

INFORMATION TO USERS

This manuscript has been reproduced from the microfilm master. UMI films the text directly from the original or copy submitted. Thus, some thesis and dissertation copies are in typewriter face, while others may be from any type of computer printer.

The quality of this reproduction is dependent upon the quality of the copy submitted. Broken or indistinct print, colored or poor quality illustrations and photographs, print bleedthrough, substandard margins, and improper alignment can adversely affect reproduction.

In the unlikely event that the author did not send UMI a complete manuscript and there are missing pages, these will be noted. Also, if unauthorized copyright material had to be removed, a note will indicate the deletion.

Oversize materials (e.g., maps, drawings, charts) are reproduced by sectioning the original, beginning at the upper left-hand corner and continuing from left to right in equal sections with small overlaps. Each original is also photographed in one exposure and is included in reduced form at the back of the book.

Photographs included in the original manuscript have been reproduced xerographically in this copy. Higher quality 6" x 9" black and white photographic prints are available for any photographs or illustrations appearing in this copy for an additional charge. Contact UMI directly to order.

UMI

A Bell & Howell Information Company
300 North Zeeb Road, Ann Arbor MI 48106-1346 USA
313/761-4700 800/521-0600

ENERGY ANALYSIS OF WATERSHEDS

By

MARIA SILVIA ROMITELLI

**A DISSERTATION PRESENTED TO THE GRADUATE SCHOOL
OF THE UNIVERSITY OF FLORIDA IN PARTIAL FULFILLMENT
OF THE REQUIREMENTS FOR THE DEGREE OF
DOCTOR OF PHILOSOPHY**

UNIVERSITY OF FLORIDA

1997

UMI Number: 9802366

**UMI Microform 9802366
Copyright 1997, by UMI Company. All rights reserved.**

**This microform edition is protected against unauthorized
copying under Title 17, United States Code.**

UMI
300 North Zeeb Road
Ann Arbor, MI 48103

ACKNOWLEDGMENTS

I am grateful for the opportunity to work with my committee chair, Dr. H.T. Odum, for his brightness, superb scientific knowledge, and unique view of the world and for the support and guidance of my committee: Dr. Mark T. Brown, Dr. G. Ronnie Best, Dr. Daniel Spangler and Dr. Wayne Swank.

Many friends provided precious support: David R. Tilley with ideas, friendship, enthusiasm and working skills; Deise Dutra and Alfredo Matheus as my surrogate family; Jose Monteiro with academic assistance; Joanne Breeze with sympathy; and students and staff of the Center for Wetlands in these last five years for a warm working environment.

Above all, I thank my parents and family for their love and unconditional support. My father gave me his love for nature and appreciation for knowledge.

I had the financial support of a Fulbright scholarship and was Graduate Assistant on the contract A8FS-9; SUP 103 between the US Department of Agriculture, US Forest Service, Coweeta Hydrologic Laboratory, NC, and the Center for Environmental Policy, University of Florida for the project “Energy Analysis of Coweeta River Basin, NC”, H.T.Odum, principal investigator.

TABLE OF CONTENTS

	<u>page</u>
ACKNOWLEDGMENTS.....	ii
ABSTRACT.....	v
CHAPTERS	
ONE. INTRODUCTION.....	1
Managing Environment with Watersheds.....	1
Concept of Geopotential-Chemical Potential Interaction in Watershed	
Organization.....	3
Study Plan.....	5
Study Areas.....	6
Literature Review.....	12
TWO. DEFINITIONS AND METHODS.....	33
Data Processing.....	33
Energies, EMERGY and Empower Evaluations by Sector.....	48
Evaluations by Stream Order.....	61
Earth Energy Flow and Elevation.....	64
Spatial Distribution of Energy Use and Empower.....	65
Energetic ratios.....	66
THREE. RESULTS.....	69
Shape of watersheds.....	69
Geopotential Energies along River Profile.....	71
Chemical Potential Energies along River Profiles.....	79
Energy Indices relating Geopotential and Chemical Potential Energies.....	90
Empower of Rain and River.....	90
Transformities of River Outflow.....	94
Energy and EMERGY Indices relating Mountain and Valley.....	94
Empower and Transformities by Stream Order.....	96
Spatial distribution of Energies Use and Empower.....	102

FOUR. SIMULATION.....	117
Impacts of river damming in the productivity of the valley.....	117
Simulation Results.....	134
FIVE. DISCUSSION.....	145
Evapotranspired Chemical Potential Energy as Measure of Productivity.....	145
Increase of Evapotranspired Chemical Potential Power Densities at Lower Elevations.....	147
Energetics of the Bowl-shaped River Basins.....	149
Energetics of the Plateau River Basins.....	158
Outflowing river energies.....	159
Empower Accumulation Downstream.....	160
Empower Densities in Bowl-shaped and Plateau Basins.....	162
The Large Geopotential Transformities in the Valley.....	164
The Chemical Potential Transformities of River Outflow.....	169
Empower Estimates Including Earth Inputs.....	170
Downstream Impacts of River Damming.....	172
Impact of Multiple Small Dams.....	176
Conclusions.....	178
APPENDICES	
A. GRAPHS OF ENERGY AND EMERGY OF EVALUATED WATERSHEDS.....	181
B. TABLES OF ENERGY AND EMERGY INDICES AND RATIOS.....	256
C. SIMULATION TABLES AND PROGRAMS.....	275
REFERENCES.....	286
BIOGRAPHICAL SKETCH.....	292

Abstract of Dissertation Presented to the Graduate School
of the University of Florida in Partial Fulfillment of the
Requirements for the Degree of Doctor of Philosophy

ENERGY ANALYSIS OF WATERSHEDS

By

Maria Silvia Romitelli

August, 1997

Chairman: H.T. Odum.

Major Department: Environmental Engineering Sciences

This research uses a new approach to study the organization of watersheds and to provide insight for their management. It evaluates work done by water energies on the landscape and explores an hypothesis that "selforganizing watersheds couple the geopotential and chemical potential energy use to maximize biological and geological production". Work of water in the mountains was measured by the geopotential energy use and related to work on terrestrial productivity of valleys measured by the chemical potential energy evapotranspired. Using data on rainfall and river flow data and topographic geographic information, spatial and temporal energy analysis and EMERGY evaluations were performed for six Brazilian watersheds of the Ribeira de Iguape River basin, and for the Coweeta River basin in North Carolina. EMERGY is the energy of one kind used directly and indirectly to make a product or service. Maps and graphs included the water energies used, empower, and river transformities. Transformity is EMERGY per unit of energy.

Evaluations revealed two typical watershed shapes- bowl- shaped and plateau basins. Bowl- shaped basins optimized the use of the water energies, with a ratio of chemical potential energy used to geopotential energy used between 1.3 and 1.5. This ratio was 0.4 to 0.6 for the plateau basins. The geopotential energy use per area and the empower densities for the bowl-shaped basins were maximum at middle elevations, coinciding with cited zones of maximum native biodiversity.

EMERGY of the river waters accumulated through the river network enabled the pulsed delivery of residual geopotential energy, nutrients and sediments to have a large effect on lowland productivity, measured by the high transformities of about $2E6$ solar emjoules per joule. About half of the rain chemical potential energy was transferred to estuaries downstream. From headwaters to delta, transformities of chemical potential energy ranged from $2E4$ to $6E4$ solar emjoules per joule.

A computer model simulated changes in the valley productivity due to construction of one or more small dams. Dams reduced flood pulses and decreased floodplain productivity by 15 to 26%. Multiple small dams minimized the impacts.

CHAPTER ONE

INTRODUCTION

In this dissertation a new approach to watersheds was studied, providing insights for their better management. Energy analysis and EMERGY evaluations of eight watersheds were made to consider the concept that self-organizing watersheds couple the geopotential and chemical potential energy of the water to maximize biological and geological production. Evaluations were made for six Brazilian watersheds of the Ribeira de Iguape River basin and for the Coweeta and Upper Little Tennessee River basins in North Carolina, with GIS maps and longitudinal graphs of characteristics. Then, the impacts of the changes in the river flow due to river damming were evaluated using a simulation model.

Managing Environment with Watersheds

Much of the land surface of the Earth is organized by the work of the hydrological cycle whether by the natural processes of landscape organization before the ascent of civilization, or by human directed organization in economic development. The highly organized network pattern developed by water flows strongly influences the use and

occupation of the landscape. Therefore, watersheds seems to have the appropriate scale for environmental management.

In the past, civilizations had flourished within watershed boundaries (such as Nile and Euphrates). Nowadays, successful administrations are done on a watershed basis. This is specially true for the management of water resources, where the use of water and land can be collectively decided by the communities living in the watershed.

The EPA (U.S. EPA, 1995) proposed a watershed protection approach to operate its water quality programs. The Agency recognized the need for an ecosystem- based approach and the participation of local communities and agencies in the solution of the environmental problems, and therefore decided for management on a watershed basis.

There is a call from the scientific community for a better understanding of the functioning of the watershed systems. NSF and EPA jointly funded a three- year project dedicated to the study of water and watersheds. Recognizing the valuable “natural capital” represented by the water and watersheds, the project emphasizes the need for a better knowledge of these natural and human- dominated systems.

Hynes (1975) recognized that streams are “part of the valley that they drain”. He urged study of the whole river system, mainly through the use of energetics. A similar message was transmitted by the Freshwater Imperative report 1995, where it was recommended that freshwater ecosystems should be managed in regional scale, and freshwater problems should be solved through understanding of the systematic factors.

Concept of Geopotential-Chemical Potential Interaction in Watershed Organization

This research focuses on the study of watershed organization, by evaluating water energy transformations in a landscape. It proposes a new concept to explain watershed organization, based on the assumption that the two water energies (geopotential and chemical potential) are used in watershed self-organization to maximize the productivity of the whole system.

Water is an amazing chemical element that can play this double role of interacting with geological and biological systems. It can do that because the rain falling from the sky carries at least two types of energy- the geopotential energy of the elevated waters capable of breaking and transporting downward rock and sediments, and the chemical potential energy of the clean, salt-free water, with osmotic potential in relation to the saltier sea water. The chemical potential of fresh water coupled with the sunlight drives the productive vegetational work.

The concept proposes that the geopotential energy is used in the uplands to spatially and temporally organize the river flows, spreading and pulsing the chemical potential energy of the water over the floodplain and coastal zones, to maximize the biological production of these lowland systems. Therefore, the productivity of the floodplain and estuarine zones is coupled to the geological work in the mountain zones (Figure 1.1).

The validation of this principle has profound implications in watershed management because it reveals the impact of river damming and channelization. Also, it

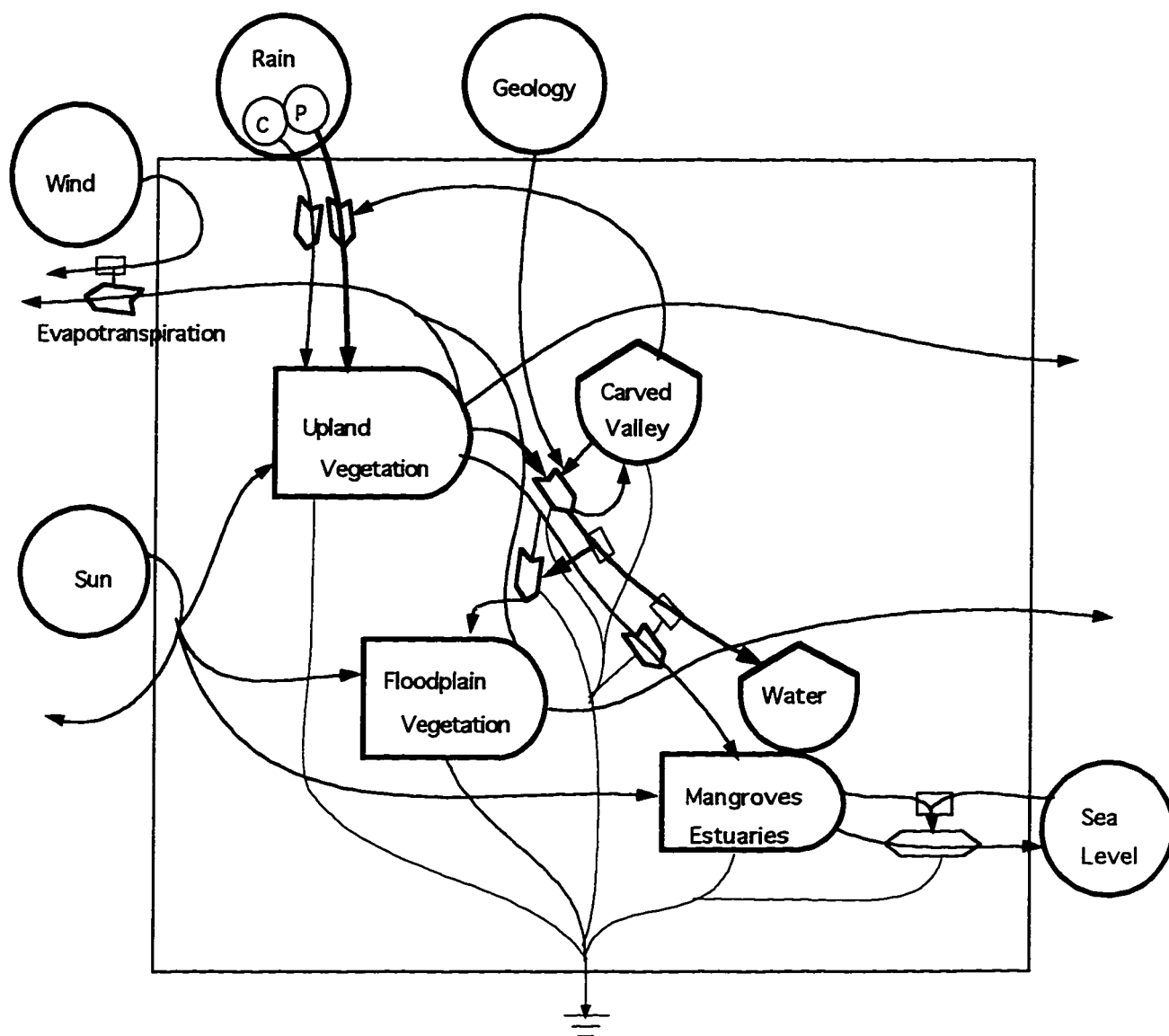


Figure 1.1. The conceptual design of the principle- " Physical energy processing the chemical energy, where G = geopotential energy and C = chemical potential energy.

allows a better evaluation of the environmental contribution of the mountain zone to the productivity of the whole system, including flood plains and valley.

Study Plan

The study used data from the Brazilian Ribeira de Iguape River watershed (southeast of Brazil) and from the Coweeta watershed in western North Carolina. The Brazilian watershed constitutes a semi-natural area where a series of dams were planned to be built. The American watershed is also a semi-natural area, much smaller than the Brazilian one, but with a rich data base accumulated over more than 65 years of research.

Energy used, EMERGY, empower, and transformities are the measures that are used in this study to evaluate the way water energies interact in the self organization of watersheds in the two regions. Estimates of water geopotential energy use indicates the intensity and pattern of water in carving the valley and building the watersheds. Evaluation of the water chemical potential energy used in evapotranspiration is related to terrestrial primary production.

This study examines the spatial distribution of the use of water energies and of empower throughout the watershed landscapes. Evaluations are done using maps and graphs of the longitudinal pattern of the water energy uses, empower contributions and river transformities. Also, indices were developed where the coupled energy use and the EMERGY contributions were evaluated for the whole-basins or for the mountain-valley sectors.

Also simulation models were used to demonstrate the essence of the watersheds upstream- downstream interactions and how they would be affected by the implementation of dams. Simulation models evaluated the impacts of one dam , or multiple smaller dams, in the productivity of the floodplain zone.

Study Areas

Ribeira de Iguape Watershed

The Ribeira de Iguape river watershed is located in the southeast of São Paulo State , Brazil, between latitudes 23 50' and 25 30' South (Figure 1.2) covering an area of about 25,000 km². The river basin is formed by two main rivers, Ribeira and Juquia, that run most of their course parallel to the coast, until they join in the valley to discharge 114 km downstream in the Atlantic Ocean (Ministerio de Minas e Energia- MME, 1984; Engecorps, 1992.a, CETESB, 1991).

The Upper Basin extends over a mountainous area (Serra Do Mar) where altitudes are over 1000 m and local amplitudes higher than 300 m. The Ribeira de Iguape river profile is very steep, descending 900m in its first 290 km (Engecorps, 1992.a, CETESB, 1991).

The Lower basin consists in a very flat floodplain where the main river and its tributaries meander and deposit their sediments. The Ribeira de Iguape profile is then very smooth, descending 5m in its last 70 km, and discharging its waters in a broad and complex estuarine zone (Engecorps, 1992.a, CETESB, 1991). Due to these topographic

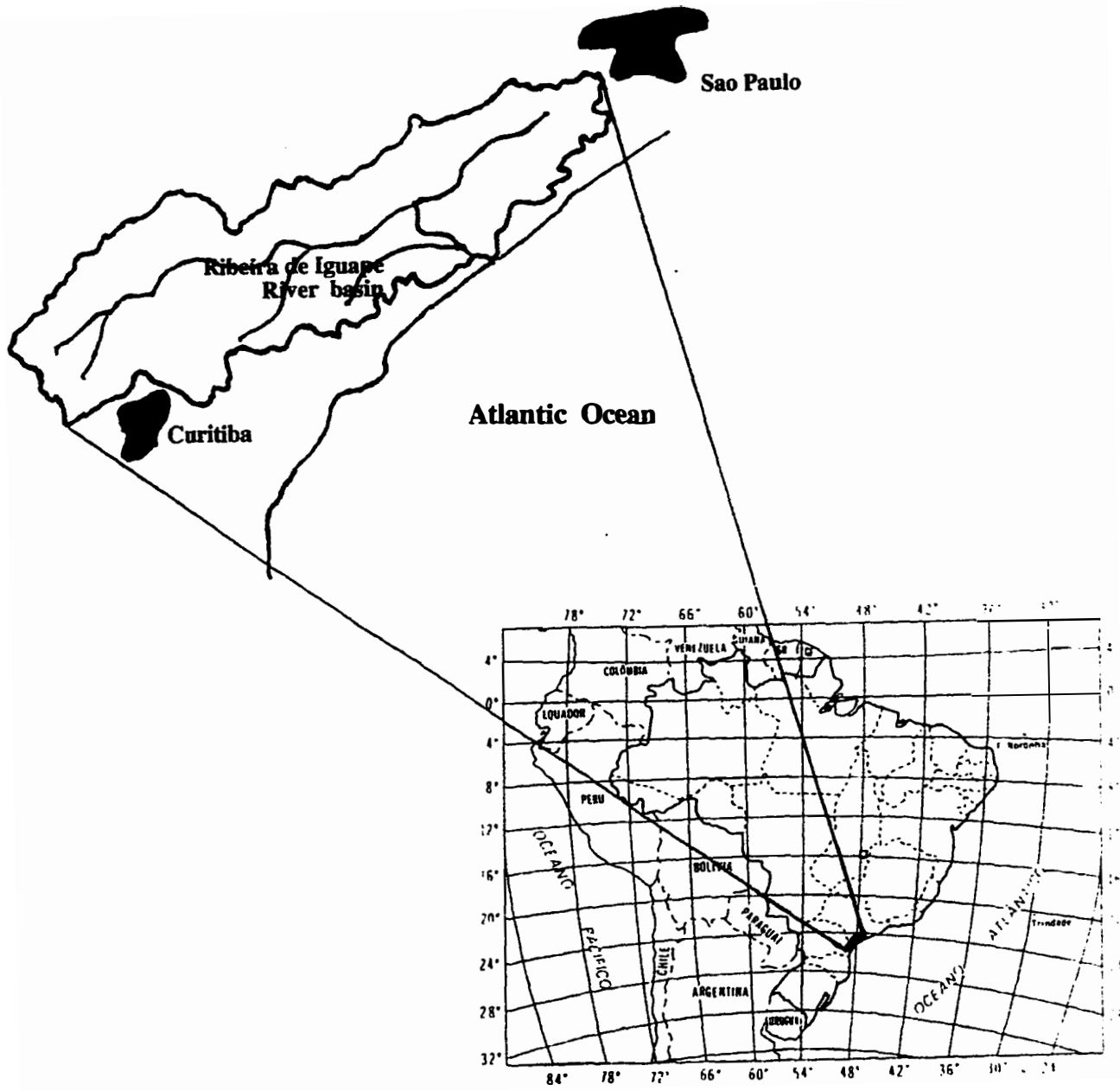


Figure 1.2. Location of Ribeira de Iguape River basin.

characteristics and geographical location, the region presents high rainfall indices (1500-1800 mm/year) with frequent floods (Engecorps, 1992, b).

A large part of the basin is composed of resistant gneiss and granites rocks. However, those zones closer to the sea are made up by the less resistant schists and filites rocks that facilitated the carving of the large valley. The erosive process took place in the last 70 million years of the Cenozoic era, and its relief was largely affected by the changes of sea level during glaciation times (Ministerio de Minas e Energia- MME, 1984).

The climate of most of the region is classified according to Koppen as humid subtropical (Cf), except in the valley which is classified as humid tropical (Af). Precipitation is more intense in the summer months (December to March) and has a heterogeneous spatial distribution over the basin(Engecorps, 1992,b). Rain is more abundant (~ 2,000 mm/yr) along the coast and over the mountain range facing the sea and much less (~1,100mm/ yr) in the deep valleys located behind of the coastal range.

The mountain zone is covered by the Atlantic rainforest, which is recognized worldwide for its rich biodiversity. This forest is the largest remnant of natural vegetation in the State, which is now reduced to 5% of its original area (Sao Paulo State, Secretariat for Environment, 1990).

The floodplain is partially occupied by monocultures such as banana, tea and citrus plantations. A large part of the floodplain is now just abandoned fields that resulted from failure of previous agricultural efforts. The poor and acidic soil of the area, lack of access to the region due to the mountain barrier, and frequent floods led to impaired development of the area when compared to the other region of the State (Lepsch et al. 1990).

The estuarine zone is part of a large, complex and very productive coastal zone, formed by lagoons, islands, channels, etc. associated with some very peculiar wetlands (restingas, mangroves, marshes, etc.). This is also the area that provides most of the natural resources (fish, shellfish, wood, palm heart, etc.), that sustain a large part of the local population (Secretaria do Meio Ambiente, 1990, SEP/DAEE, 1989).

Tourism is a new and growing activity in the area. There is some "ecological tourism" going on in the caves (karstic zones) and forests of the mountain zone. But most of the tourism occupies the coastal zone, where conflicts with production of natural resources are expected to take place.

Proposed developments for the area include the construction of dams for electrical power generation and dams for flood control. One large power generation dam (150m high, to be built over a karstic zone) will be used by a private Brazilian industrial complex to produce aluminum. Two other large hydroelectric dams will be built by the State company to serve the whole State. Planned flood control dams are smaller, but located in very pristine rivers in the forested zones.

Coweeta River Basin

The Coweeta basin is located in southwestern North Carolina (latitude 35 N and longitude 83 W), in the Nantahala Mountains of the southern Appalachians (Figure 1.2). It consists of a 1626 ha basin, formed by two 4th-order streams- Ball Creek and Shope Fork Creek- that join to form the Coweeta Creek. The latter creek drains eastward to discharge in the Little Tennessee River (Swank & Crossley Jr., 1988).

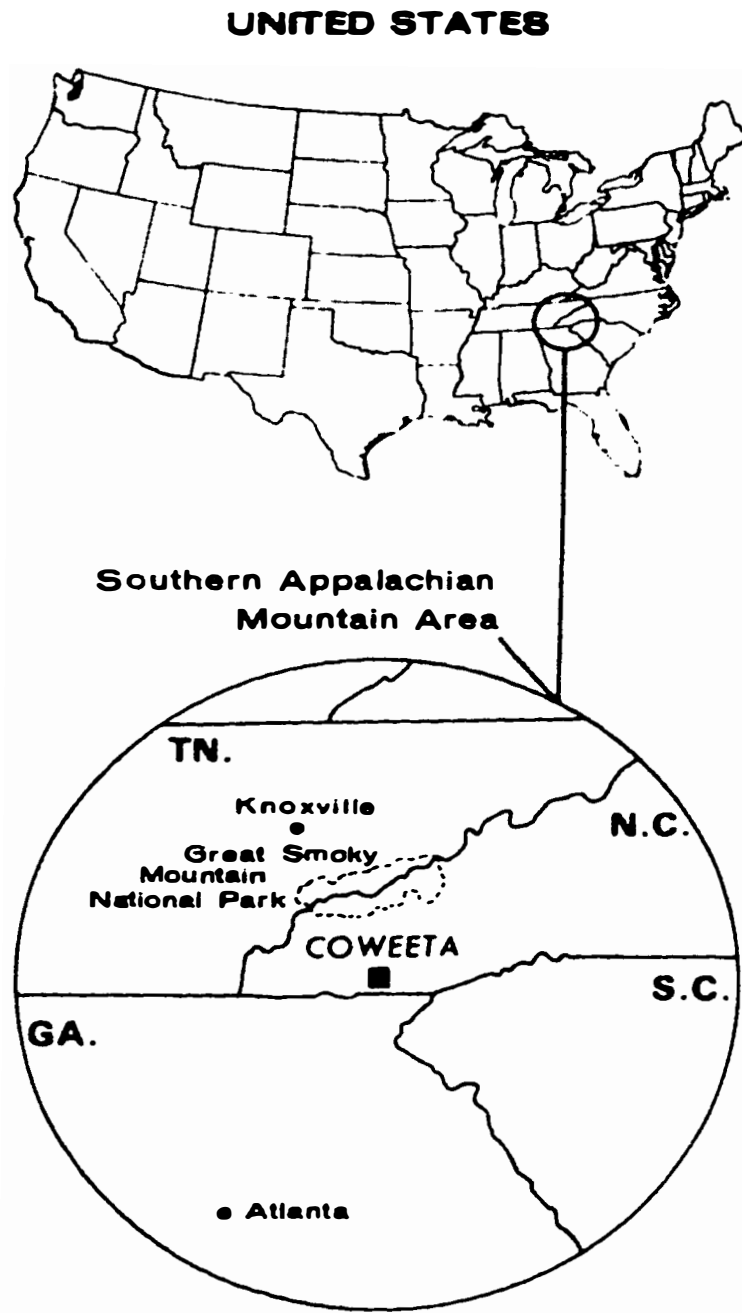


Figure 1.3. Location of Coweeta watershed.

It is a bowl-shaped valley covered by hardwood forest. Elevations range from 675 to 1592 m. Deep and permeable soils that are found in the steep slopes are primarily classified as ultisols (Typic and Humid hapludults) and inceptisols (Umbric and Typic Dystrochrepts and Typic Haplumbrepts) (Swank & Crossley Jr., 1988).

The climate in the area is very humid throughout the year with mild temperatures. It is classified according to Koppen's system as marine, humid temperatures (Cfb). Average monthly temperatures vary from 5°C during the winter to 20°C in the summer.

The basin receives about 152 mm per month of rain at Climatic Station 1 at the bottom of the area. Precipitation tends to increase about 5% per 100m of elevation in the basin, and it is fairly well distributed through the year (Swift et al. 1988)

Vegetation type in the Coweeta basin is mainly mixed-oak forest, but also includes northern hardwood, cove hardwoods and oak-pine forests (Day et al 1988). In some areas of the basin experiments led to substitution of natural vegetation by grass or white pine.

Since 1933, the basin has been part of the Coweeta Hydrologic Laboratory of the U.S. Forest Service and has been the object of intensive hydrological and ecological research (Swank and Crossley, 1988). Preliminary research focused on long-term studies on effects on water quality and quantity due to mountain farming, grazing and logging. Later on, studies evaluated the impacts of cover manipulations including forest cutting, herbicide application and fire as well as natural disturbances on biogeochemical cycles and productivity of the forest ecosystem.

More than 1000 scientific papers and 160 theses and dissertations have been done in the basin. The Coweeta Laboratory is now one of the few sites in the country selected

for the Long Term Ecological Research program (LTER) of the National Science Foundation (Stickney et al. 1994).

Literature Review

Energy and EMERGY Concepts

This study evaluates both the available and the used water energies. Available energy measures the potential energy capable of doing work and being degraded in the process. The used energy is the amount of available energy that was transformed into heat during the energy transformation process (Odum, 1996).

The geopotential and chemical potential energy of the water were evaluated. The geopotential energy is the available physical energy of the elevated water. Chemical potential energy is Gibbs free energy. It is measured in terms of concentration of dissolved solids in the fresh water in relation to sea water (Odum 1996, Odum 1983).

EMERGY offers the appropriate measure of the work done by the water energies transforming the watershed. EMERGY estimates all available energy that was used in previous transformations to make a product or provide a service. The previous energy contributions are accounted for in terms of equivalent solar energy (since it is understood that energies of different kinds have different ability to do work). The units for solar EMERGY is solar emjoules (sej) (Odum, 1996).

The rain falling in an area is a product of various previous Earth processes. Sea water had to be evaporated, condensed and transported to fall in an area. This rain-making process is coupled to many other geobiospheric process that also make wind,

tides, rivers, etc (Figure 1.4). It is understood that because they are all interconnected, they all require the global EMERGY inputs ($9.44E24$ sej/yr) to operate (Odum, 1996).

Therefore, the EMERGY of the rain falling on land in a global scale is also $9.44E24$ sej/J. In this study, the EMERGY of the rain falling in a specific watershed was calculated as a fraction of the global rain EMERGY. Estimates were based on the fraction of global rain volume that falls in the watershed area.

The network of energy transformations constitutes an energy hierarchy. Many units of energy of one kind are required to produce one unit of energy of another kind; for example, it takes roughly 4 joules of coal to make 1 joule of electricity. The output energy occupies a higher level (or transformity) in the energy hierarchy. Therefore, the transformity of one kind of energy tells us the position of this energy in the energy hierarchy. It indicates the energy quality (Odum, 1996).

Transformity is usually estimated as the ratio of the total EMERGY inputs to the energy of the output. Its unit is solar emjoules/ joule (sej/J). Estimates of the average solar transformities for earth processes are found in Odum (1996). The solar transformity for rain geopotential energy was estimated as 10,488 sej/J and for rain chemical potential as 18,199 sej/J. Average geopotential energy of river waters was calculated as 27,764 sej/J and average chemical potential of river waters was 48,459 sej/J (Odum, 1996).

The energy transformations are represented in aggregated models using the energy systems language created by Odum, 1983. The language is composed of symbols (Figure 1.5) that have energetic and mathematical meaning associated with them.

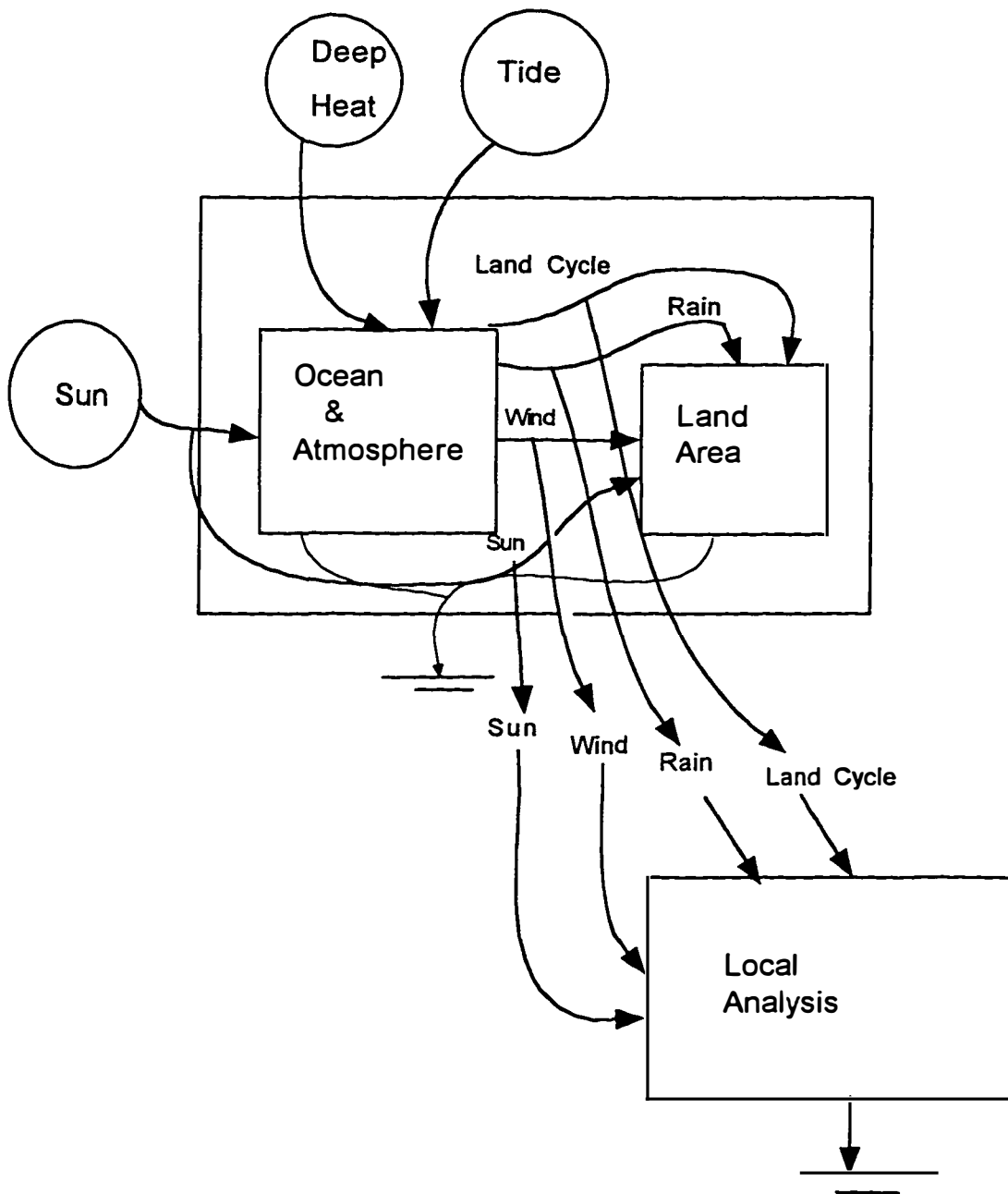


Figure 1.4. Diagram showing the interconnection of energy flows of natural sources contributing to an area (modified from Odum, 1996).

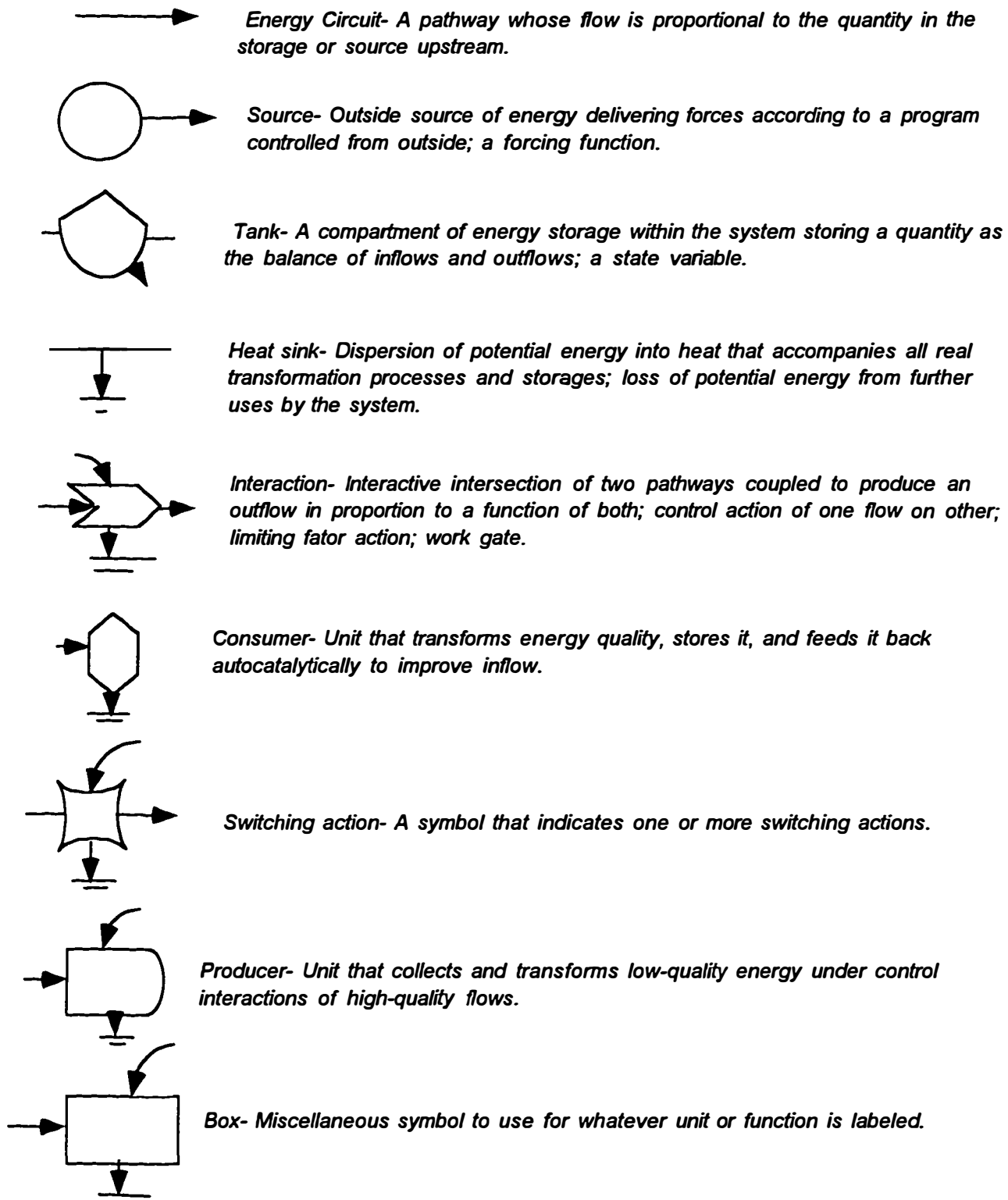


Figure 1.5. Symbols used in energy systems language (modified from Odum et al. 1986).

Previous Concepts in Watershed Systems

Many scientific fields have been studying watersheds and the river waters draining them. They all provide some insight into the functioning and organization of the watershed systems, but a more comprehensive understanding is still needed.

Geomorphology deals with the physical environment of river basins with little concern for the biotic interactions. Hydrologists keep track of the water flows and interactions of processes occurring in a watershed, but often underestimate the biotic feedback to the system. Stream ecologists are concentrated on the aquatic ecology and only recently have they started to relate to the terrestrial system.

Systematic principles of watershed systems from various fields and their major tools are described below.

Systemic view of watersheds in Geomorphology

Geomorphologists began studying watersheds in the late eighteenth century. Watersheds seem to represent an excellent fundamental unit of the geomorphic system (Ritter 1978).

A simplest systemic view of a watershed as a component of the fluvial system is diagrammed in Figure 1.6. Watershed or drainage basin, represented by the upland basins, is the production zone where water and sediments are generated. The middle zone is the transfer zone, which contains the main channel for carrying material to be settled in the deposition zone.

Major geomorphic forms in watersheds have been systematically described as a temporal product of climate and relief (Chorley et al. 1984). The litology (soil) and relief

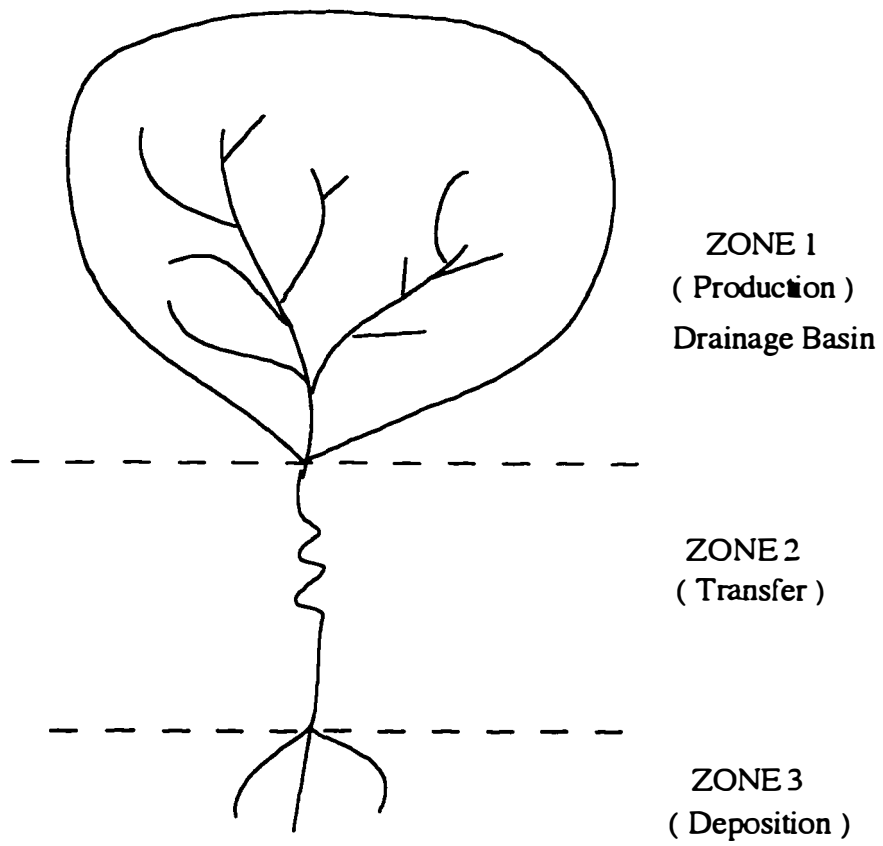


Figure 1.6. Simplistic geomorphological view of watersheds (modified from Chorley et al. 1984)

influence the vegetation, that in turn, regulate the denudation process. The climate (hydrology) acting on the relief causes the denudation process, which transfers water, soil and sediments downwards. Doing so, the major landforms in a watershed, the drainage network morphology and the hillslope morphology, are defined. Also, when material is transported downstream, the channel valley morphology and the deposition system morphology are outlined.

A hierarchical organization of the watershed landforms or stream systems has been identified by different authors. Frissell et al. (1986) described a nested hierarchy of stream systems, scaling up from microhabitat, to pool/riffle, to reach and finally to stream segment. Each spatial level was associated with certain temporal phenomena. High frequency events of low geomorphologic magnitude shape the microhabitat, pool/riffle or even reaches. Low frequency events of high magnitude cause evolutionary changes in streams and segments. Therefore, microhabitats with scales smaller than 10 m are changing due to small magnitude events occurring at more than once year. On the other hand, the stream (or watershed system) are modified by geologic events occurring at 100,000- 1,000,000 year intervals.

Chorley et al.(1984) recognized the nested hierarchy of the major watershed landforms, ascending from alluvial channel to drainage network to valley- side slopes to watershed divides. Alluvial channels are described as units of very high sensitivity and fast recovery from climatic / geologic events, whereas the divides are forms with low sensitivity and slow recovery to the same events. Leopold et al. (1964) already suggested that river channels were formed from frequent rainfall events occurring more often than once a year or two.

A classical view of the watershed is as a product of evolutionary cycles (Chorley et al 1984). According to Davis, the watershed goes through a inevitable, continuous and broadly irreversible process of change producing an orderly sequence of land transformations. A watershed system goes through youth, maturity and old age stages, as it wears down of a recent uplifted area to the peneplain. In the youth stage, soon after a flat land had been uplifted, the relief is small, the drainage is poor, the stream valleys are narrow and upland are broad and flat. During maturity, the region achieves maximum relief and the drainage network ceases to increase. Divides are narrow and major rivers present meander patterns and limited floodplain. In old age, after smoothing of relief, lowering the summits and ridge tops and broadening the valley floors, the whole region is flattened to base level (interrupted sometimes for some topographic residuals). Later on, an uplift takes place, and the cycle restarts again.

This concept has been seriously challenged, and new alternatives for the geomorphic cycle have been proposed. According to Hack (Curry, 1972), after a period of adjustments to the a tectonic event, a period of dynamic equilibrium takes place. Even if tectonic activity continues, the denudation process adjusts the rate of uplift in a way that as land is removed at same pace as it is raised. Landform processes are in equilibrium with tectonism and climate, although far from static in a geotectonic sense.

However, the evolution of a river profile, going from a flat surface to straight slope to finally to a concave profile seems to be a general pattern (Figure 1.7). Such evolution was verified by Schumm et. 1987, when studying eleven second-order basins on a clay-sand fill at Perth Amboy, New Jersey.

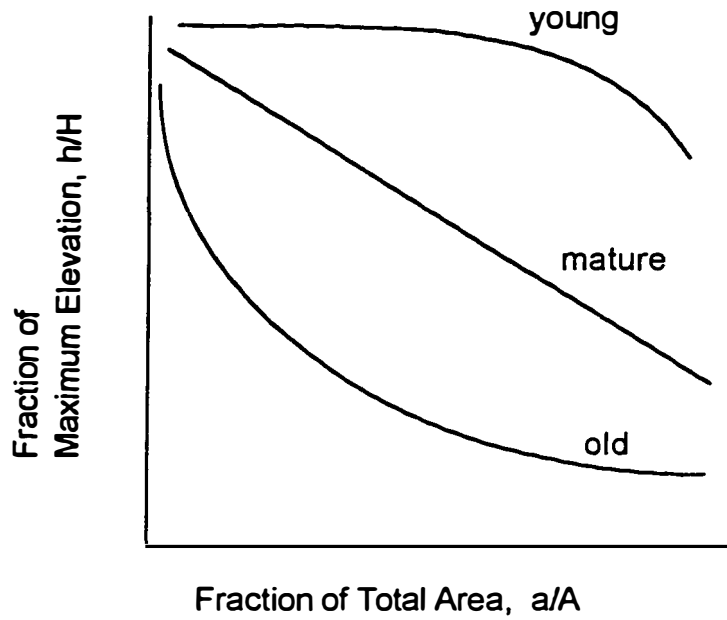


Figure 1.7. Hypsometric curves for typical stages of watersheds evolution, as verified in Perth Amboy badlands.
(modified from Schumm et al. 1987)

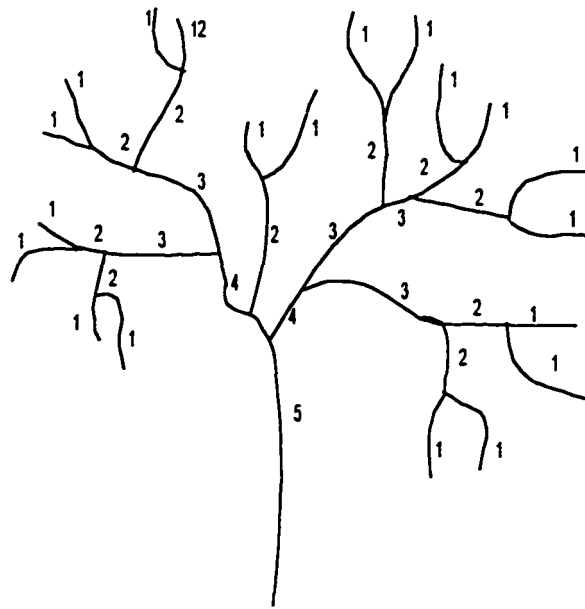
Organization of river networks. The hierarchical organization of river networks was first recognized and classified by Horton, and lately modified by Strahler. The latter author devised a classification scheme where the smallest permanent flowing river is called first order stream and the union of two streams of order n would produce a stream of order $n+1$.

Many watershed variables seem to correlate with Strahler's stream order scheme. The log number of streams are negatively correlated to the stream order whereas stream lengths are positively related to stream orders (Figure 1.8).

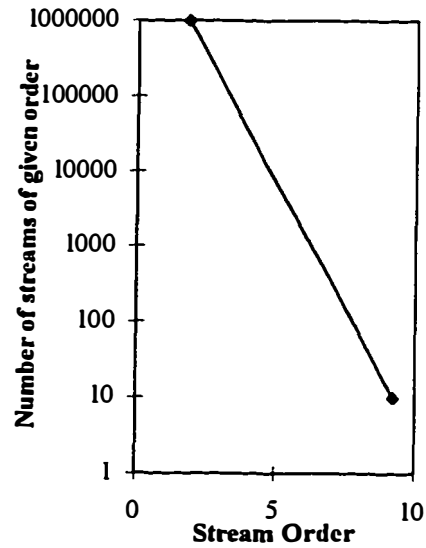
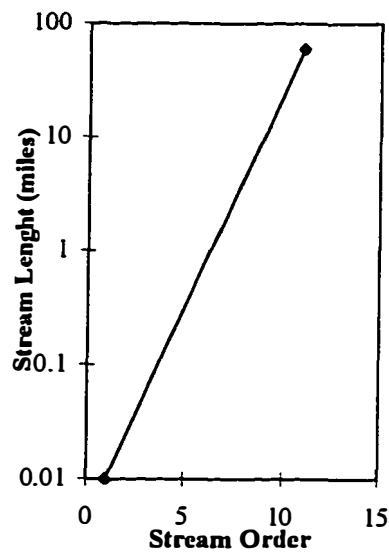
The drainage density (total stream length/ area) was seen by Glock as product of an evolutionary process. The drainage density of the river systems goes through five stages of development. The first is initiation, where the first stream patterns are established on a pristine surface. It is followed by elongation, where channels grow headward into available area, and elaboration when network is filled with addition of lower-order tributaries. Then, it goes through a stage of maximum extension where drainage density is maximum. Finally the system evolves to the integration stage where some streams lose their identity and the drainage density is reduced with time. A more hierarchically organized drainage pattern evolves after this last stage.

Drainage densities were found to be positively related to runoff and sediment yield. The higher the drainage density, the faster the rain waters are drained from the watersheds and more sediments are transported downstream.

But sediment delivery does not necessarily increase linearly with the size of watershed. In fact, the larger the drainage area, the more water and sediment is discharged from the basin, but on a unit area basis the sediment production decreases with the



A.



B.

Figure 1.8. Diagrams displaying in A.) the stream order classification according to Strahler; B) Relationship between stream orders and the number of streams or the stream length (modified from Allan, 1995).

increase in the drainage area . This is because more sediment is eroded in the headwaters, but the opportunity for sediment storages also increases downstream.

Energetics of watersheds. In the early sixties many geomorphologists started to use thermodynamics to explain how landforms were generated and maintained. They were trying to explain the idea that landforms are in dynamic equilibrium , operating in a open system framework. This new concept denied the previous idea of landscape evolution proposed by Davis, where landforms were subject to an unidirectional process toward maximum entropy.

Chorley recognized that the organization and regularity of forms in the landscapes were maintained by the continuous (but not constant) supply and removal of material. Eventually the geological work would lead to higher order, heterogeneity, differentiation and organization (Curry, 1972).

Scheidegger and Langbein (1966) proposed that steady-state in rivers was maintained by minimization of variance among river hydraulics variables, such as depth, width and velocity. An increase in the river discharges would be accommodated by minimum effect among hydraulic factors.

Leopold and Langbein (1962) advocated that the distribution of potential energy of water and sediment particles in a river system tends towards the most probable state. Using mechanical analogies and thermodynamics concepts they inferred that the most probable sequence of energy losses in successive units of river length would correspond to a uniform increase of entropy per unit of river length. This was mathematically equivalent to saying that longitudinal river profile would tend to an exponential form.

Another conclusion of their studies was that the most probable state could be reached based on the principle of minimum work. Also, the adjustment of the hydraulic variables such as depth, width, and velocity would lead to maximum probable state (and also to the minimization of work).

Odum H T (1996) identified a river network as a typical example of energy hierarchy, where small streams converge to form the large rivers. The geopotential energy of the water goes through transformation steps where a lot of energy of the rain is used to produce the small streams and a lot of small streams are needed to generate the large rivers.

Also an increase in energy quality follows the river system organization downstream. As the available energy of river water declines, the river transformity increases downstream. Diamond (1984) evaluated this hierarchical pattern when calculating the geopotential transformities for stream sectors of different orders in the Mississippi River basin.

Systematic view of watersheds in Hydrology

Watersheds are defined by hydrology meaning the land area that contributes surface runoff to any point of interest (Viessman et al. 1989). Its size can vary from hectares to thousand of square kilometers.

Hydrologists study and quantify the water inputs, flows and storages in a watershed. Today most estimates are done through the use of simulation models. These models use physical equations to describe the processes that transform and redirect the precipitated water through the earth surface.

There are a myriad of hydrological models that operate on different levels of spatial- temporal resolution (De Vries & Homadka, 1993; Fawthrop, 1994; Newson, 1994; Singh, 1989). There are the single- event streamflow models that simulate the rainfall- runoff processes after a discrete rainfall event. They include the Corps of Engineers HEC- 1 model and the Soil Conservation Service TR-20. They are mostly for flood control works.

There are also those continuous streamflow simulation models. They account for all precipitation that falls in the area and the movement of the water through the watershed to its outlet. Precipitation is tracked as direct runoff, infiltration, evapotranspiration, interflow, deep percolation, baseflow and streamflow. Typical components of a continuous streamflow simulation model are represented in Figure 1.9.

These models can be lumped, representing the watershed as a single unit or distributed, incorporating the spatial variety of rainfall, soil, slopes, and channels of the area. These later are usually combined with Geographic Information Systems providing a spatial display of the results.

Continuous streamflow simulation models include complex models such as the SWRRB (Simulator for Water Resources in Rural Basins) and the HSPF (Hydrological Simulation Program Fortran). They are used mainly in water resources planning, design and management.

There are also water quality models, linking the estimation of water quantity to the prediction of water quality of a watershed. They are found in all levels of complexity previously discussed, and they are used in pollution control and environment management. A typical water quality model is the CREAMS/ GLEAMS (Chemicals, Runoff, Erosion

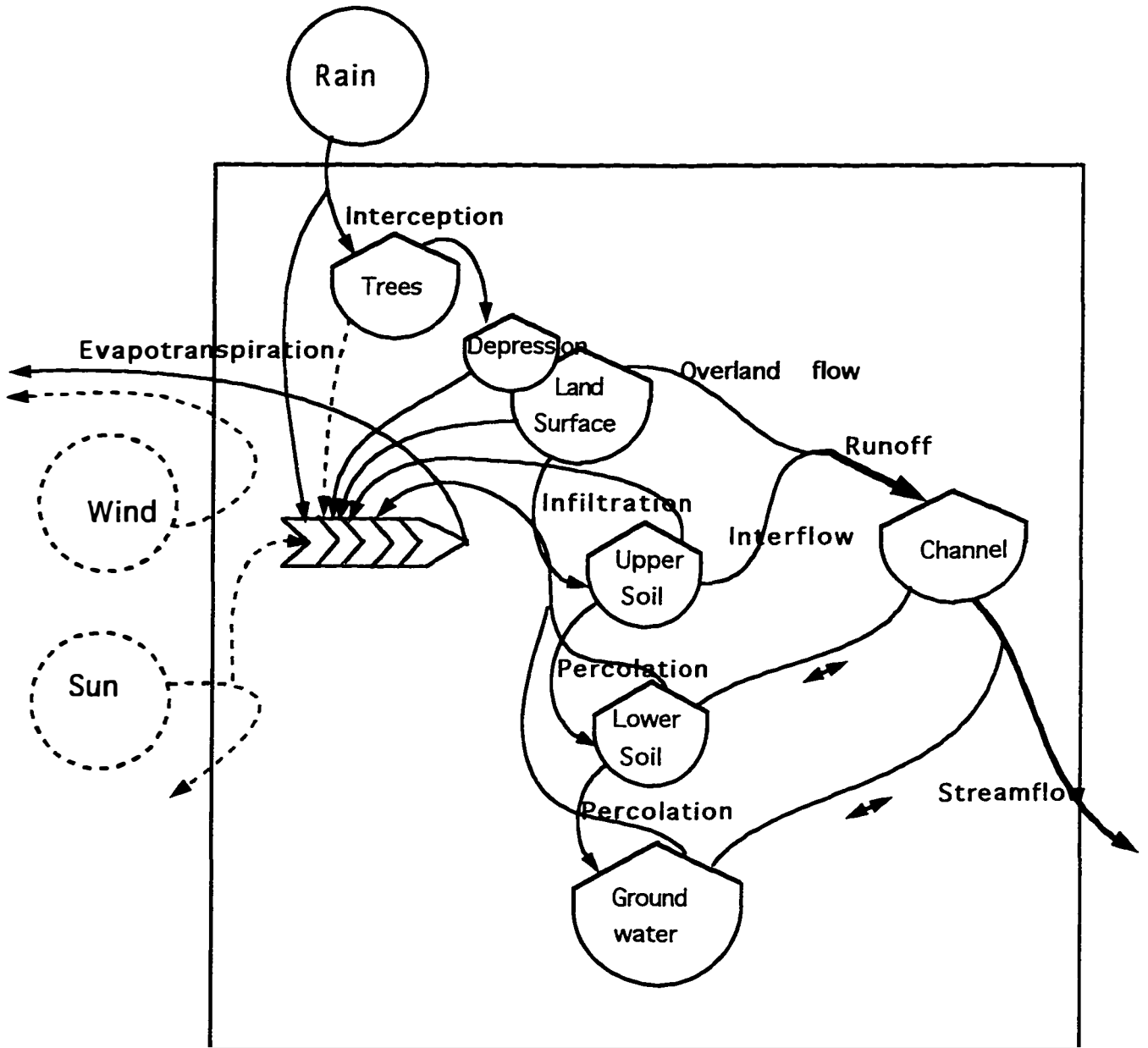


Figure 1.9. Major flows and compartments of a typical hydrological model (with dashed lines representing forcing functions indirectly considered in the model) (modified from Singh 1989)

and Agricultural Management Systems/ Groundwater Loading Effects of Agricultural Management Systems) model.

Systemic view of watersheds in Stream Ecology

Continuity. Stream ecologists have been mostly concerned with lotic communities occurring in the dynamic physical environment of the river network. However, nowadays more comprehensive concepts are being proposed looking at the connectivity of river biota to other dimensions other than the local reach of the streams.

A major concept is the river continuum concept, proposed by Vannote et al. (1980), which deals with the longitudinal connectivity of the biological production in river ecosystems (Figure 1.10). It relates the structural and functional characteristics of the lotic communities to their relative position in the stream network (i.e stream order). When in the headwaters (first to third order streams), lotic communities are largely heterotrophic and colonized by shredders and collectors, due to the shading and litterfall of the close riparian vegetation. In the mid reaches (third to fifth order streams) with larger and more illuminated channels, and with nutrient contributions from upper reaches, the lotic communities tend to be autotrophic, formed mainly of benthic algae to be consumed by scrapers. Finally, in the lower sectors (stream order higher than fifth) where the river is deeper and more turbid with high loads of organic matter from upstream reaches, the heterotrophy is favored again leading to the flourishing of collectors. Maximum diversity was proposed to take place in the middle reaches of the rivers due to the high level of environmental heterogeneity (as the diel temperature fluctuations) favoring the growth of a vast array of species.

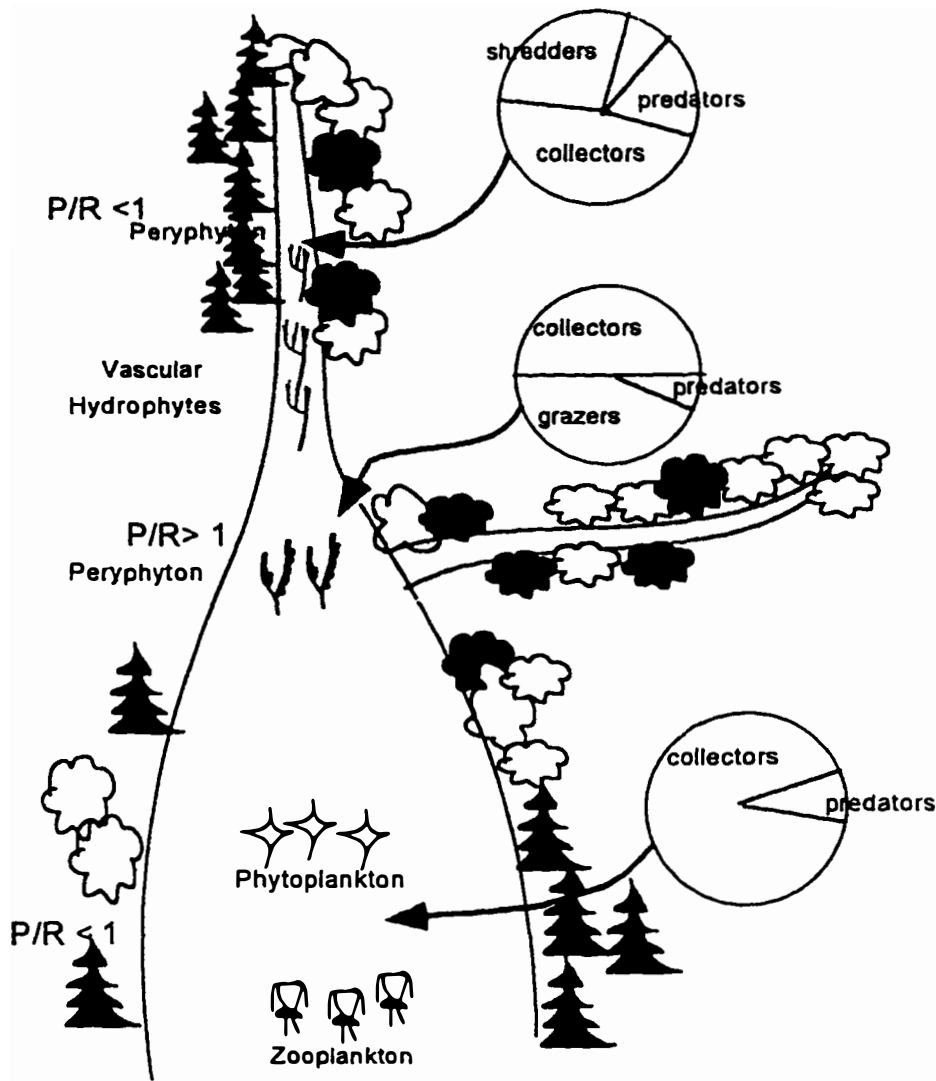


Figure 1.10. The river continuum concept that emphasizes the longitudinal connectivity of biological production in river ecosystems (modified from Vannote et al. 1980).

Lately, with the growing appreciation for the ecological importance of the floodplains zones, the significance of the river connections to two other spatial dimensions - lateral and vertical- has been recognized. The lateral connection refers to the exchange of water, resources and organisms between the river channel and the floodplain of alluvial rivers.

The flood pulse concept is an expression of such connectivity (Bailey, 1991 and Bailey, 1995). It provides a theoretical framework to analyze the adaptive strategies of organisms exploiting the alternate wet and dry phases of a large floodplain area (Figure 1.11).

The inundation of a floodplain is seen as a “moving littoral” creating a dynamic edge effect when traversing from the channel to the upland zone. Organic decomposition and nutrient cycling are accelerated when compared to permanently inundated areas. Terrestrial and aquatic organisms develop strategies to explore this periodic interface zone. This is verified extensively in central Amazonian River floodplain, where inundation lasts for 5 to 7 months a year. Terrestrial invertebrates migrate horizontally to highlands, vertically to the canopies, go dormant or develop plastron respiration to cope with the flood.

The aquatic animals also take advantage of the high productivity and diverse habitats of floodplain areas. Fish, especially in tropical zones, are highly adapted to exploit the flood pulse. They reproduce during flood season and the young find plenty of food in the previously accumulated organic matter, in the tree litterfall, and in the accelerated primary productivity of the floodplain area. Shallow water habitat with submersed vegetation offers high temperature and diversity of shelter very appropriate for the

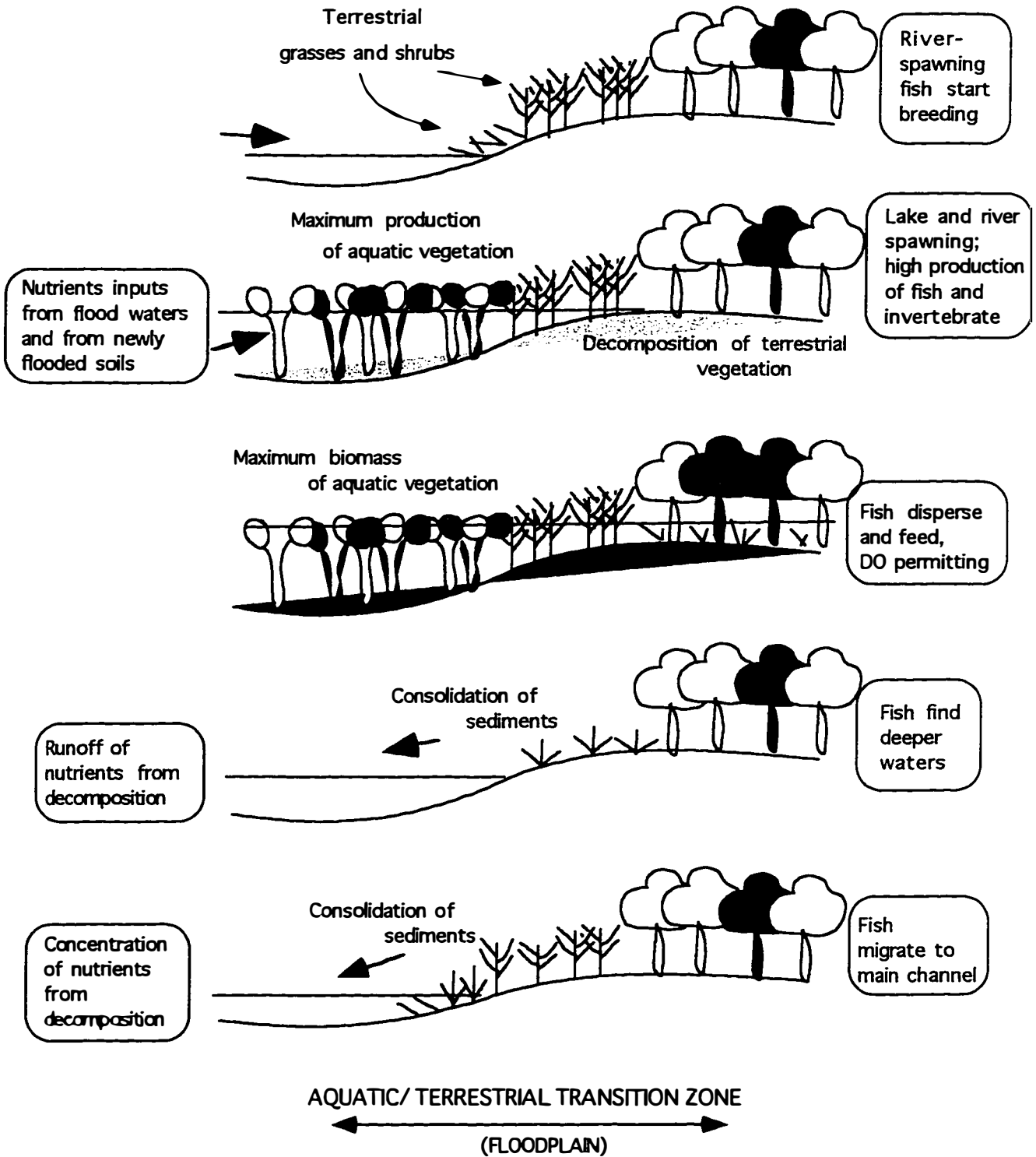


Figure 1.1 1. The flood pulse concept (modified from Bailey, 1995)

development of the young. At the same time, vegetation is helped by seed dispersal performed by fishes.

The third connection to the river channel ecology is the vertical one, recognizing that the stream biota is also correlated to the groundwater of the alluvial zones. Water, nutrients and organisms moves into the aquifer and out to the channel. Standing crop of organisms living in the interstitial zone in the sandy-gravel sediments exceeded the benthic biomass in the alluvium zone of Flathead river (Stanford & Ward, 1988). The vertical interface between surface water and groundwater acts as a physical barrier to sediments, organic matter and pollutants that can eventually contaminate the aquifer (Petts, 1994).

Discontinuity. Opposing to the previous concepts of continuity along river network, the serial discontinuity concept offers a theoretical view on how impoundments are responsible for major disruptions on the longitudinal gradient of river network. Major upstream- downstream shifts in biotic and abiotic pattern and process occur due to dam implementation (Stanford & Ward, 1987).

The serial discontinuity concept was proposed first for constrained channels and lately for a more interactive river system where floodplain are taken in consideration. This late system would represent a more complex system where three well-defined reaches were characterized - the upper constrained channel, the mid braided channel and the lower meandering channel.

The general pattern along the longitudinal profile and potential alterations due to dam implementation were predicted for the different physical and biological parameters analyzed. Figure 1.13 displays the predicted pattern and impacts of dam in the constrained and in more complex river system , when evaluating thermal heterogeneity and

biodiversity. As proposed by this concepts , the intensity of the impacts would follow the intensity of the parameter in analysis along river profile. Therefore, when considering the complex river system, more intense impacts in thermal heterogeneity and biodiversity would be observed for dams constructed in the lower meandering reaches of a river system.

Aquatic biota related to physical watershed. Some relationships have been found between river biota productivity and diversity and physical characteristics of the watershed. A linear relationship between the abundance of fish and stream width was verified in small forested streams of Panama (Angermeier and Karr, 1983). A log- linear relationship between number of species of freshwater mussels and the area of drainage basin was found in 49 rivers draining the North America Atlantic coast (Allan, 1995). The same type of relationship has been detected among species of fishes and basin area in different parts of the world (Allan, 1995). Upstream fish migration was identified as an important feedback mechanism to replenish phosphorus (and genetic information) reserves in the headwater systems (Hall, 1972).

CHAPTER TWO

DEFINITIONS AND METHODS

Data Processing

In order to evaluate the water energy hierarchy of the studied watersheds, data about areas and elevations, rainfall and river flows were collected and processed in two steps:

- River basins and sub-basins were divided in elevational and stream order sectors.
- A water budget was estimated for each sector, where rainfall and runoff were calculated from gauging data. Infiltration was assumed to be 10% of rainfall for the plateau basins and nil for the other basins. Evapotranspiration was estimated as the difference between rainfall and the outflows.

Therefore, data were processed for the evaluated watersheds as follow:

Ribeira de Iguape River Basin

Areas and elevations

To estimate the areas in the different elevational sectors of the Ribeira watershed, topographic maps of the area (scale 1: 250,000) were prepared using ArcInfo software. Digitized elevation contours included 1000 m, 800m , 500 m, 300 m and 100m contour lines (Figure 2.1)



Figure 2.1. Topographic map of the Ribeira de Iguape River basin.

The Ribeira de Iguape river basin area was also divided in 20 major sub-basins, according to system adopted by other projects in the area (Figure 2.2). Therefore, six elevational sectors were defined for the Ribeira river basin and its sub-basins. They were identified by the middle elevation point in the sector (such as 1050, 900, 650, 400, 200, 50 m) and they encompassed the area located between two consecutive contour lines. Areas of elevational sectors of Ribeira river basin and sub-basins were measured using ArcInfo , and then used in the next estimates.

Six sub-basins were evaluated in this study: Eta, Jacupiranga, Juquia, Pardo, Betari and Catas Altas.

Annual rainfall

Map of rain distribution in the Ribeira river basin (Figure 2.3) was prepared based on the average annual rainfall data of 50 gauging stations in the basin (Engecorps, 1992 a) .The volume of rainfall falling in each elevational sector of a basin or sub-basin (rain/sector) was estimated multiplying the predicted annual rain in the area by the aerial extension of the sector. The total volume of rain (total rain) that could eventually reach an elevational sector (i.e., rain in the sector plus rain in the upstream sectors) was also estimated.

River flows

Discharge data from existing and extinct gauging stations in the Ribeira de Iguape basin were gathered from different sources (Table 2.1). The runoff ratio (i.e. ratio of the river flow leaving the area to the volume of rainfall falling in the drainage area) was then calculated for each gauging station. Runoff ratios were then correlated to the middle

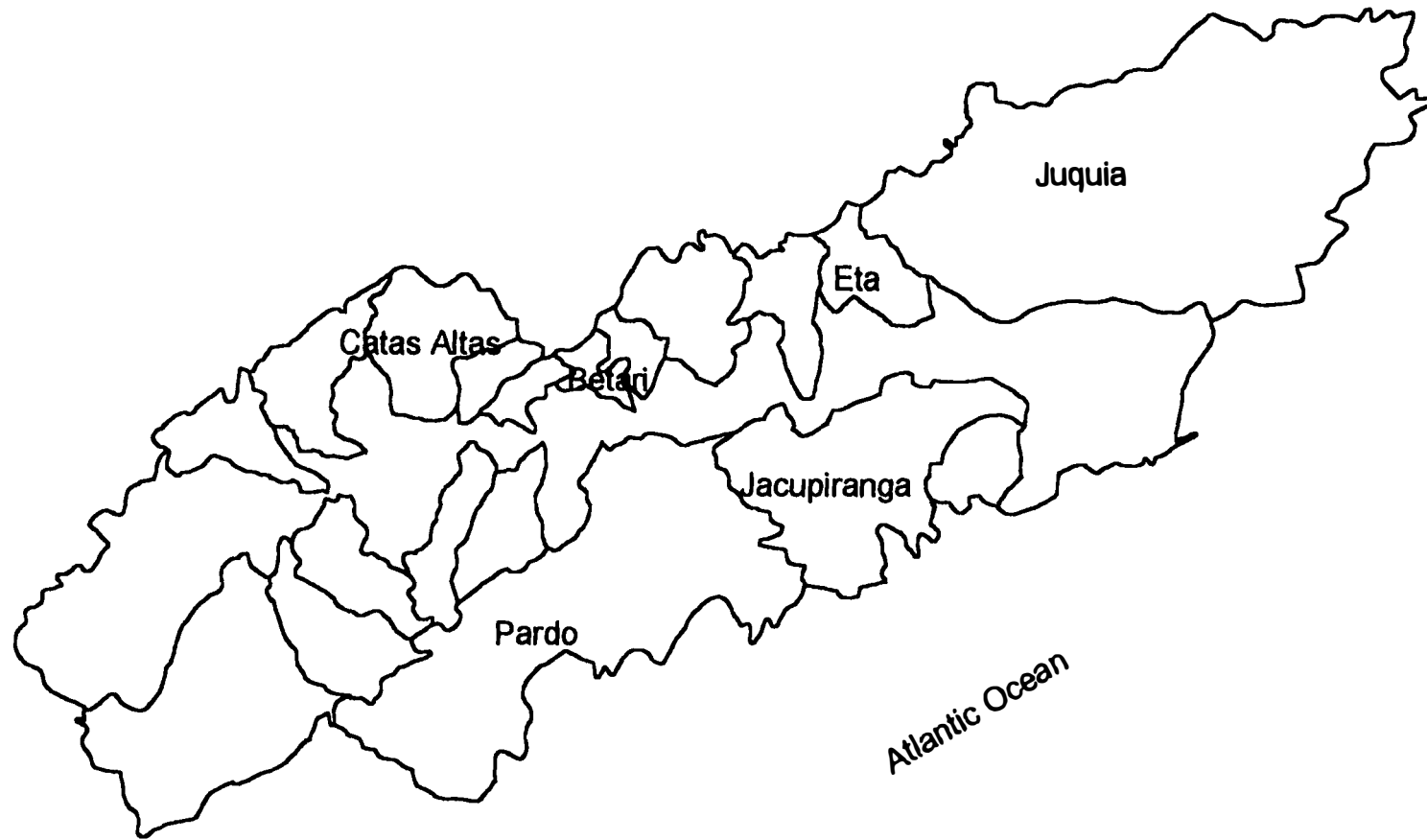


Figure 2.2. Map of sub-basins in the Ribeira de Iguape watershed

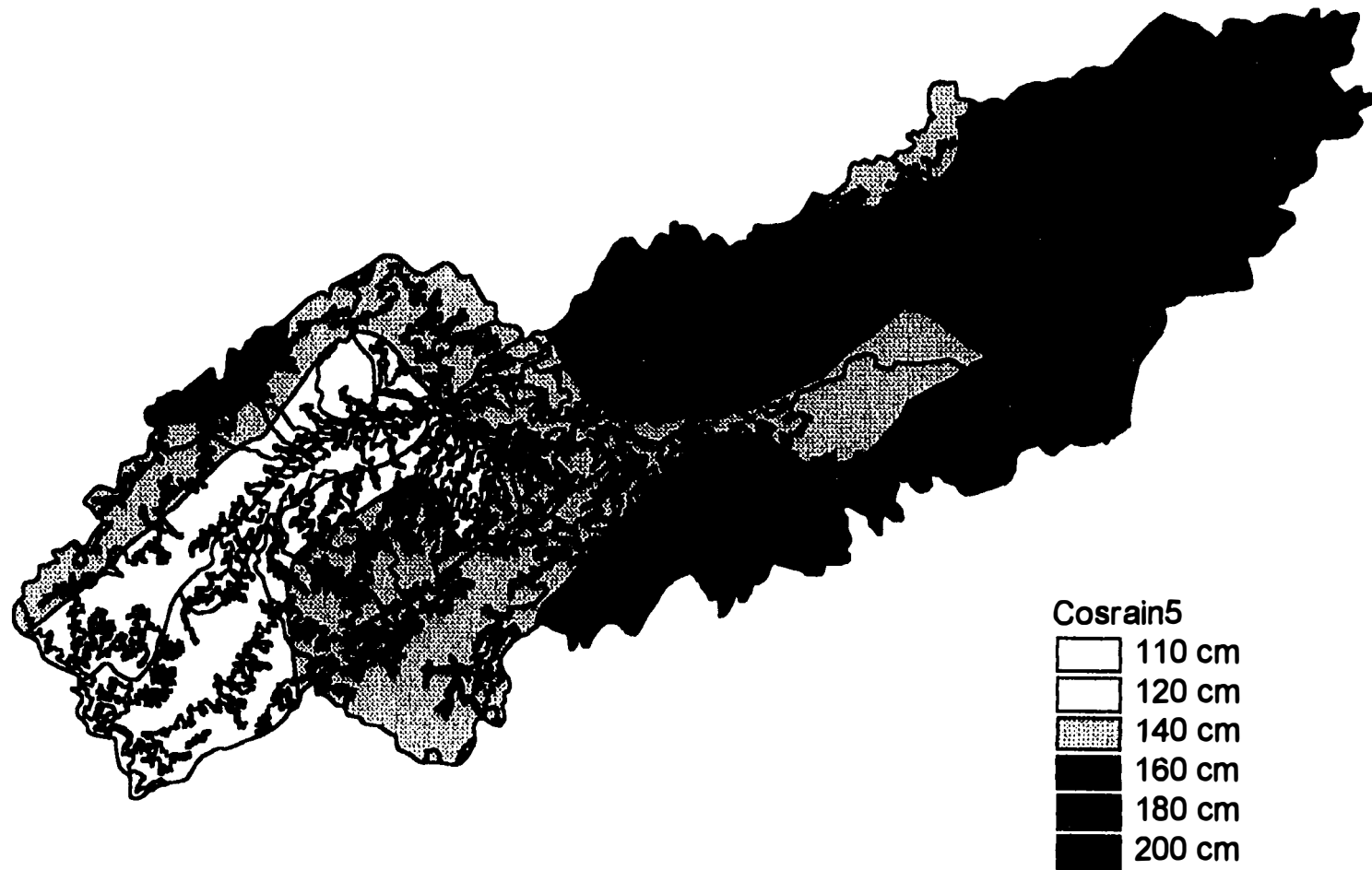


Figure 2.3. Isohyetal map of the Ribeira de Iguape watershed.

Table 2.1. Discharge data from gauging stations of Ribeira de Iguape River basin

Subbasin	Gauging Station	Drainage area (Km ²)	Period yrs (19..-19..)	Mean Discharge m ³ /s	References
Açungui (PR)	Passo do Assungui	1573	36-45	22.86	MME-DNAEE
Betari	5F - 015	177	72-83	3.84	DAEE (bulletin)
Catas Altas	Barra do Chapeu (river mouth)	128	—	2.80	Engecorps
		698	—	11.00	Engecorps
	6F-001	652	72-92	9.66	DAEE
Grande	Sitinho	189	—	3.52	MME-DNAEE
Itapirapuã	(river mouth)	505	—	7.90	Engecorps
Jacupiranga	5F-016	204	72-92	4.63	DAEE
	5F-009	148	65-93	6.53	DAEE
	4F-016	1325	63-93	31.17	DAEE
Juquia	3E - 114	35	82-93	1.60	DAEE
	4E - 025	130	80-92	5.43	DAEE
	4E - 015	236	72-87	8.72	DAEE
	4E - 026	500	81-92	14.41	DAEE
	4F- 003	2443	59-93	68.20	DAEE
	4F-018	4341	69-92	126.00	DAEE
S Lourencinho (Juquia)	4F-017	556	63-94	21.34	DAEE
Itariri (Juquia)	4F-010	22	55-71	1.702	DAEE
	4F-014	91	59-94	3.57	DAEE
	Azeite river	74	38-78	4.7	Engecorps
	4F-026	356	72-93	10.43	DAEE
S Lourenço (Juquia)	Pedro Barros	1225	38-68	42.9	Engecorps
	4F-039	1426	81-93	45.6	DAEE
	4F-007	1713	62-93	51.7	DAEE
Rib Fundo (Juquia)	4F- 036	145	80-85	3.95	DAEE
Acungui , SP (Juquia)	4F-005	410	59-93	15.04	DAEE
	4F-025	634	72-93	22.98	DAEE

Table 2.1. cont. Discharge data from gauging stations of Ribeira de Iguape River basin

Subbasin	Gauging Station	Drainage area (Km ²)	Period yrs (19..-19..)	Mean Discharge m ³ /s	References
Palmital	(river mouth)	157	___	3.40	Engecorps
Pardo	Capivari	1085	30- 67	16.94	MME- DNAEE
	5F-011	2872	69-93	49.20	DAEE
	Corrego Comprid	3076	77-91	53.30	Engecorps
Pariqueraçu	4F-023	110	72-93	2.09	DAEE
	(river mouth)	333	___	11.00	Engecorps
Peropava	(river mouth)	1058	___	26.40	Engecorps
Pilões	(river mouth)	487	___	19.00	Engecorps
Ponta Grossa	Cerro Azul	349	31-66	4.48	MME-DNAEE
Ribeira	Itapirapua riv mo	4020	___	61.50	Engecorps
	Balsa do Cerro A	4570	___	70.00	Engecorps
	5F -005	7465	62-83	112.90	DAEE
	Iporanga	12430	42-90	188.80	Engecorps
	5F-001	14582	38-92	234.60	DAEE
Rib Fundo	4F- 036	145	80-85	3.95	DAEE
S Lourencinho	Azeite river	74	38-68	4.70	Engecorps
	Itariri	356	72-93	10.43	DAEE
	4F-017	556	63-94	21.43	DAEE
Taquari	(river mouth)	412	___	14.30	Engecorps
Tijuco	Apiai	4	___	0.09	Engecorps
	(river mouth)	185	___	3.70	Engecorps

DAEE , 1994- Monthly river discharges data (per. communication)
 DAEE- Departamento de Aguas e Energia Eletrica do Est.de S Paulo.
 S Paulo, Brazil.

Engecorps, 1992. Macrozoneamento do Vale do Ribeira- Memorial Descritivo - Recursos Hidricos. Secretaria do Estado do Meio Ambiente de S Paulo.
 Coordenadoria de Planejamento Ambiental, S Paulo, Brazil.

MME- DNAEE. 1970. Boletim Fluviometrico n 25- Bacias Litorâneas dos Estados do Parana e Santa Catarina (1937- 1967). Ministerio de Minas e Energia.
 Departamento Nacional de Aguas e Eneergia Eletrica . Divisão de Agua do Segundo Distrito Sul. Belo Horizonte, MG. Brazil.

elevation of the drainage areas, and equations relating runoff ratio to elevation were prepared for each basin or sub-basin .

Runoff ratio was then defined for each elevational sector of the sub-basins. The annual river flow was estimated for each sector of a sub-basin by multiplying the total rain by the runoff ratio expected to occur in that sector.

Coweeta River Basin

Areas and elevations.

A digitized topographic map of the Coweeta watershed was provided by the University of Georgia, Institute of Ecology, GIS lab. Original coverage presented 50 ft interval contour lines, ranging from 2200 to 5000 ft.

The basin was mapped for analysis in two ways:

- Elevational sectors-defined as the areas between elevation contours at 400 ft elevation interval (Figure 2.4). They were identified by the middle elevation point (5000, 4600, 4200, 3800, 3400, 3000, 2600 and 2300 ft).
- Stream order segments-using Strahler's modified Horton numbering scheme for the stream order. First to fourth order stream sectors were identified in the Coweeta River basin, using a topographic map of the area with a scale 1: 4400 (Figure 2.5).

Energy and EMERGY were calculated for the elevational sectors of the 3rd order and 4th order stream sub-basins of the Coweeta River basin (Figure 2.6). The elevational sectors of the sub-basins, defined when overlaying the sub-basin boundaries to the topographic map, were used as the aerial units in the estimates.

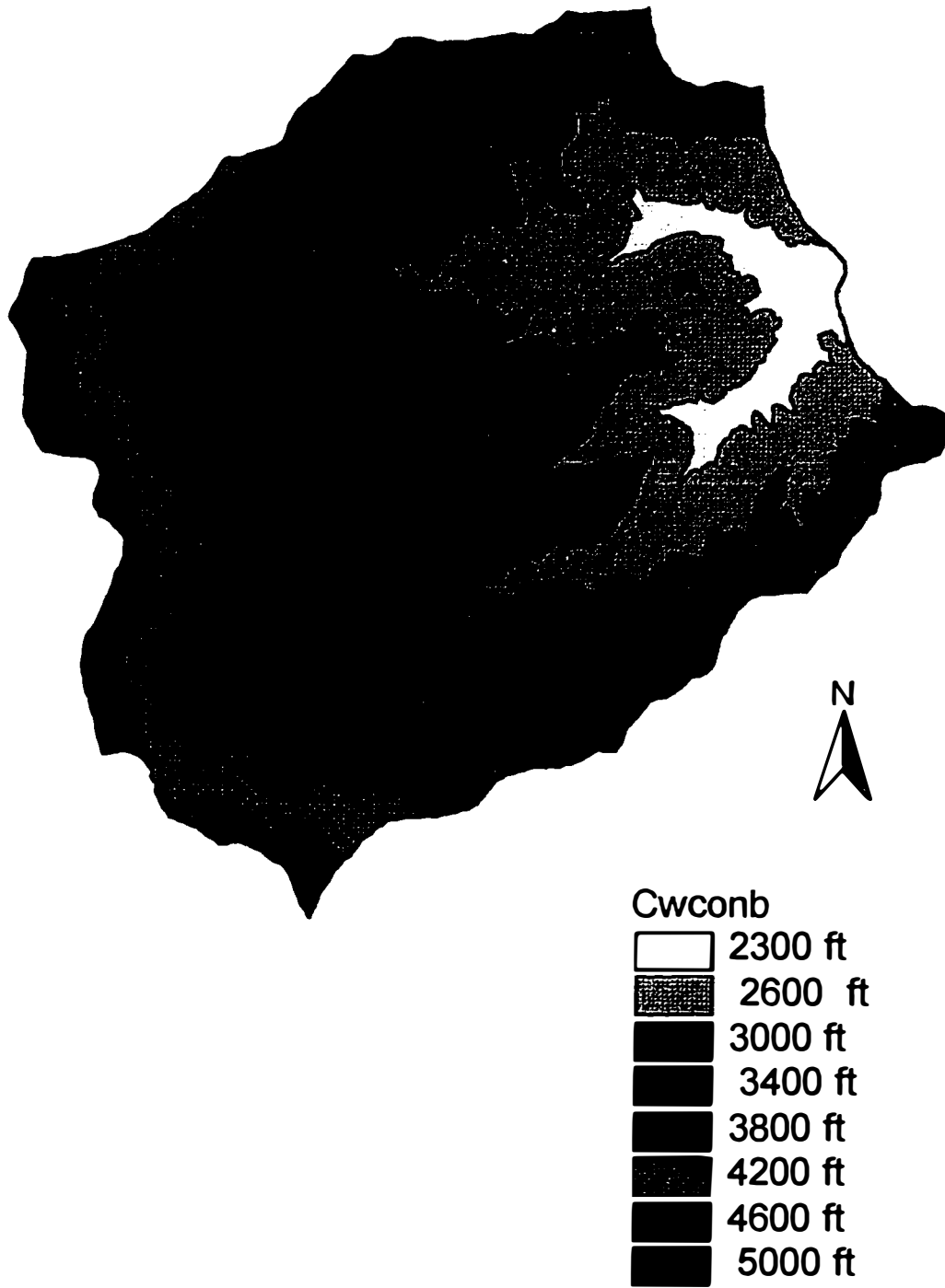


Figure 2.4. Topographic map of the Coweeta watershed.

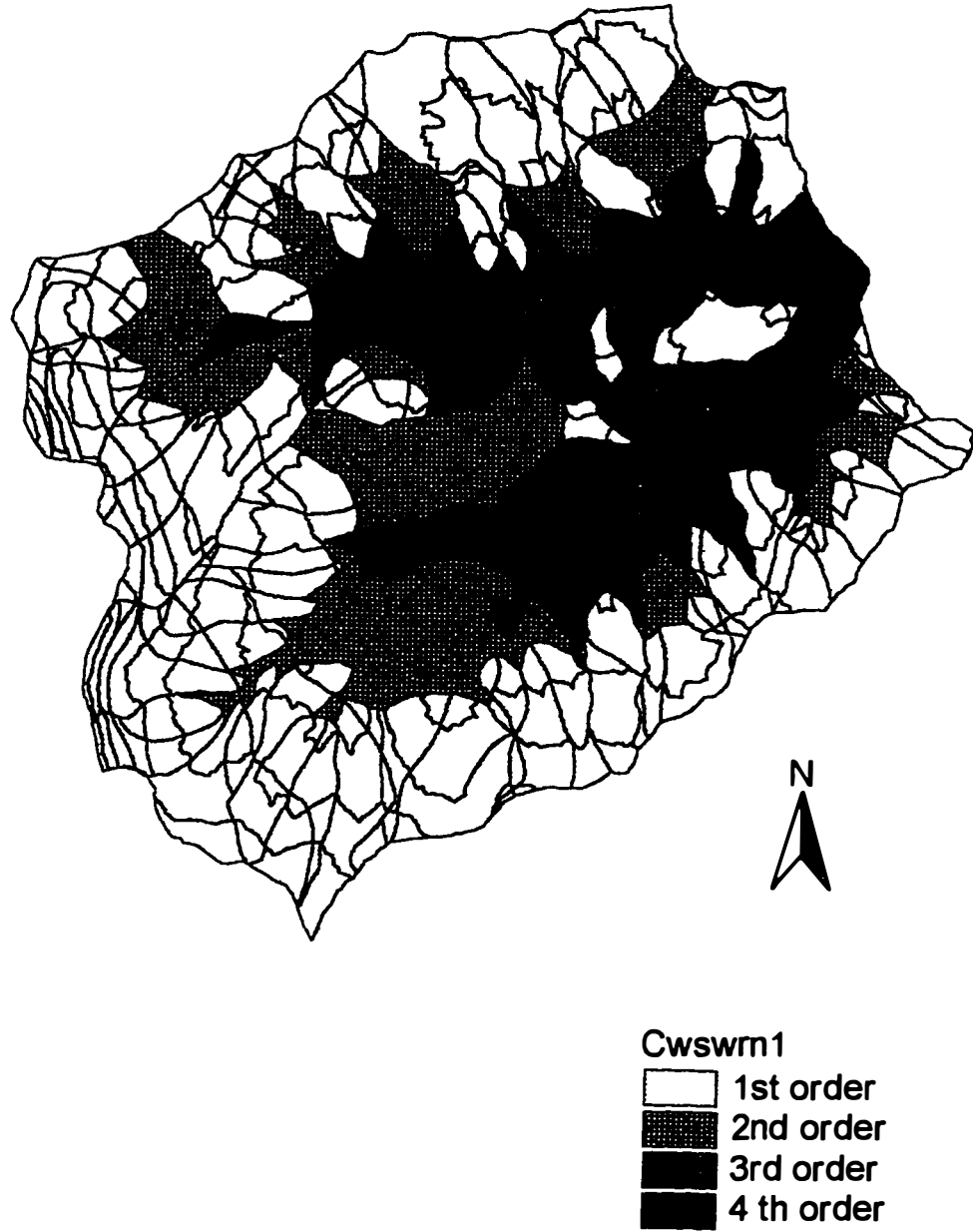


Figure 2.5. Map of the stream order sectors of the Coweeta River basin.

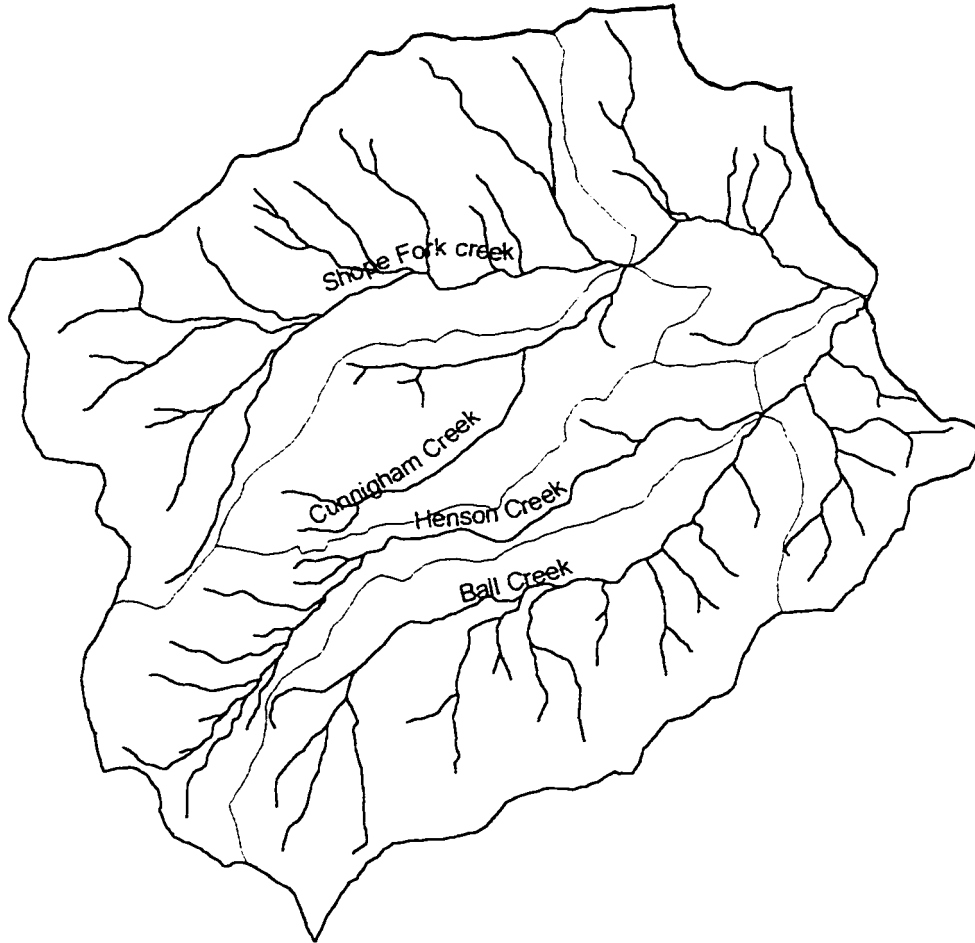


Figure 2.6. Third and fourth order sub-basins of the Coweeta watershed.

For the stream order studies, the draining areas for the stream order segments (1st to 4th order) were defined as sectors. Estimates were still done for the elevational sectors of these drainage areas, but the results were averaged for the whole stream order sectors.

Areas of the different elevational sectors and stream sectors were taken from the database of the ArcInfo coverage. Manipulation of GIS data was done with the spreadsheet Excel.

Annual rainfall.

A map of annual rainfall distribution in the basin (Figure 2.7) was digitized based on a growing season mean isohyetal pattern map for Coweeta (Swank 1986) and the rainfall data for watershed 2 of the Coweeta River basin. The annual rain falling in each elevational sector was calculated, multiplying the depth of rain falling in the area by the area of the sector.

River flows.

The annual river flows for the elevational sectors of the Coweeta basin were estimated by multiplying total (potential) rain in each area by the runoff ratio assumed for that sector. These values were based on the runoff ratio observed in the multiple weirs in the basin (Table 2.2).

Five watersheds from each major sub-basin were selected to correlate their runoff ratio to the mid-basin elevation (Table 2.3.a). Correlation was done using the trendline program in the Excel software. Significant relationships for the two major Coweeta sub-basins were identified using the following exponential equations:

for Shope Fork creek: $y = 0.2021 \exp(0.0003 x)$ $R^2 = 0.975$

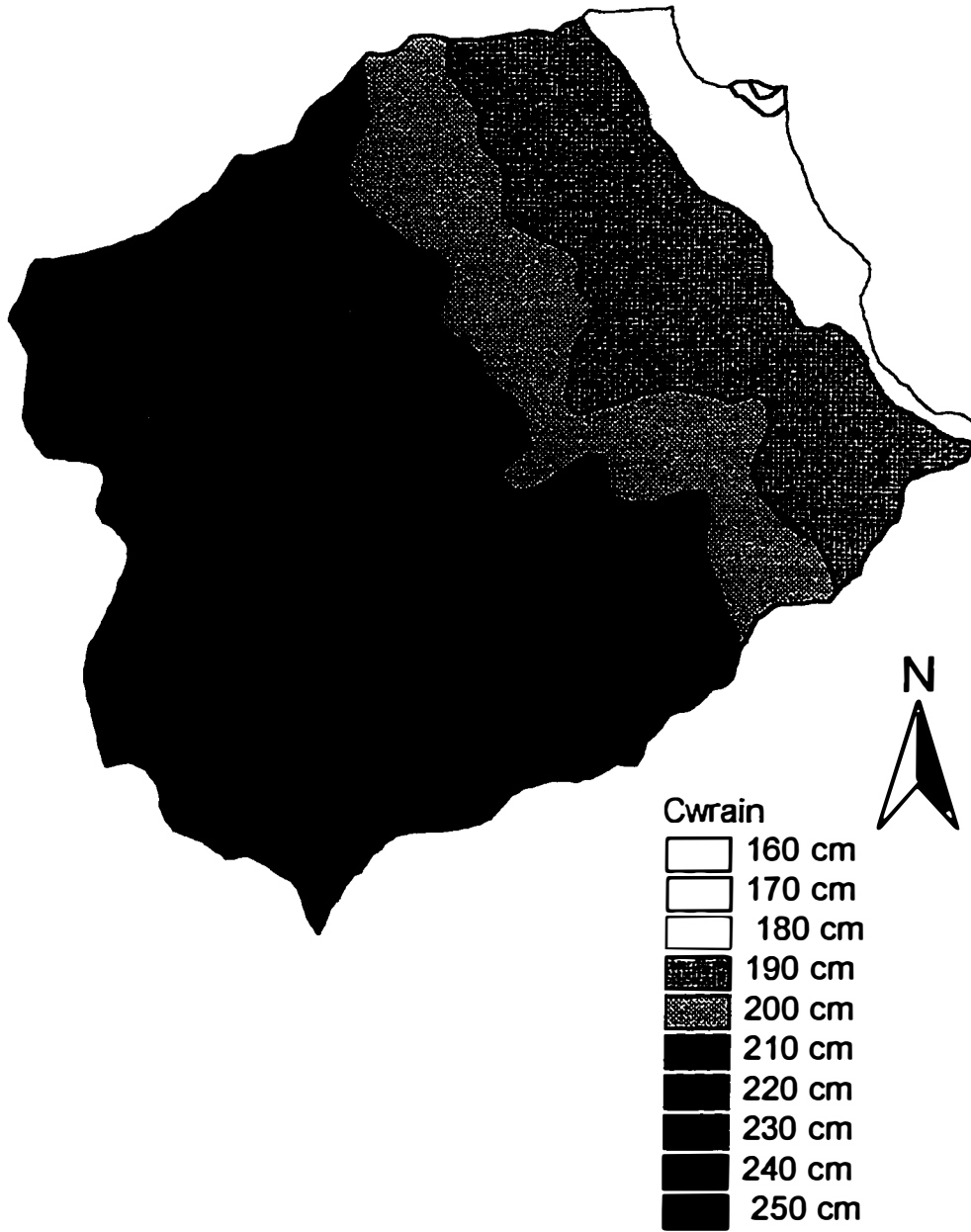


Figure 2.7. Isohyetal map of the Coweeta watershed.

Table 2.2. Discharge data from gauging stations of Coweeta river basin

Gauging Station	Drainage area	Period	Precipitation cm	Runoff cm	Runoff ratio	References
Shope Fork						
sub 36	48.6	39 yr	222	168	0.75	Swift et al.1988
sub 37	43.7	70- 83	244**	201**	0.82	per comm
sub 34	34.7	18 yr	201	117.5	0.58	Swift et al.1988
sub 10	88.08	36-54	195	111*	0.57	per commm
sub 2	12.26	37 yr	177	85	0.48	Swift et al.1988
gauge 11	303.5	36-45	184**	103**	0.56	pers comm
gauge 16	480.3	37-42	180**	105**	0.58	per comm
gauge 8	759.6	35-94	195	117.5	0.60	per comm
Ball Creeck						
sub 27	39.1	70-83	265**	187**	0.71	per comm
sub 28	144.3	70-83	277**	196**	0.71	per comm
sub 18	12.5	45 yr	206	119	0.58	Swift et al.1988
sub 14	61	44 yr	188	98.8	0.53	Swift et al.1988
sub 19	30.7	42-68	210	130*	0.62	per comm
gauge 20	199.3	38-42	232	140*	0.60	pers comm
gauge 9	723.6	35-58	219	115*	0.53	pers comm

*_ original runoff values were corrected to be compatible with the long term average rainfall values used as precipitation. Corrections were done calculating the relationship between average rainfall in the gauged period to the average long term rainfall measured in the area (35- 94 yrs).

** - precipitation and runoff data given for the same period. Therefore, no corrections were needed for runoff ratio estimates.

Table 2.3.a. Gauging stations used in the definition of the relationship between runoff ratio and elevations

Basin	Station	Mid elevation ft	runoff ratio
Shope Fork	sub 36	4175	0.75
	sub 37	4275	0.82
	sub 34	3325	0.59
	sub 10	3025	0.56
	sub 2	2788	0.48
Ball creek	sub 27	4150	0.71
	sub 28	4100	0.71
	sub 14	2785	0.53
	sub 19	3125	0.62
	sub 18	2815	0.54

Table 2.3.b. Estimated and corrected runoff ratios for the elevational sectors of Coweeta subasins

elevation ft	Estimated values		Corrected Values	
	Shope Fork	Ball Creek	Shope Fork	Ball Creek
5000	0.91	0.84	0.91	0.84
4800	0.80	0.78	0.80	0.78
4200	0.71	0.72	0.73	0.72
3800	0.63	0.66	0.66	0.66
3400	0.56	0.61	0.60	0.60
3000	0.50	0.57	0.53	0.54
2600	0.44	0.52	0.47	0.49
2300	0.40	0.49	0.44	0.46

Estimated values were calculated using the fitting equations-
for Shope Fork-

$$y = 0.2021 * (\exp 0.0003 * x)$$

for Ball Creek-

$$y = 0.3106 * (\exp 0.0002 * x)$$

Corrected values were defined after comparing discharges calculated using estimated ratios and observed average discharges in the following points:
for Shope Fork creek-
watershed 2, watershed 10, watershed 36, gauge station 8, gauge station 11.
for Ball Creek:
watershed 28, watershed 14, gauging station 20, gauging station 9.

for Ball Creek: $y = 0.3106 \exp(0.0002 x)$ $R^2 = 0.9407$

where y = runoff ratio,

x = mid sector elevation, ft.

Applying these equations for the mid point of the proposed elevational sectors resulted in runoff ratios of 0.9-0.8 for the higher sectors and about 0.5-0.4 for the lower sectors (Table 2.2a). These values were then validated, comparing the predicted runoff with the average readings for small sub-basins of the Coweeta river basin.

A slight correction in the low sector runoff ratios was then proposed for the best agreement with the readings. The corrected runoff ratios used in the estimates of river flows are included in Table 2.3.b.

Energy, EMERGY and Empower Evaluations by Sector

Geopotential and chemical potential energies of rain and river were estimated for each elevational sector of each sub-basin. Also, the rain and river empower contributions to each sector were evaluated. Estimates were done according to concepts in Figure 2.8, and equations in Table 2.4. Methodology applied in such calculations is described below:

Rain Geopotential Energy Used Up in a Sector (Gru).

Rain geopotential energy used up in a sector was calculated by subtracting the geopotential energy of the annual volume of rain leaving the area (in the form of runoff or river) from the geopotential energy of the annual volume of rain that had fallen in the area.

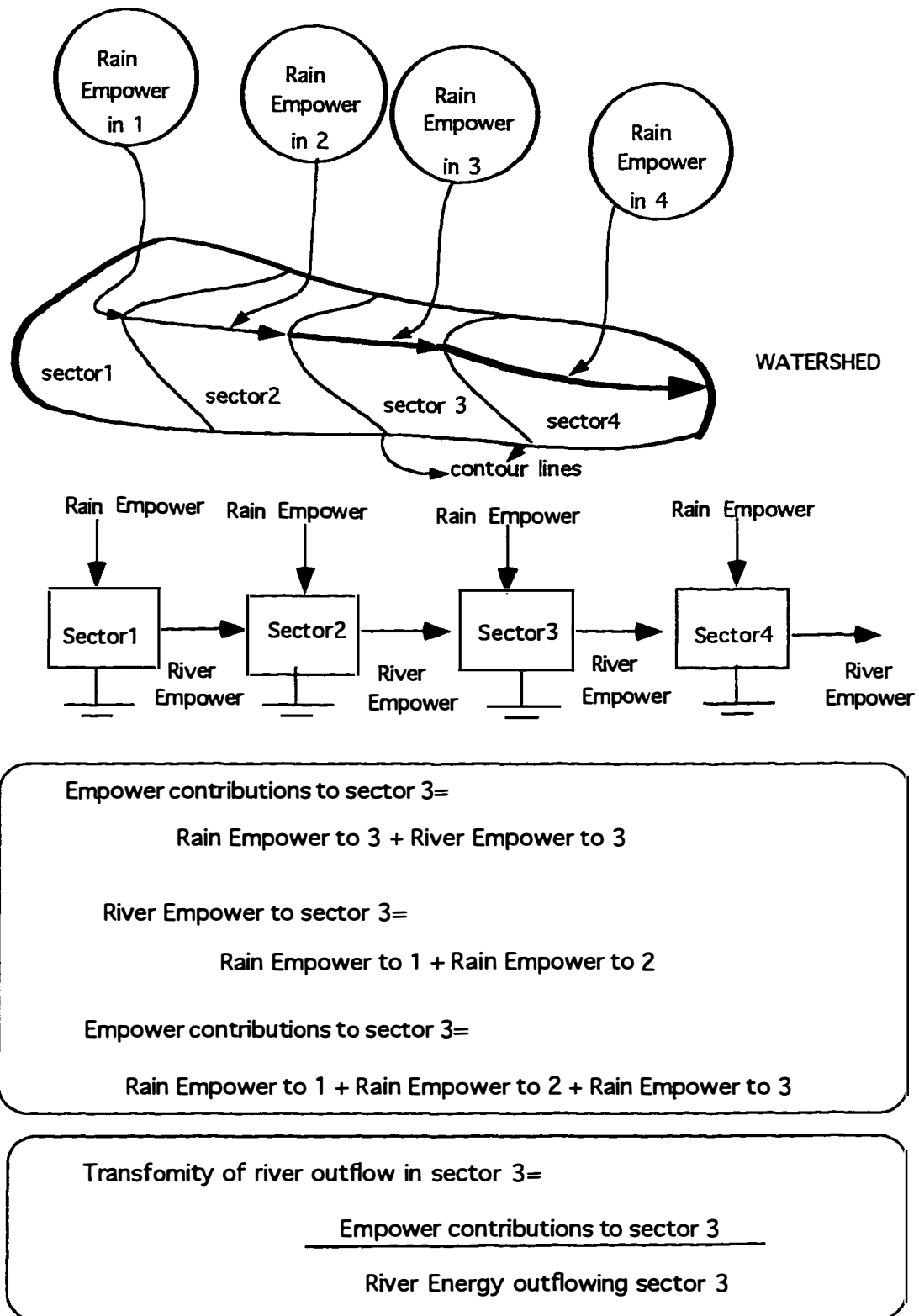


FIGURE 2.8. Diagram of methodology used to estimate Empower contributions and transformativity of river outflow

Table 2.4. Definitions and equations for variables used in energy and Emergy calculations

Variables	Definitions and Equations
Flows and Empower	
Flows(m³/yr)= J	<p>J = volume flow/ time</p> <p>(ex.J_r= rain flow; J_v= river flow; J_s= sediment flow)</p>
Empower (sej/yr)=E	E = Emergy flow= Emergy/ time
Rain Empower (sej/yr) = E_r	<p>E_r= Emergy of rain falling in the area= annual rainfall (m³/yr) * 1E6 g/ m³ * rain Emergy/ grams</p> <p>rain Emergy/ grams= global Emergy/ weight rainfall in land rain Emergy/grams = 89900 sej/ gram of rain</p>
River Empower (sej/yr) = E_v	<p>E_{v4} = available river empower for sector 4 (i.e., the 4th downstream elevational sector in the basin)</p> <p>E_{v4} = E_{r1} + E_{r2}+ E_{r3}</p> <p>E_{r1}= rain empower contributed in sector 1 (sej/yr); E_{r2}= rain empower contributed in sector 2 (sej/yr); E_{r3}= rain empower contributed in sector 3 (sej/yr).</p>
Geological Empower (sej/J)= E_g	<p>E_g = Emergy of earth cycling contributing to an area.</p> <p>E_g = erosion at elevation h* Emergy of earth cycle/gram</p> <p>erosion at elevation h= D * A * ρ</p> <p>D= denudation rates (m/yr) or</p> <p>D= (0.0001535* h- 0.01088) in m/1000m and h in m; A= area (m²) ρ = rock density (2.6E6 g/m³)</p> <p>Emergy of earth cycle = 1.0 E9 sej/g</p>

Table 2.4. Continued.

Total Empower for sector 4 (sej/yr)= Et4	<p>Et4= total available empower contribution to sector 4;</p> <p>Et4= Er4+Ev4</p> <p>Er4= rain empower contribution to sector 4 (sej/yr); Ev4= river empower inflowing in sector 4 (sej/yr).</p>
	Or
	<p>Et4*= total empower contribuion to sector 4 (including geological inputs)</p>
	<p>Et4*= Er4 + Eg4 +Ev4</p>
Empower density (sej/m2/yr)= Ed	<p>Er4= rain empower contribution to sector 4 (sej/yr); Eg4=geological empower contribution to sector 4(sej/yr); Ev4= river empower inflowing in sector 4 (sej/yr);</p>
	<p>Ed= Energy flow/ area</p>
	<p>(ex. Eg = geopotential empower density, Ec= chemical potential empower density)</p>
Geopotential energy	
Geopotential rain energy inflowing in a sector (J/yr) = Gri	<p>Gri = available energy flow (or power) of rain falling in a sector area (J/yr)</p> <p>Gri= Jri * h_m* ρ* g</p> <p>where</p> <p>Jri = annual rain volume flow (m3/yr)</p> <p>h_m= mid point elevation in a sector(m)</p> <p>ρ = water density (1000 kg/m3)</p> <p>g= gravity (9.8 m/ s2)</p>
Geopotential rain energy outflowing from a sector (J/yr)= Gro	<p>Gro= available geopotential energy flow (or power) in runoff outflowing the sector</p> <p>Gro = Jro* hl* ρ* g</p> <p>Jro= annual rain outflowing a sector (m3/yr)</p> <p>hl= lowest elevation in a sector (m)</p> <p>ρ= water density (1000 kg/m3)</p> <p>g= gravity (9.8 kg/s2)</p>

Table 2.4. Continued.

Geopotential rain energy used up (J/yr)= G_{ru}	<p>G_{ru}= available geopotential energy flow (or power) used up in an elevational sector</p> <p>$G_{ru} = G_{ri} - G_{ro}$</p> <p>G_{ri}= geopotential rain energy inflowing in a sector (J/yr) G_{ro}= geopotential rain energy outflowing from a sector (J/yr)</p>
Geopotential river energy used up (J/yr)= G_{vu}	<p>G_{vu} = available geopotential river energy flow (or power) used up in an elevational sector</p> <p>$G_{vu} = J_{ri} * \rho * g * (hh - hl)$</p> <p>$J_{vi}$= annual river volume inflowing in the sector (m³/s) ρ= water density (1000 kg/m³) g= gravity (9.8 m/s) hh= highest elevation in a sector (m) hl= lowest elevation in a sector (m);</p>
Total geopotential energy used up (J/yr) = G_{tu}	<p>G_{tu} = available geopotential rain and river energy flow(or power) used up in an elevational sector</p> <p>$G_{tu} = G_{ru} + G_{vu}$</p> <p>G_{ru} = geopotential rain energy used up (J/yr) G_{vu}= geopotential river energy used up (J/yr)</p>
Total geopotential power density (J/yr/m²)= G_{tud}	<p>G_{tud}= total geopotential energy flow (or power) used per unit area of the sector</p> <p>$G_{tud} = G_{tu} / \text{area}$</p> <p>$G_{tu}$ = total geopotential energy used up (J/yr) area= sector area (m²)</p>

Table 2.4. Continued

Geopotential river energy outflow (J/yr)- Gvo
Gvo= geopotential river energy flow (or power) outflowing from an elevational sector;

$$Gvo = Jvo * hl * \rho * g$$

Jvo= annual river outflow (m3/yr)
 hl= lowest elevation point in a sector (m)
 ρ= water density (1000 kg/m3)
 g= gravity (9.8 m/s2);

Geopotential transformity of river outflow (sej/J)_ Tvg
Tvg = geopotential transformity of the river outflowing an elevatioanal sector or a subasin.

$$Tvg = \frac{Et (sej/yr)}{Gvo (J/yr)}$$

Et = total empower contributing to a sector (sej/yr)
 Gvo= geopotential river energy outflow (J/yr)

Chemical potential energy

Rain used up- Jru
Jru = rain volume flow that falls in a sector and is used (evapotranspired) in the area.

$$Jru = (1 - \% Ro) * Jr$$

% Ro= runoff ratio = Jr/Jv
 Jr= annual rain volume falling in a sector (m3/yr)
 Jvo= annual river volume outflowing from a sector (m3/yr);

Chemical potential rain energy inflowing in a sector (J/yr)- Cri
Cri= available energy flow (or power) in the rain falling in the area.

$$Cri = Jr * \rho * \Delta F$$

Jr= annual rain volume falling in a sector (m3/yr)
 ρ= density (1E+6 g/m3)

ΔF= Gibbs Free energy (~4.94 J/g)

Table 2.4. Continued.

Chemical potential rain energy used up (J/yr)- Cru	<p>Cru= available chemical potential energy flow (or power) used up in a sector;</p> $Cru = Jru * \rho * \Delta F$ <p>Jru= rain volume evapotranspired (m3/yr) ρ= density (1E+6 g/m3) ΔF= Gibbs Free Energy for rain water (~ 4.94 J/g)</p>
Chemical potential river energy used up in evapotranspiration (J/yr) - Cvt	<p>Cvt = available chemical potential energy flow (or power) of river used up in evapotranspiration in a sector.</p> $Cvt = Jvt * \rho * \Delta F$ <p>Jvt= river volume evapotranspired (m3/yr) ρ= density (1E+6 g/m3) ΔF= Gibbs Free Energy for rain water (~ 4.92 J/g)</p>
Chemical potential river energy used up (J/yr)- Cvu	<p>Cvu = available chemical potential energy flow (or power) used up (by dissolved solids) in a sector</p> $Cvu = (Jv4 - Jv3, m3/yr) * \rho * (\Delta F_{rain} - \Delta F_{riv})$ <p>Jv4= river flowing sector4 , m3/yr (or Jv4= Jvo3) Jv3 = river flowing sector 3, m3/yr(or Jv3 = Jvo2) ρ= density (m3/yr) ΔF_{rain} = Gibbs free energy for rain (4.94 J/g) ΔF_{river} = Gibbs free energy for river(~ 150mg/l DS)- 4.92 J/g</p>
Total chemical potential energy (of rain and river) evapotranspired (J/yr)- Cet	<p>Cet = available rain + river chemical potential energy used up in evapotranspiration in an elevational sector.</p> $Cet = Cru + Cvt$ <p>Cru= chemical potential rain energy used up (J/yr) Cvt = chemical potential river energy used up in evapotranspiration (J/yr)</p>

Table 2.4. Continued.

Total chemical potential energy used up (J/yr)- Ctu	<p>Ctu= available rain + river chemical potential energy used up in a elevational sector</p> $Ctu = Cru + Cvu + Cvt$ <p>Cru =chemical potential rain energy used up (J/yr) Cvu = chemical potential river energy used up (J/yr) Cvt= chemical potential river energy used up in evapotranspiration (J/yr)</p>
Chemical potential rain power density (J/m2/yr)- Crud	<p>Crud = rain chemical potential power used up per unit area of the sector</p> $Crut = Cru/ \text{area}$ <p>Cru= rain chemical potential power used up (J/yr) area= sector area (m2)</p>
Chemical potential energy river outflow (J/yr)- Cvo	<p>Cvo- chemical potential river energy flow (or power) outflowing from a sector</p> $Cvo= Jvo * \rho * \Delta F$ <p>Jvo= annual river volume outflowing from a sector (m3/yr) ρ= water density (1E+6 g/m3) ΔF= Gibbs Free energy for river water (4.92 J/g);</p>
Chemical potential transformity of river outflow (sej/J)- Tvc	<p>Tvc = chemical potential transformity of the river outflowing an elevatioanal sector or a subasin.</p> $Tvg = \frac{Et (\text{sej/yr})}{Cvo (J/yr)}$ <p>Et = total empower contributing to a sector (sej/yr) Cvo= chemical potential river energy outflow (J/yr)</p>

The difference was taken as the annual rain geopotential energy used up in the area. The following equations were used to estimate the geopotential rain energy used up in the area:

- Available geopotential power of rainfall in a sector:

$$G_{ri} \text{ (J/ yr)} = \text{rain in sector (m}^3\text{/yr)} * 1000 \text{ kg/m}^3 * 9.8 \text{ m/ s}^2 * \text{mid point elevation (m)}$$

- Available geopotential power in a sector runoff:

$$G_{ro} \text{ (J/ yr)} = \text{rain in sector (m}^3\text{/yr)} * \% \text{ runoff} * 1000 \text{ kg/m}^3 * 9.8 \text{ m/s}^2 * \text{lowest elevation (m)};$$

- Available geopotential power of rain used in a sector:

$$G_{ru} \text{ (J/ yr)} = \text{rain energy in (J/yr)} - \text{rain energy out (J/yr)}$$

River Geopotential Energy Used Up (G_{vu}) and Energy Outflowing (G_{vo}) a Sector.

The geopotential energy of the river outflowing the area (G_{vo}) was calculated for the total runoff flowing out of a sector at the lowest point of the sector, using the following equation:

$$G_{vo} = \text{river geopotential energy outflow (J/yr)} = \text{river flow leaving the sector (m}^3\text{/yr)} * \text{lowest elevation point in the sector} * 1000 \text{ kg/ m}^3 * 9.8 \text{ m/s}^2$$

To estimate the geopotential energy used up by the river (G_{vu}) in a sector, the volume of river water flowing in a sector (n) was assumed to be constant along the sector and equal to the volume discharged by the upper sector (i.e., $J_{vn} = J_{vo \ n - 1}$). The additional volume of water brought by the rain in that sector joined the river at its lowest end of the sector, and the water energy used in the sector had already been computed as

rain energy used up. The volume of river flow in the highest elevational sector in the basin was taken as nil.

The geopotential energy used up by a river (G_{vu}) in a sector was estimated as the difference in the available energy in the river waters flowing from the upper to the lower end of the sector. The equation used to estimate this energy use was:

$$G_{vu} = \text{river energy used (J/yr)} = \text{river volume inflowing the sector (m}^3\text{/yr)} * 1000 \text{ kg/m}^3 * 9.8 \text{ m/s}^2 * (\text{highest point in a sector} - \text{lowest point in a sector, m}).$$

Rain Chemical Potential Energy Available (C_{ri}) and Used in a Sector (C_{ru})

The rain water falling in an area has potential energy of the fresh water relative to the sea of about 4.94 J/g (Odum, 1983). The available chemical potential energy in the rain falling in a sector was calculated by multiplying the annual weight of rain falling in a area to the Gibbs free energy of the rain water, as indicated below:

$$C_{ri} = \text{available chemical potential rain energy (J/yr)} = \text{rain volume in the sector (m}^3\text{/yr)} * \text{water density (1E+6 g/m}^3\text{)} * \text{Gibbs Free energy of rain water (4.94 J/g)}.$$

The chemical potential energy of rain is used in a natural area basically through the evapotranspiration of the plants. Therefore, the volume of rain evapotranspired (J_{ru}) was calculated as total rain falling in the area multiplied by the percent evapotranspired (which is equal to 1 - runoff ratio).

The chemical potential energy of rain used up (C_{ru}) in the sector was then calculated by multiplying the annual weight of rain used up in evapotranspiration to the Gibbs Free energy of rain water (~ 4.94 J/g). The equations used in these estimates were:

J_{ru} = rain used up = rain in the sector (m³/yr) * (1- runoff ratio)

C_{ru} = chemical potential rain energy used up (J/yr) = rain used up (m³/yr)

* 1E + 6 (g/m³) * Gibbs free energy for rain water (4.94 J/yr)

River Chemical Potential Energy Evapotranspired (C_{vt}) and Used Up in a Sector (C_{vu}) and Outflowing a Sector (C_{vo}).

The volume of river evapotranspired (J_{vt}) was estimated as the difference between the volume of water inflowing in sector (as rain (J_{rn}) and as upstream river (J_{vn-1})) and the volume outflowing a sector (as rain evapotranspiration (J_{ru}) and as river outflow(J_{vn})). The chemical potential energy of river evapotranspired then was calculated by multiplying the annual weight of river water evapotranspired to the Gibbs Free energy of the river waters (~4.92 J/g). The following equations applied:

J_{vt} = river water evapotranspired (m³/yr) = ($J_{rn} + J_{vn-1}$) - ($J_{ru} + J_{vn}$)

where

($J_{rn} + J_{vn-1}$) = rain in sector n + inflowing river from sector $n-1$

($J_{ru} + J_{vn}$) = rain evapotranspired in sector n + river outflowing sector n

C_{vt} = river chemical potential energy evapotranspired (J/yr) = annual runoff waters evapotranspired in a sector (m³/yr) * density (1E+6 g/m³) * Gibbs free energy of river waters (~4.92 J/g).

The chemical potential energy of river outflow (C_{vo}) from a sector was calculated for the total river flow leaving a sector with a concentration of dissolved solids around

150 mg/l (Gibbs Free energy~ 4.92 J/g). Calculation was done according to following equation:

$C_{vo} = \text{river chemical potential energy outflow (J/yr)} = \text{river flow leaving the sector (m}^3/\text{yr)} * 1E6 \text{ g/m}^3 * \text{Gibbs Free energy for river water (4.92 J/g)}$.

Calculations of chemical potential energy used up by river (C_{vu}) waters started with evaluation of additional volume of river water that was flowing into a sector ($J_v n$) compared to the volume running in the upstream sector ($J_v n-1$). This additional volume was assumed to contain dissolved solids, between the average concentrations in rain (5 mg/l, Gibbs Free Energy - 4.94 J/g) and average concentrations in river (150 mg/l, Gibbs Free Energy - 4.92 J/g). As explained before, the volume of water flowing into a sector as river was taken as the volume of river water leaving the upstream sector, $J_v n = J_{vo} n - 1$. The following equation was used to estimate the river chemical potential energy used up:

$C_{vu} = \text{river chemical potential energy used up (J/yr)} = \text{additional volume of river water in a sector compared to upstream sector} = (J_v n - J_v n - 1)(\text{m}^3/\text{yr}) * 1E6 \text{ g/m}^3 * (\text{Gibbs free energy for rain, 4.94 J/g} - \text{Gibbs Free energy for river, 4.92 J/g})$.

Rain Empower Contributing to a Sector (E_r)

In order to estimate the rain empower (E_r) contributing to a sector area, the Empower per gram of rain was evaluated. According to Odum (1996), the global annual Empower contribution to Earth is $9.44 E24 \text{ sej/yr}$ and volume of rain falling over land

surface is 105,000 km³/ yr. This volume represents 1.05 E 20 g rain/yr. Therefore,

Empower per gram of rain was estimated as:

$$\text{Rain Empower/gram} = (9.44 \text{ E } 24 \text{ sej}) / (1.05 \text{ E } 20 \text{ g}) = 89,900 \text{ sej/g}$$

The empower of the rain (E_r) contributing to a sector was calculated by multiplying the weight of rain falling in the area in grams to the rain Empower per gram.

The equation used in the calculation was:

$$E_r = \text{Rain Empower (sej/yr)} = \text{rain volume in the sector (m}^3\text{/yr)} * 1 \text{ E}6 \text{ g/m}^3 * 89,900 \text{ sej/g}$$

River Empower (E_v) and Total Empower (E_t)

Waters as they flow downstream accumulate the EMERGY of all the input sectors. Therefore, the empower of a river (E_v) flowing into a sector was calculated as the sum of the rain empower (E_r) of all upstream sectors of a basin, as indicated in Figure 2.8. It was understood that a river flowing in an elevational sector was a product of the rain falling and working in all previous upstream sectors. Therefore, the river empower (E_v) contribution to any sector was calculated as:

- $E_{v2} = \text{river empower}_2 \text{ (sej/yr)} = \text{rain empower}_1 \text{ (sej/yr)}$;
- $E_{v3} = \text{river empower}_3 \text{ (sej/yr)} = \text{rain empower}_1 \text{ (sej/yr)} + \text{rain empower}_2 \text{ (sej/yr)}$;
- $E_{v4} = \text{river empower}_4 \text{ (sej/yr)} = \text{rain empower}_1 \text{ (sej/yr)} + \text{rain empower}_2 \text{ (sej/yr)} + \text{rain empower}_3 \text{ (sej/ yr)}$.

The total empower (Et) contribution to a sector was the sum of the estimated rain and river inflow empower, as indicated in the equations:

$$\begin{aligned} - Et_4 &= \text{total empower}_4 \text{ (sej/J) } = Er_4 + Ev_4 \\ &= \text{rain empower}_4 \text{ (sej/J) } + \text{river empower}_4 \text{ (sej/J);} \end{aligned}$$

But substituting the value for river empower₄, it would be:

$$- Et_4 = \text{total empower}_4 \text{ (sej/J) } = Er_1 + Er_2 + Er_3 + Er_4 = \text{rain empower}_4 \text{ (sej/J) } + \text{rain empower}_1 \text{ (sej/J) } + \text{rain empower}_2 \text{ (sej/J) } + \text{rain empower}_3 \text{ (sej/J)}.$$

Geopotential (Tvg) and Chemical Potential (Tvc) River Transformities

Transformities of the river outflowing an elevational sector was calculated as the ratio between the total EMERGY (Et) contribution to a sector and the energy of river outflow (Gvo or Cvo). Therefore, equations used for transformities estimates would be:

$$Tvg = \text{river geopotential transformity (sej/J) } = \frac{\text{total Empower contribution to a sector (Et)}}{\text{Geopotential energy of river outflow (Gvo)}}$$

$$Tvc = \text{river chemical potential transformity (sej/J) } = \frac{\text{Total Empower contribution to a sector (Et)}}{\text{Chemical potential energy of river outflow (Cvo)}}$$

Evaluations by Stream Order

Each stream order sector was treated as a sub-basin. Therefore, the energies used up and outflowing and the EMERGY contributions were estimated for each elevational sector of a stream order sub-basin, according to procedures previously described.

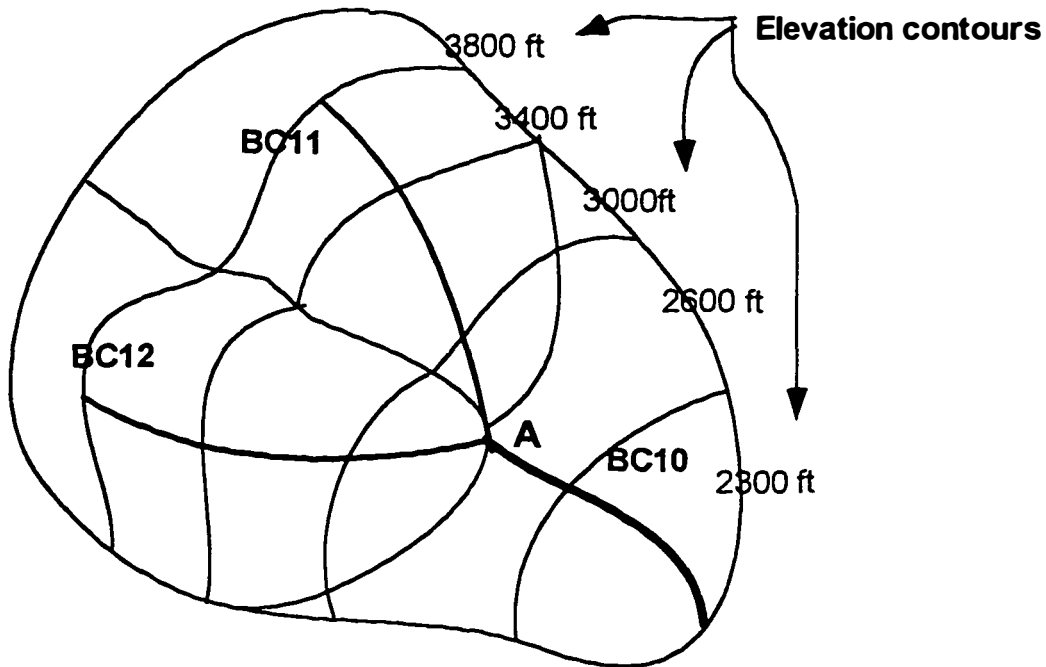
However, to evaluate the energy used up in the whole stream order sector, the values calculated for each elevational sector were added. The energy outflowing from a stream order sector was taken as the energy outflowing from the lowest elevational sector.

The total Empower contribution to a stream order sector was also taken as the empower contribution to the lowest elevational sector. Therefore, transformities for river outflowing a stream order sector were estimated as the ratio between the total Empower contribution to the stream segment and the river energy outflowing the lowest elevational sector.

Densities (energy flow per area or EMERGY flow per area) were estimated similarly. Energy flow densities in a stream order sector were evaluated dividing total energy used (i.e. the sum of energy used in all elevational sectors of a stream order sector) by the area of the stream order sector. The EMERGY density for the stream order sector would take the total EMERGY contribution to the area (which is equal to total EMERGY contribution to the lowest elevational sector of the stream order sub-basin) and divided it by the area of the stream order sector.

Empower Contributions to Higher-order Stream Sectors

Rivers outflowing a sector would carry downstream all the previous empower that contributed to its formation. Therefore, river sectors of higher order received empower contribution of rain falling in that sector, plus the empower of the lower order rivers flowing in the area (Figure 2.9). In this way, 3rd order stream sectors received river empower from 2nd order and 1st order streams flowing to the stream order sector, plus



FIRST AND SECOND ORDER STREAM SECTORS

Empower contribution for 2nd order sector BC10=
rain Empower falling in BC10 + river Empower entering in A

River Empower entering in A = rain Empower falling in BC11+
rain Empower falling in BC12

Figure 2.9. Diagram representing methodology used in the computation of total Empower contribution to the higher stream order sectors .

the empower of rain falling in the 3rd order stream sector. Ultimately, the empower contribution to the 3rd order stream was the empower of the rain falling over the whole area draining to the 3rd order stream basin.

Earth EMERGY Flow and Elevation

EMERGY contributions of the geological inputs were then calculated based on the erosion rates at different mountain elevations. The EMERGY input was calculated as the amount of geological uplift from below needed to keep up with the amount of denudation taking place on the mountain surface.

Erosion rates for different elevations were estimated using an empirical equation developed by Ahnert when studying American and Western European basins (Chorley et al., 1984):

$$D = 0.0001535 H - 0.01088$$

where D = mean denudation rates (m/1000 m) and H = mean relief (m).

Then the weight of eroded rock for the elevational sector was estimated using rock density of 2.6 ton/ m³. The denudation rate was multiplied by area of the elevational sector and by rock density to estimate weight of eroded rock, as follows:

$$\text{Rock eroded/elevational sector (g/yr)} = D * A * r$$

D = denudation rates (m/yr)

A = area of the sector (m³)

r = rock density (2.6 E6 g/m³).

The EMERGY contribution of the geological inputs for an elevational sector was then calculated, multiplying rock eroded per sector (equal to weight of rock uplift from below) by the global average EMERGY/gram of earth cycle (which is 1 E9 sej/g). The following equation was applied:

$$E_g = \text{geological EMERGY} = (\text{rock erosion/elevational sector}) * (\text{EMERGY/g of earth cycle}) * (1\text{E9 sej/ g}).$$

The total Empower contribution to a river leaving an elevational sector would include the Empower contribution from rain plus the Empower contribution from geology. Therefore, downstream sectors of the river would accumulate the rain and geological empower contributions of all upstream river sectors.

Spatial Distribution of Energy Use and Empower

To evaluate the spatial pattern of energy use and empower contribution in the Coweeta sub-basins, three methodological approaches were used to define the sub-basin units:

- First, second, third and fourth stream order sectors were used as sub-basins ("stream order" approach);
- Third order segments were used as sub-basins ;
- Fourth order segments were used as sub-basins.

Results were displayed in form of maps.

Energetic Ratios

Energy and EMERGY Indices to Evaluate the Mountain System Performance

In order to evaluate the use of geopotential and chemical potential energy by the watersheds, energetic indices and ratios were proposed. The performance of a basin was evaluated using the following indices and ratios:

- Total available rain geopotential energy;
- Total available rain chemical potential energy;
- Total geopotential used in the basin;
- Geopotential energy in the river outflowing;
- Total rain and river chemical potential evapotranspired in the basin;
- Chemical potential energy in the river outflowing;
- Geopotential energy in the river outflowing per cubic meter of river flow;
- Ratio of geopotential energy outflowing to geopotential energy available in the basin;
- Ratio of geopotential energy outflowing to total geopotential energy used in the basin;
- Ratio of total chemical potential energy evapotranspired to total geopotential used in the basin;
- Ratio of total chemical potential energy evapotranspired to total geopotential available to the basin;
- Ratio of total chemical potential energy evapotranspired to total chemical potential available to the basin;

- Ratio of total chemical potential energy evapotranspired to total chemical potential available to the basin;
- Ratio of river chemical potential energy outflowing the basin to total chemical potential available to the basin;
- Ratio of river chemical potential energy outflowing the basin to the river geopotential outflowing the basin;
- Average and maximum value estimated for the elevational sectors of total geopotential energy used per square meter of the basin;
- Average and maximum value estimated for the elevational sectors of the rain chemical potential energy evapotranspired per square meter of the basin.
- Total available geopotential per area of the basin;
- Total available chemical potential per area of the basin;
- Total river chemical potential outflowing the basin per square meter of the basin.

EMERGY indices used in the watersheds performance included:

- Total rain empower contributing to the basin;
- Rain empower density ;
 - Geopotential and chemical potential transformities of river outflow.

EMERGY and Energy Indices for Mountain-valley Relationship Evaluation.

EMERGY and energy indices and ratios were proposed to evaluate mountain and valley relationships in different watersheds. These indices especially related the empower

and geopotential work of the mountain zone to the rain and river evapotranspired in the valley. Indices estimated in this study were:

- Mountain area (m²) and valley area (m²);
- Mountain EMERGY stored (sej);
- Annual contribution of rain Empower to the mountain (sej/yr);
- Total (rain + river) annual geopotential energy used in the mountain zone (J/yr);
- Annual rain and chemical potential energy evapotranspired in the valley (J/yr)("valley transpiration");
- Ratio of geopotential energy use in the mountains to valley transpiration;
- Ratio of EMERGY stored in the mountains to valley area (sej/m²);
- Ratio of EMERGY stored in the mountains to annual evapotranspiration (sej/J/yr) in the valley;
- Ratio of annual mountain Empower to annual valley transpiration (sej/J).

These indices were applied to larger basins with floodplain areas such as Jacupiranga, Eta, Itariri and Upper Little Tennessee River basins. The limits of valley areas were roughly defined as the flat lowland zone in the basins.

CHAPTER THREE

RESULTS

Shape of Watersheds

Two typical shapes of river profile were identified among the evaluated watersheds - “bowl- shaped basins” and plateau basins. Bowl-shaped basins had concave river profiles, with extensive lowlands with floodplains. The areas of elevational sectors of a bowl- shaped basin increased exponentially towards the lower sectors. Such pattern was observed in the aerial distribution of Eta and Jacupiranga River basins, as shown in Figure 3.1.

Plateau basins were the ones with a convex river profile, with extensive highlands and narrow basin tip close to the river mouth. In this type of basin, the highest land concentration was found in the highest elevational sectors of the basin. The Pardo River basin represents a typical plateau basin, and its aerial distribution is shown in Chart C of Figure 3.1.

The shapes of the watersheds have geomorphologic as well as energetic meaning, important in the evaluation of the energy and EMERGY distributions in the river basins.

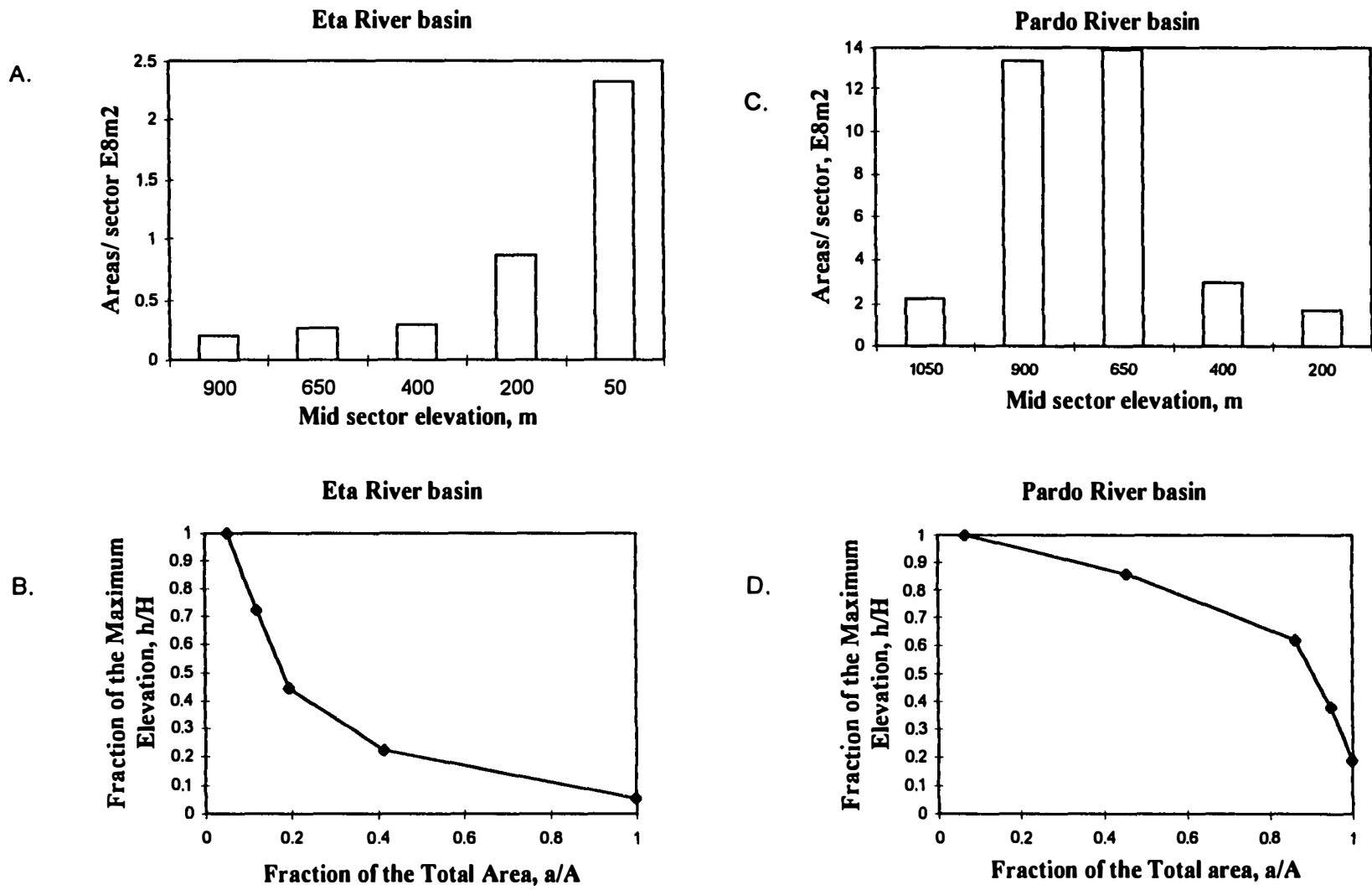


Figure 3.1. Graphs showing in: A and B. land concentration in the lower sectors of the basin and the concave hypsometric curve for the Bowl-shaped Eta River basin; C and D. land concentration in the upper sectors of the basin and the convex hypsometric curve for the plateau Pardo River basin.

Geopotential Energies along the River Profiles

Available Geopotential Energies

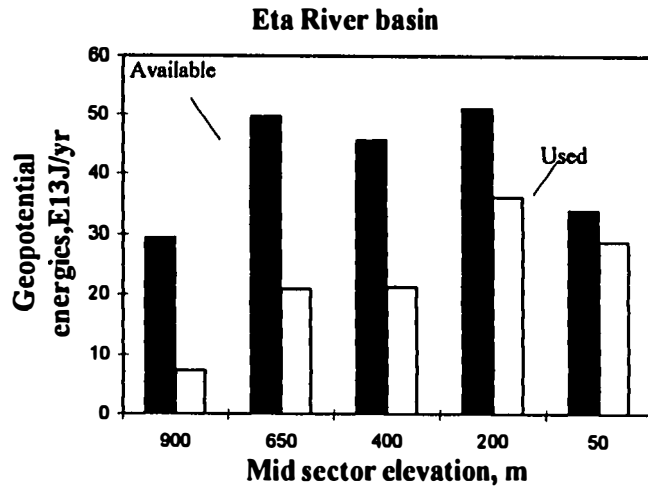
Water geopotential energy is provided to the river basins in the form of rain and partially transferred downstream through the river waters. Available geopotential energy increases with elevation and with the amount of rain falling in the basin.

The distribution of the available geopotential energy along river profiles is parabolic with peaks around 650- 700m elevation, as displayed in Chart C of Figures A.1. to A.8. However, for bowl- shaped Jacupiranga and Eta River basins, the distribution pattern of the available geopotential energy was quite flat throughout the 650m to 200m elevational sectors. Typical distribution patterns for the available geopotential energy are shown in Figure 3.2.

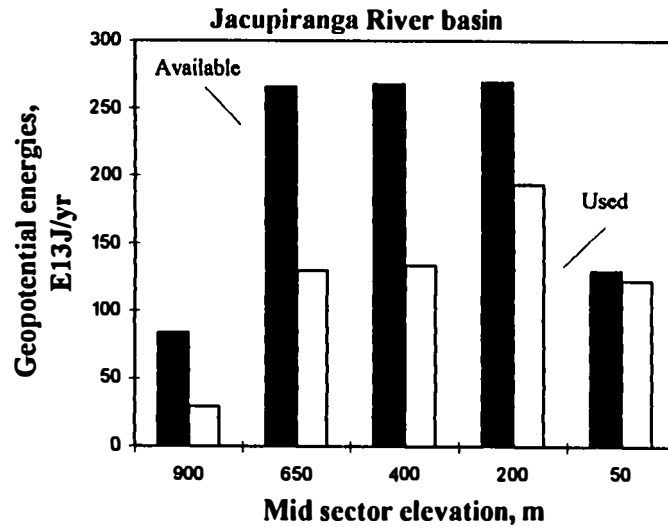
Water geopotential energy was provided for the bowl-shaped river basins in similar proportions of rain or river energy, as shown in Figure 3.3. The same pattern was verified in the Coweeta River basin (Chart D in Figure 3.3) and in the Upper Little Tennessee River basin. For the plateau basins, however, rain provided the geopotential energy for the highlands whereas river waters supplied energy to the narrow lower sectors of the basins (Chart C in Figure 3.3).

The total available water geopotential energy to the watersheds ranged from less than $10E13$ J/yr for the Coweeta sub-basins, to about $30 E13$ J/yr for the whole Coweeta basin, and from 100 - 4000 $E13$ J/yr for the large evaluated watersheds (Column 4 in Tables B.1 and B.4). On aerial basis, however, the available geopotential were more

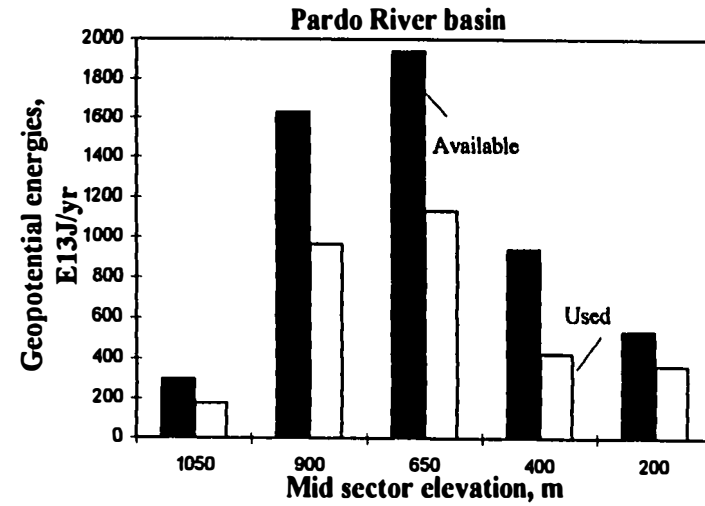
A.



B.



C.



D.

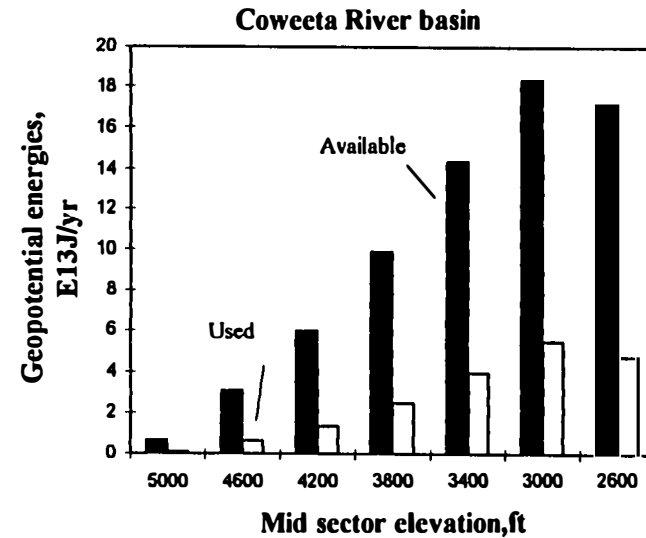


Figure 3.2. The parabolic distribution of available geopotential energy along river profiles, peaking around 650-700m, but being more flattened for the bowl-shaped Eta and Jacupiranga River basins (A and B).

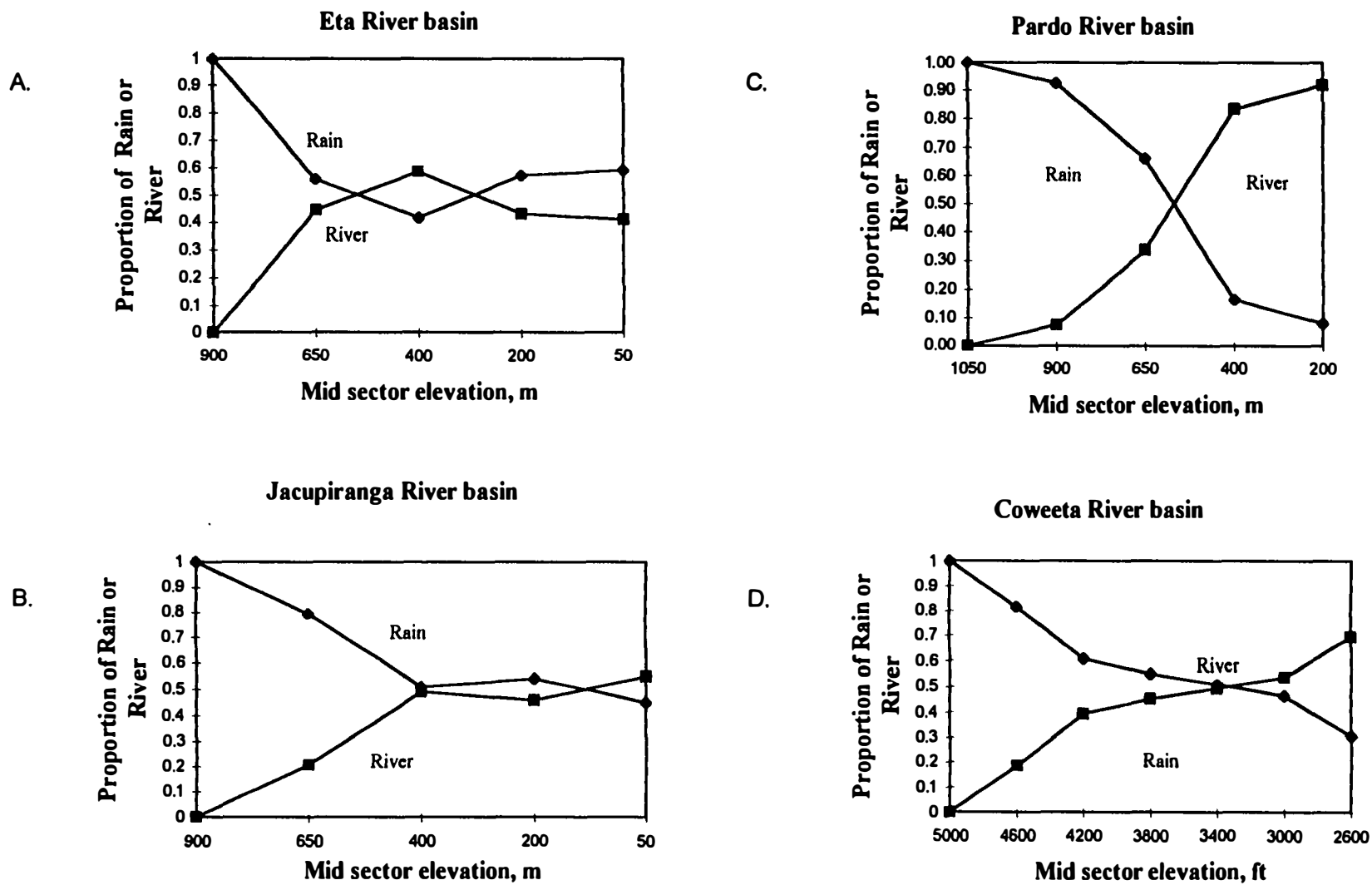


Figure 3.3. Proportion of water geopotential energy provided by rain or river for : A. and B. The bowl-shaped Eta and Jacupiranga River basin; C. The plateau Pardo River basin; D. The elevated Coweeta River basin.

intense in the Coweeta basin and sub-basins, being around 20 to 25 E6 J/m²/yr (Column 6 in Table B.5). It was less than 4E6 J/m²/yr for the bowl- shaped river basins and between 7 and 14 E6/m²/yr for the other large evaluated watersheds (Column 6 in Table B.2).

Used Geopotential Energies

Water geopotential energies used or outflowing the elevational sectors of studied river basins are shown in Chart G of Figures A.1 to A.8 and Chart A of Figures A.9 to A.14. For most basins, the use of rain geopotential energy followed closely the land distribution pattern, with the exception of the bowl-shaped Jacupiranga and Eta River basins. There, the use of rain geopotential was evenly distributed along the basin profile despite the land being more concentrated in the low sectors of the basin. Figure 3.4 displays the longitudinal distribution of land and the used rain geopotential energy for typical basins.

The geopotential energy used by the rivers increased almost linearly along the longitudinal profile, due to the gradual convergence of rain waters to the river. The use of geopotential energy of river waters was usually greater than the use of the rain geopotential energy in the lower sectors of the Brazilian watersheds, as indicated in Chart I of Figures A.1 to A.8. About 80% in the plateau basins and 50% in the bowl- shaped basins, of the water geopotential energy used in their low elevational sectors was derived from river waters. Proportions of rain or river energy use for typical river basins are shown in Figure 3.5.

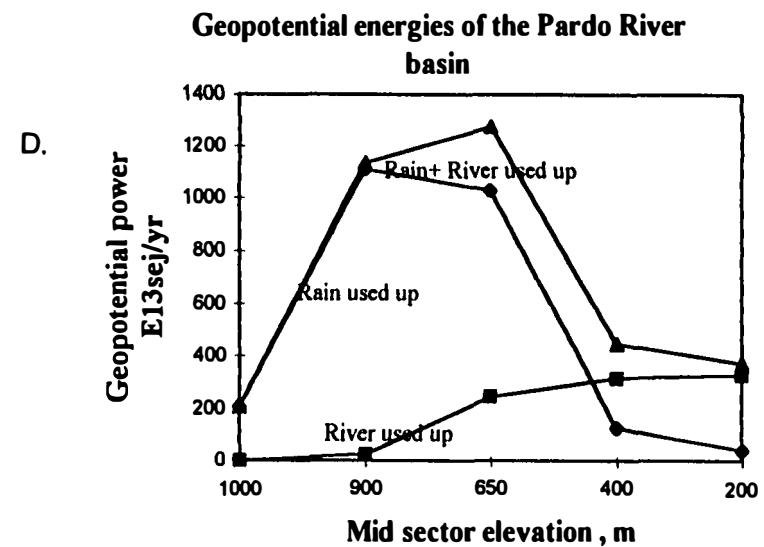
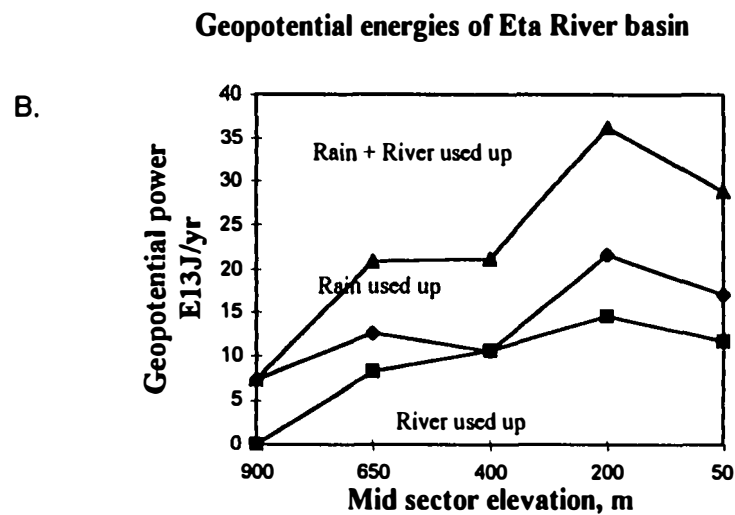
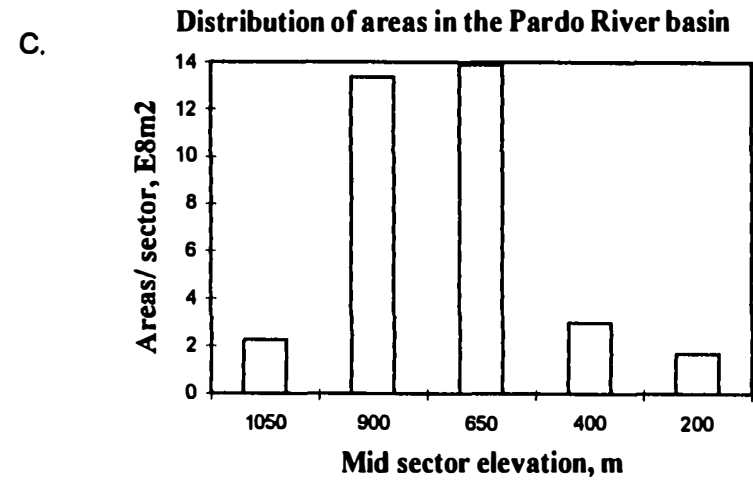
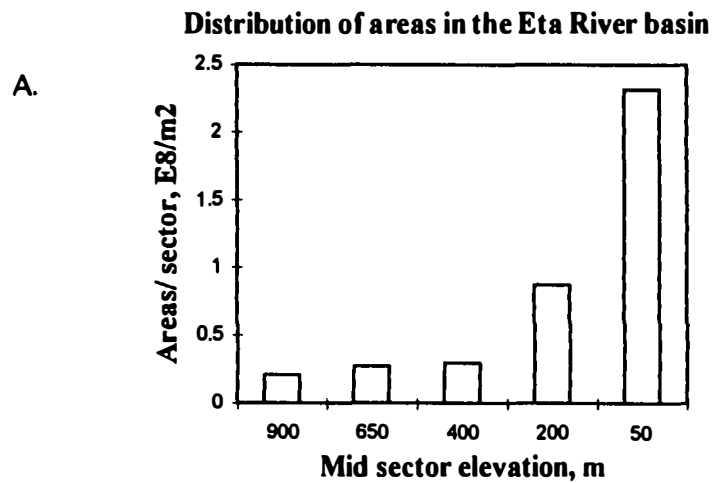


Figure 3.4. Geopotential rain energy used up following close the land distribution for most river basins (as shown for the plateau Pardo River basin in C and D), except for the bowl- shaped basin (as shown for Eta River basin in A and B).

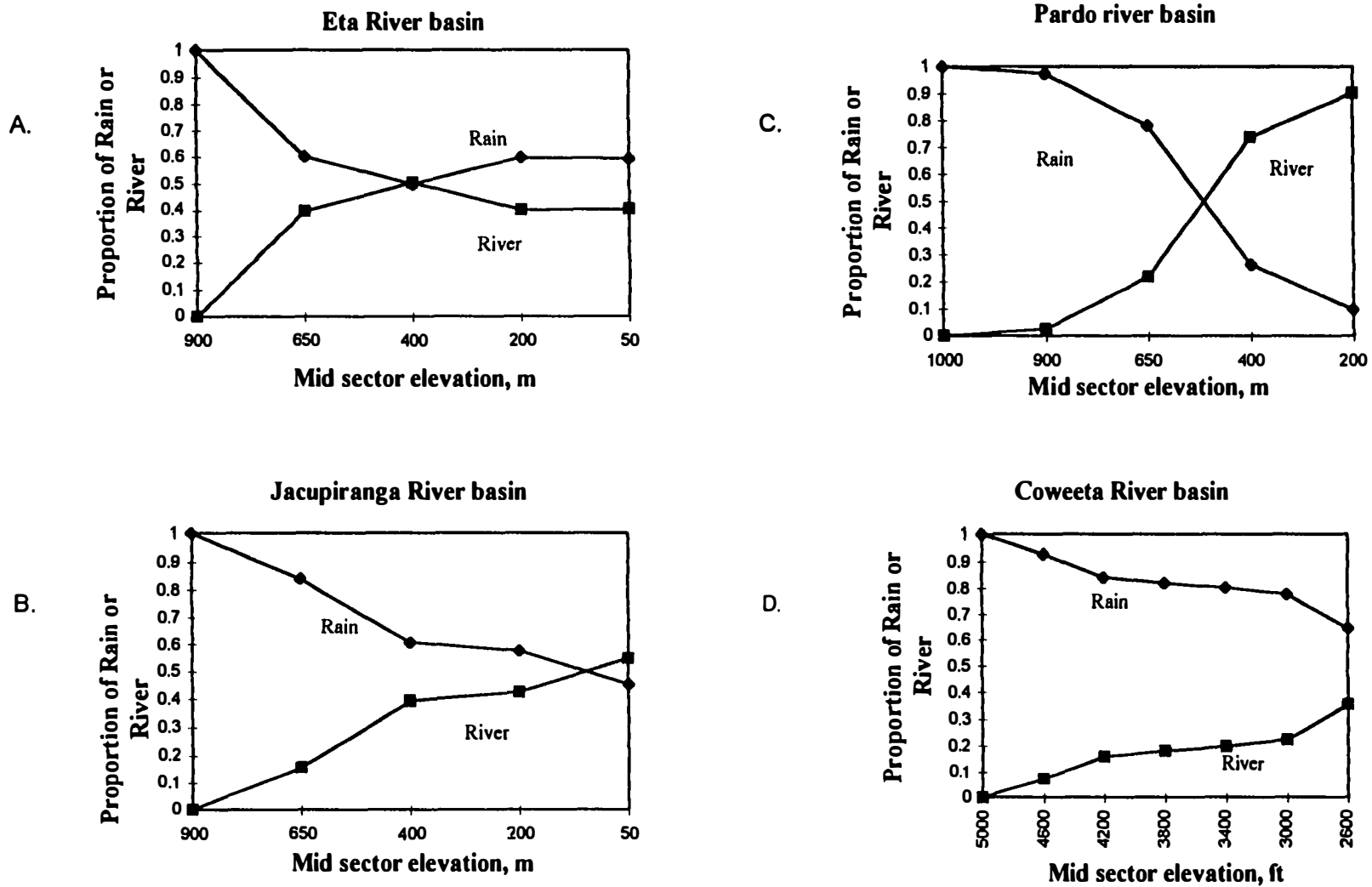


Figure 3.5. Proportion of Used geopotential energy from the rain or river in : A. and B. The bowl- shaped Eta and Jacupiranga River basin; C. The plateau Pardo River basin; D. The elevated Coweeta river basin.

The total water geopotential energy used in the watersheds was less than $7.0E13$ J/yr for the Coweeta sub-basins, around $20E13$ J/yr for the Coweeta basin, and between 100 to $4000E13$ J/yr for the large evaluated river basins (Column 6 in Tables B.1 and B.4). The geopotential energy use per area was more intense in the Coweeta basins and sub-basins, the average values being 11 to $14 E6$ J/m²/yr (Column 2 in Table B.5). In the large river basins, average geopotential energy uses were less than $9.0E6$ J/m²/yr, and less than $4.0 E6$ J/m²/yr for the bowl- shaped river basins (Column 2 in Table B.2).

Most river basins displayed a typical pattern of their geopotential energy use per area along the river profile. Intensity of the use was about constant or slightly crescent in the upper elevational sectors of the basins, and sharply increasing in the elevational sectors below 650m or 3000 ft (Chart K of Figures A.3 to A.8 and Charts C in Figures A.9 to A.14. In the bowl- shaped river basins, however, the geopotential energy use intensified in the upper sectors of the basin reaching a plateau in the elevational sectors between 650 to 400 m , and decreasing in the lower elevational sectors (Charts K of Figures A.1 and A.2). Graphs of the geopotential energy use per area for typical basins are presented in Figure 3.6.

Outflowing Geopotential Energies

Estimates of the geopotential energies of rivers outflowing the elevational sectors are displayed in Charts G of Figures A.1 to A.8 and Charts A of Figures A.9 to A.14. The longitudinal pattern of the geopotential energy outflowing the elevational sectors was of

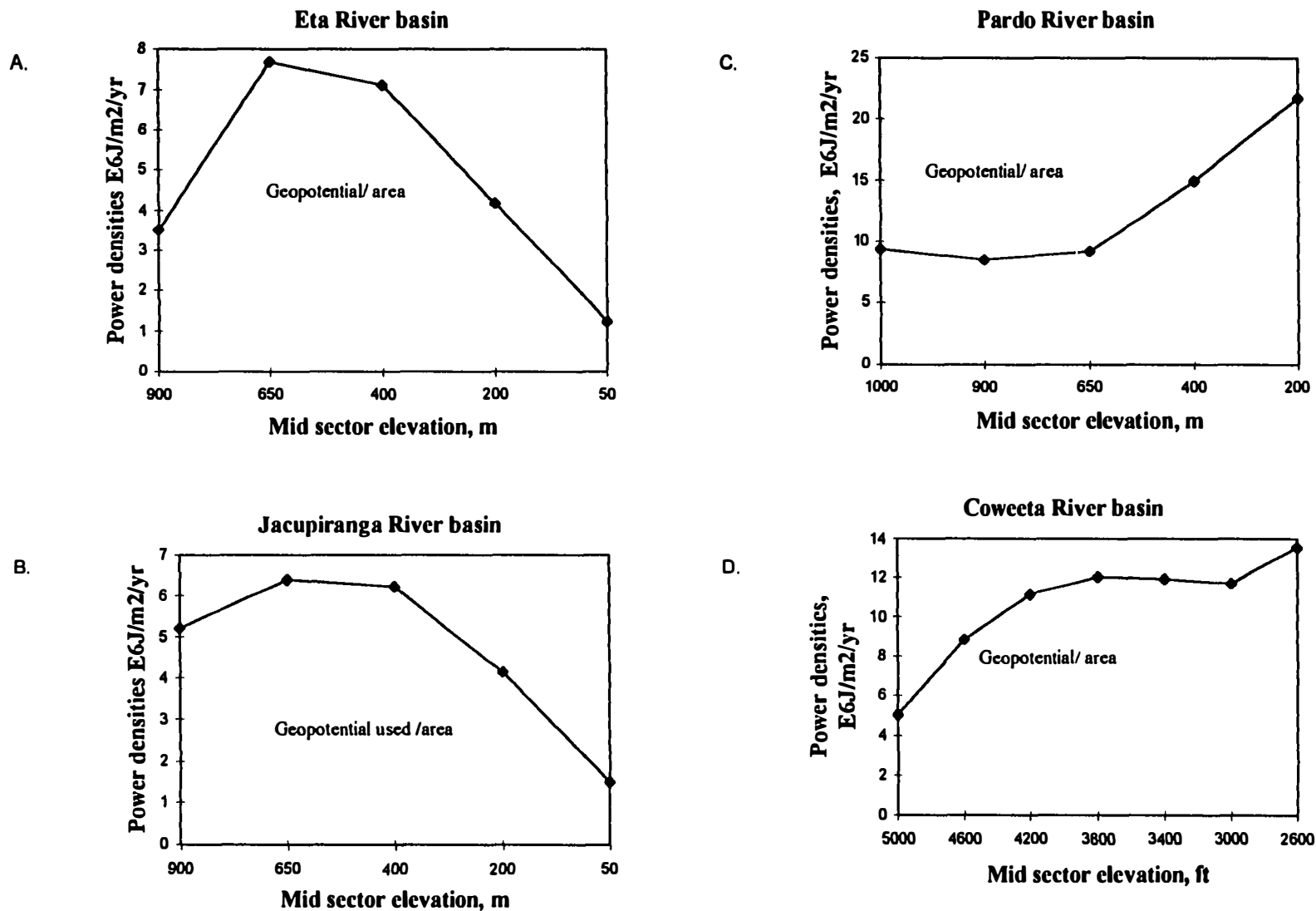


Figure 3.6. Graphs of geopotential energy use per area showing in: A. and B. A hump- shaped distribution in the bowl-shaped Eta and Jacupiranga river basins; C. and D. An exponential- shaped or mixed-shaped distribution in the plateau Pardo and the elevated Coweeta River basins, respectively.

parabolic shape, peaking usually in elevational sectors around 650m or 3000 ft , as verified in typical basins represented in Figure 3.7.

In the large Brazilian basins, the outflowing rivers had relatively little geopotential energy left. At their river mouth located below 50 m elevation, discharging waters of the Eta, Jacupiranga and Juquia Rivers had less than 5% of the available geopotential energy to provide to their watershed (Column 3 in Table B.3).

On the other hand, in the Coweeta River basin and sub-basins, that receive high annual precipitation and discharge around 700m elevation, the geopotential energy of outflowing rivers carried about 30 to 35% of total energy provided to the area (Column 3 in Table B.6). When comparing the absolute values , the geopotential energy of the river outflowing the Coweeta watershed (10.8 E13J/yr) with area of 15.8 Km² was larger than the geopotential energy outflowing the Jacupiranga River basin (7.0 E13 J/yr)with 1757 km².

Chemical Potential Energies along the River Profiles

Available Chemical Potential Energies

Rain to an area provides water chemical energy, which is partly used in plant transpiration and partly transported downstream. Therefore, the amount of chemical potential energy in an elevational sector water is basically dependent on the volume of rain and river inflowing in the area.

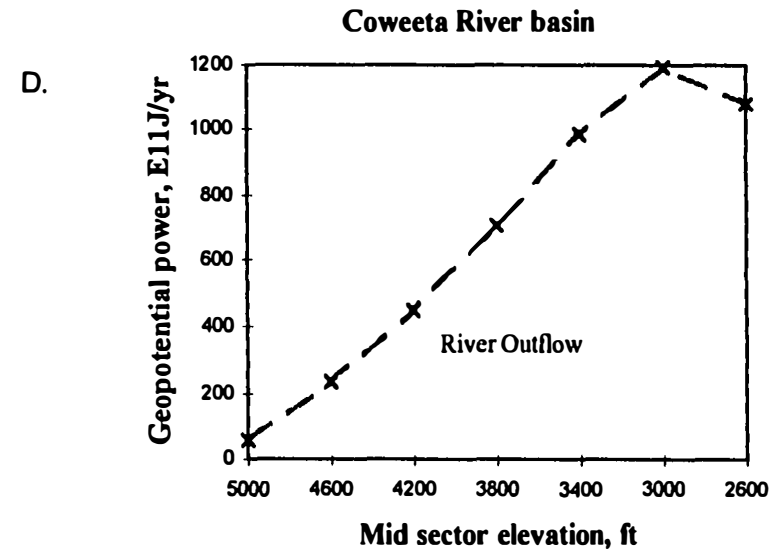
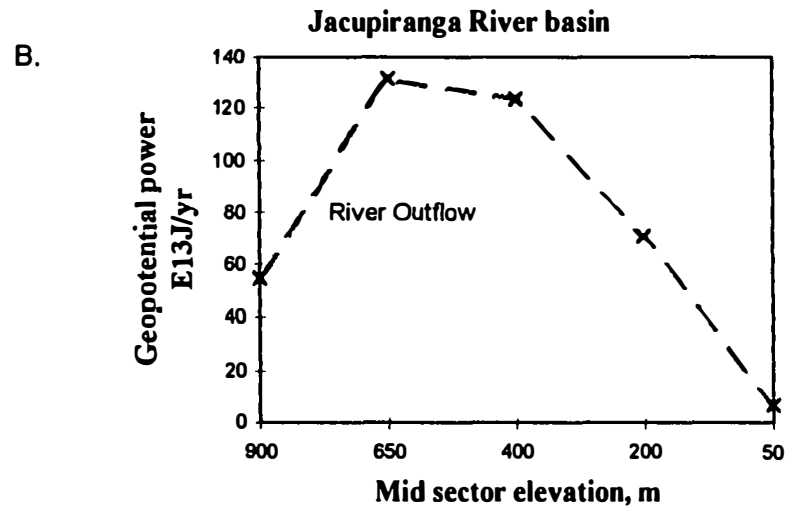
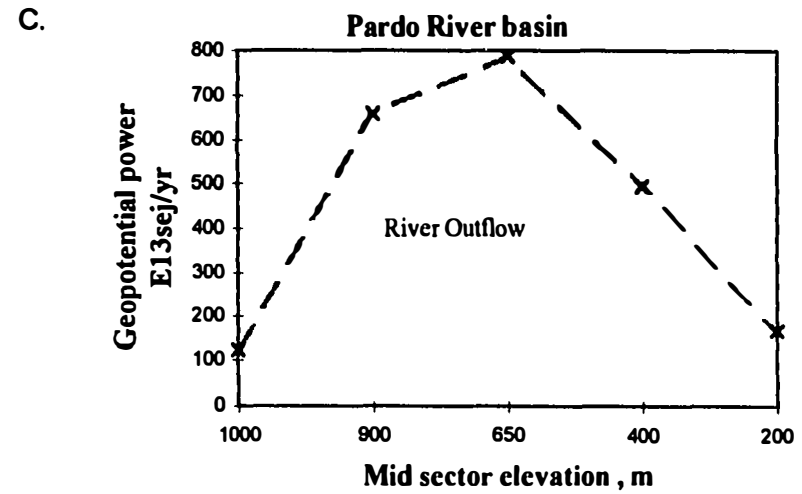
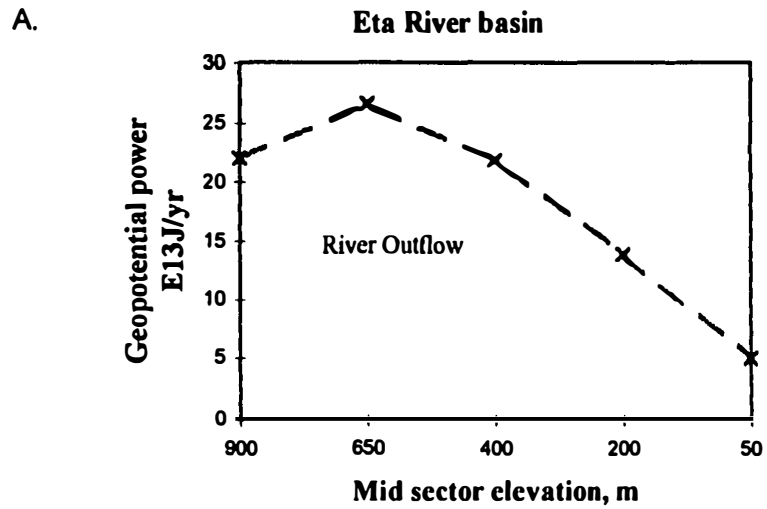


Figure 3.7. The parabolic shape of the geopotential energy outflowing the elevational sectors of: A and B. The Bowl-shaped Eta and Jacupiranga River basins; C. The plateau Pardo River basin; D. The elevated Coweeta river basin.

Most of the evaluated watersheds showed the availability of water chemical potential energies increasing downstream (Charts E of Figures A.1 to A.8). This is because of the larger areas receiving rain in the lower sectors of the basins, and increasing the volume of river waters downstream. The longitudinal profile of the available water chemical potential energy for some typical river basins are shown in Figure 3.8.

The relative contribution of chemical potential energy of rain and river, along the river profiles is shown in Chart F of Figures A.1 to A.8. The pattern is quite similar to that observed for geopotential energy, as can be seen comparing results of Figure 3.9 to those in Figure 3.3. Rain provided relatively more chemical potential energy than geopotential energy.

The total chemical potential energy available to the evaluated watersheds ranged from less than $5.0 \text{ E}13\text{J/yr}$ for the Coweeta sub-basins, to $17 \text{ E}13\text{J/yr}$ for the whole Coweeta basin, and from $100 \text{ E}13 \text{ J/yr}$ to $4600 \text{ E}13\text{J/yr}$ for the large river basins (Column 5 in Tables B.1 and B.4). On an area basis, the available chemical potential was higher in the basins with more precipitation. Concentrations of available chemical potential were around $10 \text{ E}6\text{J/m}^2\text{/yr}$ for the Coweeta basin and sub-basins (Column 7 in Table B.5) about $8 \text{ E}6 \text{ J/m}^2\text{/yr}$ for the more rainy large watersheds (such as Eta, Juquia and Jacupiranga Rivers) and about $6.5 \text{ E}6\text{J/m}^2\text{/yr}$ for the large watersheds located in more drier zones, such as Pardo, Catas Altas and Betari River basins (Column 7 in Table B.2).

Used Chemical Potential Energies

The longitudinal pattern of use of water chemical potential energy is displayed in Chart H of Figures A.1 to A.8 and Chart B in Figures A.9 to A.14. These graphs

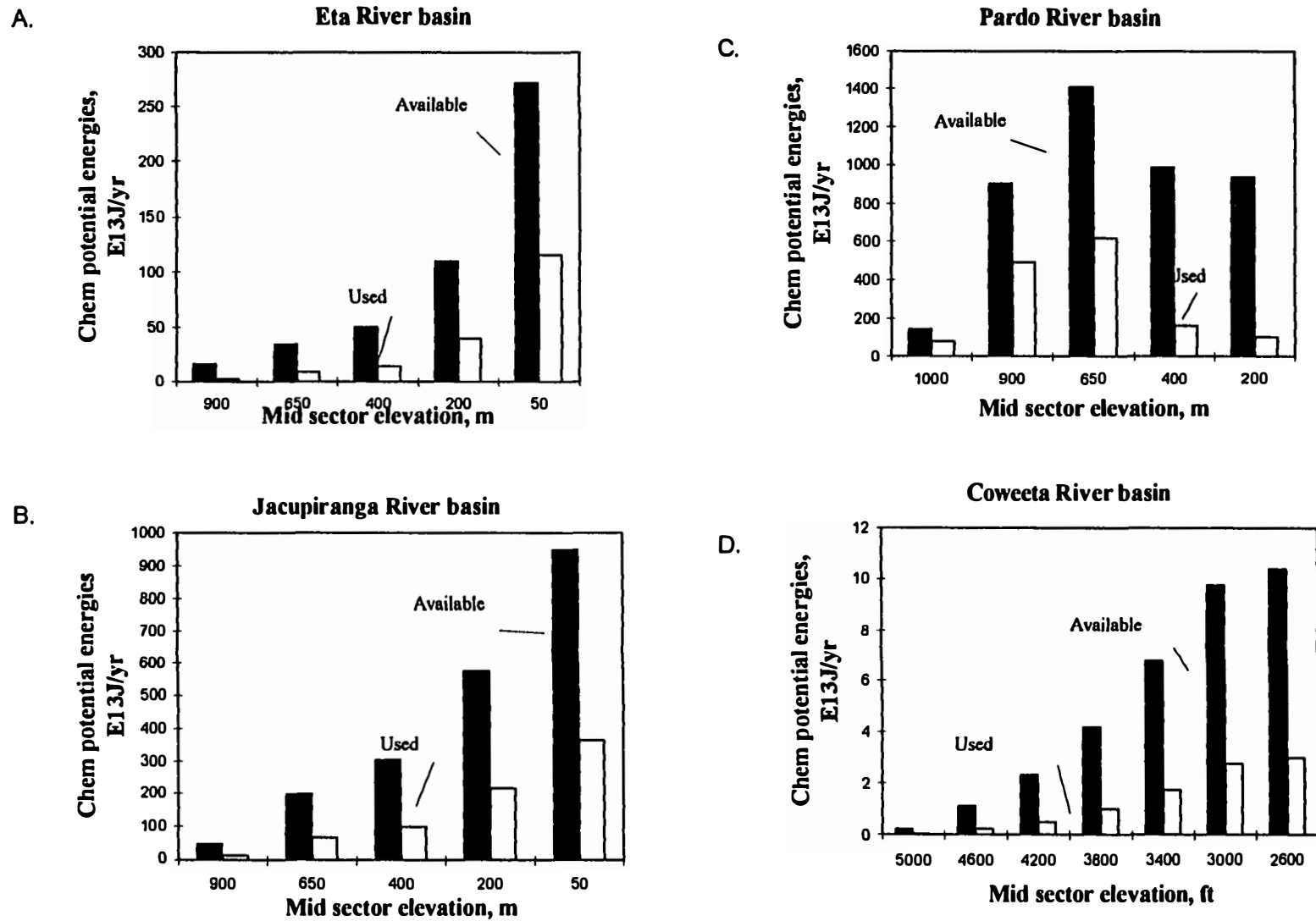


Figure 3.8. The increase of the available water chemical potential energies along river profiles of : A. and B. The bowl-shaped Eta and Jacupiranga River basins; C. The plateau Pardo river basin; D. The elevated Coweeta River basin.

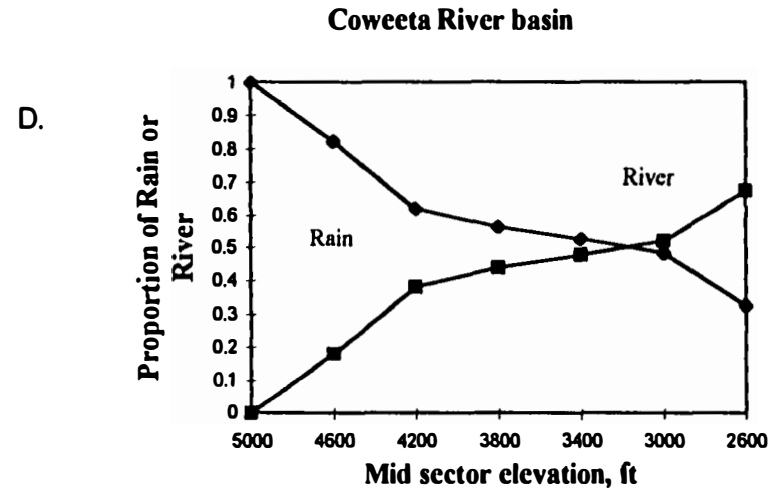
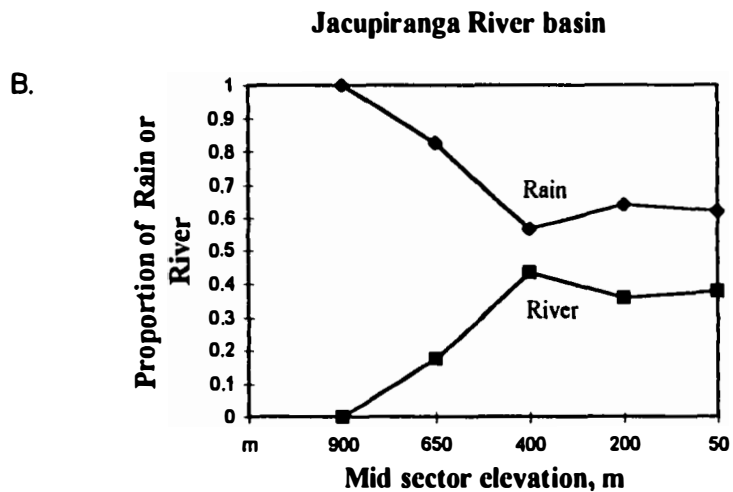
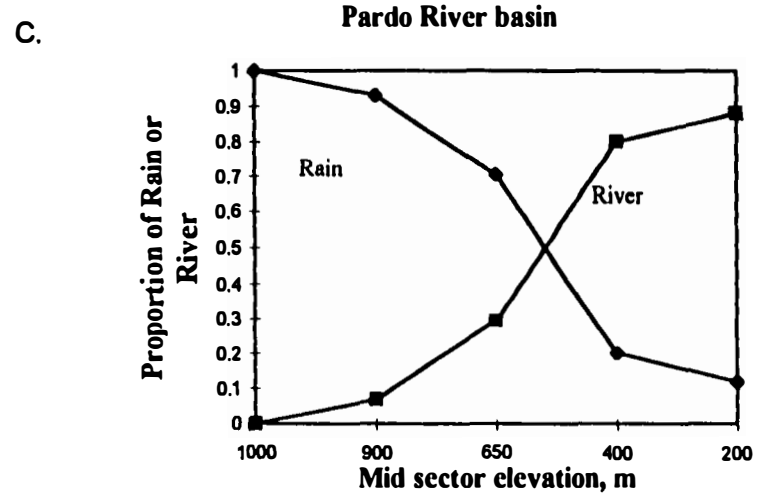
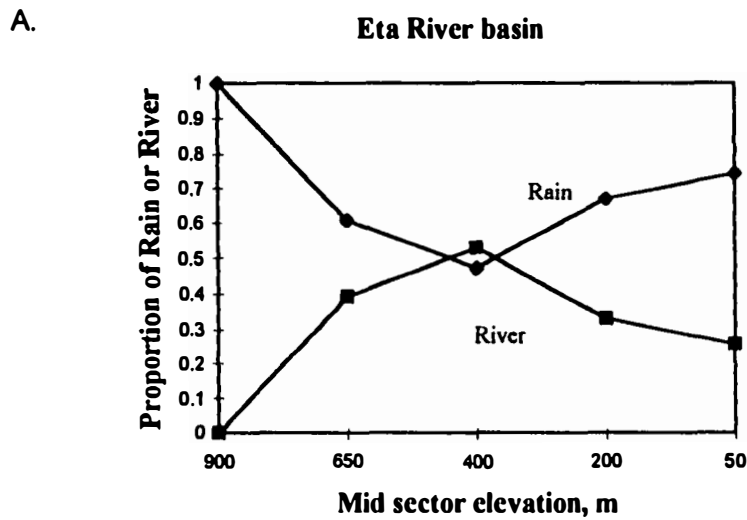


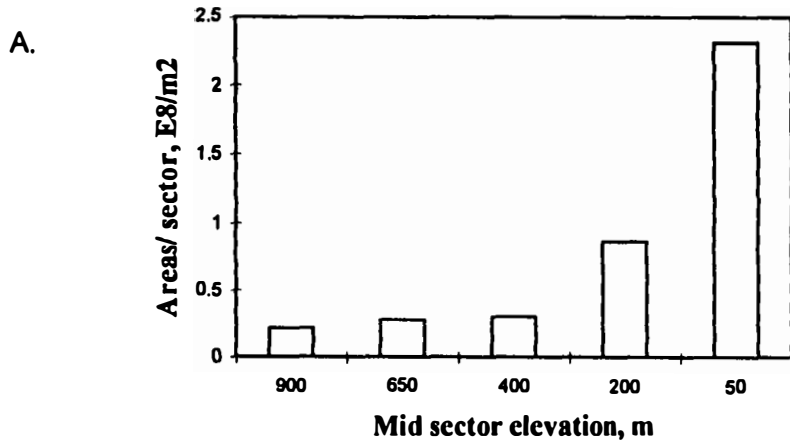
Figure 3.9. Proportion of water chemical potential energy provided by rain or river for: A. and B. The bowl-shaped Eta and Jacupiranga River basins; C. The plateau Pardo River basin; D. The elevated Coweeta River basin.

followed very close to the land distribution pattern of the basins, as verified for typical basins displayed in Figure 3.10. Water chemical potential energy was largely used by evapotranspiration of the rain. Evapotranspiration of the river waters represented minor use of the available water chemical energy, amounting 10 to 30% of the total water energy use in some sectors, as indicated in Chart J of Figures A.1 to A.8. Proportion of rain or river chemical energy used in some typical watersheds are presented in Figure 3.11.

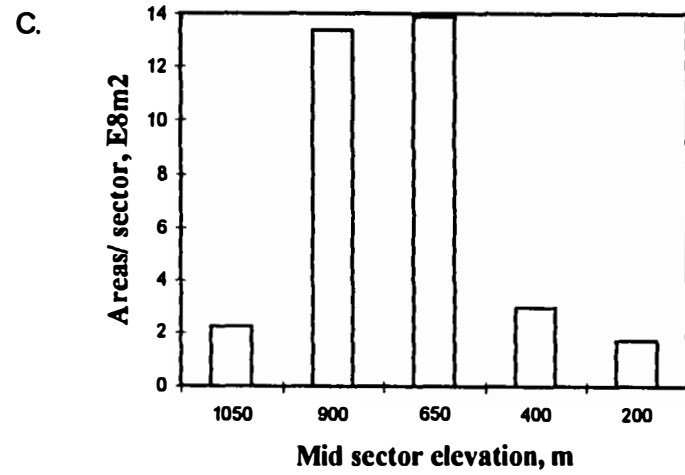
The total chemical potential energy used up in evapotranspiration in the watersheds was less than $3.0 \text{ E}13\text{J/yr}$ for the Coweeta sub-basins, about $9.0 \text{ E}13\text{J/yr}$ for the Coweeta River basin, and ranging from $50 \text{ E}13\text{J/yr}$ to $2400 \text{ E}13\text{J/yr}$ for the large river basins (Column 8 in Tables B.1 and B.4). Use was more concentrated in the Coweeta River basin and sub-basins (about $5.7 \text{ E}6\text{J/m}^2\text{/yr}$), indicating high evapotranspiration and suggesting high biological production (Column 4 in Table B.5). The average evapotranspiration rates of bowl-shaped river basins with floodplain around $4.3 - 4.6 \text{ E}6\text{J/m}^2\text{/yr}$ were slightly higher than those of the plateau basins of $3.7 - 4.2 \text{ E}6\text{J/m}^2\text{/yr}$ (Column 4 in Table B.2).

With decreasing elevation, a linear to asymptotic increase in the water transpired per area was observed in all evaluated watersheds, as shown in Chart K of Figures A.1 to A.8 and Chart C in Figures A.9 to A.14. This is expected because there are higher saturation deficit and less clouds in the valleys (Jones, 1992). The chemical potential energy use per area for some typical watersheds are displayed in Figure 3.12.

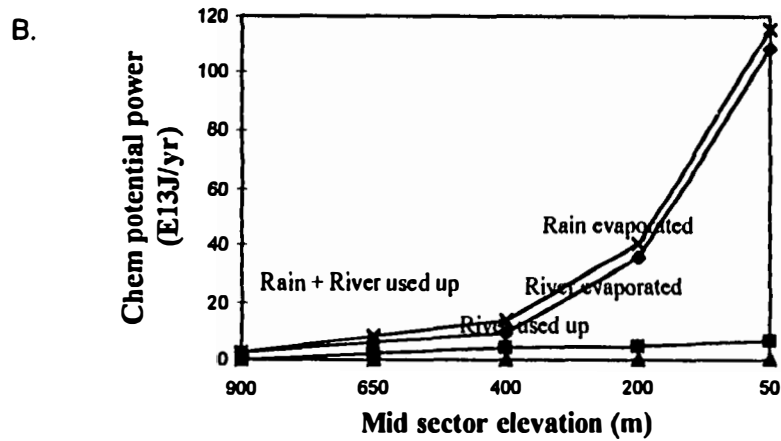
Distribution of areas in the Eta River basin



Distribution of areas in the Pardo River basin



Chemical potential energies of Eta river basin



Chemical potential energies for the Pardo River basin

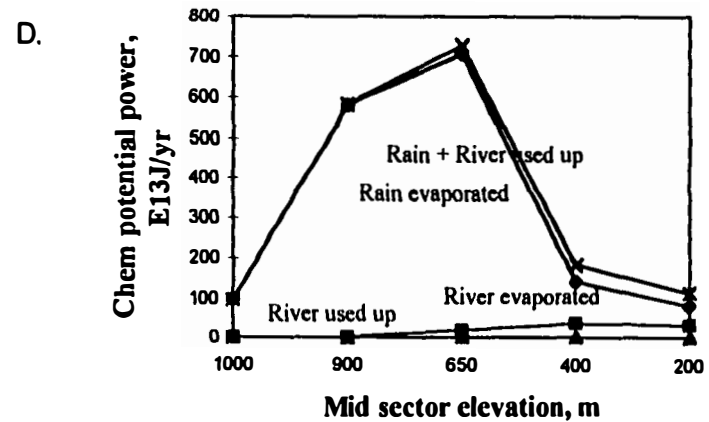


Figure 3.10. The rain chemical potential energy used up according to the land distribution pattern in A and B. The bowl shaped Eta river basin; C and D.. The plateau Pardo river basin

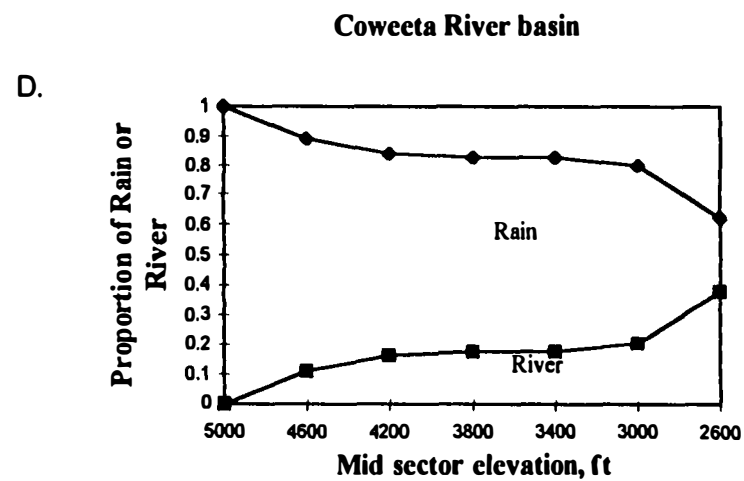
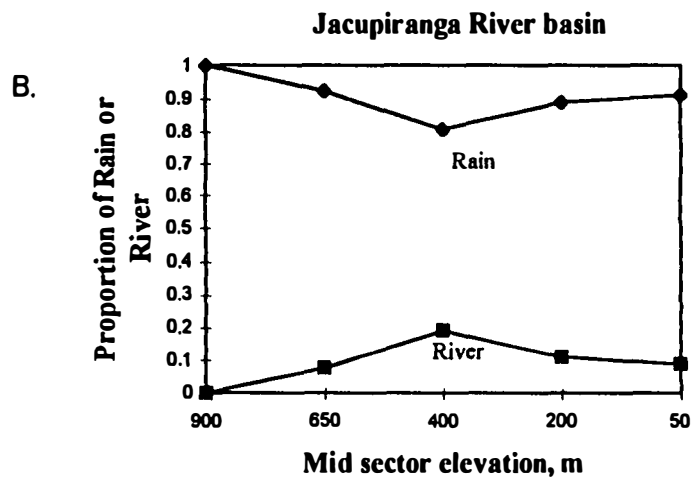
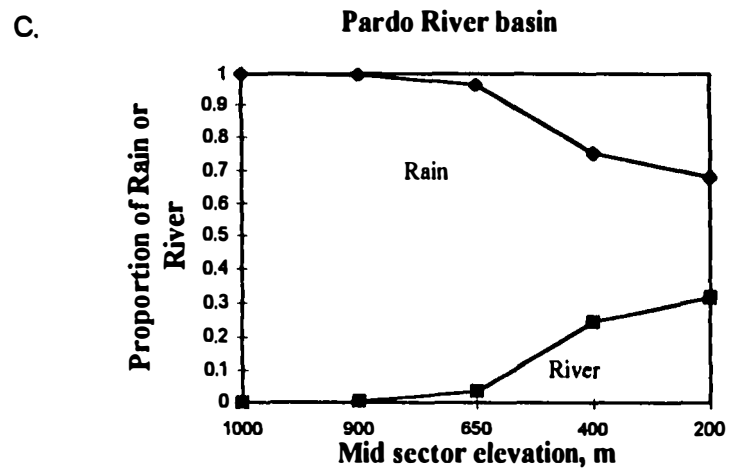
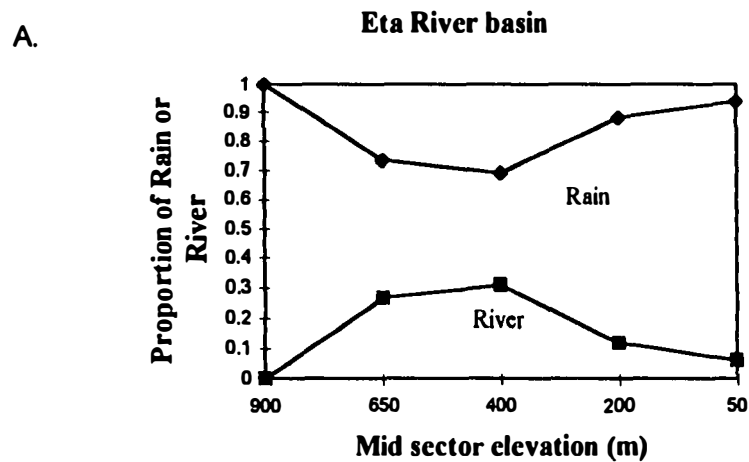


Figure 3.11.. Proportion of Used chemical potential energy from the rain or river in : A. and B. The bowl- shaped Eta and Jacupiranga River basin; C. The plateau Pardo River basin; D. The elevated Coweeta river basin.

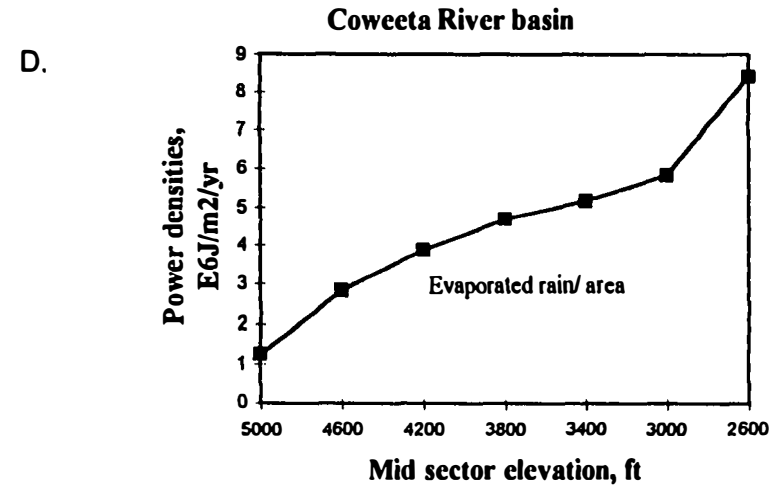
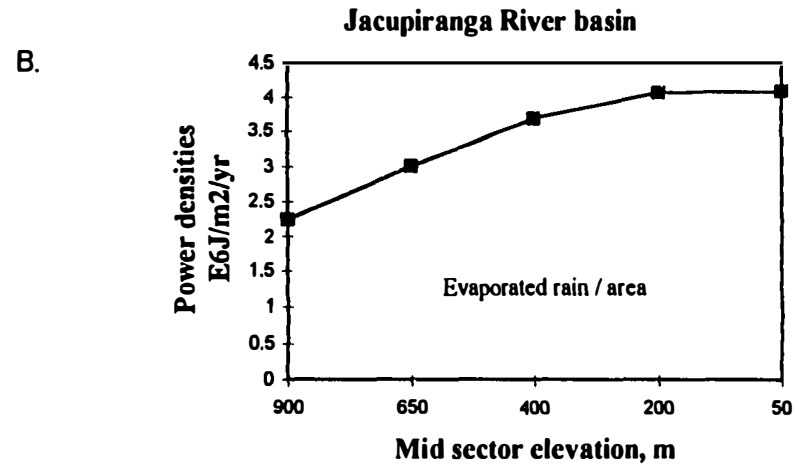
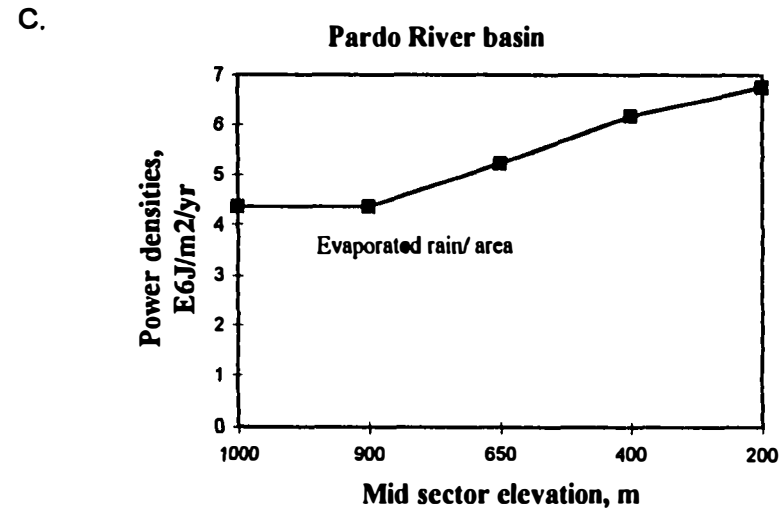
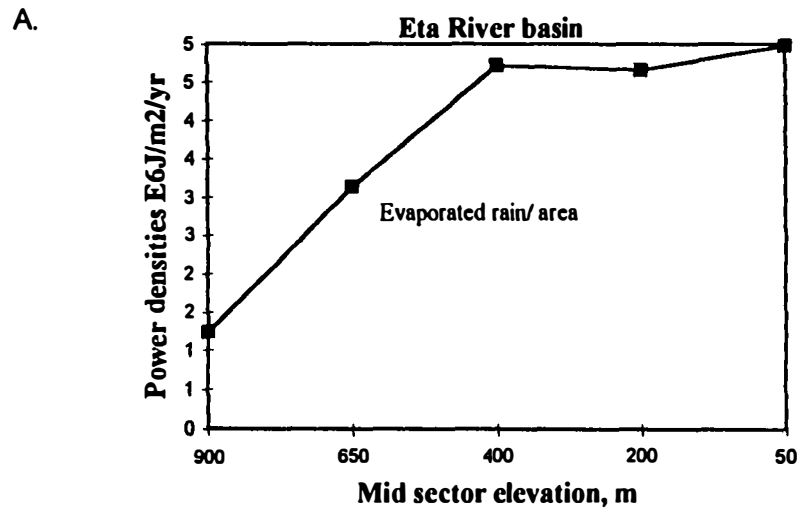


Figure 3.12. The log- shaped increase of chemical potential energy use per area in the downstream sectors of : A. and B. The Bowl-shaped Eta and Jacupiranga River basin;C. The plateau Pardo River basin; D. The elevated Coweeta River basin.

Chemical Potential Energy of River Outflow

Chemical potential of river outflow increased along the river profile with an increase of the water volume in the rivers, and therefore reached its maximum in the lowest sector of the evaluated watersheds. Estimates of the chemical potential energy of river outflowing the elevational sectors are displayed in Charts H of Figures A.1 to A.8 and Charts B in Figures A.9 to A.14. The longitudinal pattern of the pattern was exponential to log-shaped, as verified in typical river basins depicted in Figure 3.13.

Chemical potential in the waters discharging the evaluated watersheds was less than 2.5×10^{13} J/yr in the Coweeta sub-basins, around 7.5×10^{13} J/yr for the Coweeta River basin, and ranging from 50×10^{13} J/yr to 2300×10^{13} J/yr for the large watersheds (Column 8 in Tables B.2 and B.5) The concentration of chemical potential energy outflowing per square meter of the river basin area was around 5.0×10^6 J/m²/yr for the Coweeta basins and sub-basins, about 4.0×10^6 J/m²/yr for the rainy large basins, and ranging from 2.0 to 3.0×10^6 J/m²/yr for the drier basins.

In all evaluated watersheds, except for the two drier river basins Catas Altas and Pardo, the chemical potential outflowing the river basins were around 44 to 49% of the total available chemical potential provided to the basin (as shown by the estimates on Column 8 of Tables B.3 and B.6). Also, in all evaluated watersheds the water chemical potential use in evapotranspiration ranged from 51 to 63% of the available chemical potential in the area (Column 7 of Tables 3.3 and 3.6).

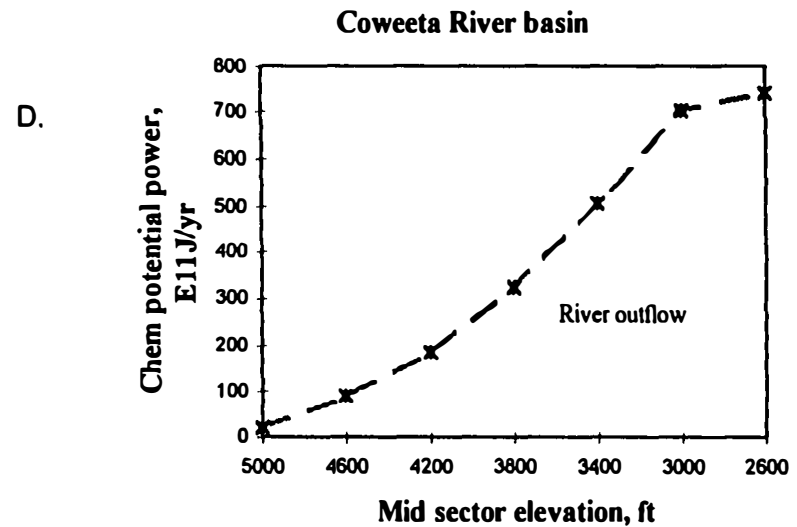
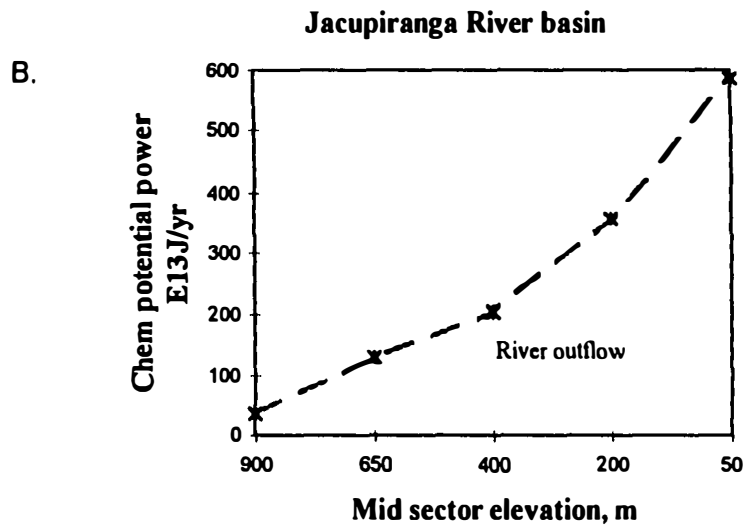
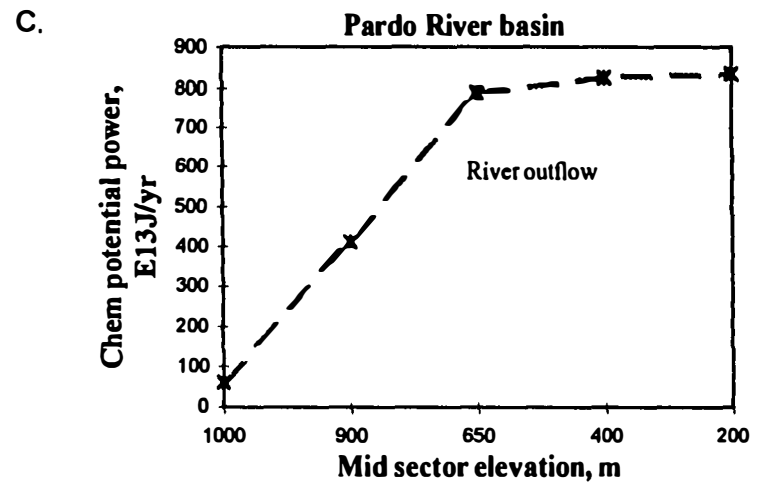
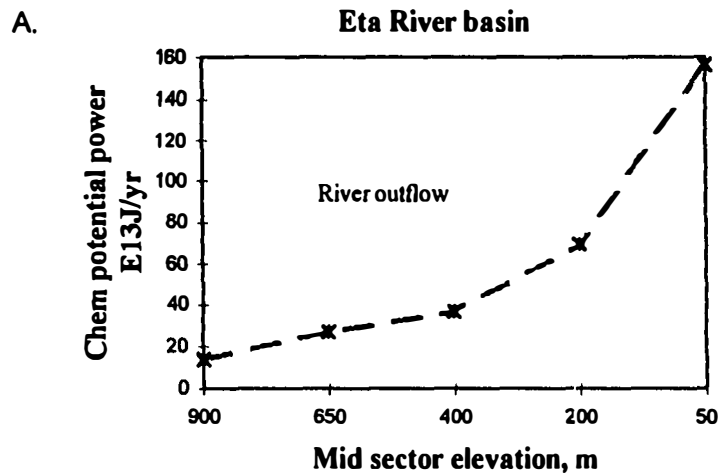


Figure 3.13. The exponential to log-shaped growth of the chemical potential energy outflowing the elevational sectors of: A and B. The Bowl-shaped Eta and Jacupiranga River basins; C. The plateau Pardo River basin; D. The elevated Coweeta river basin.

Energy Indices relating Geopotential and Chemical Potential Energies

Water geopotential energy is least in the lower sectors of the watersheds compared to the chemical potential energy, but both are important in the valley production. Therefore, a good index to test the watershed performance is the ratio of chemical potential evapotranspired to the geopotential energy used in the watershed upstream (Column 5 of Tables B.3 and B.6). This ratio was around 0.4 to 0.6 for the high elevation Coweeta River system and for the large plateau basins. For the bowl-shaped Eta and Jacupiranga River basins, the ratio was 1.58 and 1.24 respectively, indicating their efficiency in using their limited supply of geopotential energy to process chemical potential energy in the downstream valleys.

Empower of Rain and River

The total empower contribution by rain to the elevational sectors increased downstream, since the rain empower of the upper sectors were transferred to the lower sectors in form of river (Chart M of Figures A.1 to A.8 and Chart E of Figures A.9 to A.14). An exponential to log-shaped increase of the total empower was observed along the river profile, as represented for some typical river basins in Figure 3.14.

The total rain and river empower contributions to the Coweeta system ranged from less than $1.0E18$ sej/yr for the sub-basins, to $3.0E18$ sej/yr for the Coweeta River basin and to about $160E18$ sej/yr for the Upper Little Tennessee River basin (Column 2 in Table B.8). For the Brazilian watersheds, the empower contribution was less than $100E18$ sej/yr

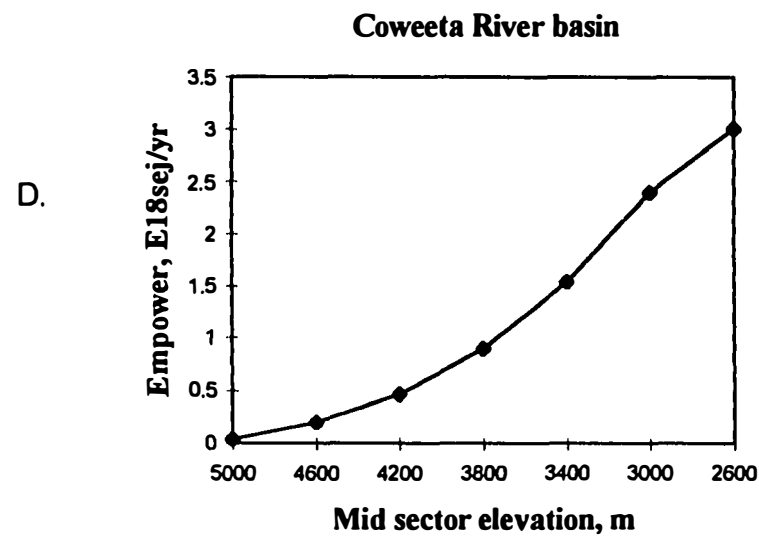
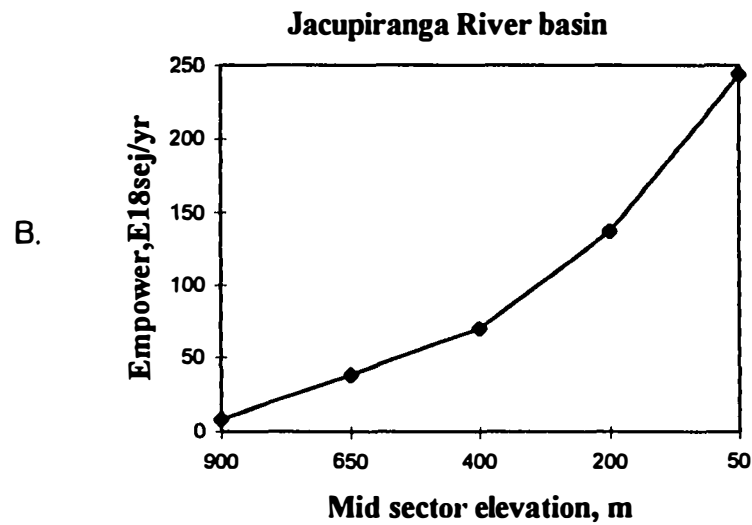
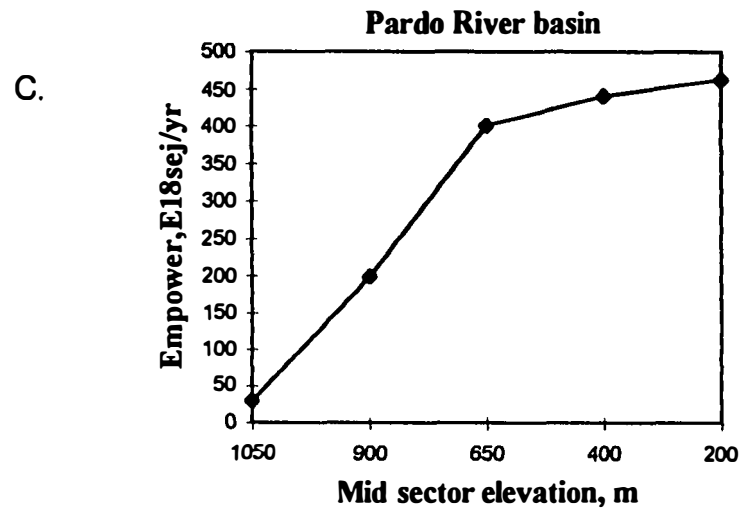
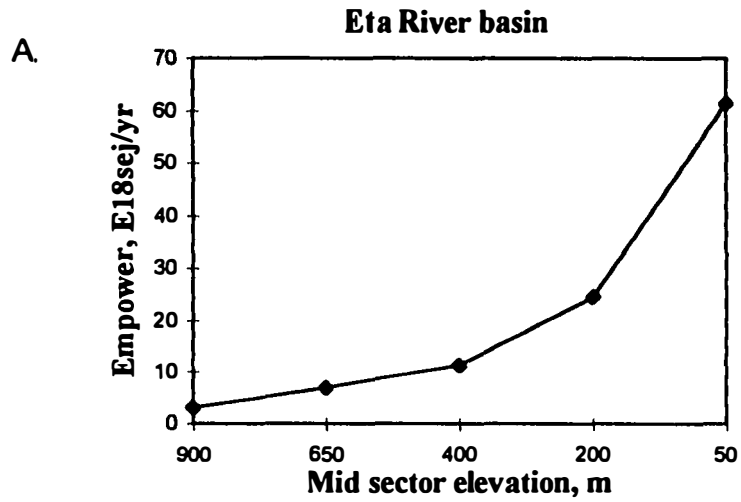


Figure 3.14. The exponential to log-shaped increase of total empower in: A and B. The bowl-shaped Eta and Jacupiranga river basins; C. The plateau Pardo River basin; D. The elevated Coweeta River basin

for the medium sized Eta , Betari and Catas Altas River basins but $200E18$ to $800E18$ for the large-sized Jacupiranga, Pardo and Juquia River basins (Column 2 in Table B.7)

The empower density in the elevational sectors increased in an exponential shape towards the lower sectors of the river basin in most evaluated watersheds (Charts M of Figures B.1 to B.8 and Charts E of Figures B.9 to B.14) However, the empower density of the elevational sectors of the bowl-shaped Jacupiranga and Eta River basins was parabolic, with maximum density in the middle elevation sector about 400 m high. Graphs of the empower density for these typical basins shapes are depicted in Figure 3.15.

The average concentrations of rain and river empower were higher for the small Coweeta sub-basins and basin ($5.0 - 7.0E11$ sej/m²/yr), due to the high precipitation in the area and the intense convergence of runoff due to shape of the basin (Column 4 in Table B.8). In the large Brazilian basins, average rain and river empower was less than $3.0E11$ sej/m²/yr in the bowl-shaped river basins, around $4.0 - 5.0E11$ sej/m²/yr for the plateau basins with relative downstream runoff convergence and almost $10.0E11$ sej/m²/yr for the Pardo river basin due intense runoff convergence in the river mouth (Column 4 in Table B.7).

Similar ranking among river basins was found for the total energy use per area (Column 6 in Tables B.7 and B.8). The high concentration of energy use in the Coweeta, Upper Little Tennessee and the Brazilian plateau basins was due to the greater geopotential work in the elevated sectors of the basins.

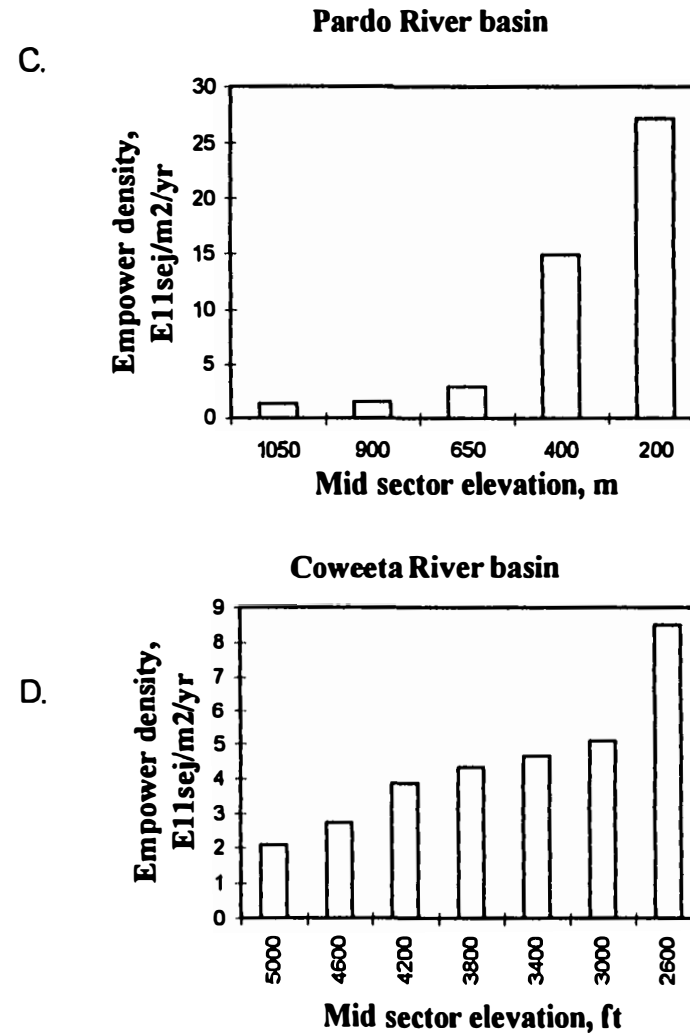
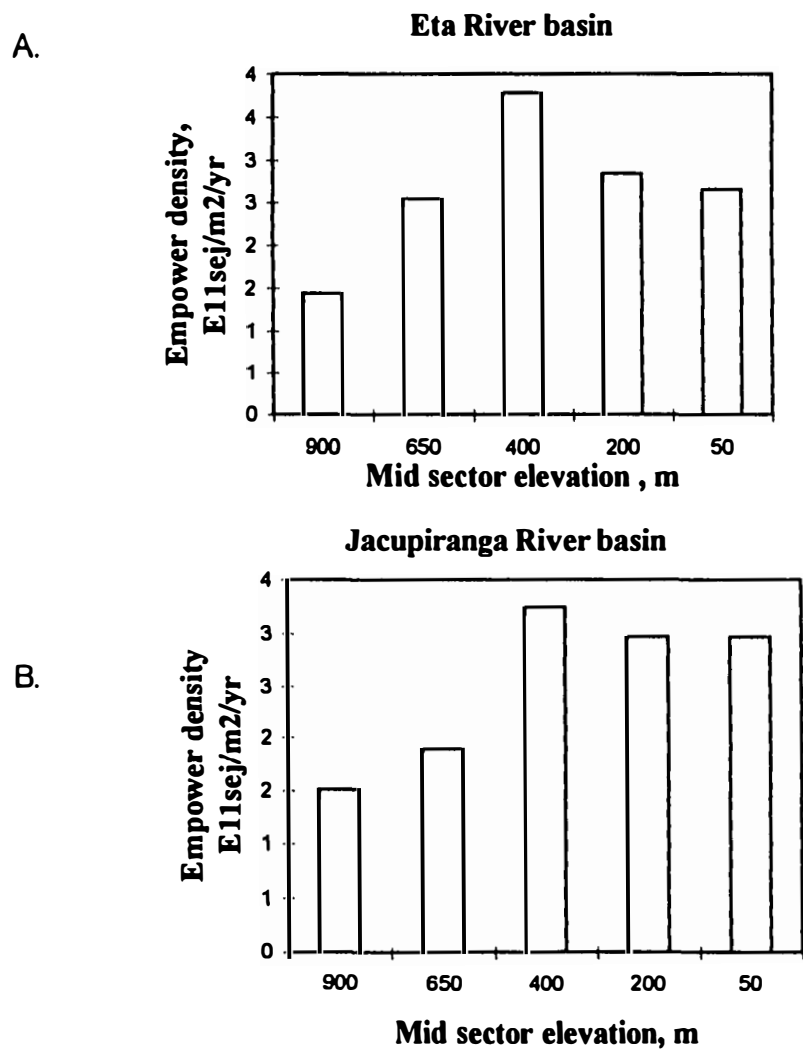


Figure 3.15. Graphs of empower density showing in: A. and B. A hump-shaped distribution in the bowl-shaped Eta and Jacupiranga river basins; C. and D. An exponential-shaped or mixed-shaped distribution in the plateau Pardo and the elevated Coweeta River basins, respectively.

Transformities of River Outflow

Transformities rise downstream representing an increase in the spatial and temporal organization in the river system downstream (Charts N of Figures B.1 to B.8 and Charts F of Figures B.9 to B.14).. Geopotential transformities increased with an exponential shape as the chemical potential transformities increased in a straight pattern, as depicted in Figure 3.16 for some typical river basins.

In the Coweeta River system, the river geopotential transformities ranged from 10,000 sej/ J to 30,000 sej/J and the chemical potential transformities varied from 20,000 sej/J to 40,000 sej/J. The transformities for chemical potential were always higher than those for geopotential.

However, the pattern was reversed with the river transformities of sectors lower than 650m high. In the Brazilian watersheds, maximum values for the transformities of river chemical potential were around 55,000 sej/J. Transformities of geopotential of river outflow were about 1,000,000 to 3,500,000 sej/J in the large bowl- shaped basins.

Energy and EMERGY Indices relating Mountain and Valley

Ratios of mountain energy and EMERGY to valley productivity ratios were estimated for the floodplain watersheds of the Eta River basin, the Jacupiranga River basin, the Itariri River basin and the Upper Little Tennessee River basin (Table B.9) with the following results:

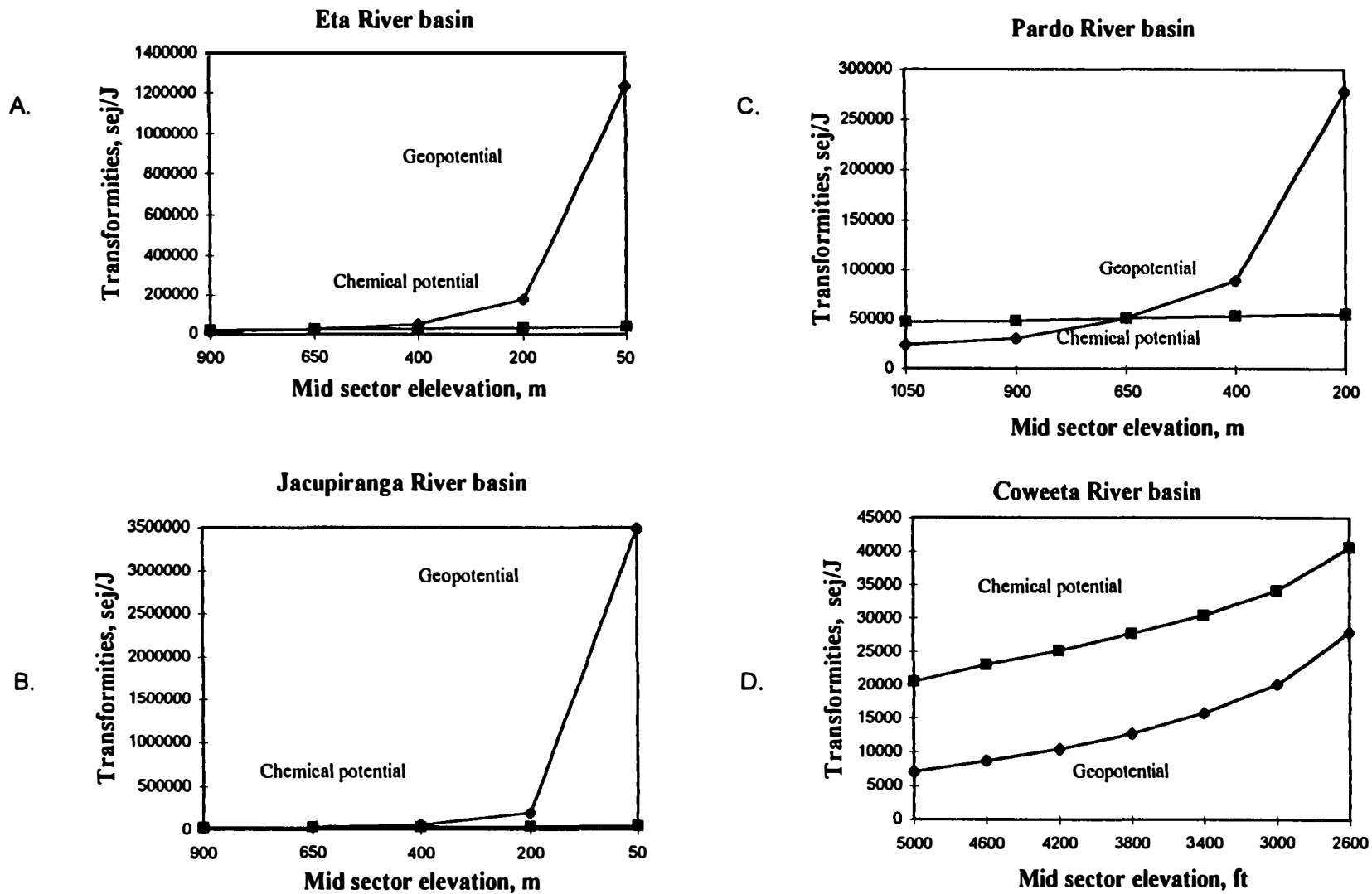


Figure 3.16. Geopotential transformities increased in an exponential shape as chemical potential transformities increased in a straight pattern for: A. and B. The bowl-shaped Eta and Jacupiranga River basins; C. The plateau Pardo River basin; D. The elevated Coweeta River basin.

- Ratios of stored ENERGY in the mountain structure to the area of the valleys were of same order of magnitude about $E18 \text{ sej/m}^2$ (Chart B in Figure 3.17).
- Ratios of geopotential energy used in the mountain sector to the rain chemical potential energy used in the valleys were similar, approximately 1.0 for the three Brazilian watersheds with valleys close to the sea level (Chart A in Figure 3.17)
- The Upper Little Tennessee River basin, with an elevated valley had a ratio of geopotential to chemical potential of 2.14. However if valleys further downstream are included, the ratio for the whole watershed is areas is closer to 1.0.
- Ratios of mountain ENERGY use to chemical potential energy evapotranspired in the valleys ranged from $1.5E11 \text{ sej/J/yr}$ to $7.5E11 \text{ sej/J/yr}$. Ratios of annual mountain empower to chemical potential energy transpired in the valley were around $2E5$ to $4E5 \text{ sej/J/yr}$ (Figure 3.18).

Empower and Transformities by Stream Order

Areas and Geopotential Energies Used in the Stream Order Sectors

Average areas of the first and second order stream sectors of the Coweeta sub-basins were relatively small, usually around 10 to 15 ha. The fourth order sectors with their oblong shape were much larger, with areas of 70 to 80 ha. The fourth order sectors varied from 35 ha for Ball creek and about 65 ha for the Shope Fork (Chart A of Figure 3.19).

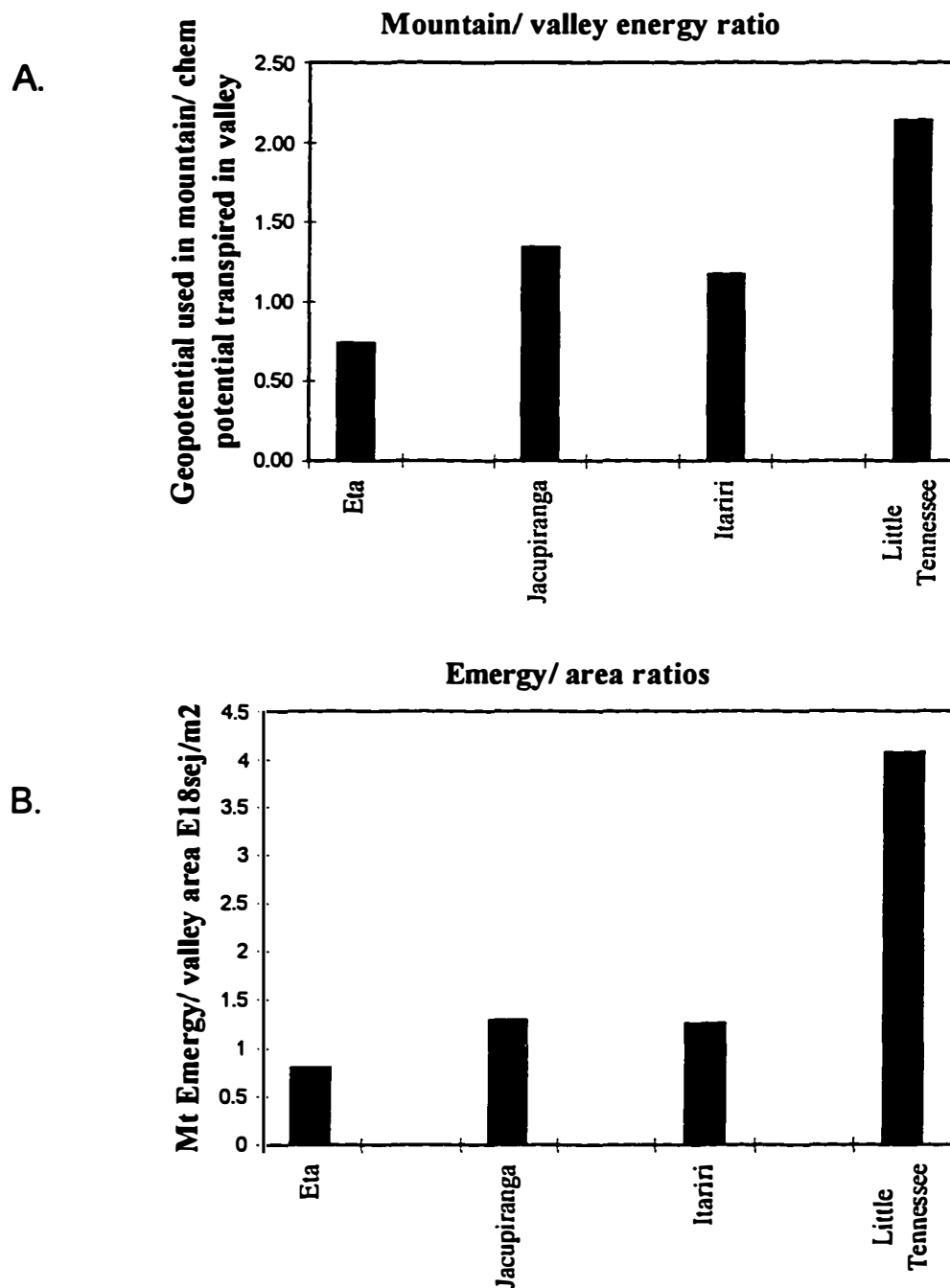


Figure 3.17.A. Ratios of geopotential energy used in the mountain per rain chemical potential transpired in the valley for four floodplain river basins; B. Ratios of energy of the mountain zone to area of the valleys for the floodplain river basins.

Mt Energy/ chem potential transpired in the valley, E11 sej/J/yr
Mt Empower/ chem potential transpired in the valley, E4 sej/J

Mountain and Valley Energy and Empower ratios

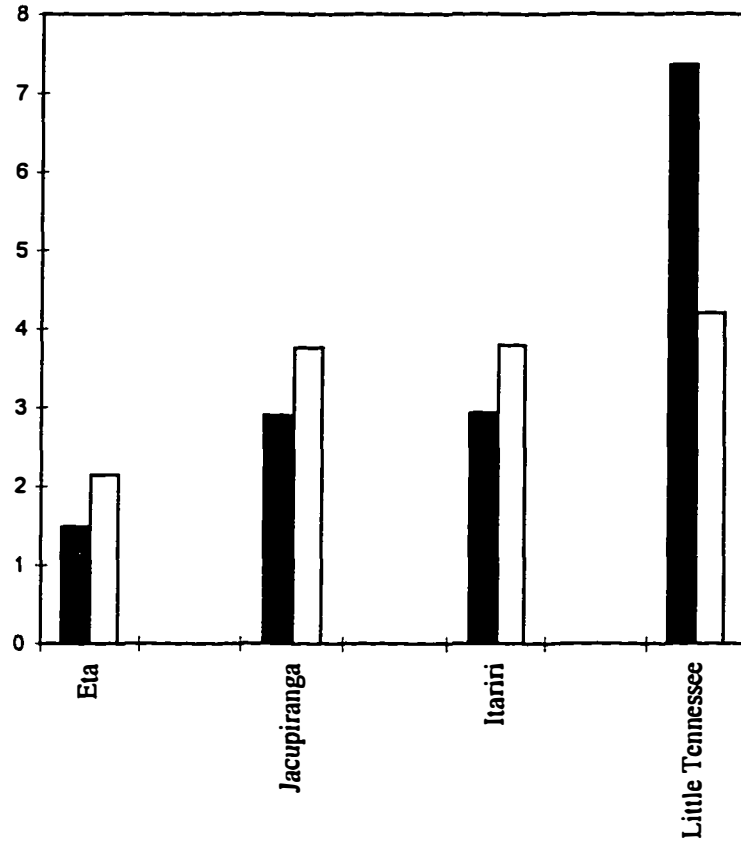


Figure 3.18. Ratios of mountain energy (dark bars) or mountain annual empower (white bars) to rain chemical potential evapotranspired in the valley for some floodplain river basins.

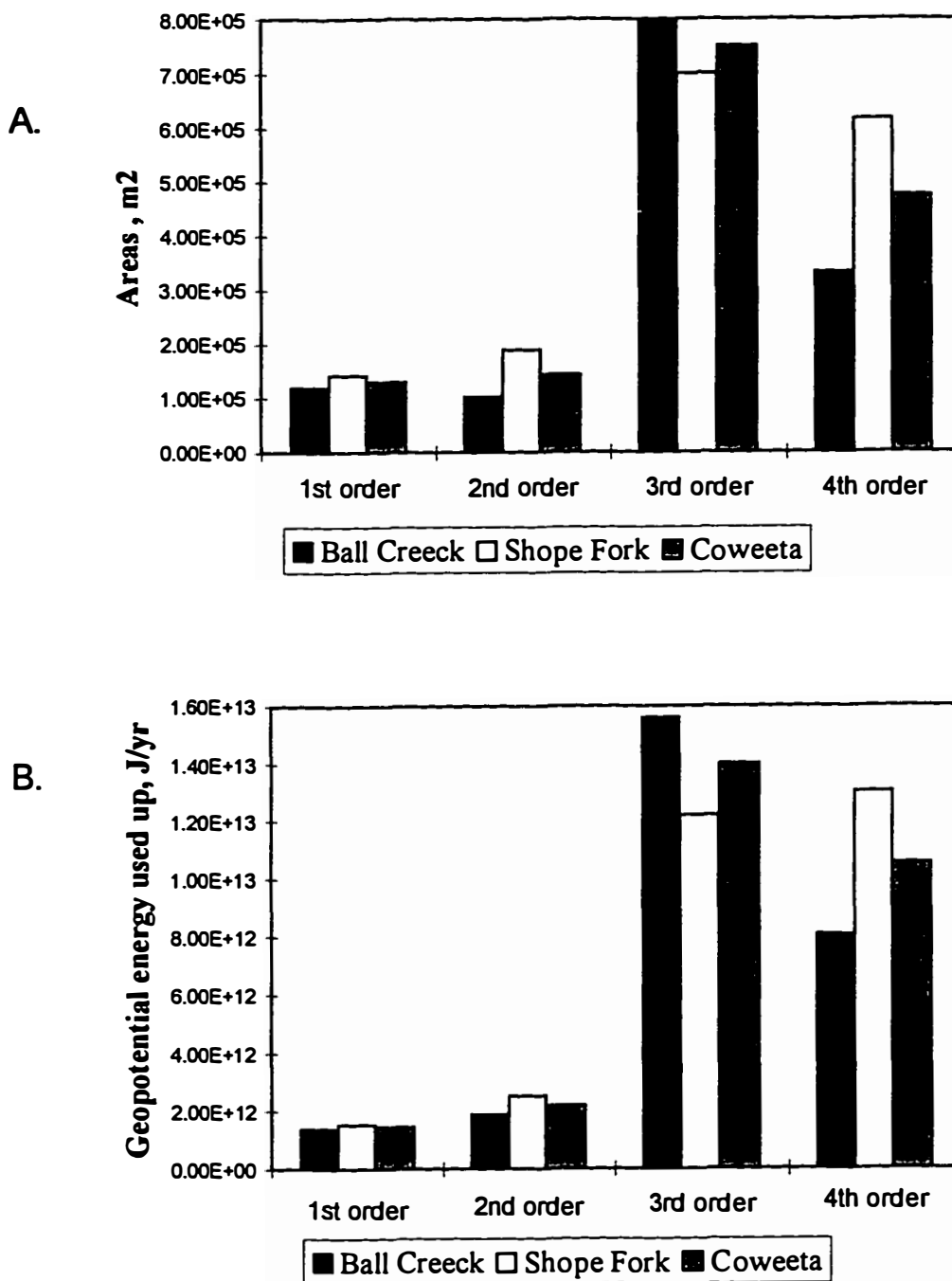
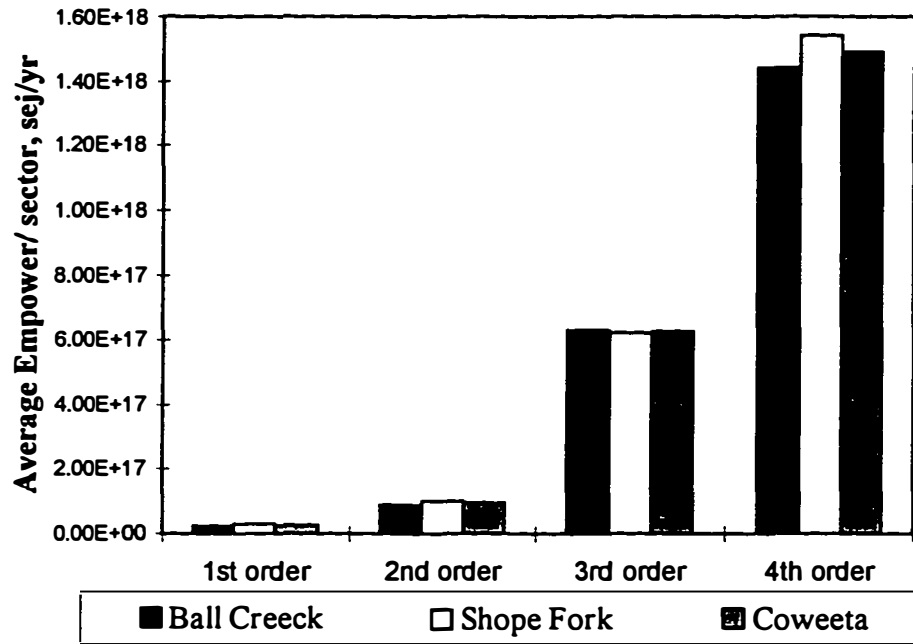


Figure 3.19. Energy and energy indices and ratios for the stream order sectors of Coweeta river basin, representing in: A. average areas of the sectors; B. average geopotential energy used in the sectors; C. average total (rain+ river) Empower contribution for the sectors; D. average transformities of river outflowing (T_{vg}) the sectors.

C.



D.

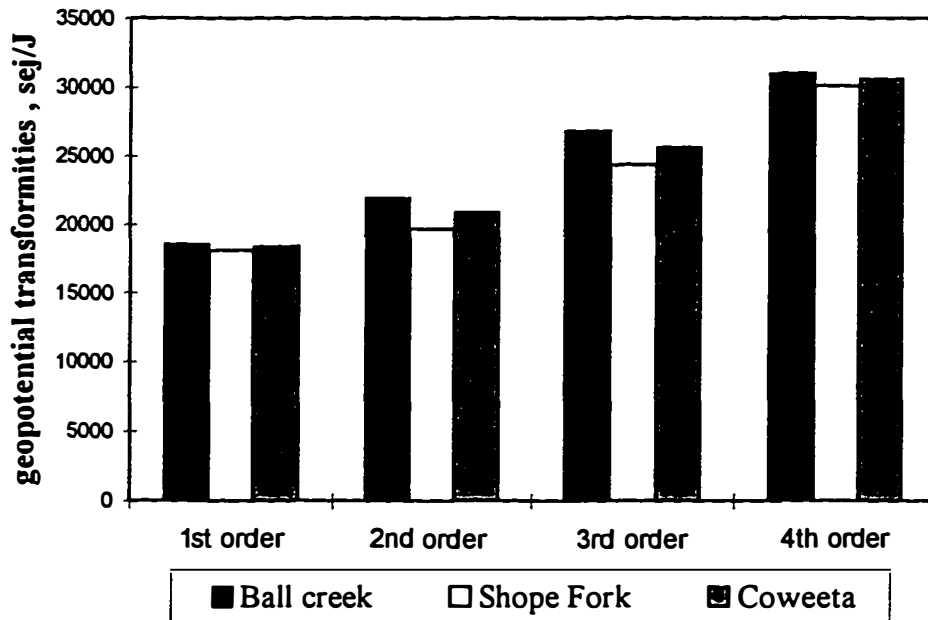


Figure 3.19. Continued.

The geopotential energy used up in the sectors followed very closely the pattern identified for the elevational sector areas (Chart B of Figure 3.19). This is because the geopotential energy was most used when rain was transformed into runoff. The calculation of such energy use was largely dependent on the size of the areas.

Empower Contribution to Stream Order Sectors

Total empower contribution increased with exponential shape along the stream order sectors (Chart C of Figure 3.19). Average empower contribution ranged from $5E16$ sej/yr for the first order stream sectors, $9E16$ sej/j for the second stream order sectors, $6 E17$ sej/yr for the third order stream sectors and $1.5E18$ sej/yr for the fourth order stream sectors. This pattern was predictable. Since rain EMERGY from the uplands (first and second order stream sectors) was conserved in the river outflowing these basins, the downstream segments of higher river order accumulated the rain empower of all upstream segments of lower river order.

Geopotential Transformities of River Outflowing the Stream Order Sectors

As small streams concentrated and organized themselves into higher order streams, their stream transformities increased. This pattern was observed in the Coweeta sub-basins (Chart D in Figure 3.19).

Average transformities ranged from 18,000 sej/J for the first order stream sectors, 22,000 sej/J for the second order stream sectors, 27,000 sej/J for the third order stream sectors and about 32,000 sej/J for the fourth order stream sectors.

Spatial Distribution of Energy Use and Empower

Spatial Pattern of Total Geopotential Energy Use.

Spatial patterns of geopotential energy use in the Coweeta sub-basins are displayed in Figures 3.20, 3.21 and 3.22 using three different methods- (1) basin-stream order sectors, (2) analysis based on 3rd order sectors and (3) analysis based on 4th order sectors. All three maps indicated increased concentrations of water energy use that takes place when major streams converged in the downstream sector.

The map based on the stream order sectors (Figure 3.20) best indicated the different zones of high geopotential energy use and thus potential erosion in the Coweeta River basin. Concentration was especially intense along the narrow Henson Creek sub-basin and some other zones along Upper Ball Creek and Upper Shope Fork Creek.

Figure 3.21 based on 3rd order sub-basins also showed some of the intensification of the geopotential energy use along secondary streams and their zone of convergence. But the map based on 4th stream order (Figure 3.22) was too coarse to represent the rivers work process.

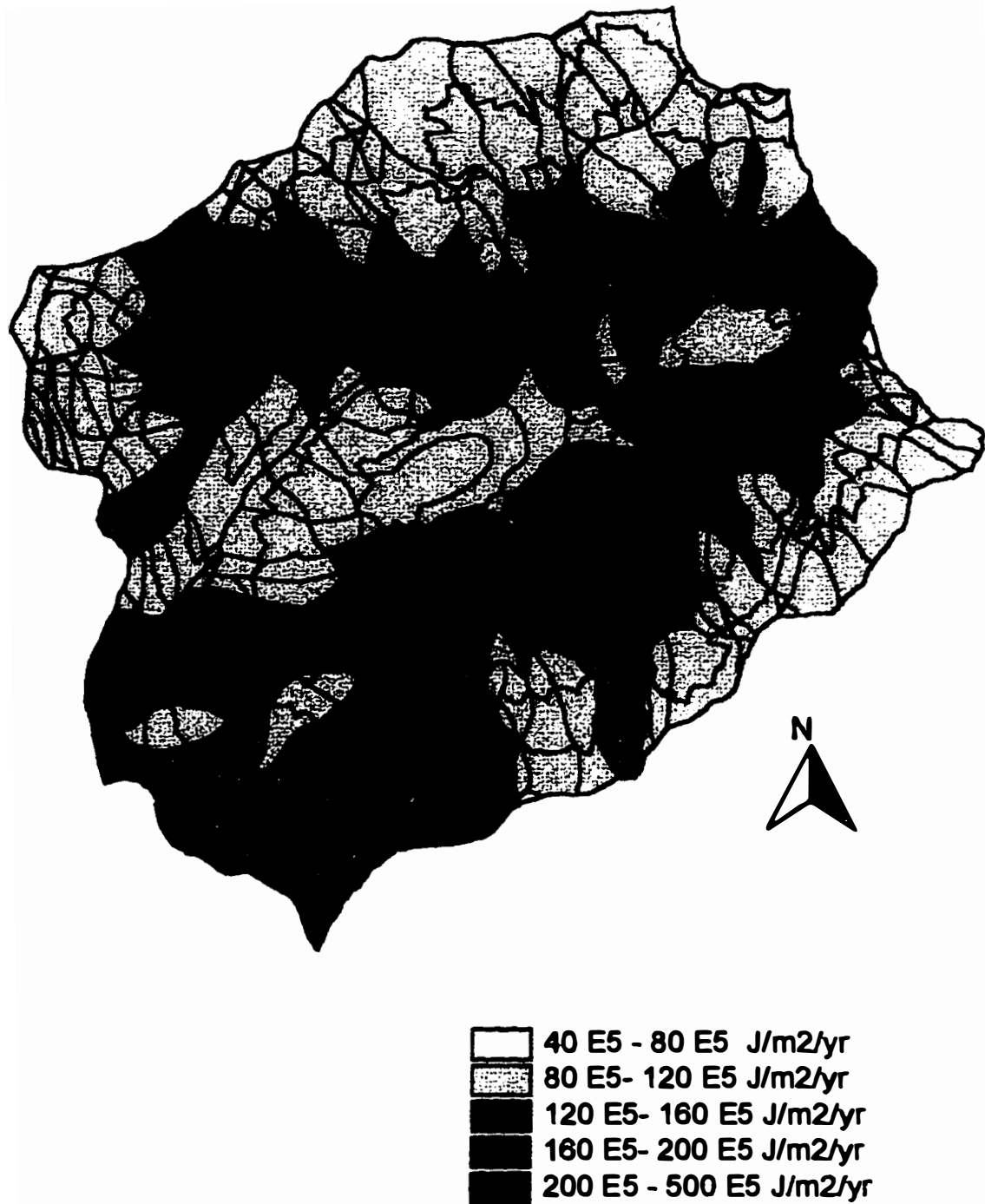


Figure 3.20. Map of density of total geopotential power use (Gtud) of the Coweeta River basin (based on stream order sectors).

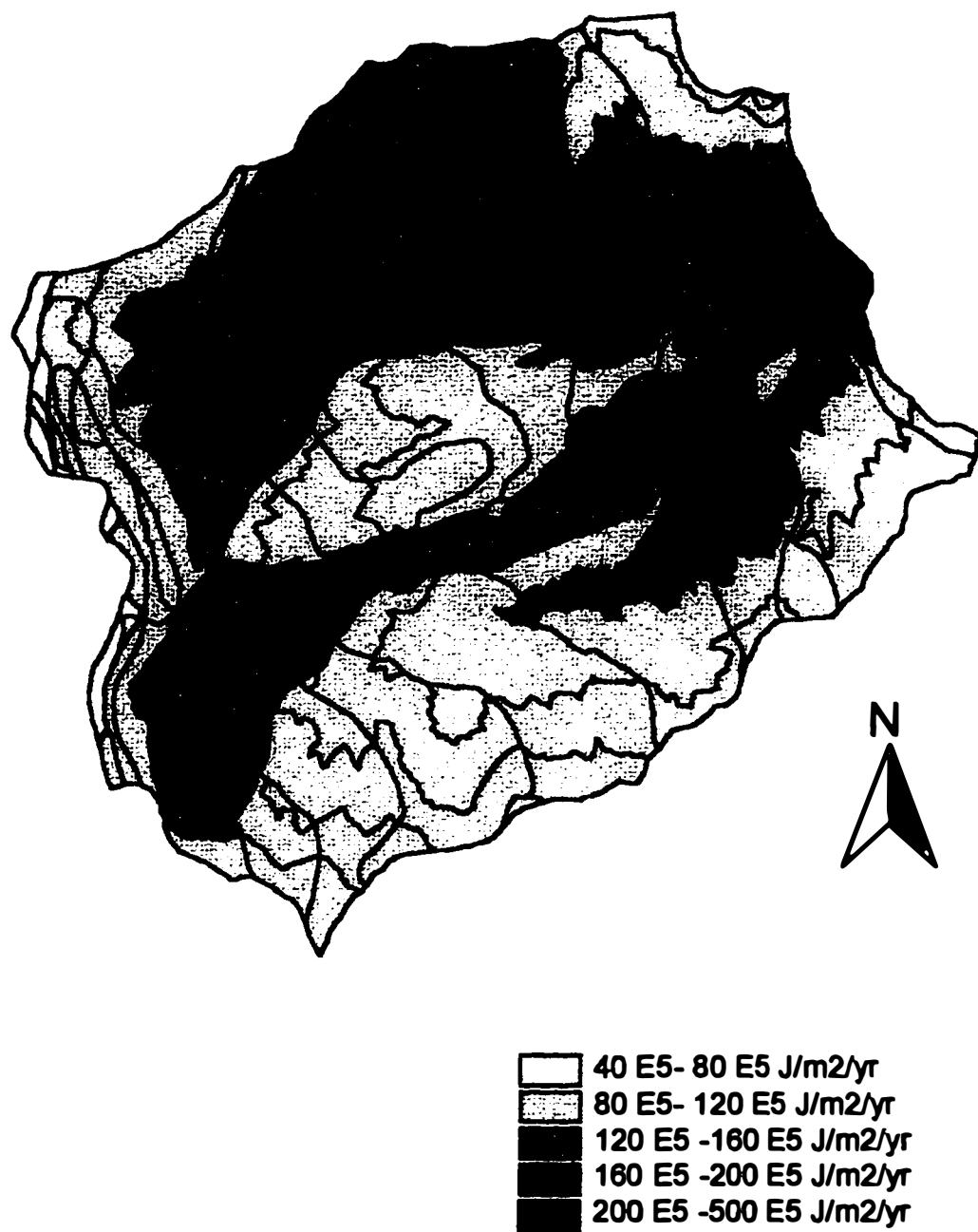


Figure 3.21. Map of density of total geopotential power use (Gtud) of the Coweeta River basin (based on third order sector sub-basins).

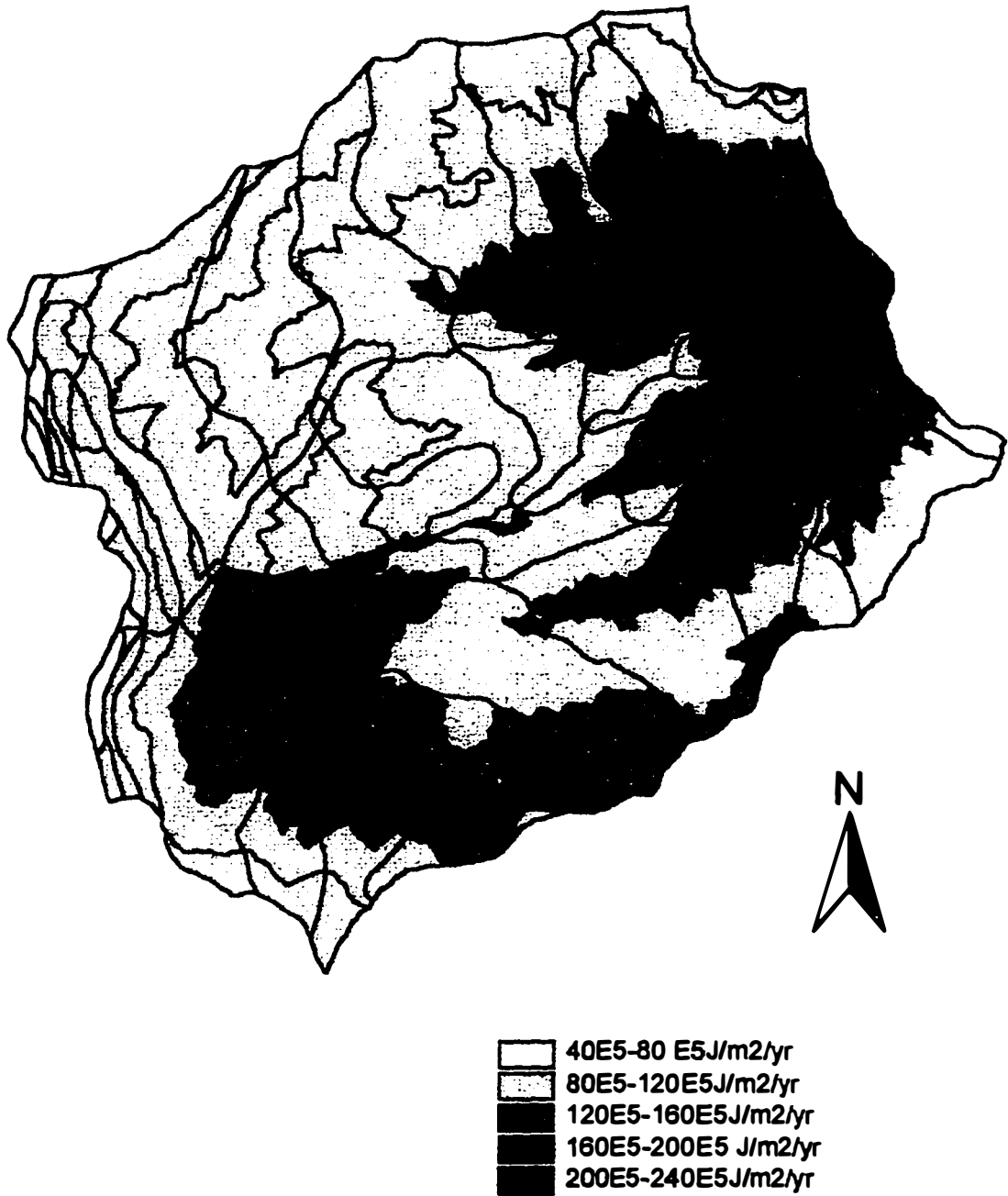


Figure 3.22. Map of density of total geopotential power use (Gtud) of the Coweeta River basin (based on fourth order sector sub-basins).

The geopotential power density used in the Coweeta River basin ranged from 4.0×10^6 to 5.0×10^7 J/m²/yr. This range of values was similar in all three maps prepared with the different methods.

Spatial Pattern of the Rain Chemical Potential Energy Use.

Figures 3.23, 3.24, and 3.25 show the spatial pattern of the rain chemical potential energy use in Coweeta River basin when the area was divided into the stream order sectors, 3rd order sectors, and 4th order sectors, respectively. These maps represent the spatial distribution of the plant transpiration, and by inference the primary production, of the Coweeta River basin.

All three maps showed a concentration of the rain chemical potential use in the lower sectors of the basin. Chemical potential energy use of the rain was higher than 4×10^6 J/m²/yr in more than 70 % of its area.

Spatial Pattern of Rain and River Empower Contribution.

Spatial concentration of rain and river Empower along the major streams of the Coweeta River basin was shown in maps prepared by dividing the area by stream order sectors (Figure 3.26) and 3rd order sectors (Figure 3.27). Highest empower densities were found in the lower sectors of the major sub-basins.

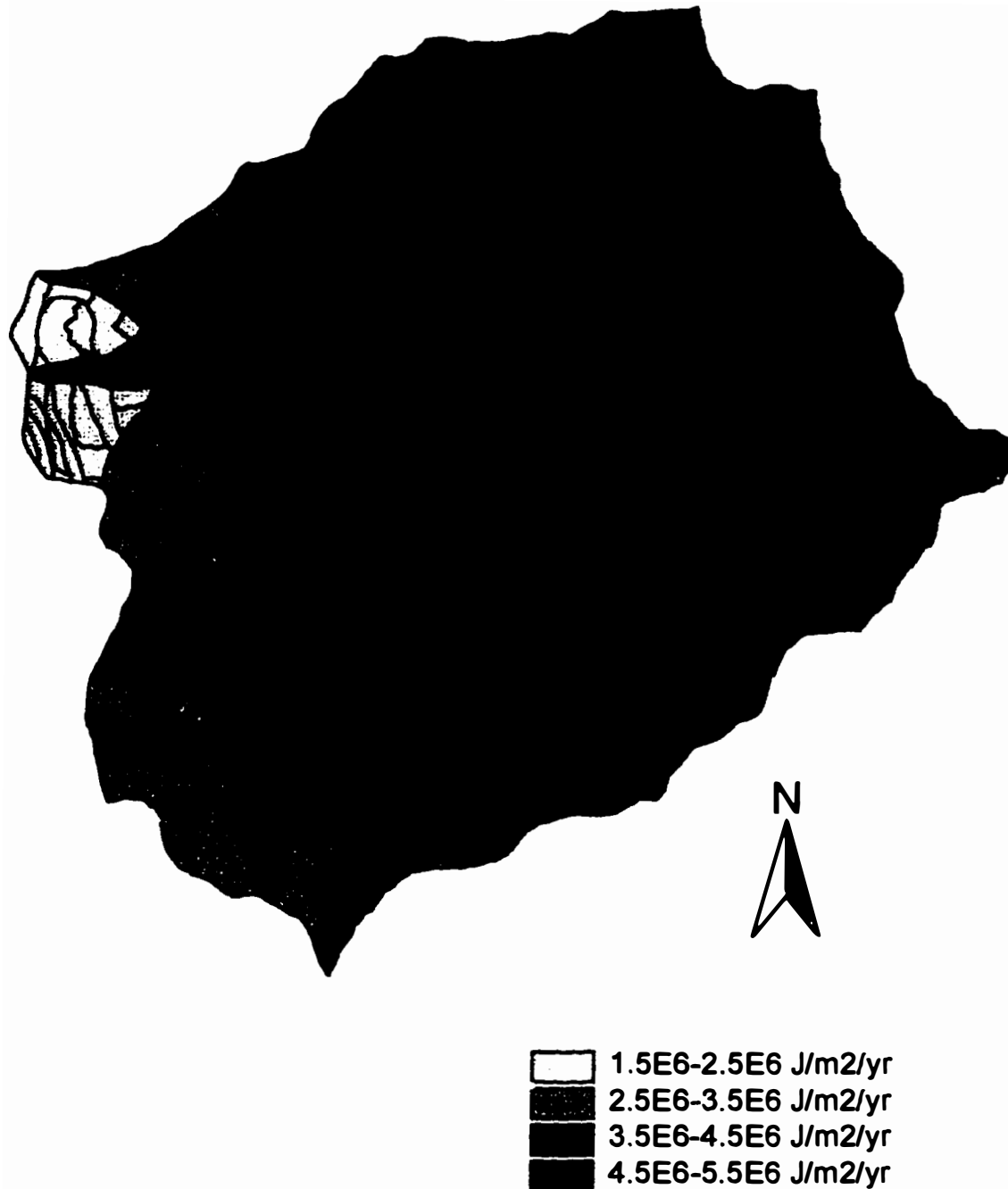


Figure 3.23. Map of density of rain chemical potential power use (Crud) of the Coweeta River basin (based on stream order sectors sub-basins).

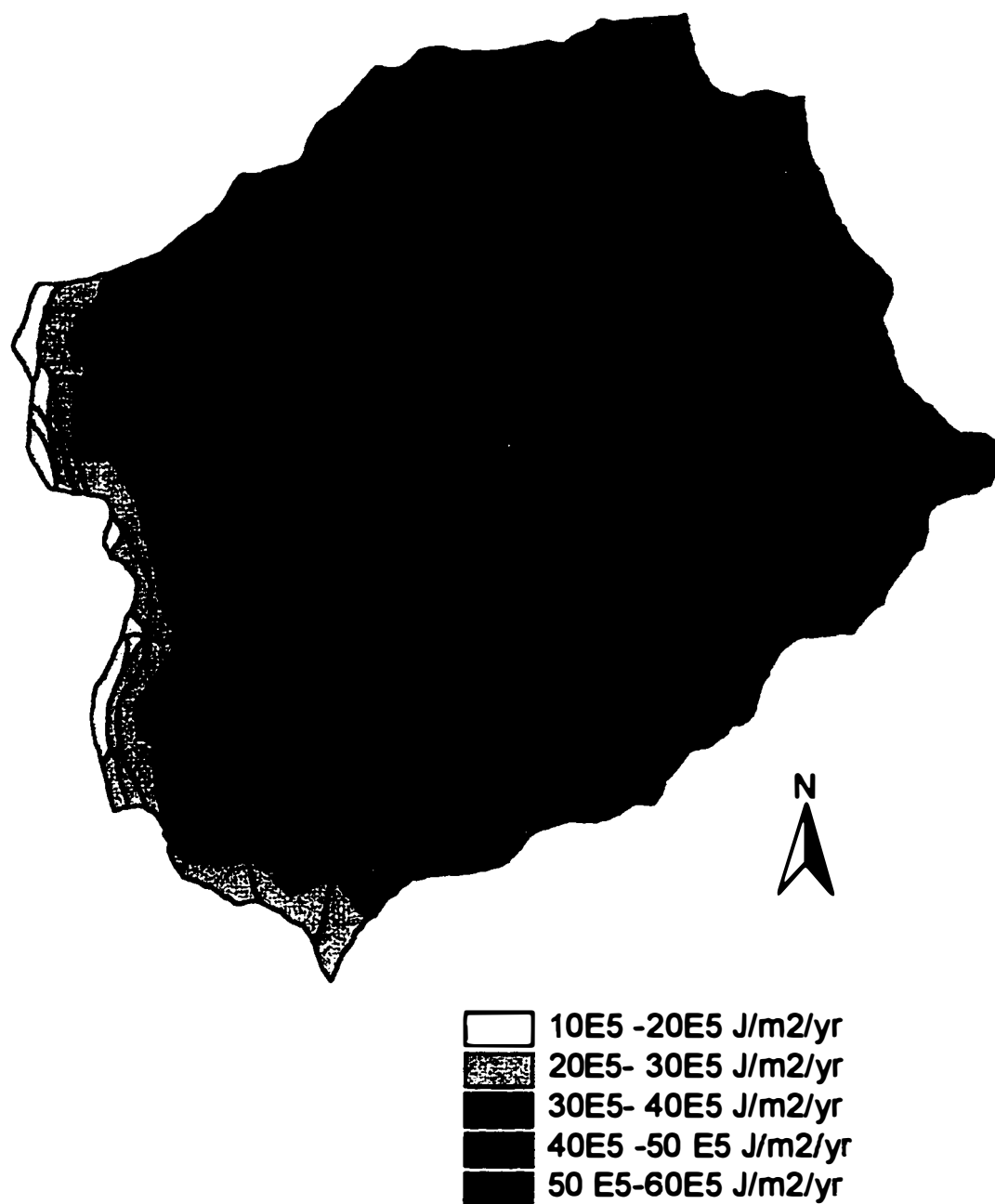


Figure 3.24. Map of density of rain chemical potential power use (Crud) of the Coweeta River basin (based on third order sectors sub-basins).

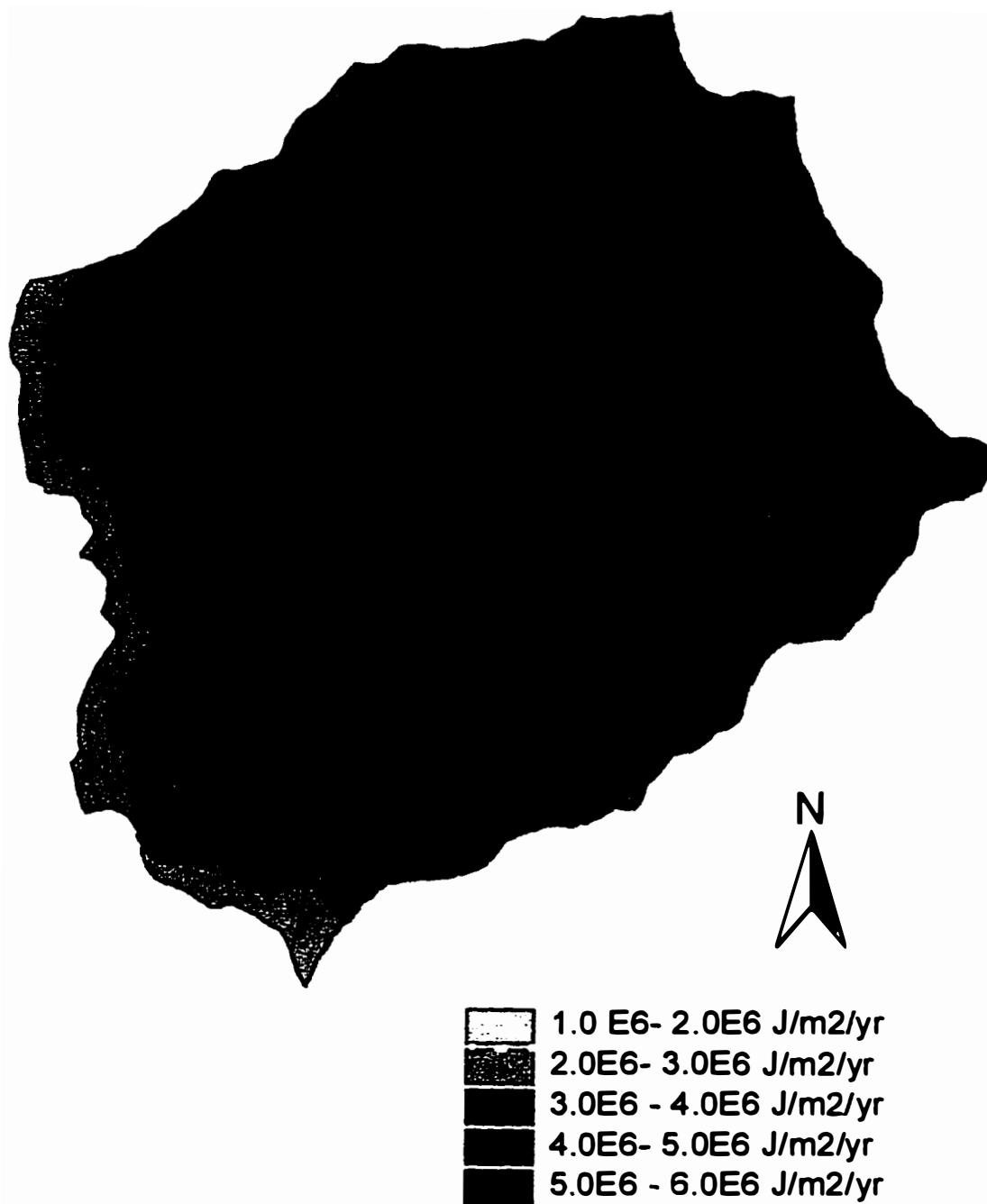


Figure 3.25. Map of density of rain chemical potential power use (Crud) of the Coweeta River basin (based on fourth order sectors sub-basins).

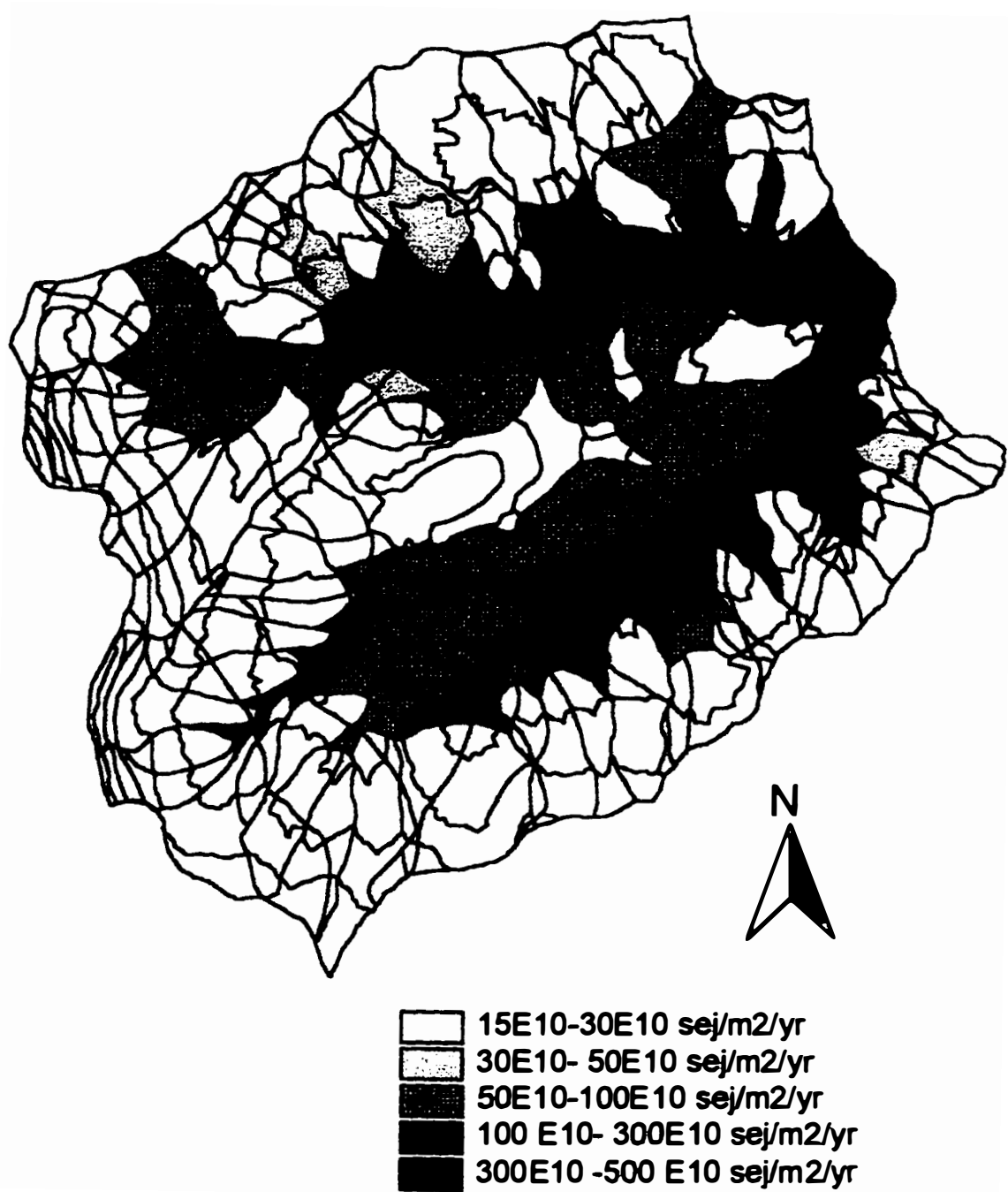


Figure 3.26. Map of total (rain +river) empower density (Ed) of the Coweeta River basin (based on stream order sectors sub-basins).

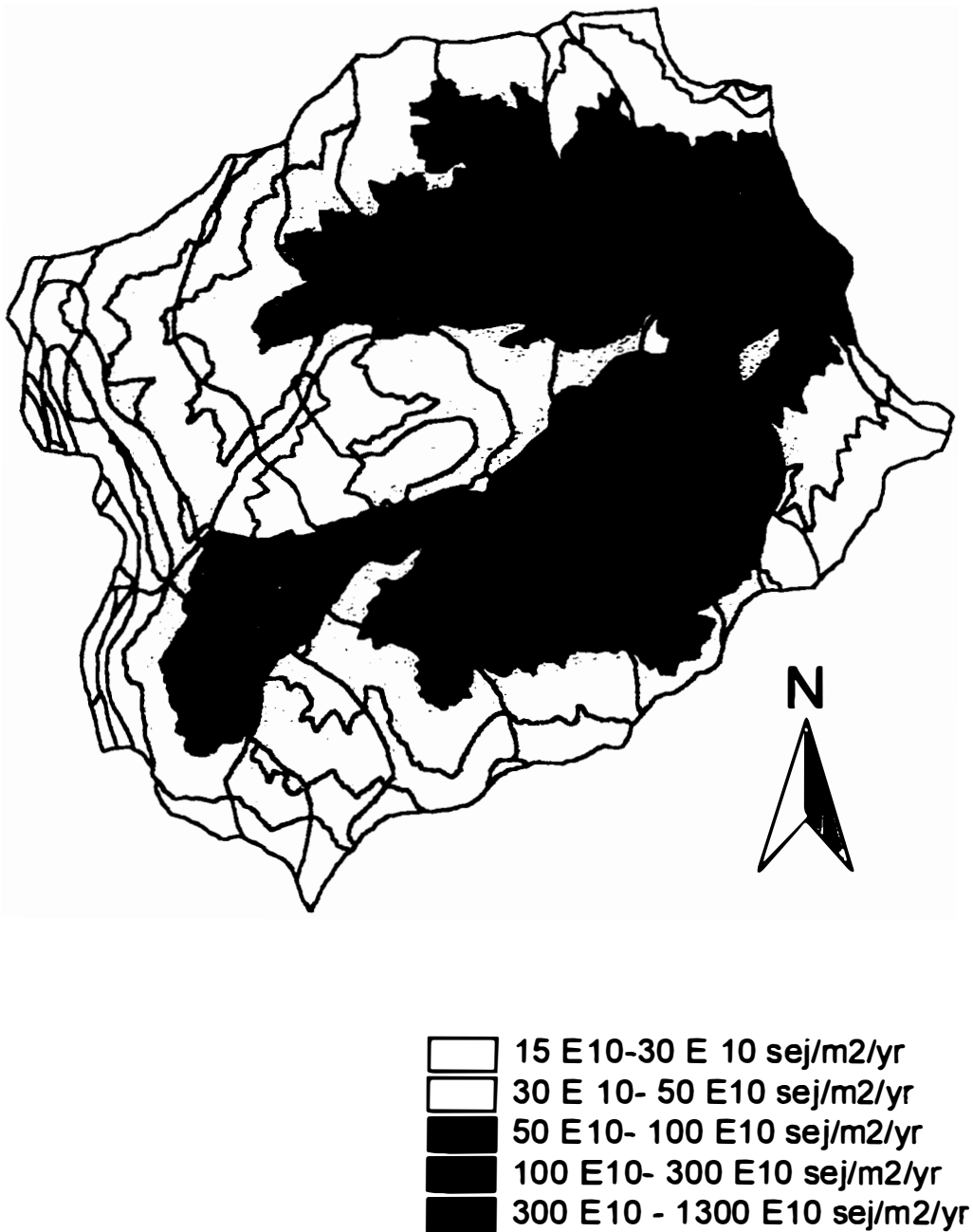


Figure 3.27. Map of total (rain +river) empower density (Ed) of the Coweeta River basin (based on third order sectors sub-basins).

In the stream order maps, the highest empower was found in the lowlands of Ball Creek. With more rainfall and a narrower shape, Ball Creek sub-basin had zones of higher energy use and EMERGY concentration.

Spatial Pattern of Transformities of River Outflow.

Maps of geopotential transformities that were based on stream order sectors (Figure 3.28) and 3rd order sectors (Figure 3.29), displayed a similar pattern. There was a gradual increase in the transformities as water moved downwards. Highest geopotential transformities of river outflow were found in the Lower Shope Fork Creek sub-basin.

Downstream increases were also observed in the transformities of chemical potential of river outflow calculated by stream order sectors (Figure 3.30) and 3rd order stream sectors (Figure 3.31). In both cases, maps made by dividing the area into 3rd order sectors failed to represent the intensification of the geopotential and chemical potential transformities along the secondary streams of Shope Fork creek sub-basin.

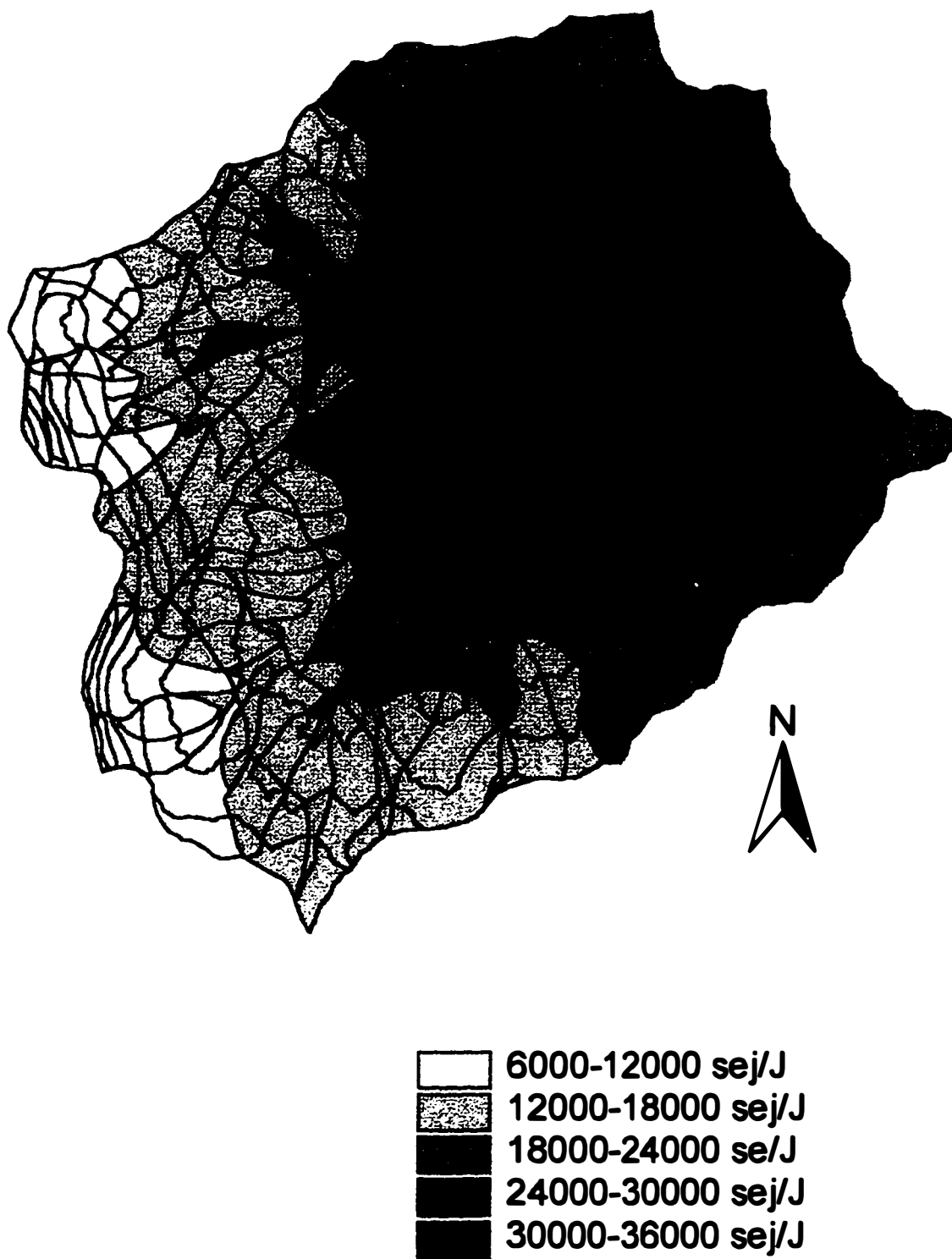


Figure 3.28. Map of geopotential transformities (Tvg) of the Coweeta River basin (based on stream order sectors sub-basins).

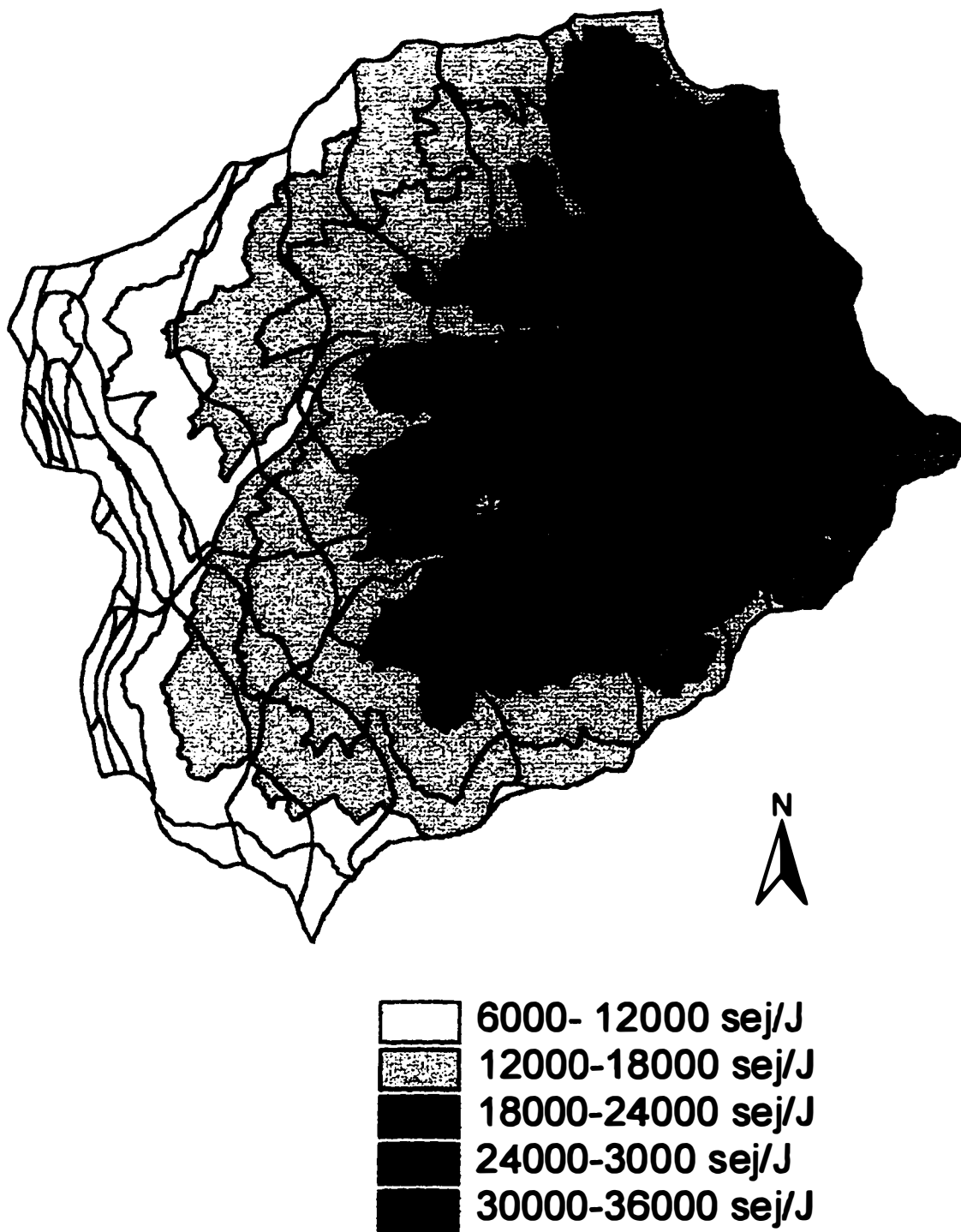


Figure 3.29. Map of geopotential transformities (T_{vg}) of the Coweeta River basin (based on third order sectors sub-basins).

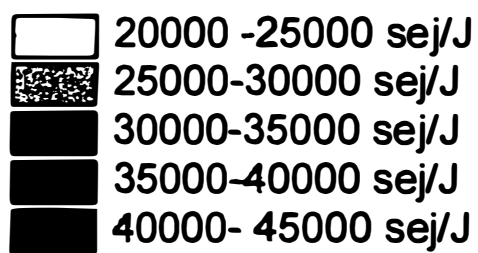
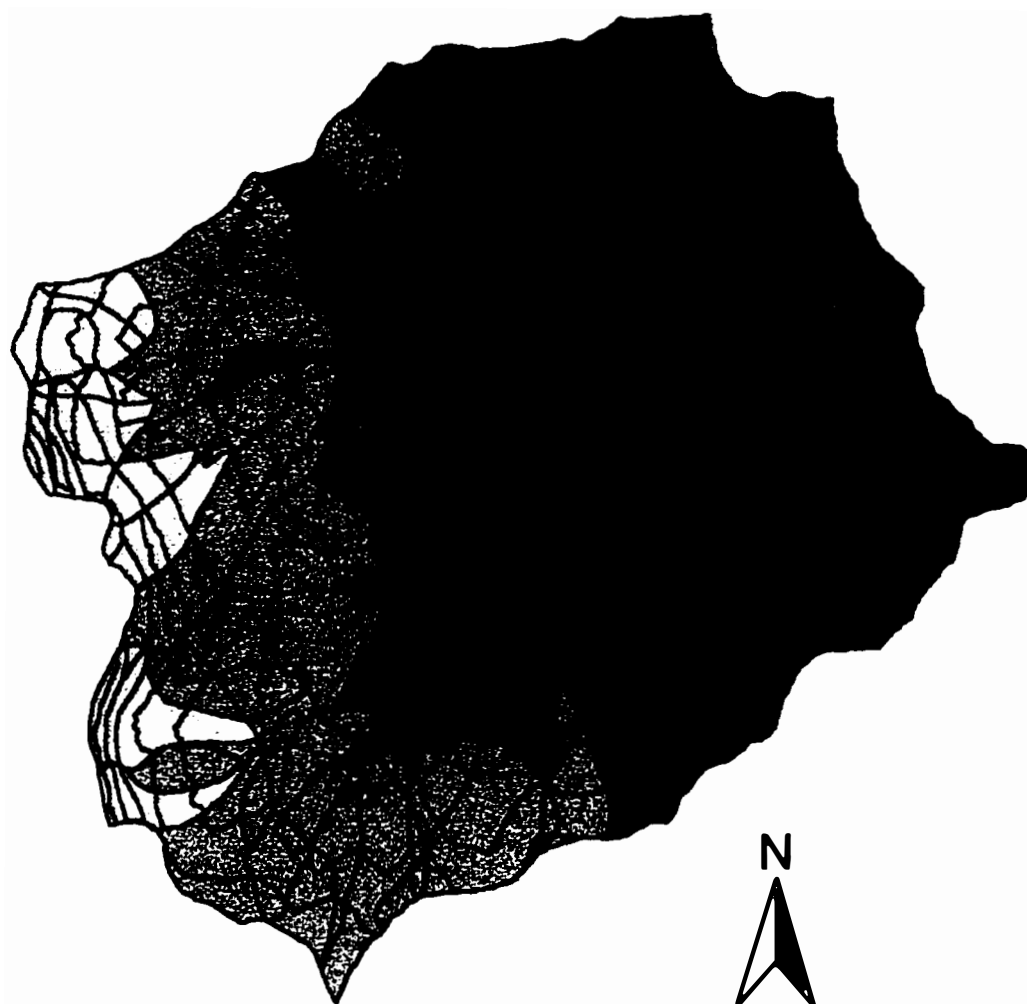


Figure 3.30. Map of chemical potential transformties (Tvc) of river outflow (based on stream order sectors)

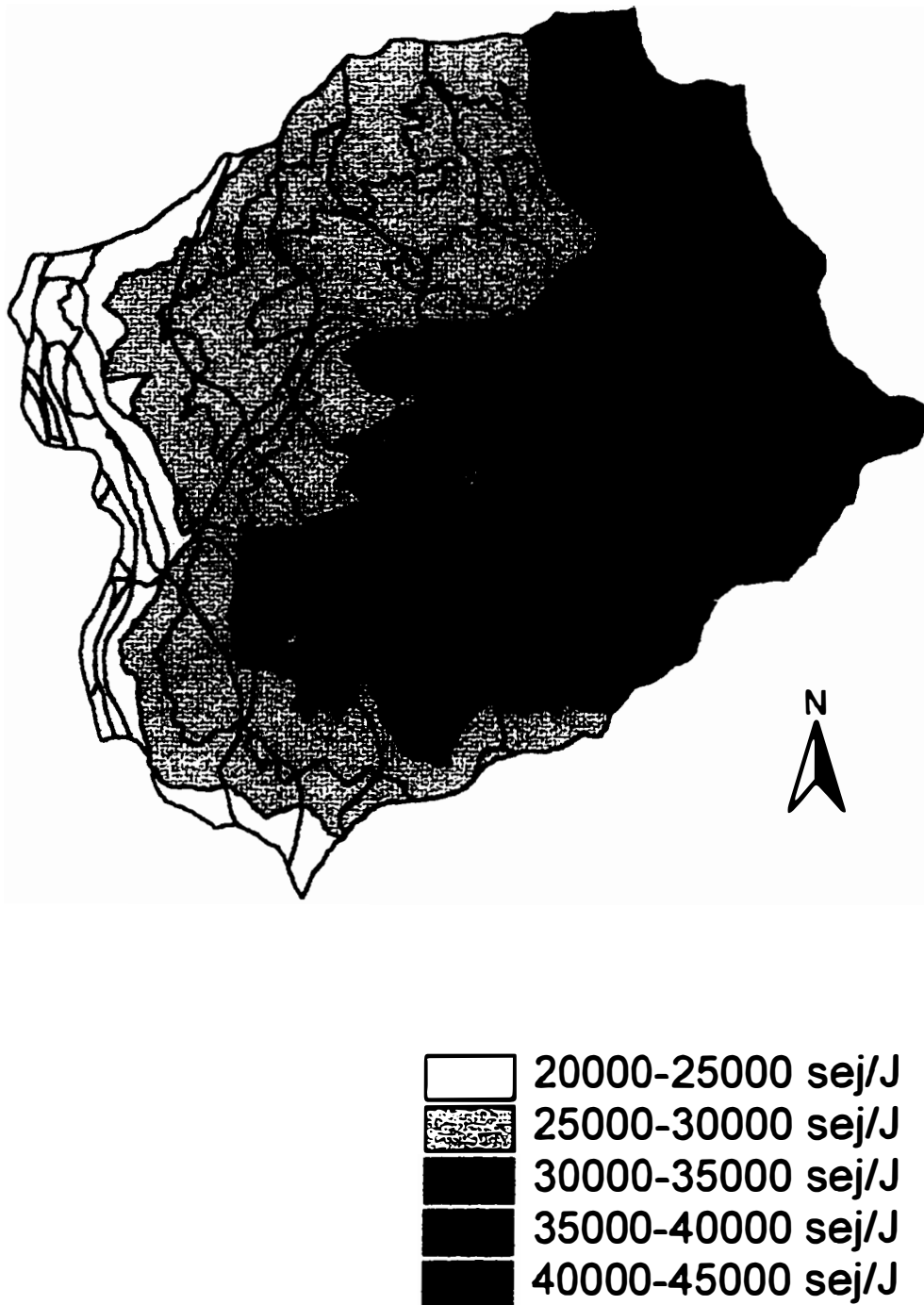


Figure 3.31. Map of chemical potential transformties (T_{vc}) of river outflow (based on third order sectors)

CHAPTER FOUR

SIMULATION

Impacts of River Damming in the Productivity of the Valley

An aggregated energy model, with the essence of the upstream- downstream relationship, was drawn to consider the impacts of river damming on the productivity of the valley. The first model represented a natural watershed, called here the No- Dam alternative (Figure 4.1). Then the model was modified to include the dams (Figure 4.2), allowing the simulation of the One Dam, Two- Dams and Four- Dams alternatives.

Description of the Model

These models included the main processes occurring in a watershed that were understood to be related to the river damming. Therefore, processes such as the production of the mountain structure (M), the production of the valley structure (V) and the river flow transferring water, sediments and nutrients from the mountain to the valley during floods, were represented using energy systems language.

The main flows and storages represented in the model are, as indicated in Figures 4.3 and 4.4 :

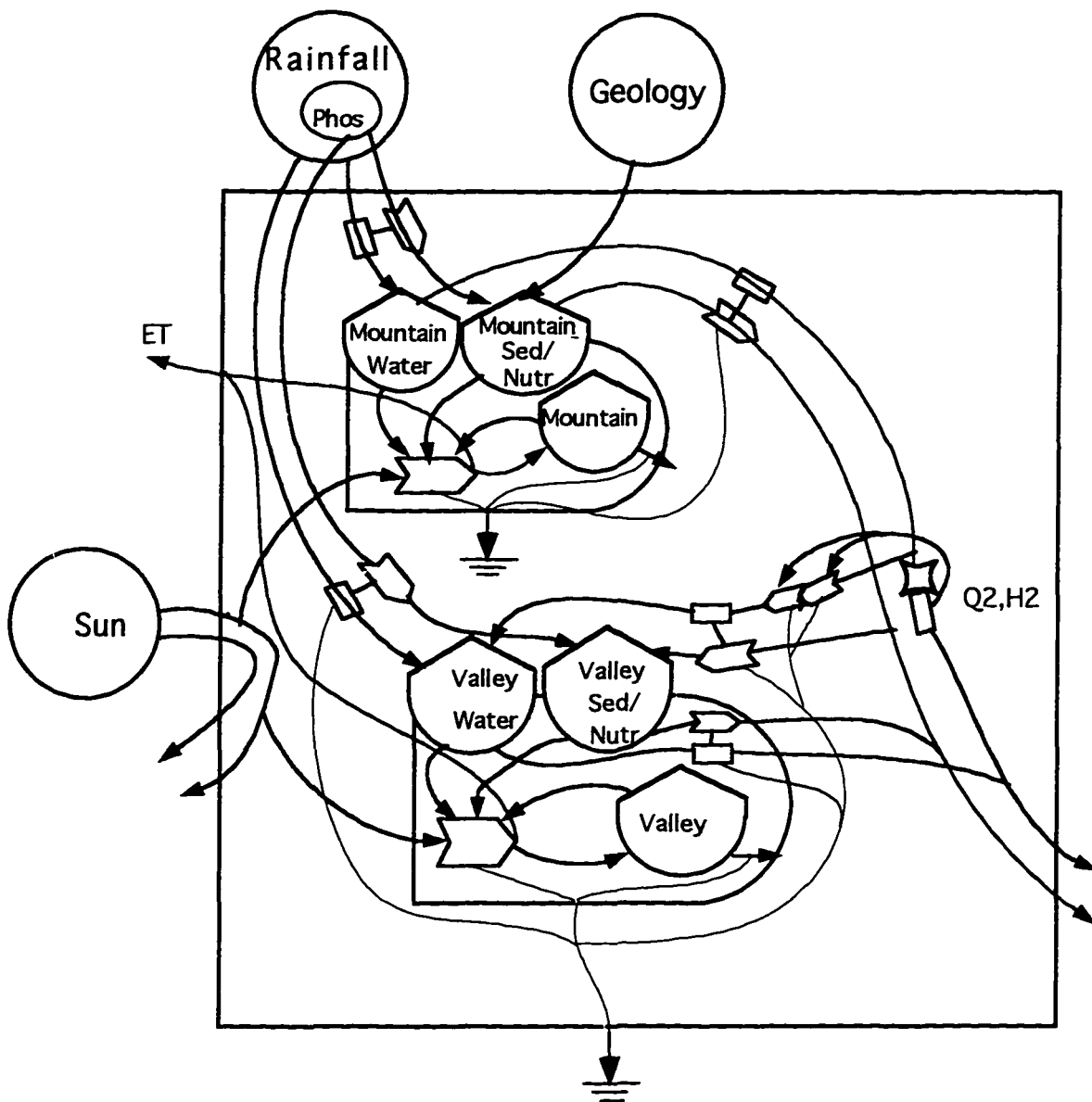


Figure 4.1. Aggregated energetic model for a natural (No-Dam) watershed (where Sed/ Nutr= nutrients in sediments and Phosp = phosphorus in rain)

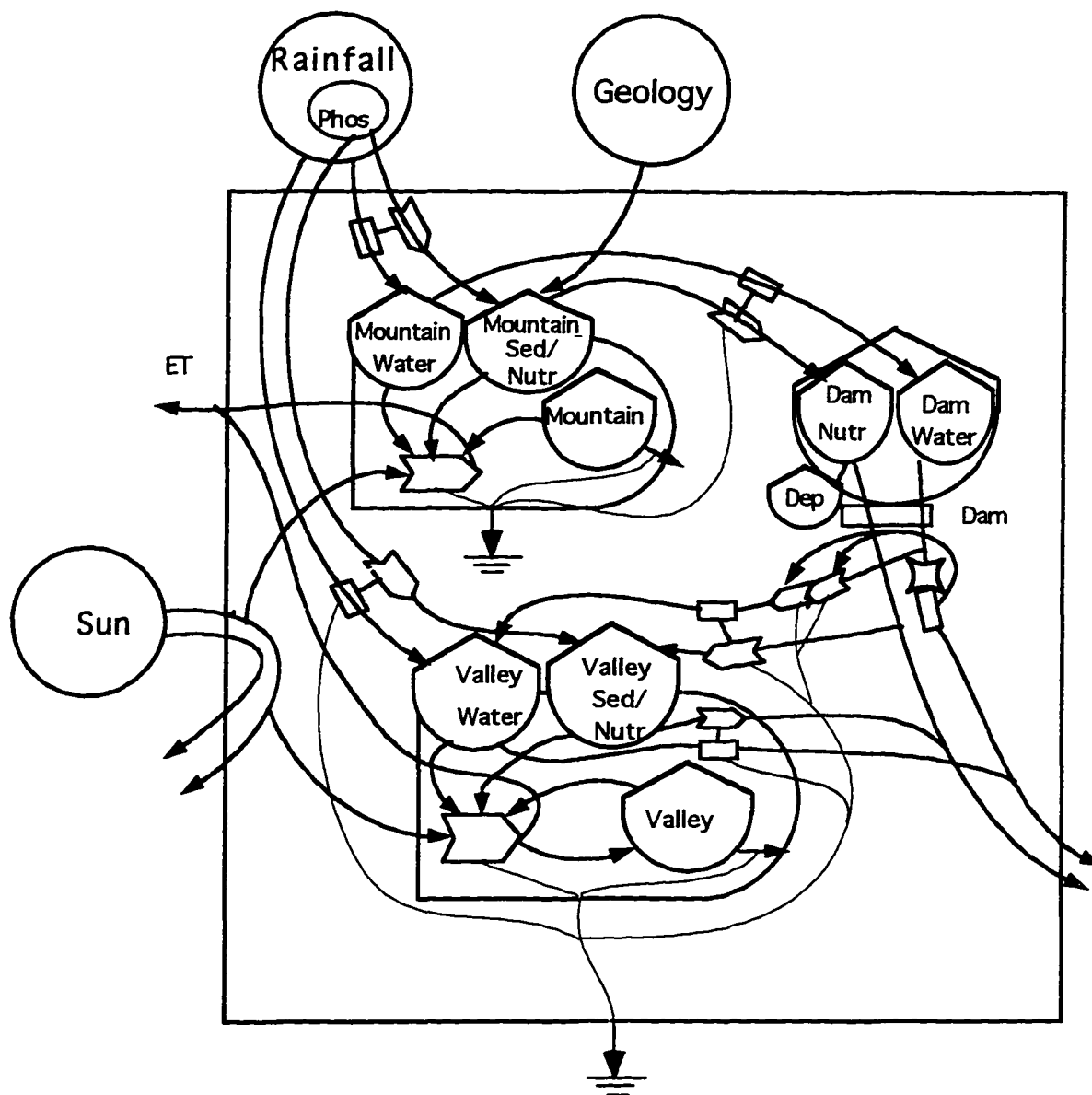
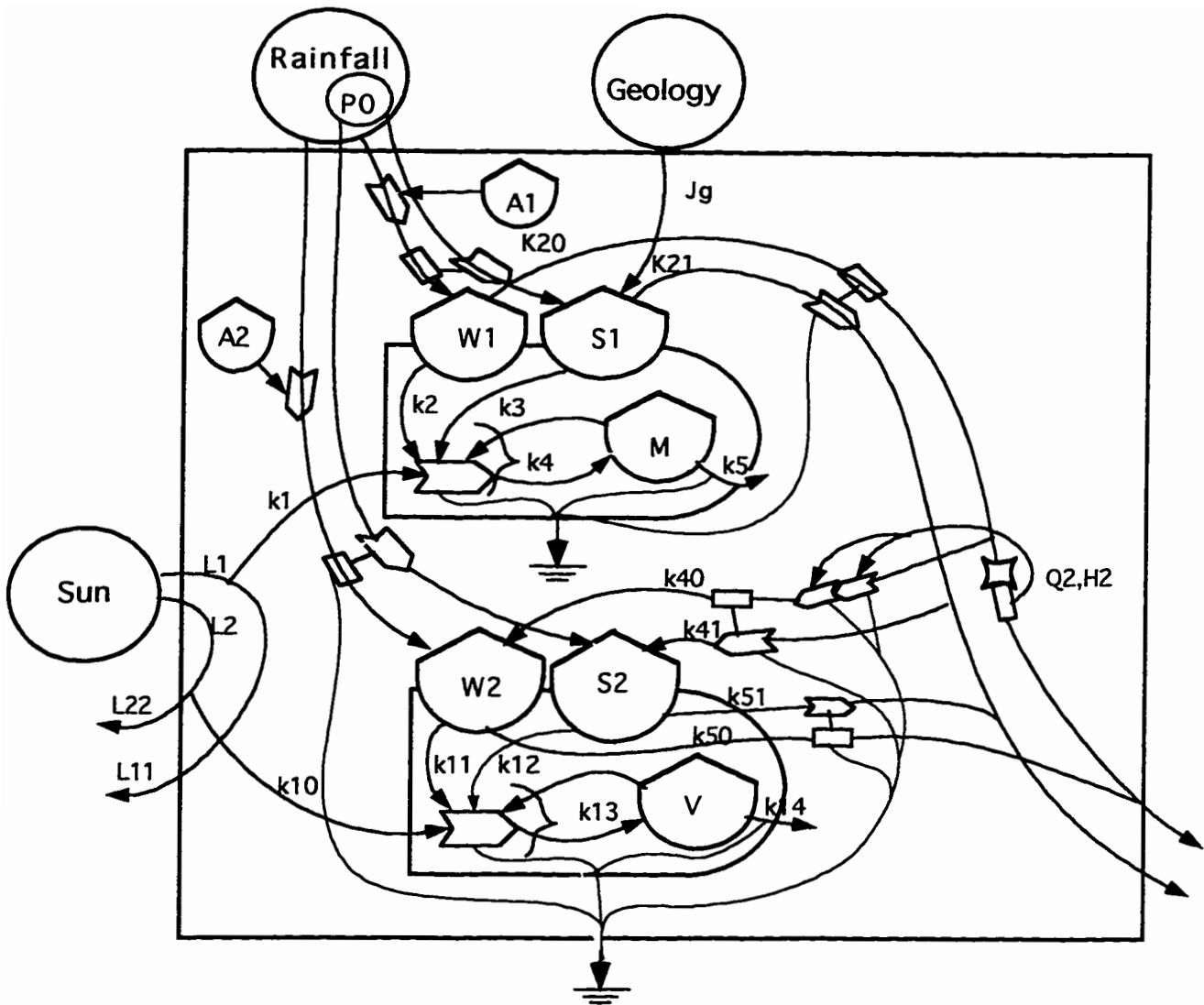
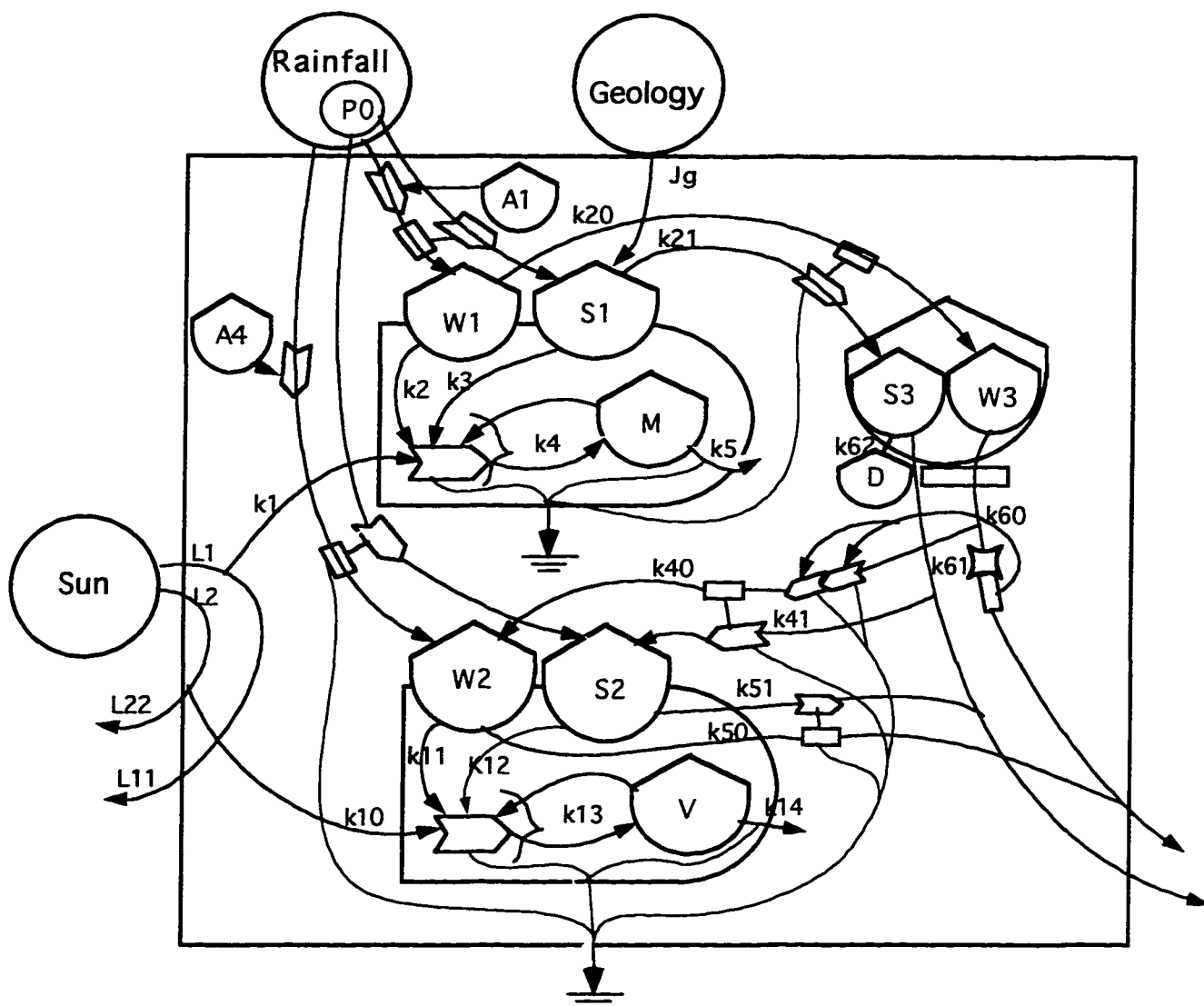


Figure 4.2. Aggregated energetic model for a watershed with dams (where Sed/ Nutr= nutrients in sediments, Phosp= phosphorus in rain and Dep= deposited phosphorus).



$$\begin{aligned}
 L11 &= L1(I) / (1 + K1*W1*S1*M) \\
 L22 &= L1(I) / (1 + K10*W2*S2*V) \\
 DM &= K4*L11*W1*S1*M - K5*M \\
 DV &= K13*L22*W2*S2*V - K14*V \\
 DW1 &= R0(I)*A1 - K2*L11*W1*S1*M - K20*W1 \\
 DS1 &= R0(I)*A1*P0 + Jg - K3*L11*S1*W1*M - K21*W1*S1 \\
 Q1 &= K20*W1 \\
 Q2 &= (((1 + 4*(K40/K)*Q1) ^{0.5}) - 1) / (2*(K40/K)) \\
 H2 &= Q2 / K \quad Q3 = K40 * ((Q2)^2) / K \\
 DW2 &= R0(I) * A2 + Q3 - K11*L22*W2*S2*V - K50*W2 \\
 DS2 &= K41*((Q2)^2) / K*S1 + R0(I) * A2*P0 - K12*L22*W2*S2*V - \\
 &\quad K51*W2*S2
 \end{aligned}$$

Figure 4.3. Equations relating main flows and storages for the No-Dam simulation model.



$$L11 = L1(I) / (1 + K1 * W1 * S1 * M) \quad L22 = L1(I) / (1 + K10 * W2 * S2 * V)$$

$$DM = K4 * L11 * W1 * S1 * M - K5 * M$$

$$DV = K13 * L22 * W2 * S2 * V - K14 * V$$

$$DW1 = R0(I) * A1 - K2 * L11 * W1 * S1 * M - K20 * W1$$

$$DS1 = R0(I) * A1 * P0 + Jg - K3 * L11 * S1 * W1 * M - K21 * W1 * S1$$

$$Q1 = K60 * W3$$

$$Q2 = (((1 + 4 * (K40 / K) * Q1) ^{0.5}) - 1) / (2 * (K40 / K))$$

$$H2 = Q2 / K$$

$$Q3 = K40 * ((Q2)^2) / K$$

$$DW2 = R0(I) * A4 + Q3 - K11 * L22 * W2 * S2 * V - K50 * W2$$

$$DS2 = K41 * ((Q2)^2) / K * S3 + R0(I) * A2 * P0 - K12 * L22 * W2 * S2 * V - K51 * W2 * S2$$

$$DW3 = K20 * W1 - K60 * W3$$

$$DS3 = K21 * W1 * S1 - K61 * W3 * S3 - K62 * S3$$

Figure 4.4. Equations relating main flows and storages for the One-Dam simulation model.

Rain falling in the mountain area (JR1) brings nutrients (JP1) to the area. They infiltrate into the mountain soil where they are stored for a brief period of time in W1 and S1 respectively. They are used together with the sunlight (L11) to produce the mountain structure (M). The geology of the mountain also reinforces the flow of nutrients (Jg) to the mountain system.

The water not used by the mountain system during the evapotranspiration process starts to move down hill, organizing the river network. It carries with it sediments and nutrients. During floods (i.e., when river stages are higher than a threshold depth (H2)), they are transferred to the valley system as water flow and nutrient flows. The transferring process to the valley is a function of the discharge (Q2) and river depth (H2) which is also a function of Q2. Therefore it is represented by a square function of river discharges ($Q2^2$).

The flooding water gives to the water storage in the valley (W2) and the nutrients and sediments to the sediment storage (S2). The rain falling in the valley also feeds these storages with water (JR2) and nutrients (JP2). The production of the valley (V), fueled by the sunlight reaching the area (L22), tap these storages of water and nutrients.

The stored water not used in the production process returns back to the downstream river. It takes with it some of the sediments and nutrients stored in the valley.

The construction of the dam is represented by the storages of water (W3) and nutrients (S3) in the reservoir (and a deposit of sediment and nutrients in the bottom of the reservoir (D)). River flows draining the mountain system are

dammed before reaching the valley. River flows leaving the dam take sediments and nutrient not retained by the dam to the downstream system.

Calibration of the Models

Models were calibrated for steady- state conditions (flow in = flow out) with monthly time step. Fig 4.5 and 4.6 display values assumed for the inputs, storage and flows in the No-Dam and One-Dam simulation models used to simulate the construction of dams in a Brazilian watershed (Jacupiranga river basin). The One-Dam alternative was based on the construction of a fictitious dam of 70 km² and about 70m deep in a major tributary (the Guarau river) of Jacupiranga river basin. The Two-Dam or Four-Dam alternatives are just river partitions of the One-Dam alternative. They represent the option of building two 35m dams or four 17.5m dams instead of one 70m dam.

Models were calibrated with local data or with data from similar ecosystems to those found in the area (Table 4.1). The 12 months rainfall and sunlight data used in simulation were based on average readings in the area. However, every three years a peak rainfall season was assumed, where the first 5-months rainfall data were 10 to 40% larger than the those assumed for the average years. River flows leaving mountain and valley systems were estimated from runoff ratios previously calculated in the emergy analysis of Jacupiranga river basin.

The mountain area (A1) draining to the dam was measured from a map. The valley area affected by the dam (A2) was estimated after defining the ratio of the dam drainage area to the total mountain area of the Jacupiranga river basin. The same ratio was then

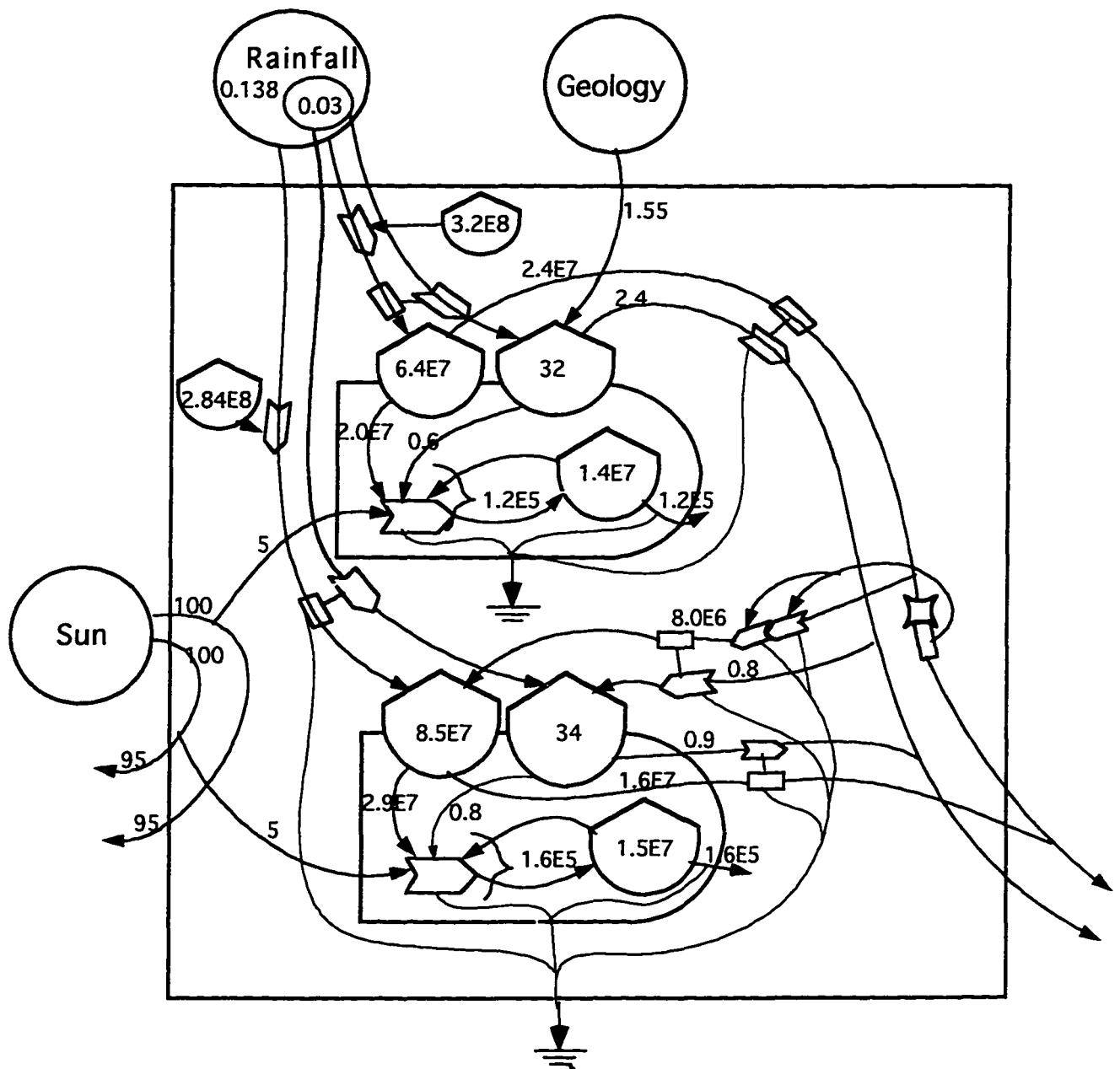


Figure 4.5. Calibration values for the No-Dam simulation model.

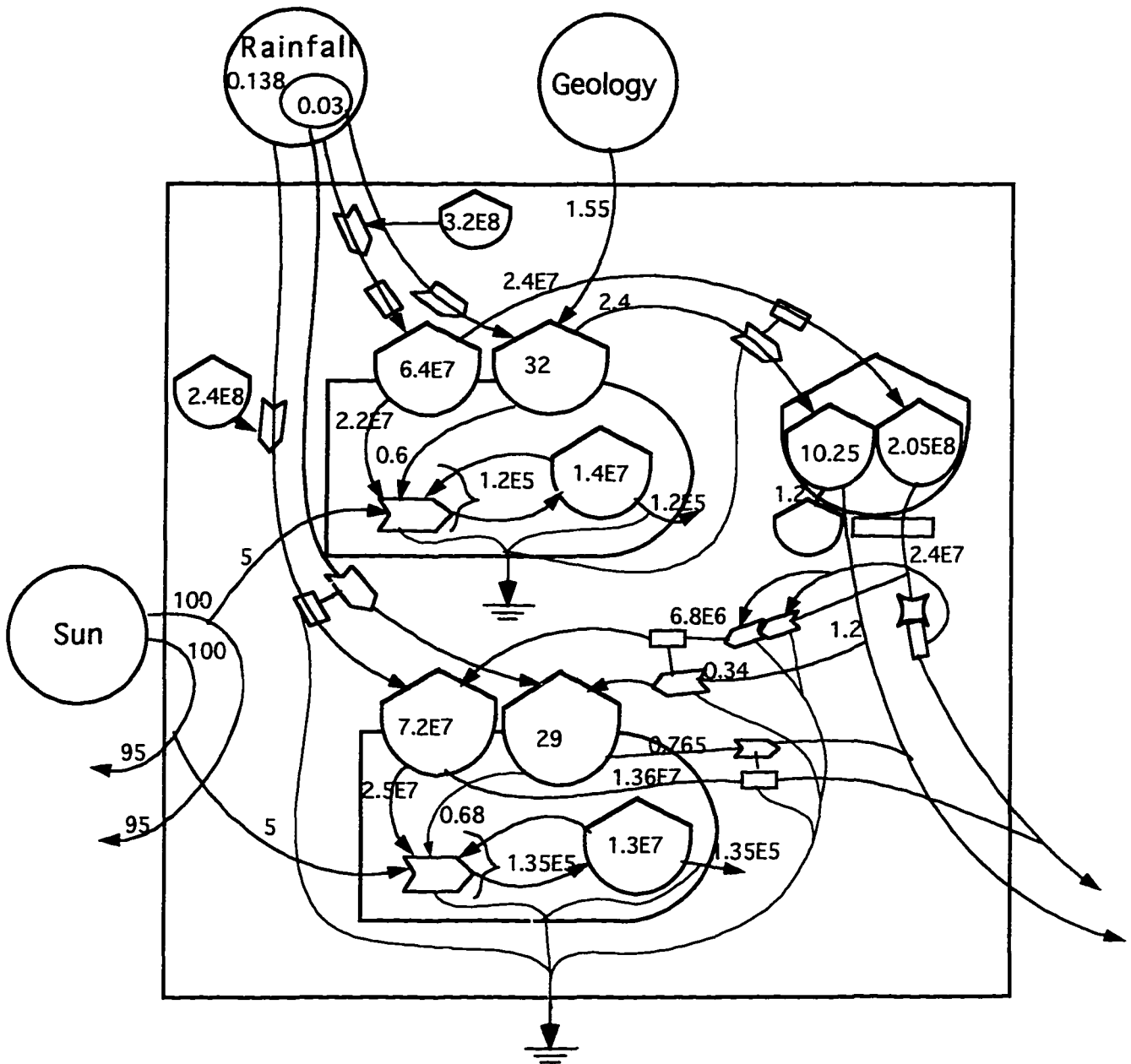


Figure 4.6. Calibration values for One-Dam simulation model.

Table 4.1. Data used in the calibration of models.

Symbols	Description	Values
L1	Solar insolation- Assumed average value was 100 and it would varied according to variation in insolation readings in the area. The monthly measurements in cal/ cm ² /yr from January to December were - 540, 500, 375, 290, 230, 200, 225, 270, 250, 340, 500, and 480. (Tundisi, 1982?)	from January to December- 154, 143, 107, 83, 66, 57, 64, 77, 71, 97, 143, 137.
R0	Rainfall- Average value for the whole basin was assumed to be 1.65 m/yr (or 0.1375 m/ month). The monthly rainfall was predicted to vary following data from Eldorado Paulista gauging station (24 31S and 48 06 W), where average monthly precipitation in mm during 1940 to 1991 would be :- 235.3, 220.2, 190.1, 97.2, 86.7, 75.3, 69.9, 53.5, 93.5, 123.8, 112.6, 163.5.(Engecorps,1982)	From January to December (normal year)- 0.26, 0.24, 0.21, 0.11, 0.09, 0.08, 0.08, 0.06, 0.10, 0.13, 0.12, 0.18. From January to April(for rainy year)- 0.29, 0.30, 0.29, 0.12.
A1	Mountain area- Upland area draining to the dam . (It was based on the upland areas of Guarau river in the Jacupiranga river basin, where dam was assumed to be built).	3.2E8 m ²
A2	Valley area- Floodplain area downstream of A1. (It was estimated as about 1/3 of the floodplain area of the Jacupiranga river basin , as A1 would represent 1/3 of the upland area in the basin).	2.84E8 m ²
A4	Valley area after construction= A2 minus area of the dam .	2.4E8 m ²
A5	Area of the dam	0.7E8 m ²

Table 4.1. Continued

P0	Phosphorus concentration in the rain was assumed to be 0.03 mg/l (according to global budget presented in Shlesinger, W H.1991)	0.03 mg/l
M	Mountain structure represented by the forest and soil biomass of a tropical rainforest. The total biomass was calculated the sum of tree biomass (276 ton/ha- tropical moist forest in the dry season in Panama- from Golley FB et al. 1975) and soil biomass (152 ton/ha, from Odum & Pigeon,1970)	428 ton/ha
V	Valley structure represented by the forest and soil biomass. Total biomass was the sum of plant biomass (377 ton/ha - tropical moist forest in the wet season in Panama- from Golley F B et al. 1975) and soil biomass (152 ton/ha, from Odum & Pigeon,1970).	530 ton/ha
W1	Water volume in the forest soil in the mountain system. It was assumed an average soil depth of 1m and porosity around of 0.2. Water volume was calculated as : W1= mountain area (A1)* soil depth* porosity = 3.2E8 m ² * 1m* 0.20= 6.4E7 m ³	6.4E7 m ³
W2	Water volume in the forest soil in the floodplain system. Calculations were done assuming average soil depth of 1.5m and porosity of 0.2. Then: W2= valley area(A2)* soil depth* porosity= = 2.84E8 m ² * 1.5m * 0.2= 8.5E7 m ³	8.5E7 m ³
W3	Water volume in the forest soil of the floodplain system after dam construction. Esimates were done for soil depth of 1.5m and porosity of 0.2, as follow: W3= valley area after dam (A4)* soil depth* porosity= = 2.4E8 m ² * 1.5m* 0.2= 7.2E7 m ³	7.2E7 m ³

Table 4.1. Continued.

S1	Available total Phosphorus in mountain soil compartment was assumed as 1 kg P/ ha. Therefore, for mountain area of 32000 ha , the Phosphorus weight would be: $S1 = 32000 \text{ ha} * 1 \text{ kg/ha} = 32000 \text{ kg} = 32 \text{ ton P.}$	32 ton
S2	Available Total Phosphorus in the valley soil compartment. Assuming 1.2 kg P/ha, the total Phosphorus in the valley compartment was: $S2 = \text{valley area (A2)} * \text{P concentration in soil} = 2.84 \text{ E4 ha} * 1.2 \text{ kg/ha} = 34080 \text{ kg} = 34 \text{ ton P.}$	34 ton
S3	Available total Phosphorus in the valley soil after dam construction , assuming Phosphorus concentration in the soil as 1.2 kg/ha: $S3 = \text{valley area after dam (A4)} * \text{P concentration} = 2.4 \text{ ha} * 1.2 = 28800 \text{ kg} = 29 \text{ tonP.}$	29 ton
JR1	Average volume of rain falling in the mountain system during a month period was estimated as the average monthly rain (0.1375 m/month) multiplied by the mountain area (A1).	4.4 E7 m3/ month
JR2	Average volume of rain falling in the valley system during a month period was estimated as the average monthly rain (0.1375 m/month) multiplied by the valley area (A1). (When dam was included , monthly rain was multiply by A4).	3.9 E 7 m3/ month (3.3 E7 m3/ month)
JP1	Average weight of Phosphorus in the monthly rain (JR1) falling in the montain system was estimated as JR1 multiplied by P0.	1.32 ton/ month
JP2	Average weight of Phosphorus in the monthly rain (JR2) falling in the valley system was estimated as JR2 multiplied by P0. (The same calculation was done for the alternative with dam, using the" with dam" JR2)	1.17 ton/ month (0.99 ton/ month)

Table 4.1. Continued

JG	Average Phosphorus contribution from the Geology of the mountain system. was estimated as the amount needed to balance Phosphorus use and output in the mountain system. Then $JG = (J2 + J21) - JP1$.	1.6 ton/month
J1	Percent of sunlight used by the mountain system. It was assumed as 5 out of 100.	5
J2	Soil water used in the production ("transpiration") of the mountain system was estimated as 45% of the rain falling in the mountain area. Then $J2 = 0.45 * 4.4E7 m3/month$	2.0 E7 m3/month
J3	Phosphorus from mountain soil used in the production system, assuming that most phosphorus used in production was recycled in the system and just 0.6 ton total P/ month was required for production.	0.6 ton/ month
J4	Gross primary production(GPP) less forest biomass used in the production process was estimated based on the assumption that net primary production (NPP) in form of litterfall and wood production was 12 ton/ha/yr. Taken NPP as 25% of GPP, this later would be equal to 48 ton/ha/yr. Assuming that 3 ton/ha/yr would return to production, the J4 flow was 45 ton/ha/yr or 3.75 ton/ ha/month. For the whole mountain area was 1.2E5 ton/month (or 3.75* 3.2E4 ha).	1.2E5 ton/month
J5	Mountain production used by consumers and respired. The system was assumed in steady-state and therefore $J5 = J4$.	1.2E5 ton/month
J10	Percent of sunlight used in the production of the valley system. It was assumed as 5 out 100.	5

Table 4.1. Continued

J11	Soil water used in the production (“transpiration”) of the valley system was estimated as 75% of the rain falling in the valley area. This means $J12 = 0.75 * R0 * A2$ m3/month. (When dam was included, $J12 = 0.75 * R0 * A3$ m3/month)	2.9E7 m3/month (with dam- 2.5E7 m3/month)
J12	Phosphorus from the valley soil used in the production system was assumed that most phosphorus would recycled in the system and just 0.8 ton/month was necessary to replace some losses in the system. (When dam was included J13 was assumed 15% less(0.68) following the reduction in floodpain area).	0.8 ton/month (0.68 ton/month)
J13	Gross primary production(GPP) less forest biomass used in the production process was estimated based on the assumption that net primary production (NPP) in form of litterfall and wood production was 18 ton/ha/yr. Taken NPP as 25% of GPP, this later would be equal to 72 ton/ha/yr. Assuming that 4 ton/ha/yr would return to production, the J4 flow was 68 ton/ha/yr or 5.7 ton/ ha/month. For the whole mountain area was $J13 = 5.7 * A2$ without dam or $J13 = 5.7 * A3$ with dam.	1.6E5 ton/month (with dam 1.35E5 ton/ month)
J14	Valley production used by consumers and respired. The system was assumed in steady-state and therefore $J5 = J4$.	1.6E5 ton/month (with dam, 1.35E5 ton/month)
J20	Runoff from soil water in the mountain. was estimated as the difference between rainfall and water used by the production system (“Evapotranspired”). Then $J20 = JR1 - J2$	2.4E7 m3/month
J21	Phosphorus from mountain soil carried by the runoff flow (J20). It was assumed that runoff had concentration of 0.1 mg P/l. Then , total phosphorus carried by J20 would be: $J21 = J20 * 0.1 \text{ g/m}^3 * 1\text{E-}6 \text{ ton/g}$	2.4 ton/month

Table 4.1. Continued

J40	Average river flow that runs through the floodplain was assumed that about 33% of river flows through the floodplain. This means that $J40 = 0.33 * J20$. (When dam was included, and valley area reduced 15%, then assumed value for J40 also reduced 15%. Then J40 for the dam alternative was $6.8E6$ m ³ /month).	8E6 m ³ /month (6.8E6 m ³ /month)
J41	Phosphorus that is taken to the floodplain with the flooding waters (J40) was estimated multiplying river waters overbanking by phosphorus concentration in river waters ($J41 = J40 * 0.10g/m^3 * 1E-6ton/g$). (The same consideration was used for the estimates with dam, considering the modified J40)	0.8 ton/ month (0.68 ton/month)
J50	Runoff from floodplain water storage (W2) in the valley system. It was calculated as the difference between inputs (JR2+ J40) and the output (J12). Then $J50 = (JR2+J40) - J12$. (However, because J40 can assume very different values than the calibrated value and most of them equal zero, the value considered in this equation was $J40 - 0.1E6$. Then $J50 = (JR2+J40-0.1E6) - J12$. (When dam was included, the original flow was reduced 15% following the 15% reduction in floodplain area).	1.6E7 m ³ /month (with dam 1.36E7 m ³ /month)
J51	Phosphorus leaving the floodplain with J50. It was calculated as the difference between the inputs (Jp2 +J41) minus the output (J13). The same correction on the estimates of J50 was applied here. Then $J51 = (Jp2 + J41 - 0.1) - J13$. (flow of phosphorus was reduced when dam was included, equivalent to the water runoff decrease).	0.9 ton/month (with dam 0.765 ton/month)
J60	River flow leaving the water storage in the reservoir. It was estimated as equal as the flow entering in the dam which is equal to the runoff from the mountain system(J20).	2.4E7 m ² /month

Table 4.1. Continued.

J61	Phosphorus leaving the dam with the river flow was estimated as half of total P entering in the dam (J21). The other half is entrapped in the dam.(J62).	1.2 ton/month
J62	Phosphorus deposited in the dam.	1.2 ton/ month

applied to the total floodplain area of Jacupiranga river, to define the valley area affected by the dam (A2).

Considering that the reservoir would be used for hydroelectric production, it would be maintained as full as possible, and water would be released from the surface of the lake. Therefore, just minor percent of the total volume would fluctuate with changes in the inflow. It was assumed that just 6 % of the total volume would fluctuate, resulting in an “active” volume of $2.05E8$ m³ for One-Dam alternative, $9.80E7$ m³ for Two-Dams alternative and $4.9E7$ m³ for Four-Dams alternative.

Equations

Differential equations were written for each storage , the input flows and the flooding phenomena. They defined how variables would change with time. They were based on systems concepts presented in the “System Ecology “ book (Odum, 1983). Figures 4.3 and 4.4 shows the variables and coefficients , followed by the equations used in the models.

Coefficients

A spreadsheet program was used to estimate the coefficients. They are calculated from the mathematical expression defining the flows and the calibrated value assumed for that flow. Tables C.1, C.2, C.3 and C.4 were prepared for the calculation of coefficients of the No Dam, One-Dam, Two-Dams and Four-Dam models respectively.

Program

The simulation model program was written in Qbasic. It included statements to introduce the starting variables, the coefficient values, the changing equations, and the plotting statements. The main program (No Dam model) was written to simulate the

natural contribution of the uplands to the valley production during flood events (Figure C.1) .Then the program was modified to include statements that would represent the construction of one dam between uplands and lowlands zones (Figure C.2).

Two other alternatives- the Two- Dams and the Four Dams alternatives- were evaluated using the One- Dam model program, but changing the values for the reservoir water storage (W3) and phosphorus storage (S3).

Simulation

Models ran for a period of 300 months. Rainfall was given a large pulse every three years. Simulation was done in Qbasic and the values assumed by the state variables were transferred to Excel spreadsheet. Graphs were then produced, displaying and comparing results of No Dam, One- Dam, Two-Dams and Four-Dams simulations.

Simulation Results

Rainfall , River Stages and Water Storages

No Dam alternative

Rainfall was programmed to display a “regular” annual fluctuation for two consecutive years and a “peak” rainfall season in the third year. Maximum rain depth was 0.26 m/month during regular year and 0.30 m /month during the “peak” rainfall year. Rain depths fluctuated as shown in Chart A of Figure 4.7. River stages oscillated during regular and peak years, causing river water overbaking, flooding and fertilizer the valley.

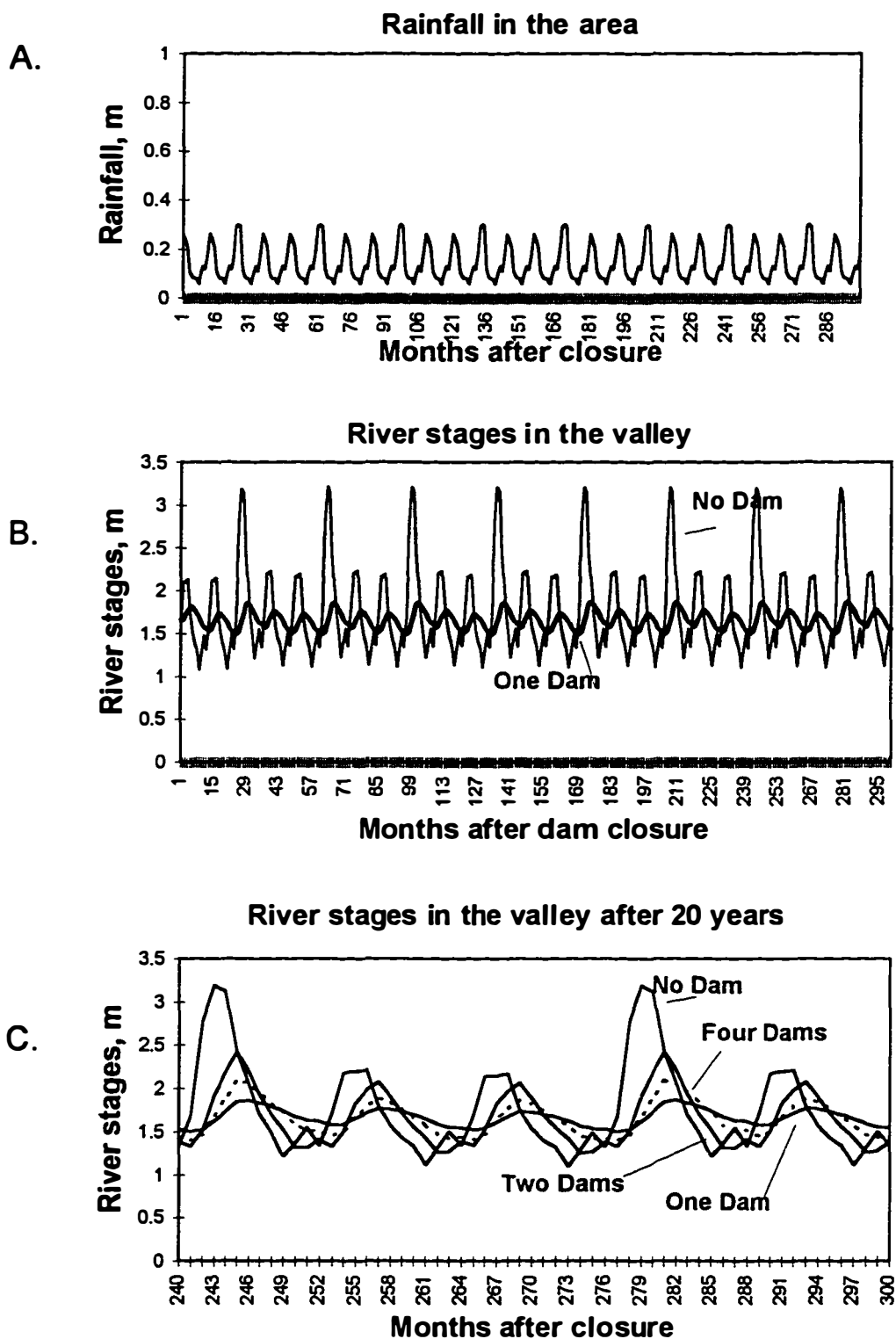


Figure 4.7. A. Simulated monthly rain depths. B. River Stages for the No- Dam and One- Dam simulated alternatives. C. River stages for the steady- state conditions of No- dam, One-Dam, Two- Dams and Four- Dams alternatives.

They reached 2.1m during a regular year and about 2.7 m during peak years (Charts B and C in Figure 4.7).

The shallow water storages in the mountain (W1) and valley (W2) fluctuated with the rainfall and river stages. More accentuated fluctuations occurred in the valley water, where water volume ranged from $6.0E7$ to $17.5E7$ m³ (Charts A and B in Figure 4.8). These large increase of water volume in the valley were caused by the excess of river waters overbanking in to the floodplain . The intense evapotranspiration and accelerated production following the flooding events caused the drawdown of the valley waters.

With Dams Alternatives

When dams were included in the simulation, it caused a dampening in the pulsing of the downstream flow as shown in Charts B and C of Figures 4.7. Maximum river stages reached by the One-dam alternative would be around 1.8 m.

For the Two-Dams and the Four- Dam alternatives , river reached maximum stages of 2.1m and 2.2 m respectively. Therefore the Two and the Four-Dams alternatives provided equivalent stage fluctuation to the No- Dam alternative in the regular rain years. But during peak rainfall years, these alternatives did not reproduce the extension of flooding of the No-Dam alternative. For the One-Dam alternative, the downstream fluctuation would be always much smaller than the No-Dam alternative.

The water storages for the all alternatives with dams fluctuated according to the monthly variation of rainfall (Figure 4.8), but with reduced amplitude when compared to the fluctuation in the No-Dam alternative. There was less river water supplied to the valley, and mainly there was reduced production. In fact, simulation results for all

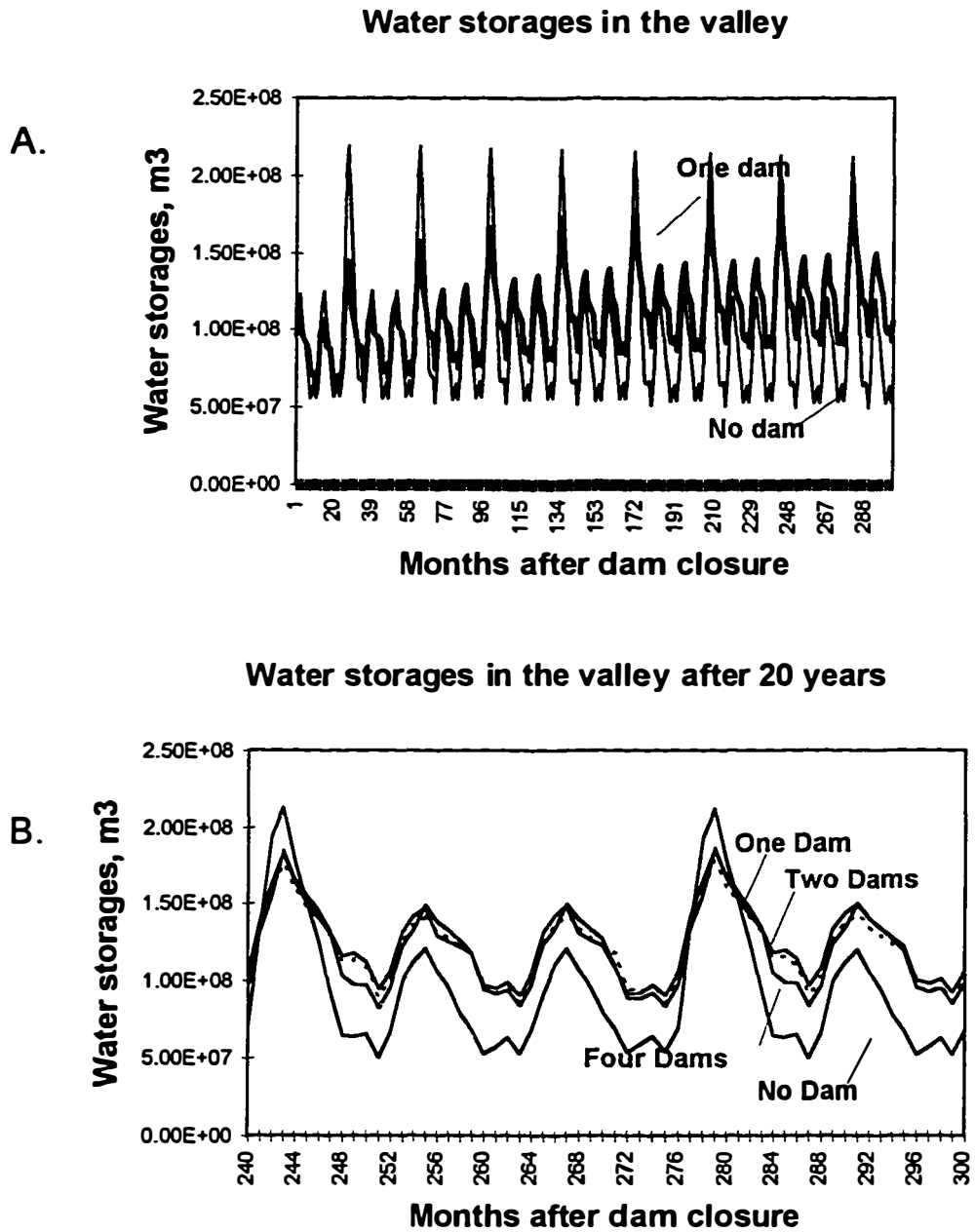


Figure 4.8.A.Simulated results of water storages in the valley for No- Dam and One-Dam alternatives.B. Water storages for the steady- state conditions of the No- Dam, One- Dam, Two- Dams and Four- Dams simulation models.

alternatives with dams indicated an increase in the water storages in the valley (Chart A in Figure 4.8), leading to potential changes in plant composition in the area.

Phosphorus

When the No-Dam model was simulated, the available phosphorus increased in the mountain storage during regular rainfall years, and subsequently was washed out to the downstream sectors in the peak rainfall years. The flooding water transferred much of the phosphorus to valley storage, reaching a maximum after the mountain wash out.

The construction of dams reduced the transference of the phosphorus to the valley. Some phosphorus was held in the dam and less phosphorus reached the floodplain area due to reduction in the flood pulse. Simulation results indicated a significant decrease in the available phosphorus storage in the valley after dam closure for all alternatives with dam (Chart A in Figure 4.9). Average stored weight of phosphorus in the floodplain area decreased to around 20-25 ton, when the original values for the No-Dam alternative was around 33 ton (Chart B in Figure 4.9).

Biomass and productivity

The construction of dams caused a decline in the valley standing biomass/ area (Chart A in Figure 4.10). After 20 years of dam construction, the standing biomass/ area was around 405 ton/ ha, 430 ton/ ha or 440 ton/ ha for the One- Dam, Two- Dams and

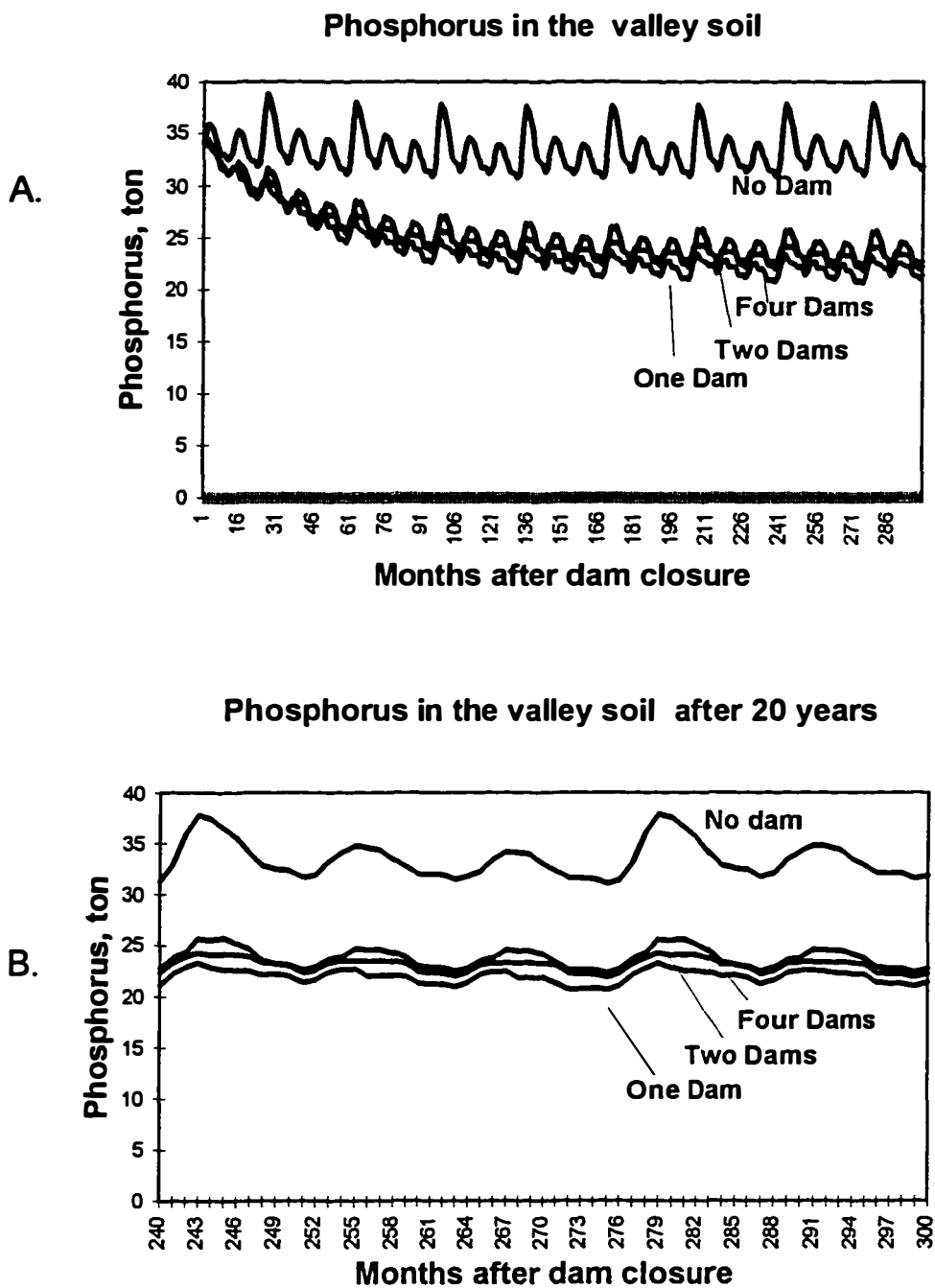


Figure 4.9. A. Simulated results of available phosphorus in the valley for the No-Dam, One-Dam, Two- Dams and Four- Dams alternatives. B. Phosphorus storages in the valley for the steady- state conditions of the No- Dam, One- Dam, Two- Dams and Four- Dams simulation models.

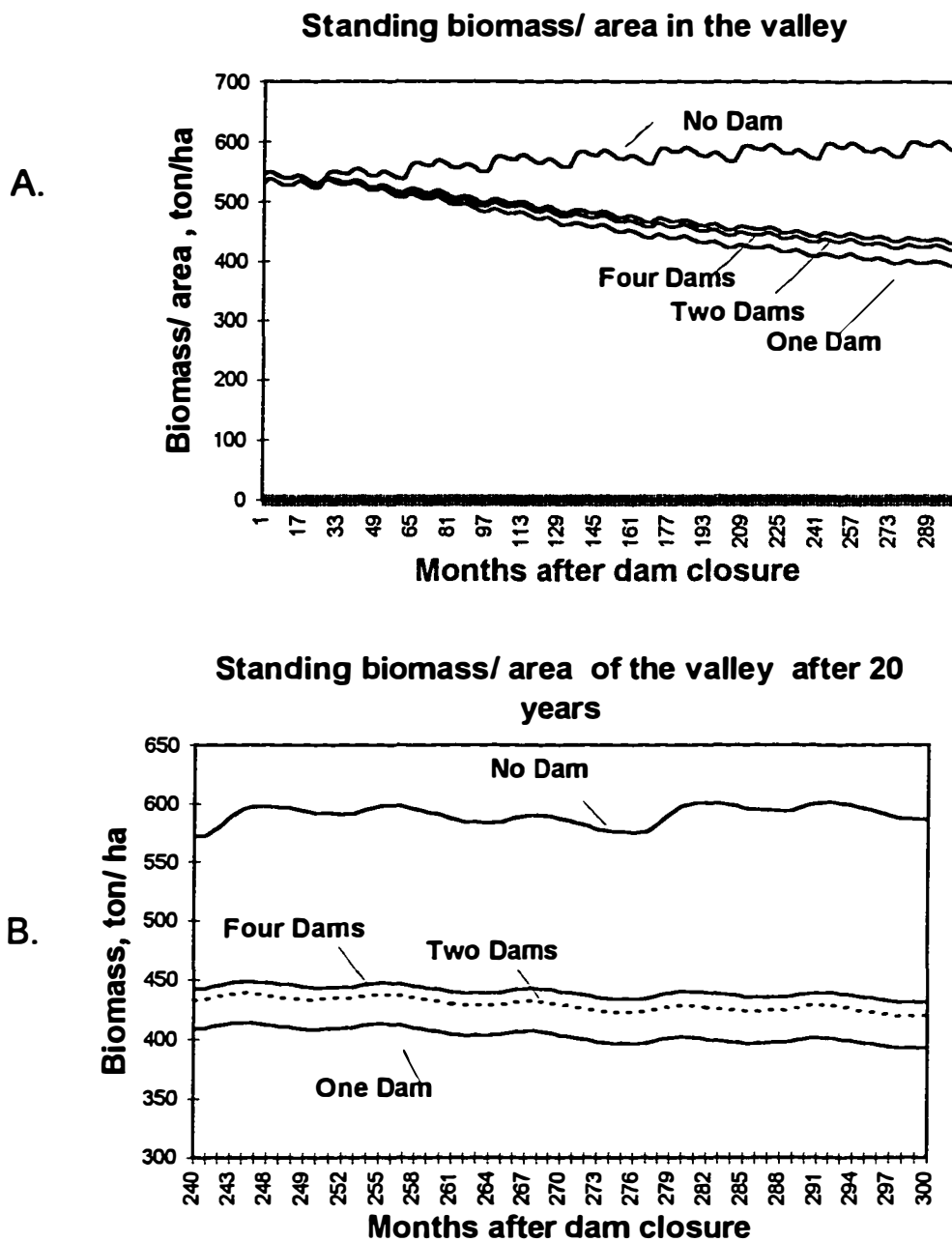


Figure 4.10.A. Simulated results of Standing Biomass/ area in the valley for the No- Dam, One-Dam, Two- Dams and Four- Dams alternatives. B. Standing biomass/ area in the valley for the steady- state conditions of the No- Dam, One Dam, Two- Dams and Four- Dams simulation models.

Four- Dam alternatives respectively. The original standing biomass/ area for the No- Dam alternative was around 500 ton/ ha (Chart B in Figure 4.10).

The productivity of the valley showed a very large amplitude during regular, and especially during peak years, for the simulation of the No-Dam alternative. It ranged from 3 to 8.5 ton/ha/month during regular years and 3 to 9.5 ton/ha/month during peak years (Chart A in Figure 4.11).

However, when the alternatives with dams were simulated, the range of productivity progressively decreased with time (Chart A in Figure 4.11). After 20 years, the maximum productivity ranged from 5.0 ton/ha/month for the One- Dam alternative to 6.5 ton/ha/month for Two and Four- Dam alternatives.

Average Results of the Steady- State Conditions

Simulation models started to reach steady state conditions after running for about 20 years. Average 5 year- monthly results, from simulation of the 20th to the 25th year, were compared (Table 4.2). Ratio of the results for alternatives with dams to the results of the No Dam simulation model were also estimated (Figure 4.12).

Average results for the water stages did not differ very much. Alternatives with dams had average water stages around 1.66m whereas the No- Dam alternative had average water stage of 1.67 m.

However, the average volume of water overflowing the river channel differed for the simulated alternatives. In One, Two or Four dams alternatives the volume of flooding waters was 58% , 74% and 85% respectively of the volume of the No Dam alternative. The differences in flooding water resulted in different monthly productivity in the valley.

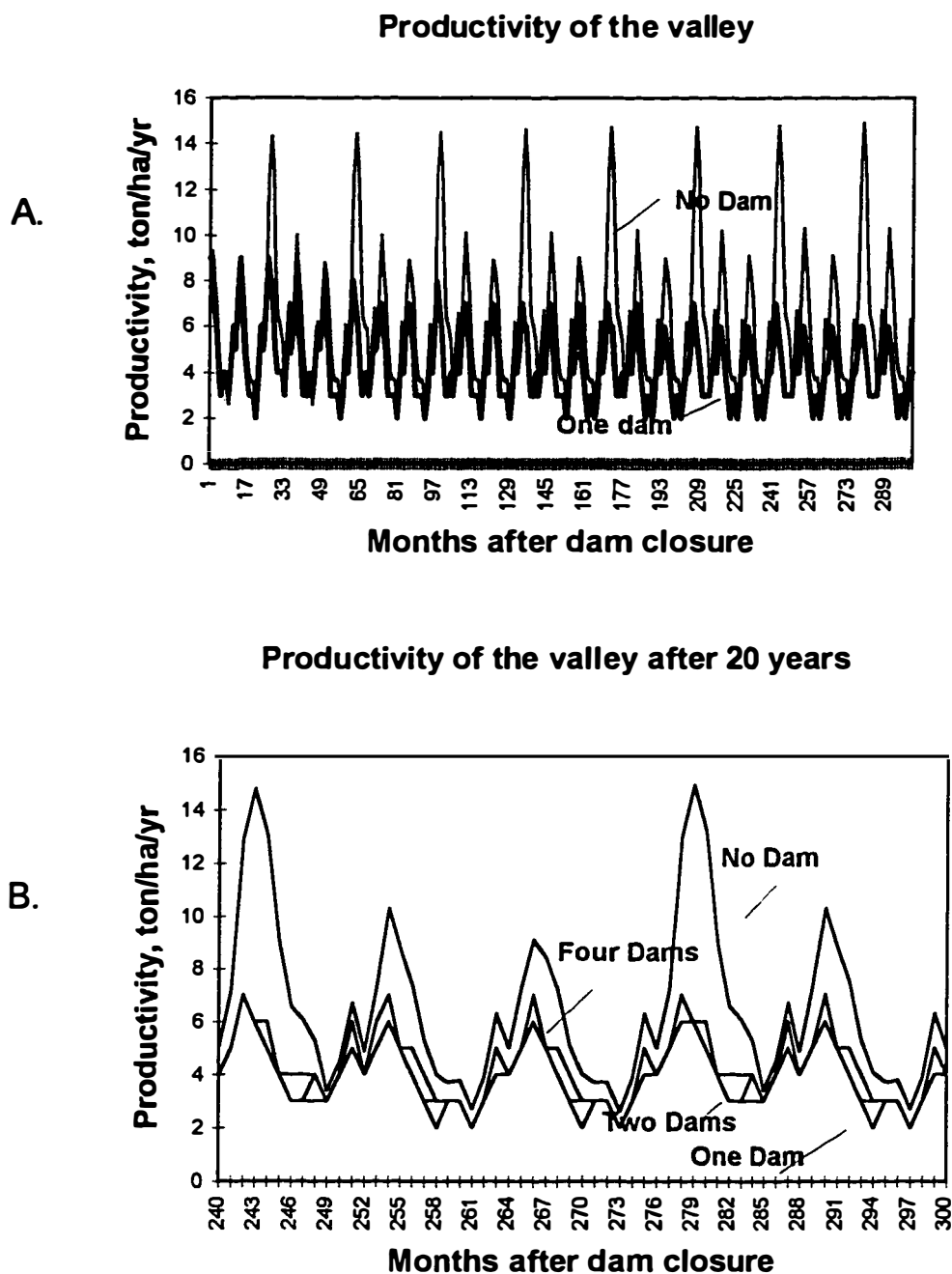


Figure 4.11.A. Simulated results of productivity in the valley for the No- Dam, One-Dam, Two- Dams and Four- Dams alternatives. B. Productivity in the valle for the steady- state conditions of the No- Dam, One- Dam, Two- Dams and Four- Dams simulation models.

Table 4.2.
Comparison of 5-years monthly average results of the simulated model.

Parameter	No-Dam	One-Dam	Two-Dams	Four-Dams
Water Stages(H2)	1.77	1.67	1.66	1.65
	1.00	0.94	0.94	0.93
Overflow(Q3)	6.89E+06	2.91E+06	3.70E+06	4.26E+06
	1.00	0.42	0.54	0.62
Productivity	6.52	3.92	4.16	4.33
	1.00	0.60	0.64	0.66
Primary Production	591	403	429	440
	1.00	0.68	0.73	0.74

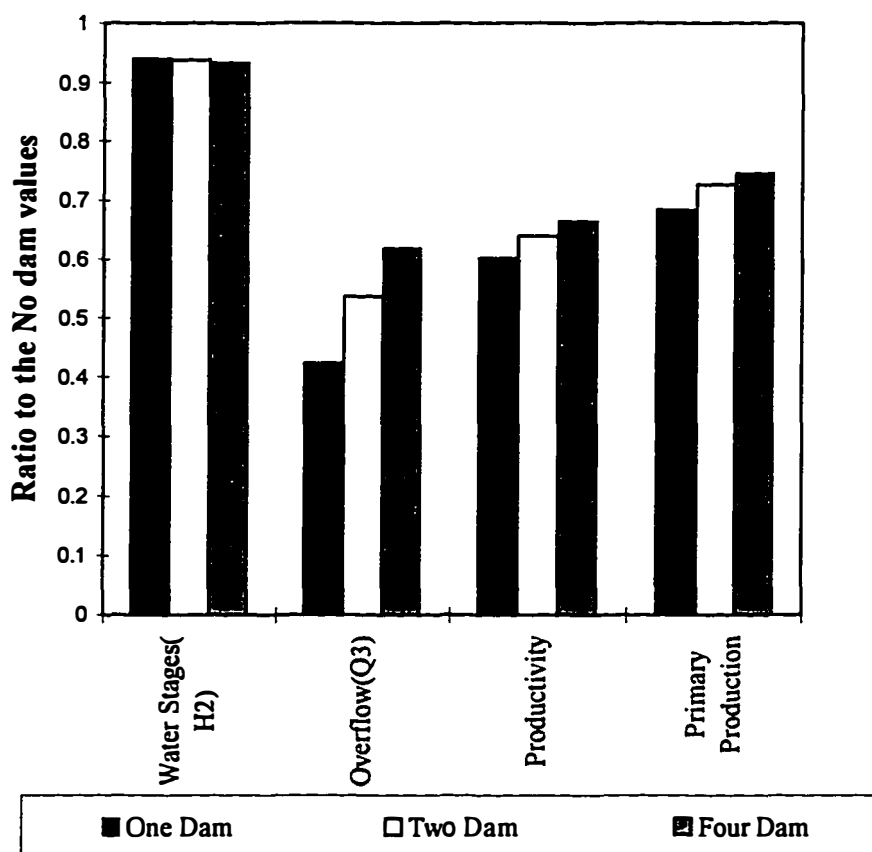


Figure 4.12. Ratio of values for alternatives with dam to values for No- Dam alternative.

Average monthly primary production varied from 3.9 ton/ha , 4.2 ton/ha and 4.3 ton/ha for the One, Two and Four- Dams alternatives respectively, whereas it was 5.3 ton/ha for the No-Dam alternative.

Variations in average standing biomass followed those of the productivity closely. Standing biomass for One, Two and Four-Dams simulation models were respectively 80%, 85% and 87% of the biomass of No-Dam alternative.

CHAPTER FIVE

DISCUSSION

Evapotranspired Chemical Potential Energy as Measure of Productivity

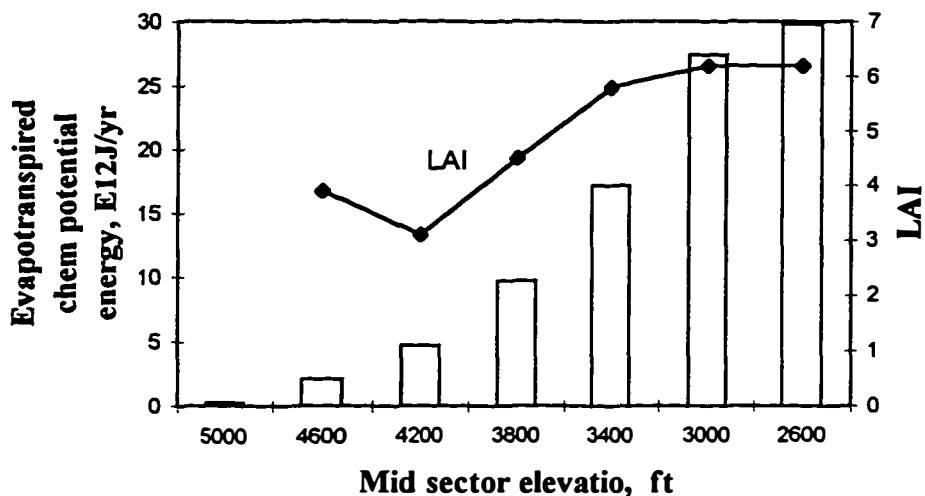
This study uses the energetic measurements of transpiration, in the form of evapotranspired chemical potential energy, as a predictor of the primary productivity in the area. Previous studies have shown the correlation between transpiration and primary productivity. Rosenzweig (1968), working with worldwide data from mature terrestrial plant communities, found a linear correlation between the net above ground productivity and actual evapotranspiration for those systems. He attributed the relationship to the fact that actual evapotranspiration measured simultaneously the availability of water and solar energy, which are the most important resources in photosynthesis.

Meentemeyer et al. (1982) verified that worldwide data on leaf and total litter production correlated very well ($r = 0.89$) with estimates of annual actual evapotranspiration. A linear relationship between daytime fixation of carbon and evapotranspiration was also observed by Burns (1978) when studying the productivity of the wetland communities in Fakahatchee Strand area in South Florida.

In this study, the estimated evapotranspired chemical potential energy in the elevational sectors of Coweeta river basin correlated well with Leaf Area Index measurements done in the area ($r^2 = 0.86$) (Figure 5.1). The volume of water

Evapotranspired chemical potential energy and Leaf Area Index in the Coweeta watershed

A.



B.

Correlation between evapotranspired chemical potential energy and Leaf Area Index in the Coweeta watershed

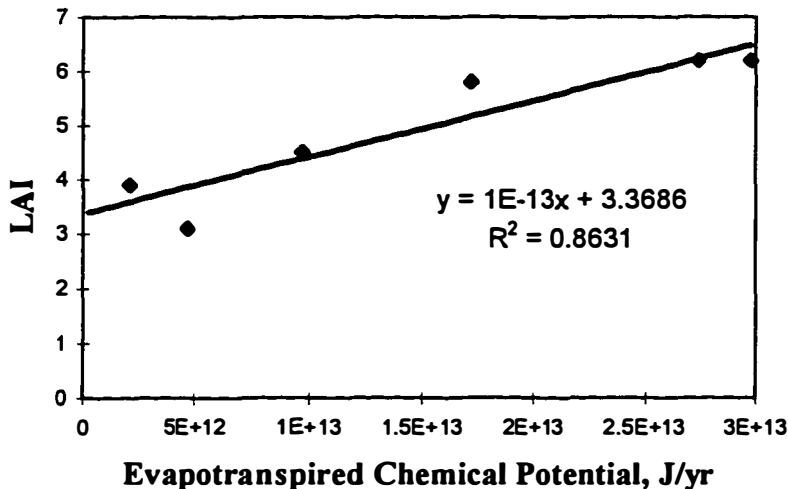


Figure 5.1. Correlating evapotranspired chemical potential energy (Cet) with productivity at different elevations of the Coweeta watershed, using : A. Estimated values for the evapotranspired chemical potential (Cet) and Leaf Area Index (LAI) measurements in the Coweeta watershed. B. Correlation curve and equation for the evapotranspired chemical potential (Cet) and LAI data of the Coweeta watershed.

evapotranspired was calculated as the actual evapotranspiration, as suggested by Rosenweig 1968, by subtracting runoff and infiltration from the precipitation in the area.

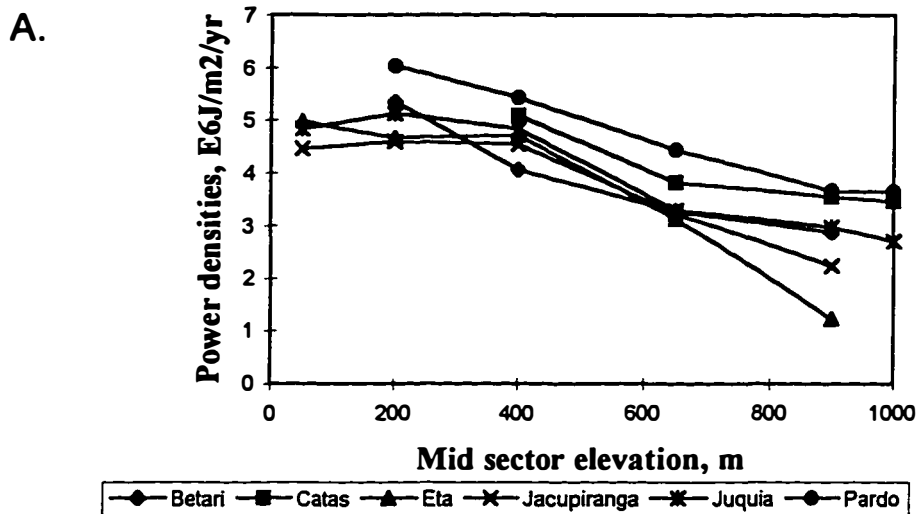
Increase of Evapotranspired Chemical Potential Power Densities at Lower Elevations

The evapotranspired chemical potential power densities (Cetd) was observed to increase in a straight or asymptotical shape towards the lower sectors of all evaluated watersheds (Charts A and B in Figure 5.2). An increase in evapotranspiration (and consequently primary production) towards the lower elevations of the basins was explained by an increase in the vapor pressure deficit and a decrease of the cloudiness in the lower elevations (Jones, 1992).

The aboveground net primary production of climax forests of the Great Smoke Mountain was found to increase asymptotically towards lower elevations of the mountain (Wittaker and Marks, 1975). Also, litterfall data from tropical mountain forests assembled by Grubb (1977) indicated the same trend. Litterfall measurements ranged from 5.0 to 6.5 t/ha/yr in upper mountain forests (above 1500m elevation) to 7.5 to 13.5 t/ha/yr in the lowlands rainforests (below 200m elevation).

In the Brazilian watersheds, the chemical potential evapotranspired power density (Cetd) increased from $3.0 \text{ E6 J/m}^2/\text{yr}$ at the 1000m mountain top to about $5.5\text{E6 J/m}^2/\text{yr}$ at 50m valley (Chart A in Figure 5.2). For the Coweeta river system, the evapotranspired chemical potential power density (Cetd) increased from 5.0E6 to $8.0\text{E6 J/m}^2/\text{yr}$ when elevations decreased from 1000m to 600m. (Chart B in Figure 5.2). These results indicated that relatively more transpiration (and therefore production) was occurring in the Coweeta

**Evapotranspired chemical potential power densities
for the large Brazilian watersheds**



**Evapotranspired chemical potential power densities
of the Coweeta river system**

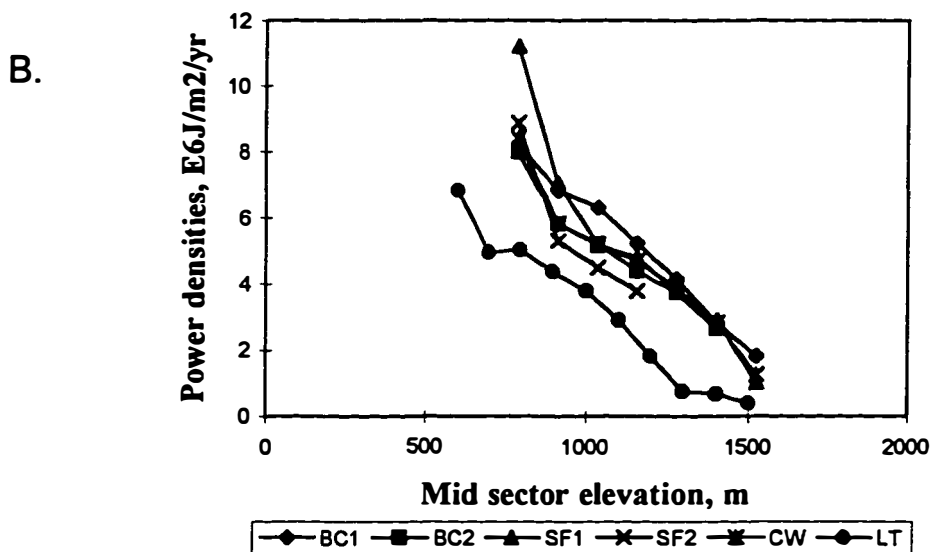


Figure 5.2. Increasing the evapotranspired chemical potential power densities (Cetd) with decreasing elevations in the basin, in :A. The large evaluated Brazilian watersheds; B. The Coweeta river system.

river system than in the Ribeira de Iguape watershed. However, it may be not appropriate to compare the *absolute* rates estimated for individual sectors of the Coweeta River basin to the Brazilian watersheds, because of the differences in latitudes.

Energetics of Bowl-shaped River Basins

Leopold et al. (1964) proposed that due to the typical increase in discharge and decrease in the particle sizes in downstream sectors of the rivers, their longitudinal profile tended to be concave upward. This makes a bowl-shaped basin. However, these authors also recognized that even rivers flowing in arid regions could develop a concave profile, suggesting that the decreasing gradient downstream depended on more than just increasing discharges. Moreover, they also verified that there were rivers with portions of their profiles convex to the sky, such as the plateau basins evaluated in this study.

They proposed an energetic explanation for the concave shape. The shape is the result of a uniform use of power per unit length of river channel, where the principle of the minimum rate of work (Prigogine, 1947) was operating.

Availability and the Use of the Geopotential Energies

The energetic evaluation of the concave river basins in this study revealed that the available geopotential energy inflowing in the system was evenly distributed along the basin profile, although the land area increased in the lower sectors of the basin (Chart A.1 in Figure 5.3). Also, that the available geopotential energy was provided to the river basin

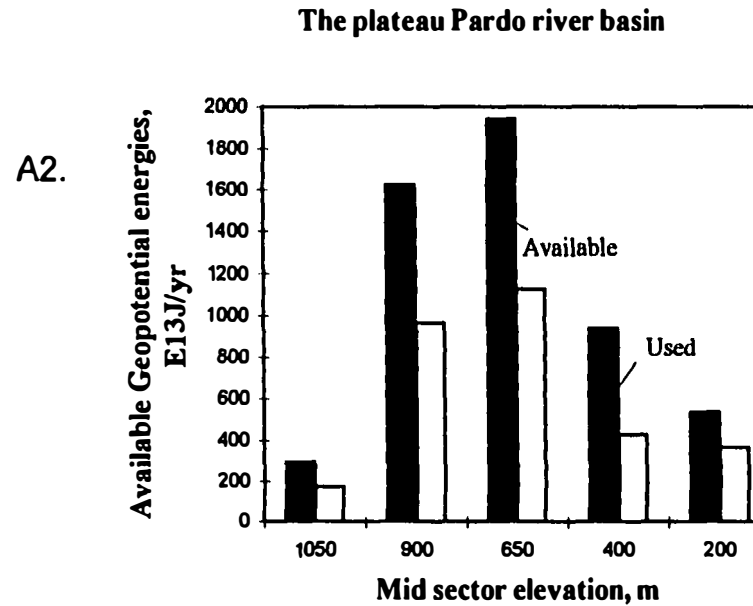
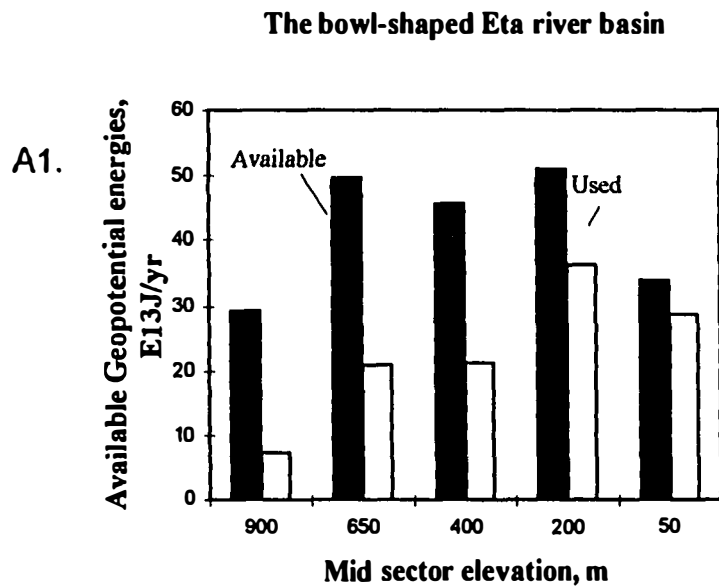
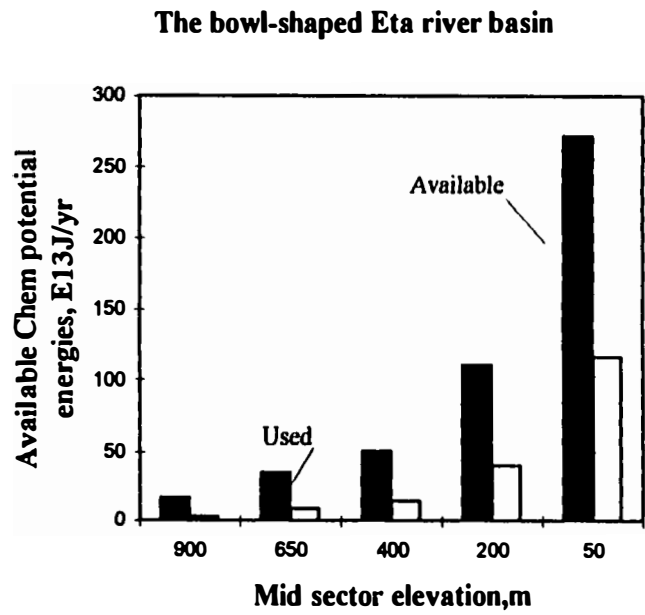


Figure 5.3. Comparison between water energy distribution in a bowl-shaped Eta river basin (left) and a plateau Pardo river basin (right): **A.** Available water geopotential energy; **B.** Available water chemical potential energy; **C.** Proportion of the geopotential energy available in form of rain and river; **D.** Proportion of the geopotential energy used in form of rain and river; **E.** Proportion of chemical potential energy available in form of rain and river; **F.** Proportion of chemical potential energy used in form of rain and river; **G.** Fraction of the available geopotential and chemical potential used in the basin. **H.** Used geopotential and chemical potential energy per area.

B1.



B2.

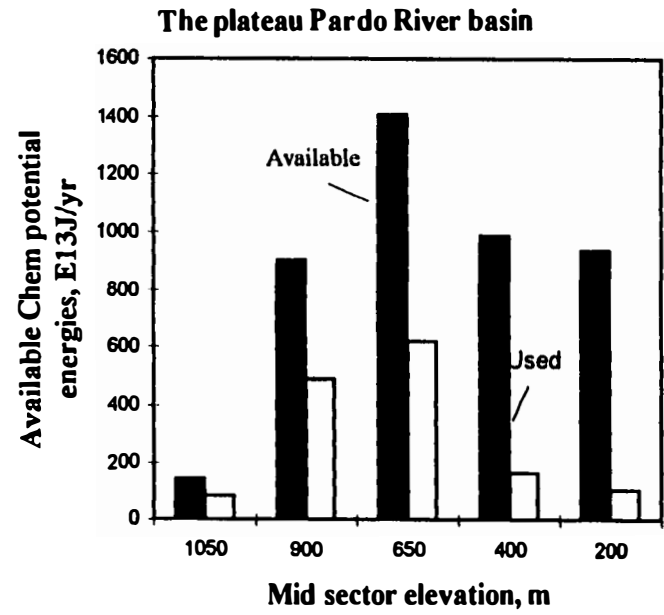
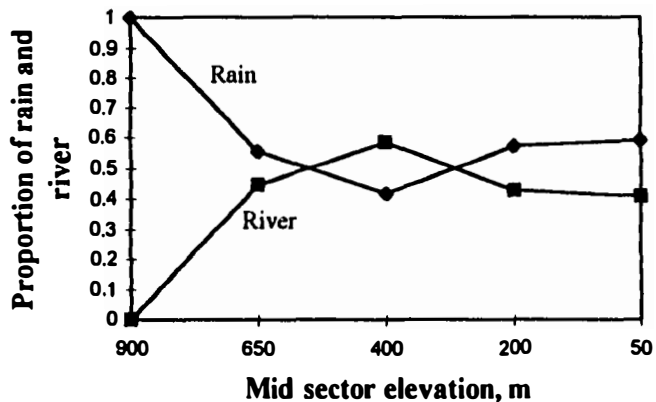


Figure 5.3. Continued.

The bowl-shaped Eta river basin

C1.

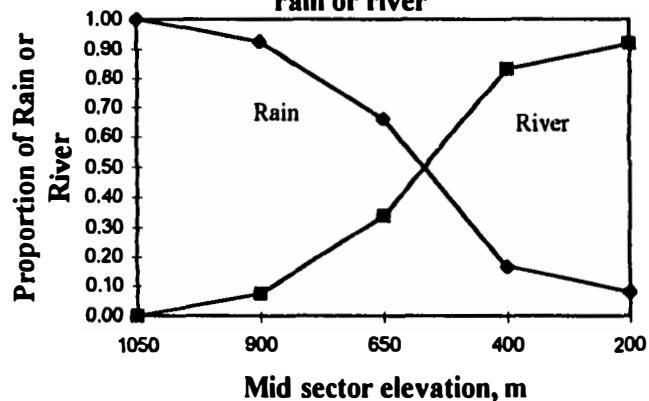
Available geopotential energy provided by rain or river



The plateau Pardo river basin

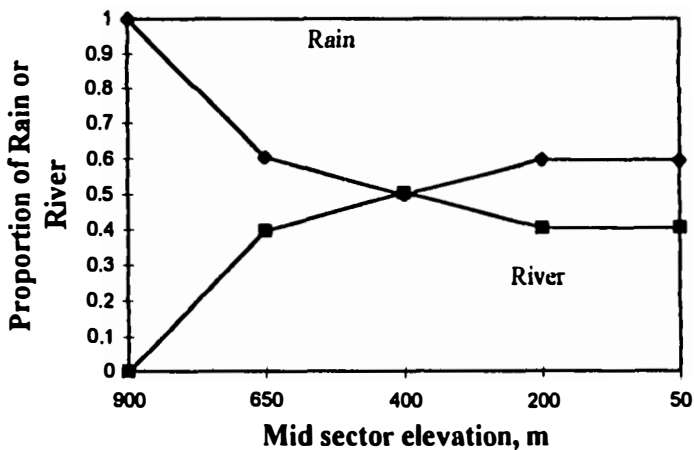
C2.

Available geopotential energies provided by rain or river



D1.

Proportion of Used Geopotential of rain or river



D2.

Proportion of Used Geopotential energies from rain or river

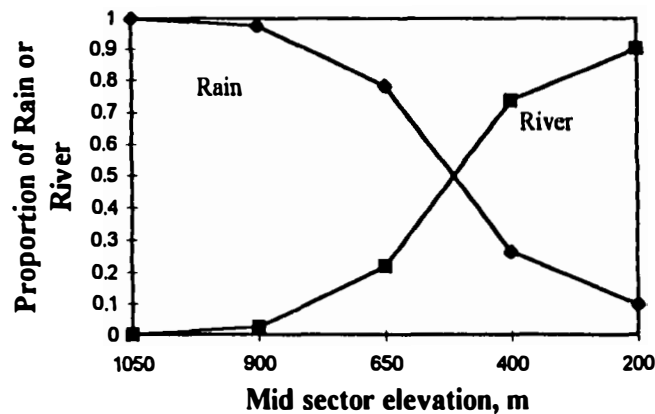
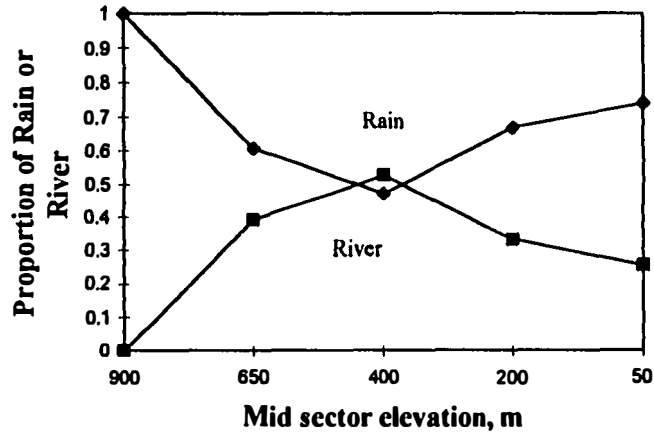


Figure 5.3. Continued.

The bowl-shaped Eta river basin

Available chemical potential provided by rain or river

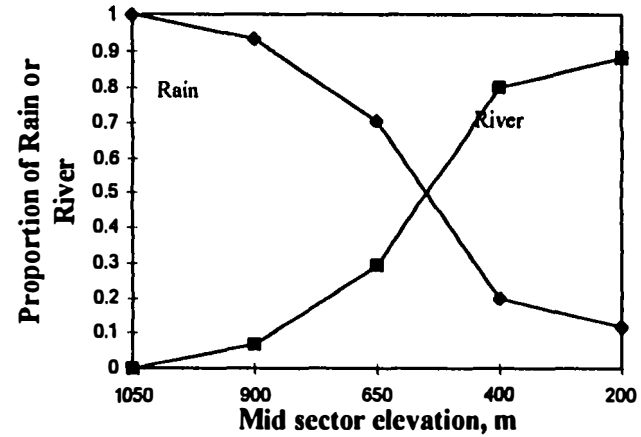
E1.



The plateau Pardo river basin

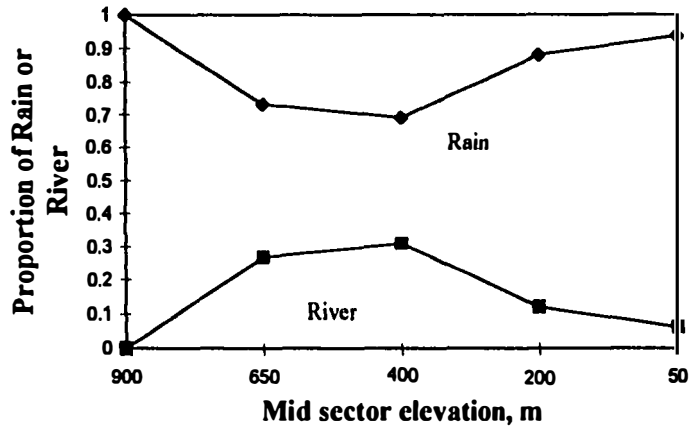
Available chemical potential energies provided by rain or river

E2.



Proportion of Used Chemical potential energies of rain or river

F1.



Proportion of Used Chemical potential energies from rain or river

F2.

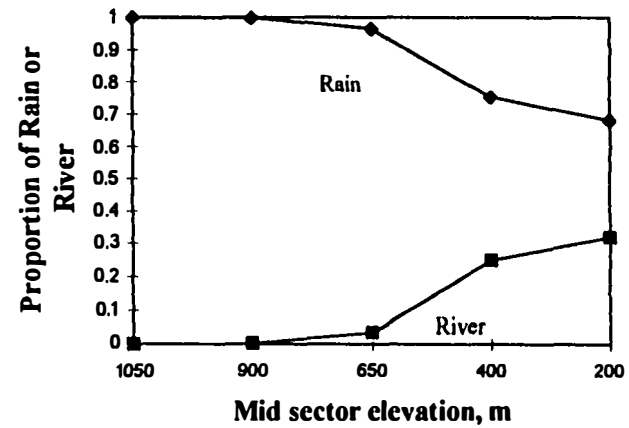
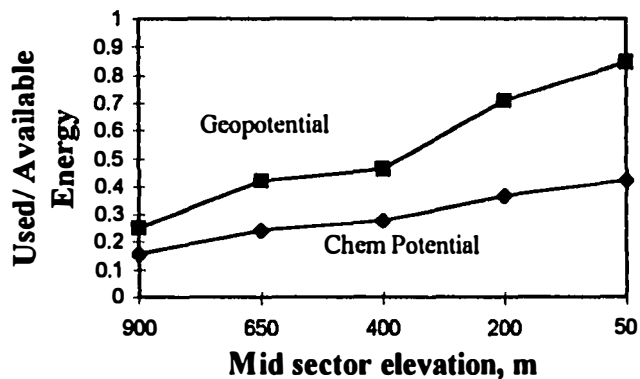


Figure 5.3. Continued.

The bowl-shaped Eta river basin

Fraction of available geopotential and chemical potential energy used

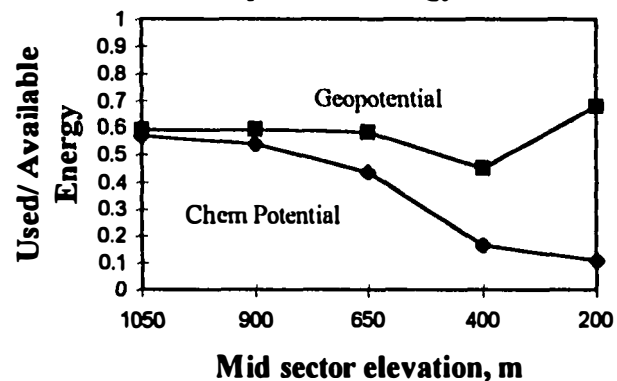
G1.



The plateau Pardo river basin

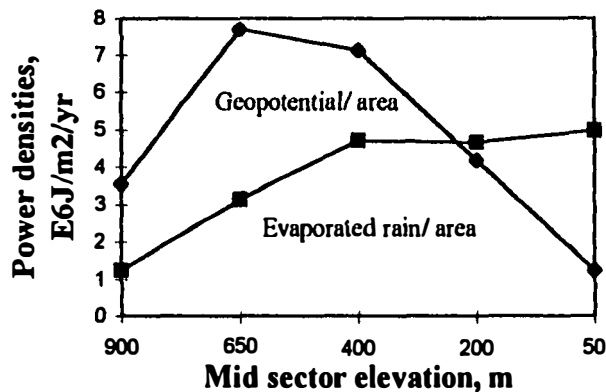
Fraction of available geopotential and chemical potential energy used

G2.



Geopotential and chemical potential power densities

H1.



Geopotential and Chemical potential power densities

H2.

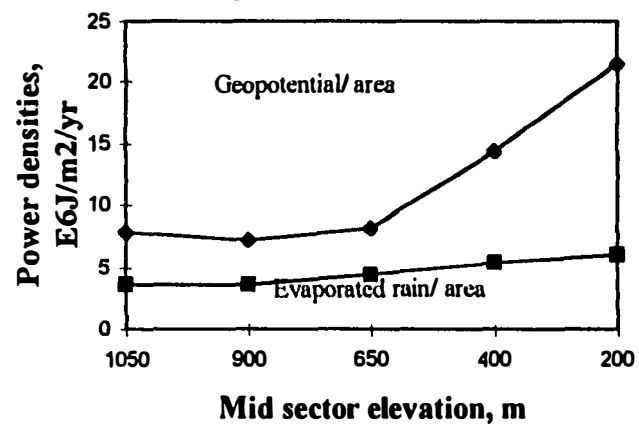


Figure 5.3. Continued.

in equivalent proportion of rain and river geopotential energy throughout the river profile (Chart C.1 in Figure 5.3).

This means that, throughout the river basin, there was availability of water energy resources (such as the rain and river energies) with slight different turnover times and different transformities. In other words, the whole watershed landscape could benefit from the availability of these sources of water energies. The more predictable and organized river geopotential energy was available throughout the river profile, instead of being limited to the lower sectors of the basin as observed in the plateau basins.

The use of rain and river geopotential energies in the large bowl-shaped Brazilian river basins followed the same pattern of their availability .Both rain and river energy resources were used throughout the river profile (Chart D.1 in Figure 5.3). In the elevated bowl shaped Coweeta and Upper Little Tennessee, the rain geopotential energy was used more than the river energy (Chart I in Figures 3.7 and 3.8).

Availability and Use of the Chemical Potential Energies

Total availability and use of chemical potential energy increased in an exponential shape towards the lower end of the basin (Chart B.1 in Figure 5.3). Although rain and river provided equivalent amount of chemical potential energy throughout the river profile (Chart E.1 in Figure 5.3), the watershed systems seemed to draw larger proportion of energy requirements from the rain (Chart F.1 in Figure 5.3).

The productivity of the valley depended more on the chemical potential of the rain than on in the river runoff. Moreover, the productivity of the valley depended on an

efficient use of the river geopotential energy (and eventually of the chemical potential energy of other elements, such as nutrients and sediments carried by the limiting geopotential energy of river waters (Chart G.1 in Figure 5.3).

Maximum Geopotential Energy Use per Area at Middle Elevations

When the geopotential energy use per area was evaluated along the basin profile, a hump shape was revealed, with maximum geopotential power densities of about 6 to $8 \text{ E6 J/m}^2/\text{yr}$ found at 650 to 400 m elevations, and the energy use per area decreasing downstream (Chart H.1 in Figure 5.3). This pattern suggested the existence of a zone of convergence of water and energy in the highlands, followed by a zone of divergence in the lowlands. The shape of this curve also indicated that ,at least in basinwide scale, the geopotential power used throughout the profile was not uniform as Leopold et al. (1964) predicted for the energy use in the river profile.

This sector of the river, where maximum energy use was found, is also the zone of maximum intensity for other phenomena observed in river systems. For example , it is the sector on the river profile where maximum fluctuations in water temperature take place (Allan, 1995 ; Stanford et al. 1996) .More importantly, it is the zone, where maximum native biodiversity is expected to occur (Stanford et al. 1996). Also, it has been observed as attractive zones for economic developments, as the interface of piedmont and coastal plain of the Southern United States, where major urban centers are located.

In the Brazilian bowl-shaped river basins the average geopotential energy use per area were around $3.0 \text{ E6 J/m}^2/\text{yr}$, which is much less than the average 6 E6 to 9 E6

J/m²/yr found in the Plateau Brazilian river basins. Therefore, it seems correct that concave watersheds use relatively less geopotential energy, as proposed in Leopold et al. (1964). This does not necessarily mean that the system is minimizing work, but rather that the concave shape allows the river to optimize the use of the limiting geopotential energy on the lowlands of river basins.

Evapotranspired Chemical Potential Power Densities

The evapotranspired chemical potential power densities of the Brazilian watersheds increased asymptotically towards the lower sectors of the basin, reaching rates of energy use of about 4.0- 5.0 E6 J/m²/yr in those lowlands located at the sea level (Chart H.1 in Figure 5.3). Those rates of energy use were less than those identified for the lower sectors of the plateau Brazilian river basins (5.0- 6.0 E6 J/m²/yr) (Chart H.1 in Figure 5.3). However, the average chemical potential energy use for the entire bowl-shaped basins (4.3- 4.6 E6 J/m²/yr) were slightly higher than those verified in the plateau basins (3.7 -4.3 E6 J/m²/yr).

These results suggested that bowl-shaped basins favor higher average productivity for the whole basin. On the other hand, the plateau basins would present higher absolute productivity rates at the mouth of their watersheds.

Evapotranspired Energy per Unit of Used Geopotential Energy Index

An index relating the chemical potential used in evapotranspiration per total geopotential used in watershed also indicated that bowl-shaped river basin are efficient energy users. The index was 1.58 and 1.24 for the bowl-shaped Eta and Jacupiranga River basins, whereas it varied from 0.47 to 0.63 for the Plateau river basin (Column 5 in Table 3.3). The bowl-shaped basins seems to lead to higher biotic production per unit of geopotential energy used in the basin.

Energetics of the Plateau River Basins

Along the longitudinal profiles of the plateau river basins, the available water geopotential energy presented a parabolic distribution, peaking around the 650m-elevational sectors (Chart A.2 in Figure 5.3). Such maximum is due to the typical land concentration in the elevated sectors of the basins. The water geopotential energy was available largely in form of rain in upper sectors of the basins and then, largely in form of river in the lower sectors of the basins (Chart E.2 in Figure 5.3).

The availability of chemical potential energy followed similar pattern to the geopotential one, with a small increase in the available chemical potential energy towards the lower sectors of the basins (Chart B.2 in Figure 5.3). Also, the energy use in the basins was compatible with the pattern of energy availability (Charts D.2 and F.2 in Figure 5.3). However, as it happened in the bowl-shaped basins, the chemical potential use was drawn largely from the rain energy (Chart F.2 in Figure 5.3)

Both geopotential and evapotranspired chemical potential power densities increased towards the lowest sectors of the basins. The increase in chemical potential energy use was straight and the increase in geopotential energy use was of exponential shape.

The fact that the plateau river basins displayed a strong intensification in energy use immediately before discharging into a major river , which eventually opens in a flat and large floodplain area, suggests that the plateau basins are just part of a large bowl-shaped basins. In the case of the Brazilian rivers, the plateau basins are part of the bowl-shaped Ribeira de Iguape River basin. They seem to represent the convergence zone of these large bowl- shaped basin. Subsequent divergence zone is expected to occur in the river valley and/or in the river estuaries.

Outflowing River Energies

Because the geopotential energy of an unit water volume decreases linearly with decreasing elevation, but the volume of river waters increases downstream, the longitudinal pattern of the outflowing geopotential energy of the rivers displayed a parabolic shape, peaking around 650-700 m (or 3000 ft). Rivers discharging at sea level had almost no geopotential energy left in their waters. In the evaluated watersheds, the river waters outflowing the Jacupiranga, Juquia and Eta River basins had just 1 to 4% of the available geopotential energy of the basins(Column 3 in Table 3.3). However, the waters the Coweeta River and the Upper Little Tennessee River discharging at about 600

m high, had about 35 to 29 % of their available geopotential energy available transferred to downstream sectors (Column 3 in Table 3.6).

The chemical potential energy of the outflowing river waters just accumulated as the volume of river waters increased in the downward sectors. An increase of exponential shape was observed for all evaluated watersheds.

The chemical potential energy outflowing most evaluated watersheds was about 50% of the total chemical potential energy available to these river basins (Column 7 of Tables 3.3 and 3.6) . Just for the drier basins (Pardo, Catas and Betari), the proportion of outflowing chemical potential energy was a little less (~ 40% of available chemical potential energy). These results suggest that, with exception for watersheds located in very dry zones, most river basins transfer large proportion of their available chemical potential energy to the downstream river basin.

Empower Accumulation Downstream

The empower contribution to an elevational sectors was calculated, taking into consideration rain empower input to that sector and the rain empower inputs to all upstream elevational sectors. The total empower contribution increased in an exponential shape along the longitudinal profile of the river, due to of the accumulation of rain empower from the upper sectors into the lower sectors of the basin.

The total empower contribution for the evaluated watersheds was function of the volume of rain falling in the area. Therefore, total empower contribution to a basin was related to the drainage area (Figure 5.4)

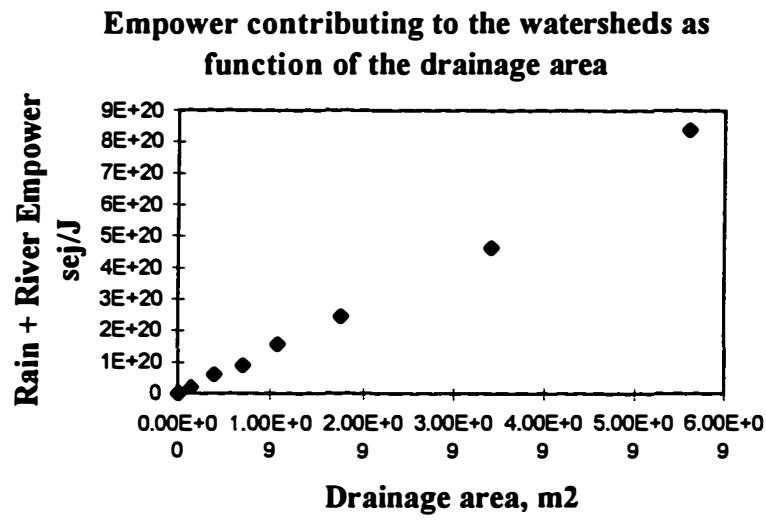


Figure 5.4. Rain and upstream river empower contribution to the watershed as function of their drainage area.

The larger the river basin, the more empower is contributing to the basin. More empower leads to more production, organization and complexity in the system. This may justify the findings where the fish and mollusks specie diversity were log -linearly related to the river basin area (Allan, 1995).

The annual empower for Coweeta River basin and subbasins ranged from 0.3 to 3.0 E18 sej . For the Brazilian watersheds, it ranged from 20E18 to 840 E18 sej.

Empower Densities in Bowl-shaped and Plateau Basins

The distribution of empower densities along the river profile had similar shape to those observed for the power densities (Chart A in Figure 5.5). Therefore the bowl shaped basins had also maximum empower densities at middle elevations (400 m). Again the maximum empower zone coincided and may explain the zone of maximum native biodiversity in the middle sectors of the river (Stanford et al. 1996). It also may explain the high economic attraction of the piedmont zones of river basins.

Plateau shaped river basins had the empower densities increasing in an exponential shape towards their lower ends (Figure 5.5.B). Mouth of watershed are zones high EMERGY convergence, and therefore, they might be zones of high production, organization and diversity.

In the watershed 7 of Coweeta river basin, the precut standing biomass of the cove hardwood located at the mouth of this watershed was 25 to 40% higher than biomass of other forests communities in the same watershed. (Boring et al 1988). Maps of empower

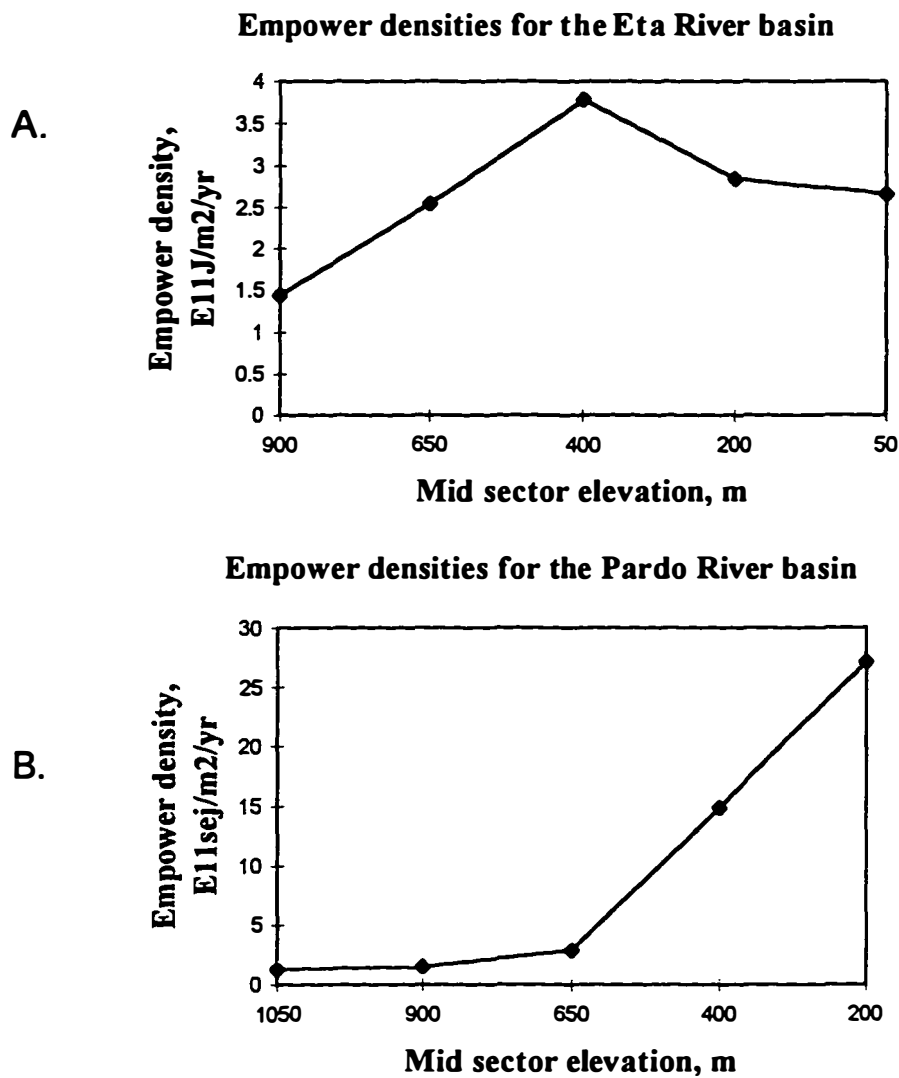


Figure 5.5. Comparison of the empower densities estimated for: **A.** The Bowl-shaped Eta River basin; **B.** The Plateau Pardo River basin.

density prepared for the Coweeta subbasins (Figures 3.26 and 3.27) strongly indicated maximum intensity being along convergence zones in the mouth of the watersheds.

However, the absolute values for the estimated empower densities have to be taken cautiously. The empower densities estimated according to the methodology proposed in this study depended on the size of the elevational sectors considered. When empower density for the Upper Little Tennessee river basin was estimated dividing the basin in 10 elevational sectors, the empower density for the lowest sector was about three times the value estimated when basin was divided in 5 elevational sectors (Chart A in Figure 5.6).

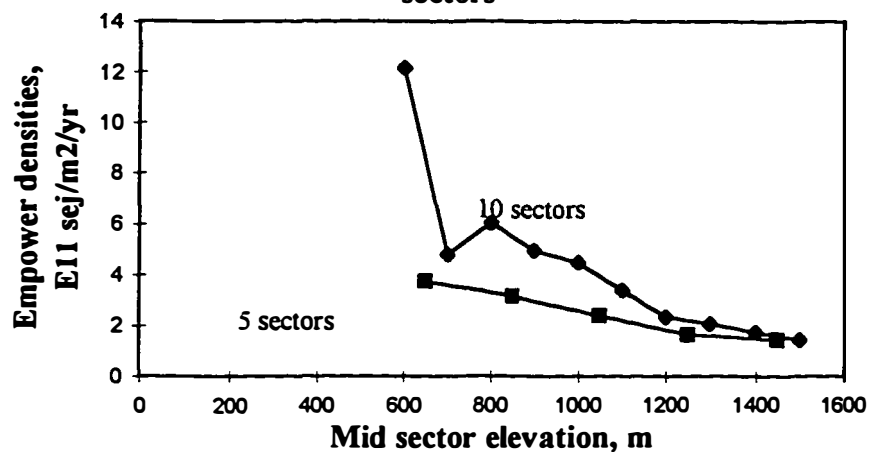
The same procedure was applied to the estimates of the geopotential and chemical potential power densities of the Upper Little Tennessee river. In this case, the estimates of power density based on 10 elevational sectors were similar to those estimates calculated for the 5 elevational sectors (Chart B in Figure 5.6).

Therefore, the proposed methodology is adequate to study the spatial distribution of energy but needs some improvement regarding the evaluation of the empower density. A methodological alternative would be to divide the basin in stream-order sectors. Or, eventually to divide the basin in elevational intervals, similar to the elevational range found in the stream- order sectors.

The Large Geopotential Transformities in the Valley

Geopotential transformities of river outflow increased downstream following the increase in spatial and temporal organization in the river systems on the downstream

Comparing empower densities for the Upper Little Tennessee river for basin divided in 5 or 10 elevational sectors



Comparing power densities for Upper Little Tennessee river for basin divided in 5 or 10 elevational sectors

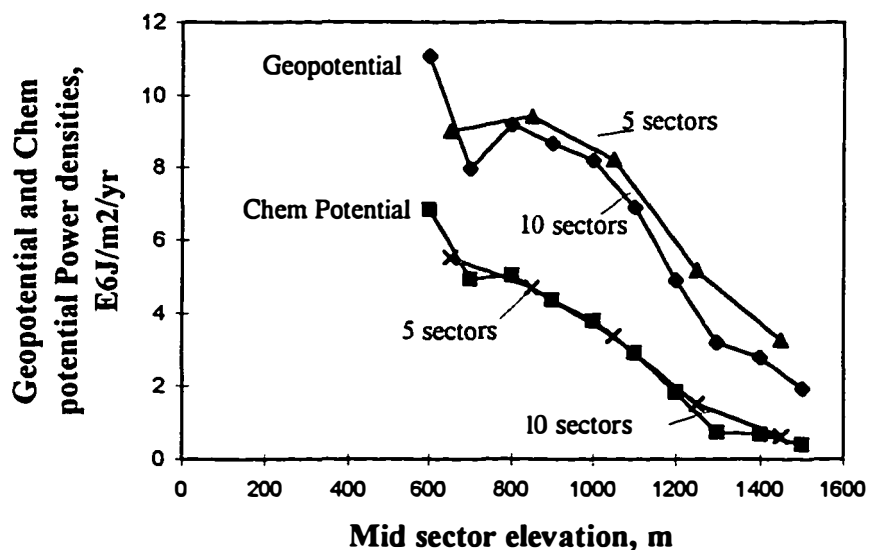


Figure 5.6. **A.** Comparison of the empower densities estimates for Upper Little Tennessee River, when basin divided in 10-100 m elevational sectors or 5 - 200m elevational sectors; **B.** Comparison of the power densities for Upper Little Tennessee River, when basin divided in 10-100 m elevational sectors or 5 - 200m elevational sectors.

sectors. Geopotential transformities increased as an inverse power function of elevation (Figure 5.7.A). It ranged from 10,000 to 30,000 sej/J in the elevated Coweeta River basins and from 15,000 sej/J to 1,500,000- 3,500,000 sej/J in the Brazilian watersheds.

These estimated geopotential transformities for the lowland of the large river basins are orders of magnitude higher than the average global solar transformities estimated for the geobiospheric processes (Odum, 1996). The estimated global transformity for the physical energy in stream flow is 27,764 sej/J, and it was calculated for river running at the average continental elevation (875 m high).

However, the geopotential transformity estimated in the study seems to refer to the ability of the river to organize its own physical characteristics and the characteristics of the valley. Rivers are permanently reorganizing their canal characteristics (such as depth, width, velocity), their trajectory along the valley, their distribution of sediment in the valley and indirectly their upstream network. The river stages are intrinsically related to the groundwater levels in the valley, and together they define the hydroperiod of the valley, and consequently the distribution of the plant community in the area. During flood period, the river waters act as a geological agent modifying the landscape. The whole land use occupation is then subject to the empower of the river network. Flooding effects are quite similar to hurricane effects.

According to the EMERGY algebra, the empower contribution to a system is transferred in a chain of processes, until the final product is dispersed in the background environment again. At this point, the energy availability is lost and with it the empower (Odum, 1996). In the case of the geopotential energy of river waters, the background level is the sea level. Therefore, a question can be raised, whether after some point in the river

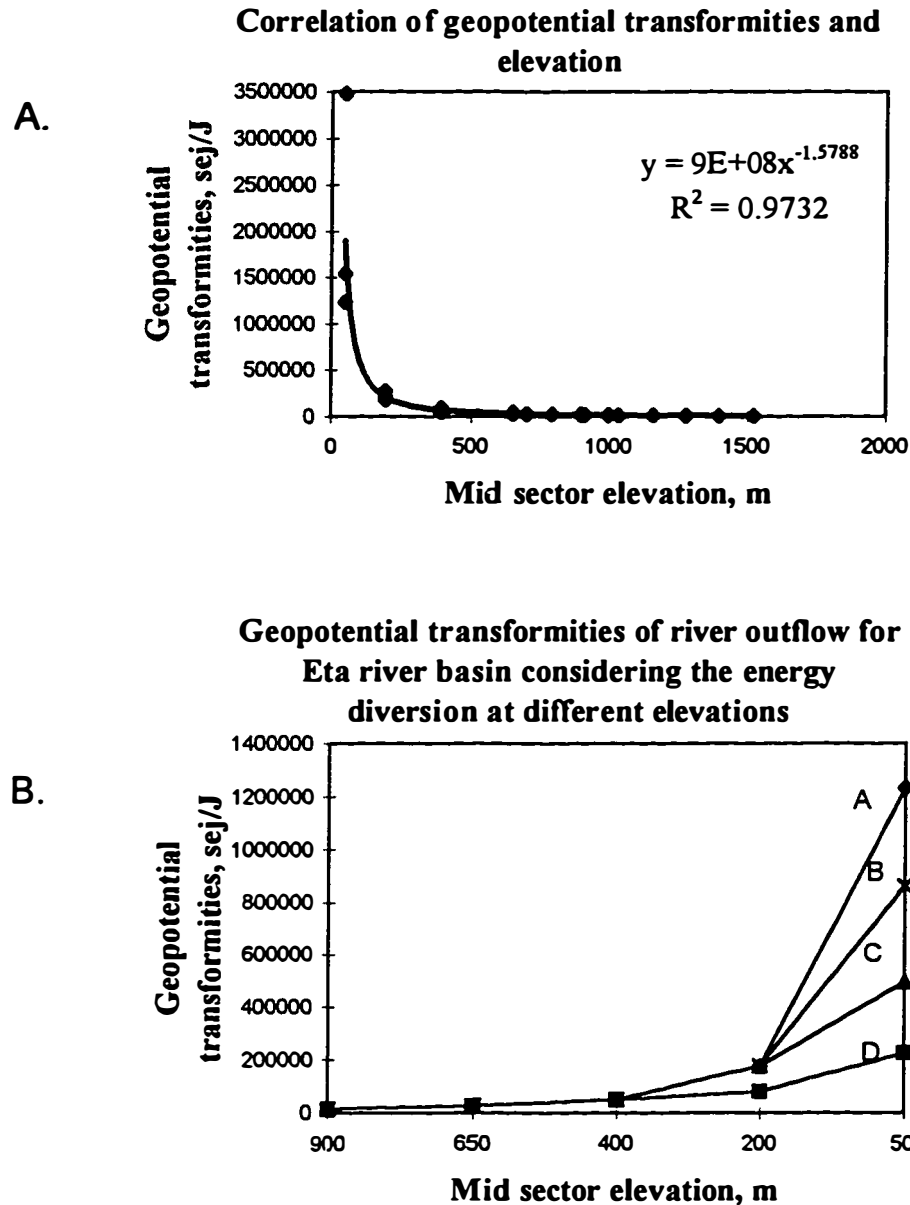


Figure 5.7. A. Correlation of the estimated geopotential transformities of river outflow with elevation. B. Estimated of geopotential transformities of river outflow for the Eta river basin with diversion occurring at: A. Below river mouth; B. Halfway in the lower 50-m elevational sector; C. Below 200-m elevational sector; D. Below 400m- elevational sector.

profile (may be, at the maximum point in the hump shaped curve for empower density), the river system begins dispersing EMERGY instead of concentrating it (as assumed in the present methodology) . If this is the case, the rain empower falling in the dispersion zone is operating separately, contributing to the empower of the land but not to the empower of river crossing the valley.

To examine this theoretical question, geopotential transformities of river outflow were calculated, considering that dispersion taking place at different elevational sectors of the Eta River basin. A new procedure was applied, where just the rain and river empower inputs to the elevational sectors above the dispersion point were considered as contributing to the empower of the downstream sectors of the basin . Results indicated that if dispersion happened at 400m elevational sector, the estimated geopotential transformity of river outflowing the 50-m elevational sector of Eta river basin would be about 200,000 sej/J. However, if dispersion would occur at river mouth, then the transformity would be 1,300,000 sej/J (Chart B in Figure 5.7). Therefore, the geopotential transformities for major rivers flowing through lowlands seems to be always of large magnitude ($2E5$ to $2E6$ sej/J), when compared to the transformities of other biogeospheric energy flows.

Other evaluations were performed to verify the adequacy of the high geopotential transformity for the floodplain rivers. Measurements of the hierarchical organization (percent of first order stream discharging in second order stream and percent of second order stream discharging in third order stream and so on) and also the drainage density were performed for sample sub-basins in different elevations of the Jacupiranga river

basin. The idea of these evaluations was to check the ability of river to maintain its organization in the lowlands, despite of the reduction of its inputs of geopotential energy.

Results of these evaluations indicated that the hierarchical organization was about the same in all samples, although the drainage density decreased in the lower sectors. These results suggested that, although the lowlands rely on less geopotential energy (therefore less drainage density), the high transformity of the main river was able to support the same hierarchical organization in lowlands as those found in other parts of the basin.

The Chemical Potential Transformities of River Outflow

The chemical potential transformities of river outflow increased towards the lower elevations, following the relative increase in transpiration and terrestrial productivity in the basin. They ranged from 20,000 sej/J to about 60,000 sej/J for the Brazilian watersheds and from 20,000 to 40,000 sej/J in the Coweeta River system.

The chemical potential transformities of river outflow were higher than the geopotential ones in the upper sectors of the basins (above 600m) and much lower in the low sectors of the basins. Such comparatively low values for the chemical potential transformities can be explained by the relative little use of the abundant water chemical potential energy available to these studied areas in form of rainfall. About half of the available chemical potential energy outflowing the river basins was transferred downstream, to be processed in the estuarine zone. There, the chemical potential transformities should reach enormous values.

Empower Estimates Including Earth Inputs

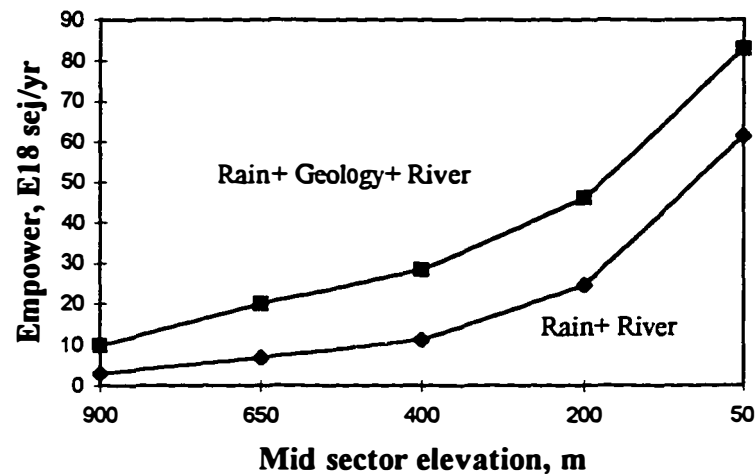
According to Chart A in Figure 5.4, the empower contribution to a watershed was almost largely related to the size of the watershed. The depth of the rain falling in the area was the other parameter influencing the empower estimates.

However, it is quite evident the importance of the geology of the area in the processes taken place in the watershed. The rain empower estimates done in this study already account for some of the geological inputs. When the continents wear down due to the erosion caused by the rainfall, they become lighter and then uplift (isostasy). This uplift is part of the same geobiospheric processes that produces the rainfall, from where our rain empower estimates were taken.

But mountains are usually the result of pulsing geologic processes. They were raised in past geologic time and are eroding in the current period of analysis. Mountains represent stored EMERGY that contributes to the coupled watershed processes, by catching the rain, supplying rock material for soil formation and supplying mass to form the basin structure. Therefore, there is some supply of EMERGY in the mountain that is not a co-product of current earth processes, and it should be added to the inputs of rain EMERGY.

Figure 5.8 represented the empower contributions to a bowl-shaped basin (Chart A) and to a plateau basin (Chart B), when estimates were done with and without the Earth inputs. Results indicated that considering the Earth empower inputs corrected for the presence of mountain in both cases. About 200 % increase in empower contributions were

A. **Total Empower contribution to the Eta River basin (estimated with and without Earth inputs)**



B. **Total Empower contributions to the Pardo River basin (estimated with and without Earth Inputs)**

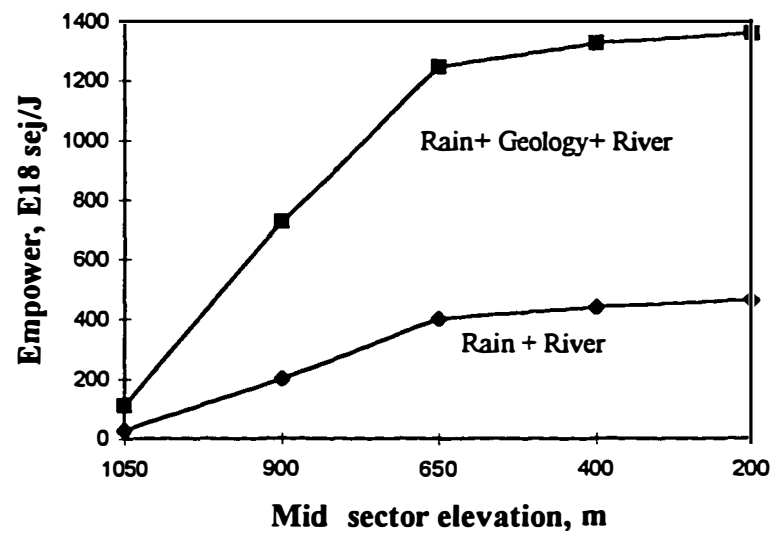


Figure 5.8. Estimating empower contribution with and without the Earth inputs for: **A.** The Bowl-shaped Eta river basin; **B.** The Plateau Pardo river basin.

verified in the upper elevational sectors of both watersheds. However, because the mountains were not prevalent features in the bowl-shaped basins, the empower estimated for their whole basin was just 35% higher than the estimated without Earth inputs. In the plateau basins, however, the Earth inputs increased the total empower contribution to the basins in 200%. It seems reasonable to take into consideration the empower of geologic inputs in future EMERGY analyses of mountainous areas.

The transformities of river outflow were also estimated with and without Earth empower inputs (Charts A to D in Figure 5.9). Geopotential and chemical potential transformities in both basin types increased, when included Earth inputs were accounted, in a similar pattern to the increase of the empower. Therefore, a relative higher increase for transformities in the upper sectors of the basins was observed. Chemical potential transformities displayed a decrease with elevation, when the Earth inputs were accounted.

Downstream Impacts of River Damming

Simulation suggested that river damming would reduce productivity of the valley significantly. The reservoirs formed by dams damped the fluctuation of the river waters in the valley, and less waters overflowed into the floodplain area. Therefore, less sediments, nutrients, organic matter and kinetic energy become available for the productivity of the valley.

Results from simulation indicated without the nutrients transported by the flood, productivity decreased. After 20 yr of the dam closure, the average volume of water overflowing the river banks was reduced to 58% of the flooding volume prior to

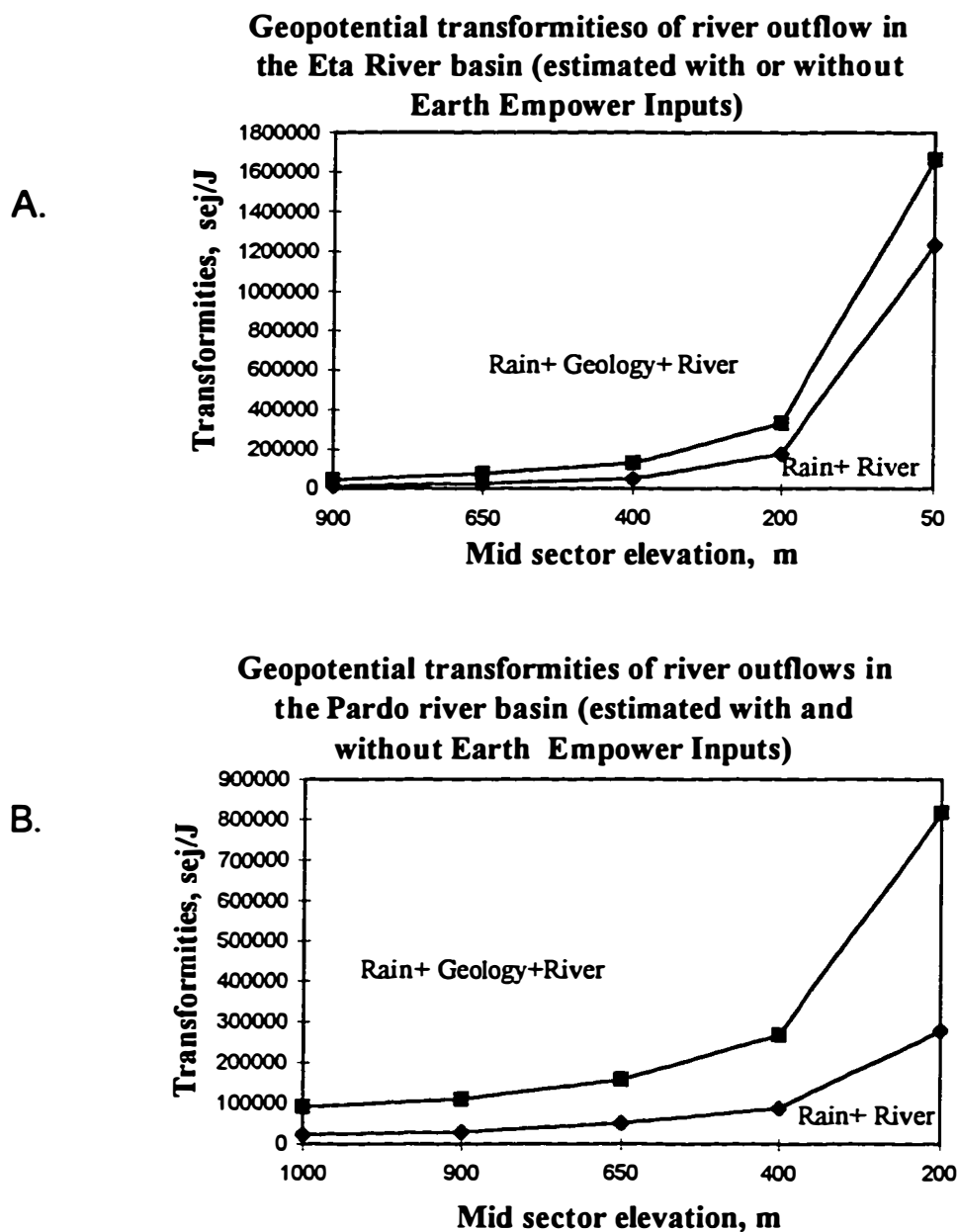
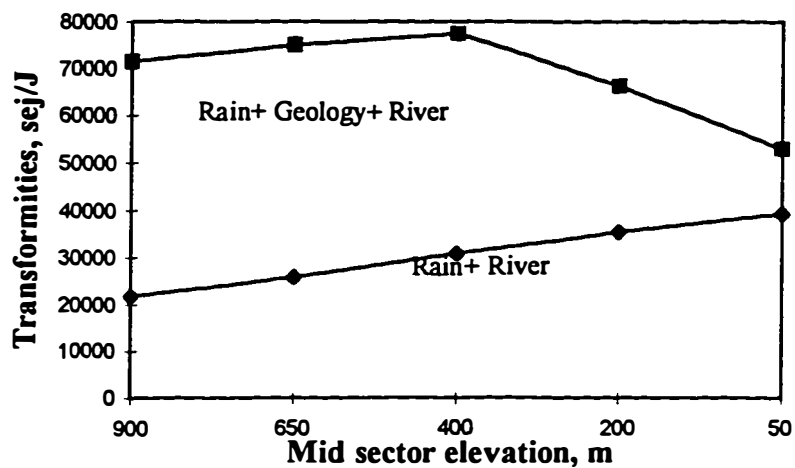


Figure 5.9. Transformities of river outflow with and without of the Earth inputs: **A.** Geopotential transformities for the Bowl-shaped Eta river basin; **B.** Geopotential transformities for the Plateau Pardo river basin; **C.** Chemical potential transformities for the Bowl-shaped Eta river basin; **D.** Chemical potential transformities for the Plateau river basin.

C. **Chemical potential transformities of river outflow for the Eta River basin (with or without Earth empower inputs)**



D. **Chemical Potential Transformities of river outflow for the Pardo River basin (with and without Earth Empower Inputs)**

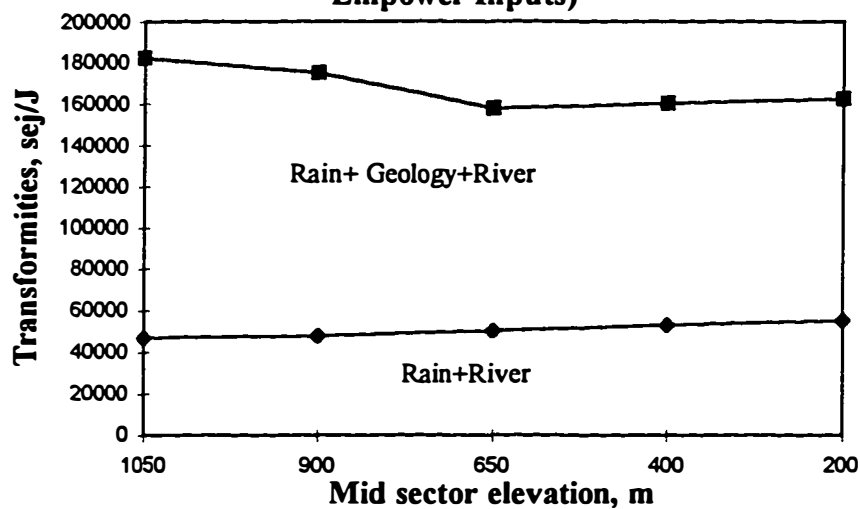


Figure 5.9. Continued.

damming. The average productivity of the floodplain decreased to 74% and the standing biomass to 80 % of those found prior dam construction.

Impacts on floodplain vegetation due to river regularization have been reported in literature. Reily and Johnson (1982), evaluating the effects on vegetation below Garrison dam in North Dakota found similar results to those predicted by the model. Tree growth and survivorship was adversely by the changes in the flow regime imposed by the dam. Nilsson and Jansson (1995), studying effects of the regulation in an entire river system in Sweden, found out that the species richness per 200 m- long sites were lower and almost all group of species were species- poor per site in the regulated rivers when compared to the free- flowing rivers. Davies (1979), described the impacts of Lake Kariba and Lake Volta on floodplains of African rivers. After dam closures, the changes in flood regime led to the encroachment or replacement of macrophytes, the dying off of the fodder trees *Acacia* with adverse consequences for the large animals (hippopotamus and crocodiles) living in the area.

Different mechanisms have been pointed out as responsible for the impacts on the riparian and floodplain vegetation downstream of a dam. Reily and Johnson 1982, indicated that alteration of seasonal streamflow pattern led to elimination of overbanking flooding and the lowering of water table during early growing season, reducing the moisture available to the upper terraces species. Alteration of the flood regime also led to lack of scouring (leading to replacement of vegetation), reduction in silt deposition (and related nutrients) and the lack of inputs of aquatic biota to the floodplain forest (e.g. seed dispersal contribution).

Results of this study indicated that damming the river affected the role of the river as organizer of the physical landscape of the valley, and as the carrier of physical chemical elements to the terrestrial production. Therefore, although in the model a limiting nutrient was represented as the mechanism altered by the dam construction, all other previously cited mechanisms could be causing the downstream impacts. In fact, it seems that phosphorus is not always the limiting factor in a floodplain forest as reported by Mitsch et al 1991.

Also, the model limited to show the impacts of a dam on the downstream floodplain. But there is a vast literature reporting impacts of dam on species diversity, composition and productivity of the aquatic biota (Ward & Stanford, 1979, Bonetto AP et al. 1989, Petts G E 1984, Blinn D W et al. 1995, Davies B 1979, Krenkel et al. 1979). Also, adverse impacts of river damming on the productivity of estuaries were documented (Prowse et al. 1996).

Impact of Multiple Small Dams

The simulation model was used to evaluate the downstream impacts of using multiple small dams instead of one large dam. The partition of a large dam into smaller units was an attempt to keep the river working closer to its natural conditions. Evaluation was then done for the No-Dam, and One- Dam, Two-Dam and Four-Dam alternatives . Results indicated that this design helped to minimize the downstream impacts.

In the simulation, the average river stages did not vary much among the alternatives (with or without dams). However, striking differences were found in the

pulsing intensity. With the No- Dam alternative, the water levels reached 3.2m depth whereas in One- Dam alternative the maximum depths were around 1.8m. Also, there was a lag (delay of about 2 months) in the timing of pulse in the alternatives with a dam, with flooding taking place late in summer or early fall when sunlight reaching the area was already decreasing.

Because of the river bank threshold (H2), differences in pulse intensity caused remarkable differences in the volume of the flooding waters for the evaluated alternatives. In steady- state conditions, the flooding waters for One Dam alternative was just 58 % of the overbanking waters of the natural pulsing conditions.

Fortunately, the impacts on plant productivity in the valley were less noticeable than the impacts in the flood intensity. In steady -state conditions, the simulated average productivity of One Dam, Two Dams and Four Dams design was around 74, 78 and 82% of the natural conditions evaluated by the No Dam alternative. Nutrients from rain falling in the valley and reserves of nutrients stored in the sediments kept the productivity of valley from being more adversely affected by the dams.

The impacts on the standing biomass in the valley were still less. After 20 years, the simulated standing biomass of the alternatives with dams were about 80 to 87 % of the biomass of the natural conditions. In fact, very rich initial conditions of the simulated floodplain of tropical or subtropical areas gave resilience to the changes in pulsing caused by the dams.

Conclusions

1. The geopotential energy of the river waters is a physical carrier for the physical-chemical resources (such as nutrients, sediments, water) required to enhance the terrestrial productivity of the floodplains. The geopotential energy is a limiting resource in the lowlands of the rivers.
2. The shape of the basin helps optimize the simultaneous use of the water geopotential and chemical potential energies in a basin. The concave shape of the bowl-shaped basin provides that rain and river energies can be available and used throughout the whole basin profile. Also, the geopotential energy use per area in a bowl-shaped basin is less intense than the energy used per area in the plateau basins (as predicted by Leopold et al 1964). Relatively more chemical potential energy is evapotranspired (more plant production) for unit of geopotential energy used. A whole basin index relating the water chemical potential energy used per unit of geopotential used was around 1.3 to 1.5 for the bowl-shaped basins whereas it was limited to about 0.4 -0.6 for the plateau basins.
3. The shape of the basin is helpful in optimizing the use of energy, but it is the EMERGY of the river water, acquired through the existence of a river network, that helps the lowland river perform its many roles in the landscape. In this study, the high quality of the river work on the lowlands was identified by their large geopotential transformities (1,500,000- 3,500,000 sej/J).
4. In the bowl-shaped basins, maximum empower density and geopotential power density were found in the middle basin elevations. This zone coincides (and may be it can explain) the zone of maximum native biodiversity in the middle sectors of the river pointed by

Stanford et al. 1996. It also may explain the attractiveness of the piedmont zones of river basins for economic development.

5. Considering that the evaluated watersheds were located in very rainy areas, there were always plenty of aquatic chemical potential energy available throughout the whole basin. Results indicated that the river chemical potential energies were little used in the basins and that about half of the available energies were flowing out of the basins. The estuaries seem to profit from the rich chemical potential energy provided by these rivers waters. It can justify the correlation of productivity of the estuaries to the supply of fresh waters indicated by Day Jr. et al. (1989).

6. Evapotranspired chemical potential power densities (and therefore productivity) increased towards the lower elevations of the basins. However, the scarcity of data did not allow us to do a more detailed assessment of the water energetics in the floodplain and estuarine zone. Such subjects seem to be extremely relevant for the management of watersheds, deserving future research.

7. The construction of dams seems to cause a break in the river network. Some of this embodied information acquired through the network was lost. The flood pulse, which is a result of the river basin processing the rain falling in its basin area, is altered by the presence of the reservoirs.

7. Simulation models of dam construction indicated losses in the downstream terrestrial productivity. After 20 yr of the dam closure, the average volume of water overflowing the river banks was reduced in 58% of the flooding volume prior dam. The average productivity of the floodplain decreased to 74% and the standing biomass to 80 % of those found prior dam construction.

8. The use of multiple small dams instead of one large dam helped to minimize the downstream impacts. After 20 years, the average productivity in the valley was reduced in 82% with Four Dams design instead of to decrease 74% with One Dam design.

9. This study proposes questions for future research about the functioning and organization of watersheds and their management, such as:

- How much is the EMERGY losses for the floodplain and estuarine systems in rivers where one dam or multiple dams are constructed?
- How do water energies works in the floodplain and in the estuarine zone? How are they related to productivity and diversity in these ecosystems?
- How is the natural and economic use of land related to the energetic use of the water in the watersheds?
- How are the evaluated EMERGY of river waters and organization of drainage system related? How are they related to the biodiversity in the system?
- What determines the shape of the basin? Is shape related to the empower of the weather and geological pattern?

APPENDIX A

GRAPHS OF ENERGY AND EMERGY OF EVALUATED WATERSHEDS

Graphs A.1 to A.8 showing the energy and EMERGY evaluations along longitudinal profile of the Eta, Jacupiranga, Juquia, Betari, Catas Altas, Pardo, Upper Little Tennessee and Coweeta River basins, presented in the following charts:

A. Aerial distribution; **B.** Hypsometric curve; **C.** Available (Gri) and Used (Gtu) geopotential energies; **D.** Proportion of rain (Gri) and river (Gvo) in the inflowing geopotential energies; **E.** Available (Cri) and Used (Ctu) chemical potential energies; **F.** Proportion of rain (Cri) and river (Cvo) in the inflowing chemical potential energies; **G.** Geopotential energies used (Gru, Gvu, Gtu) and outflow (Gvo); **H.** Chemical potential energies used (Cru, Cvt, Cvu, Ctu) and outflow (Cto); **I.** Proportion of rain (Gru) and river (Gvu) in the geopotential energy used up; **J.** Proportion of rain (Cru) and river (Cvu) in the chemical potential energy used up; **K.** Geopotential used up (Gtud) and evapotranspired chemical potential (Cetd) power densities; **L.** EMERGY/ total used energy (Et/(Gtu+Ctu) ratios; **M.** Total empower (Et) and empower densities (Ed); **N.** Geopotential (Tvg) and chemical potential (Tvc) transformities of river outflow.

Graphs A.9 to A.14 showing the energy and EMERGY evaluations along longitudinal profile of the Upper Shope Fork, Cunningham, Lower Shope Fork, Henson, Upper Ball, and Lower Ball Creek su-basins, presented in the following charts:

A. Geopotential energies used (Gru, Gvu, Gtu) and outflow (Gvo); **B.** Chemical potential energies used (Cru, Cvt, Cvu, Ctu) and outflow (Cto); **C.** Geopotential used up (Gtud) and evapotranspired chemical potential (Cetd) power densities; **D.** EMERGY/ total used energy (Et/(Gtu+Ctu) ratios; **E.** Total empower (Et) and empower densities (Ed); **F.** Geopotential (Tvg) and chemical potential (Tvc) transformities of river outflow.

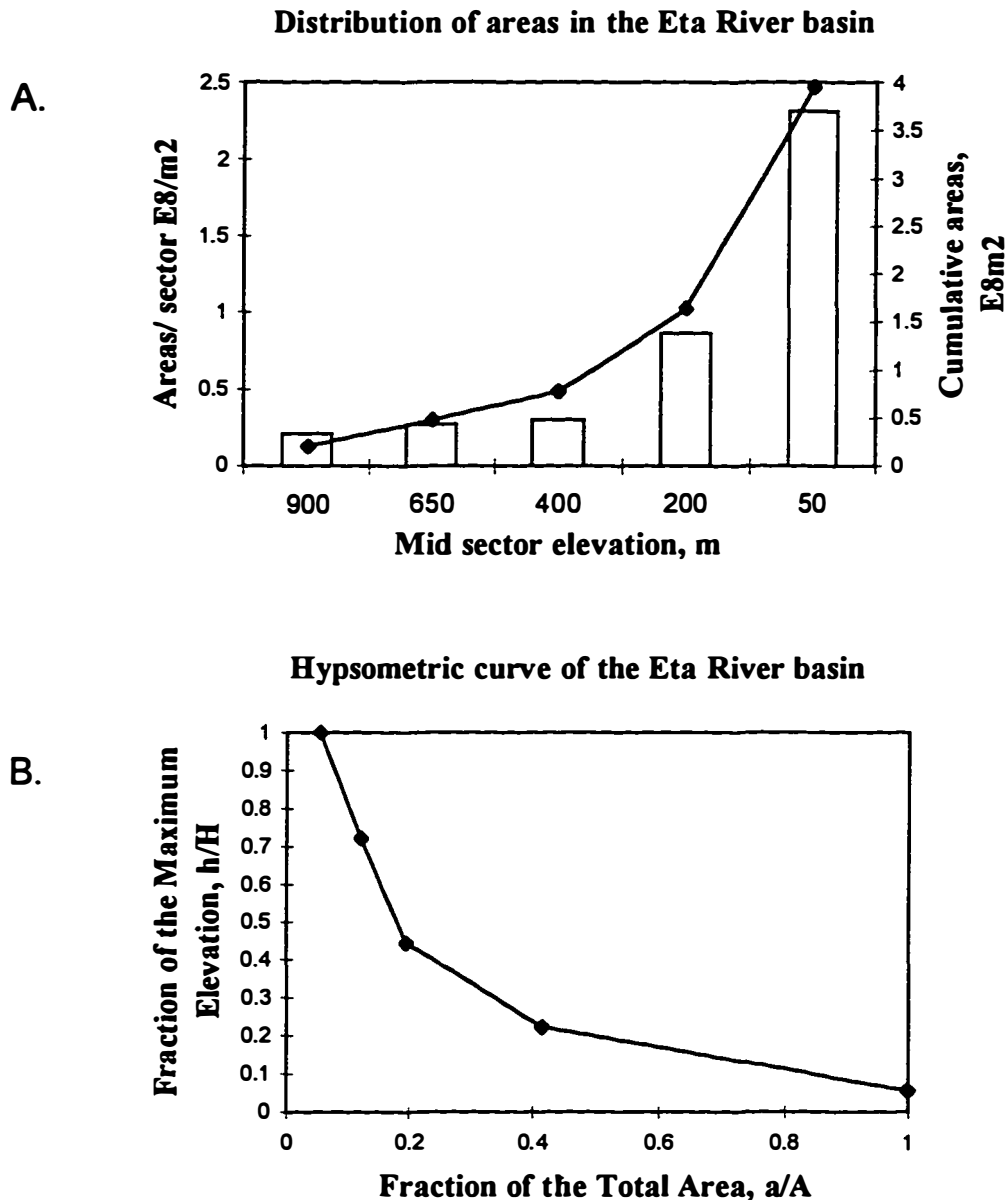


Figure A.1. Areas, energy and energy evaluations for the elevational sectors of Eta river basin, representing in: **A.** Aerial distribution; **B.** Hypsometric curve; **C.** Available (G_{ri}) and Used (G_{tu}) geopotential energies; **D.** Proportion of rain (G_{ri}) and river (G_{vo}) in the inflowing geopotential energies; **E.** Available (C_{ri}) and Used (C_{tu}) chemical potential energies; **F.** Proportion of rain (C_{ri}) and river (C_{vo}) in the inflowing chemical potential energies; **G.** Geopotential energies used (G_{ru}, G_{vu}, G_{tu}) and outflow (G_{vo}); **H.** Chemical potential energies used ($C_{ru}, C_{vt}, C_{vu}, C_{tu}$) and outflow (C_{to}); **I.** Proportion of rain (G_{ru}) and river (G_{vu}) in the geopotential energy used up; **J.** Proportion of rain (C_{ru}) and river (C_{vu}) in the chemical potential energy used up; **K.** Geopotential used up (G_{tud}) and evapotranspired chemical potential (C_{etd}) power densities; **L.** Energy/ total used energy ($E_t / (G_{tu} + C_{tu})$) ratios; **M.** Total empower (E_t) and empower densities (E_d); **N.** Geopotential (T_{vg}) and chemical potential (T_{vc}) transformities of river outflow.

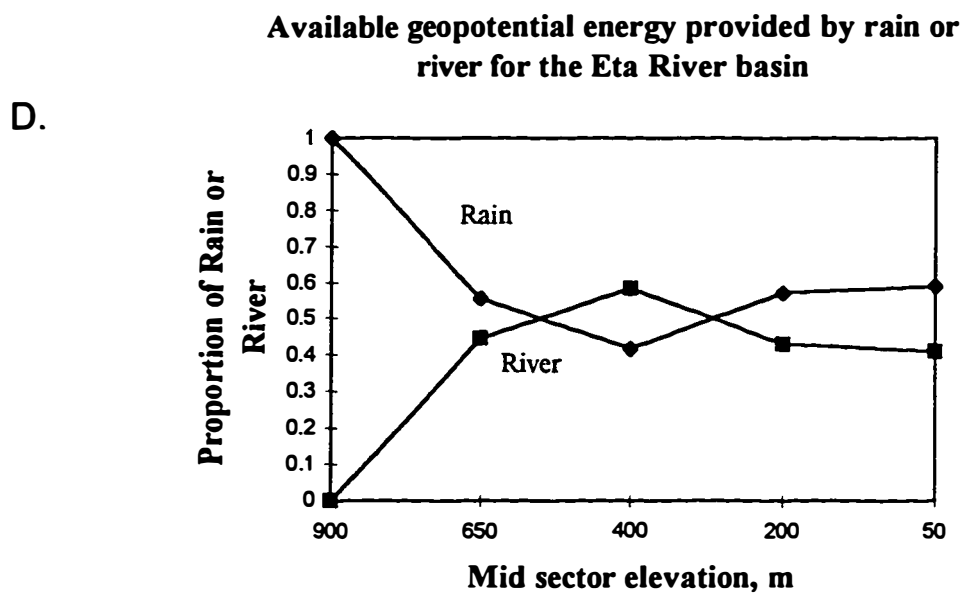
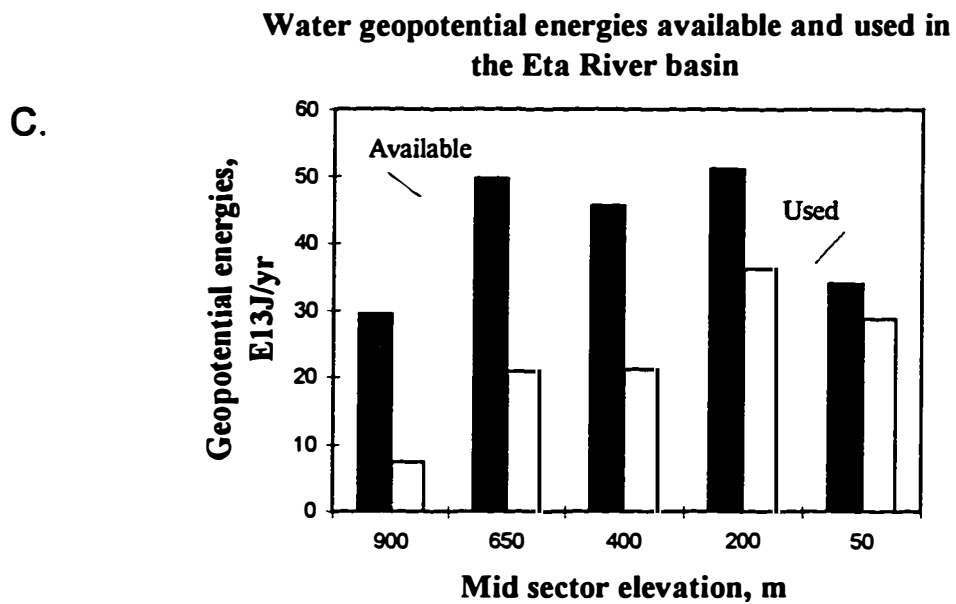
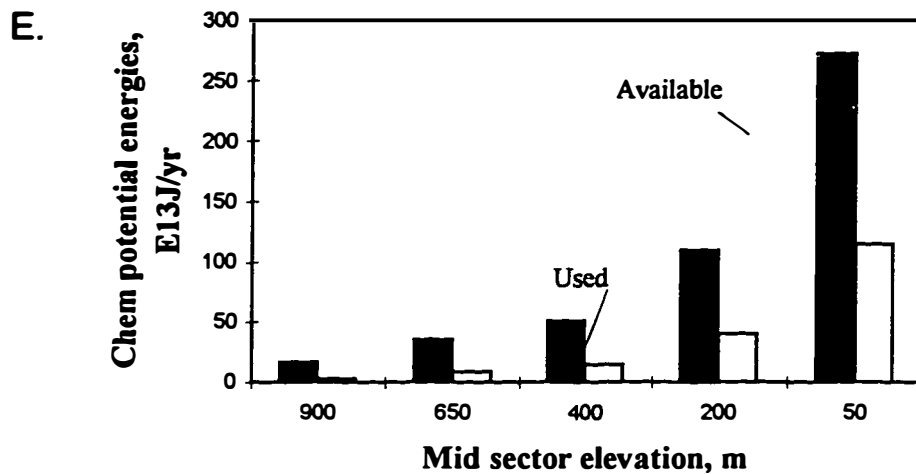


Figure A.1. Continued

**Water chemical potential energies available and used
in the Eta River basin**



**Available chemical potential provided by rain or river
for the Eta River basin**

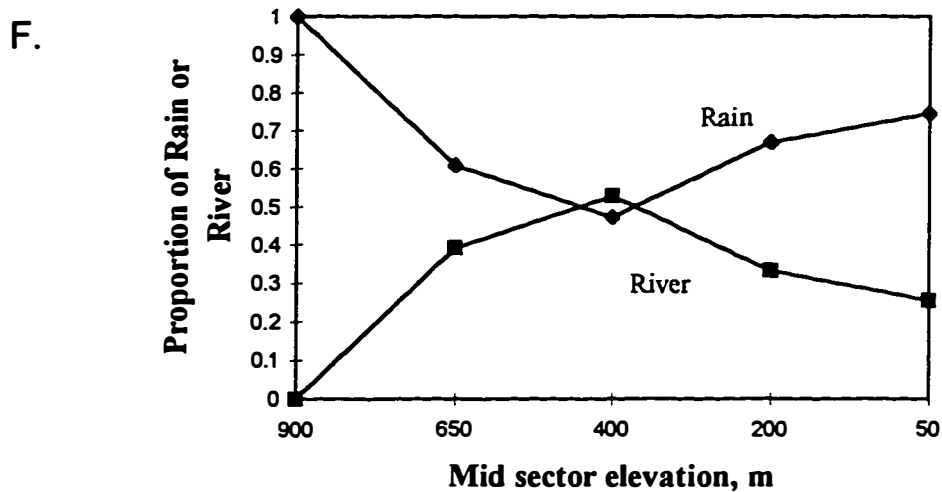


Figure A.1. Continued

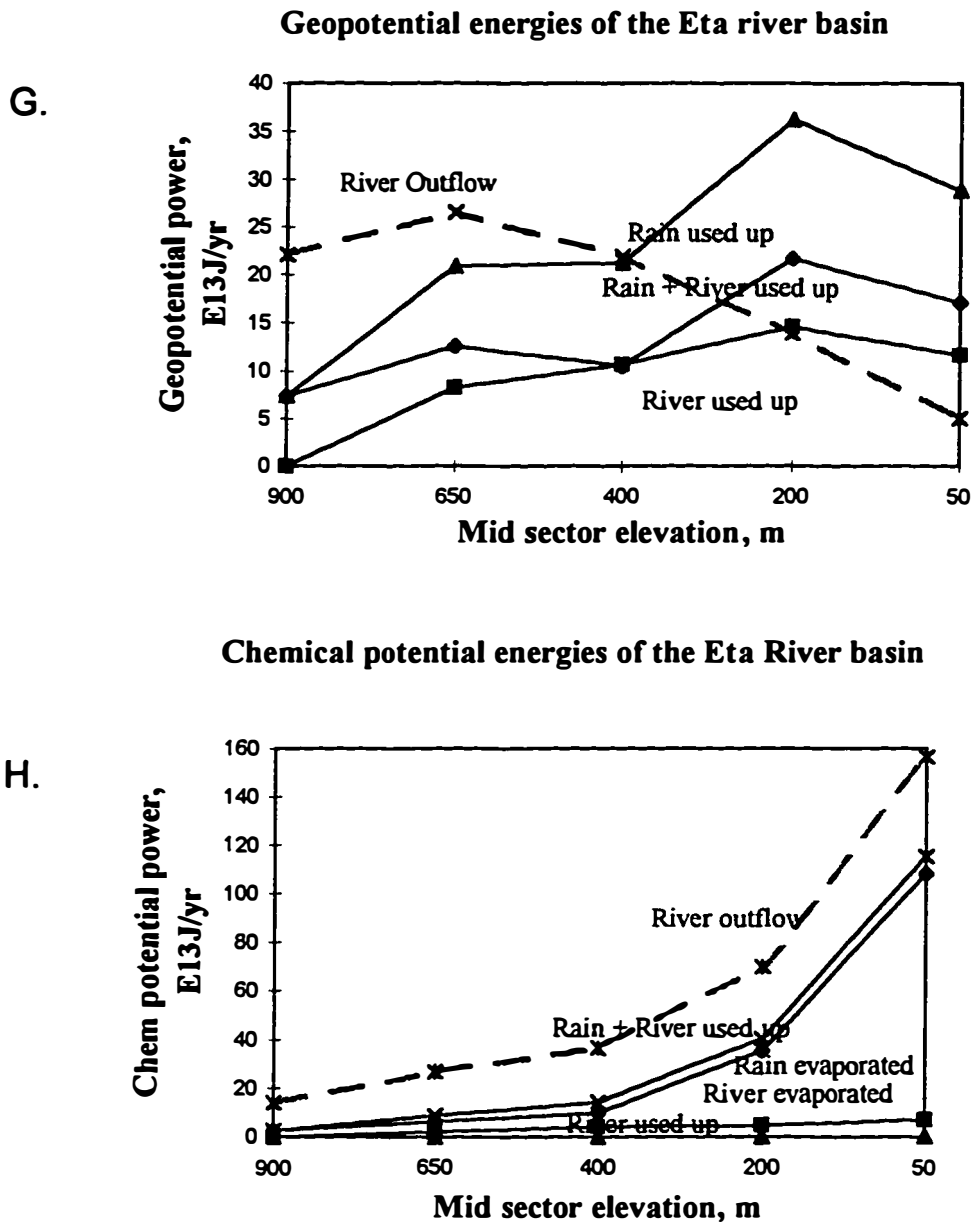
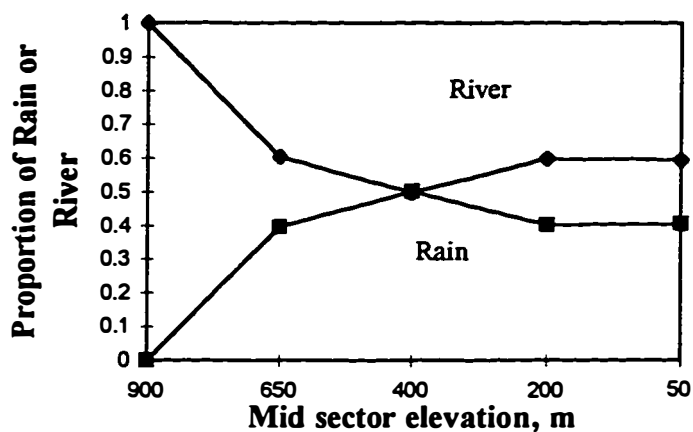


Figure A.1. Continued

Proportion of Used Geopotential energies from rain and river in the Eta River basin

I.



Proportion of Used Chemical potential energies from rain and river in the Eta River basin

J.

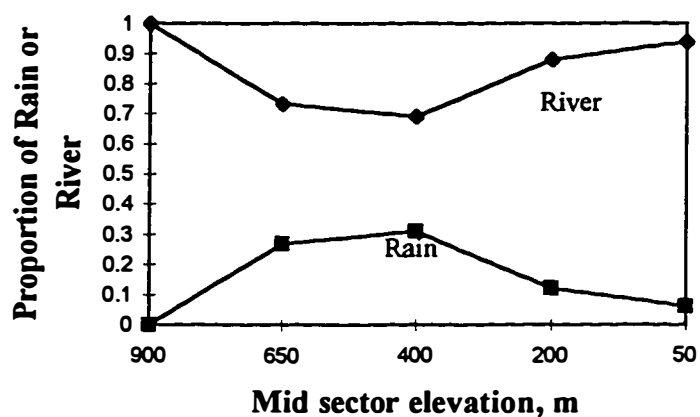
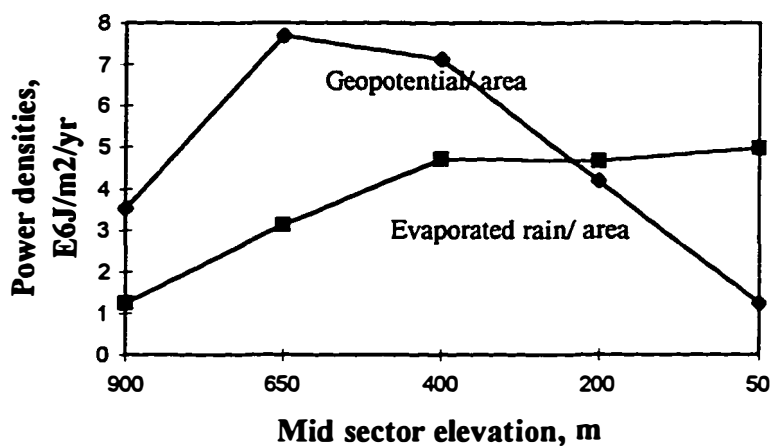


Figure A.1. Continued

K.

**Geopotential and chemical potential power densities
for the Eta River basin**



L.

Energy/ used energy ratio for the Eta River basin

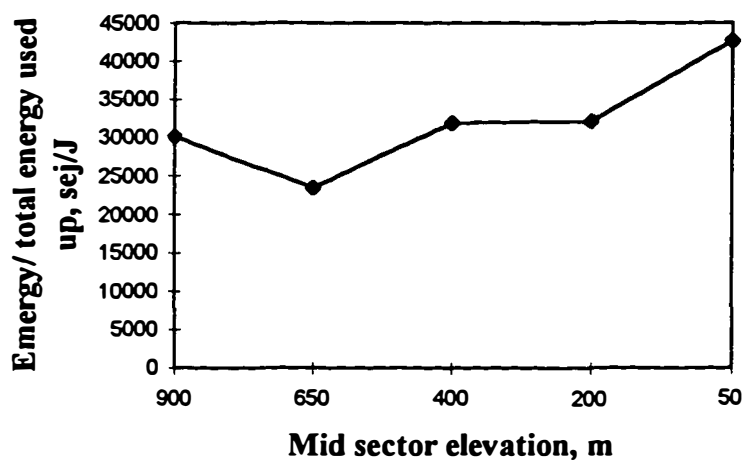


Figure A.1. Continued

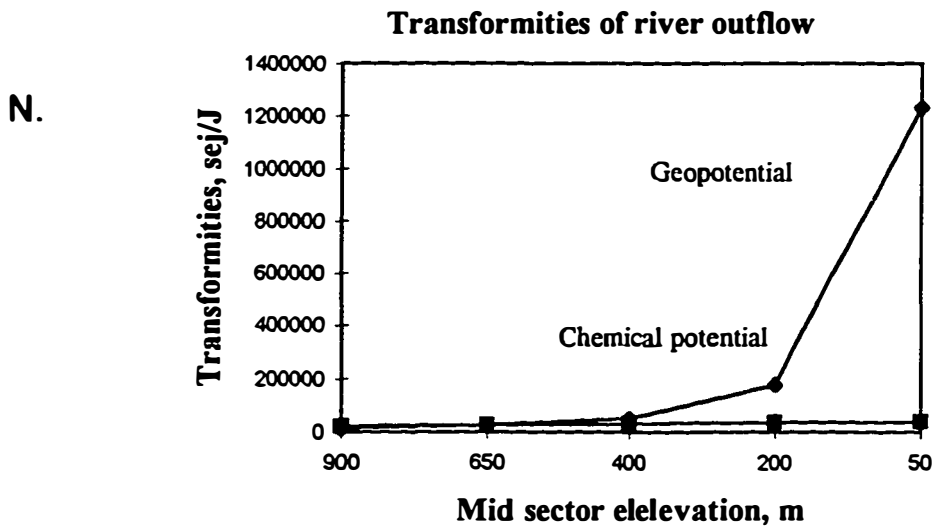
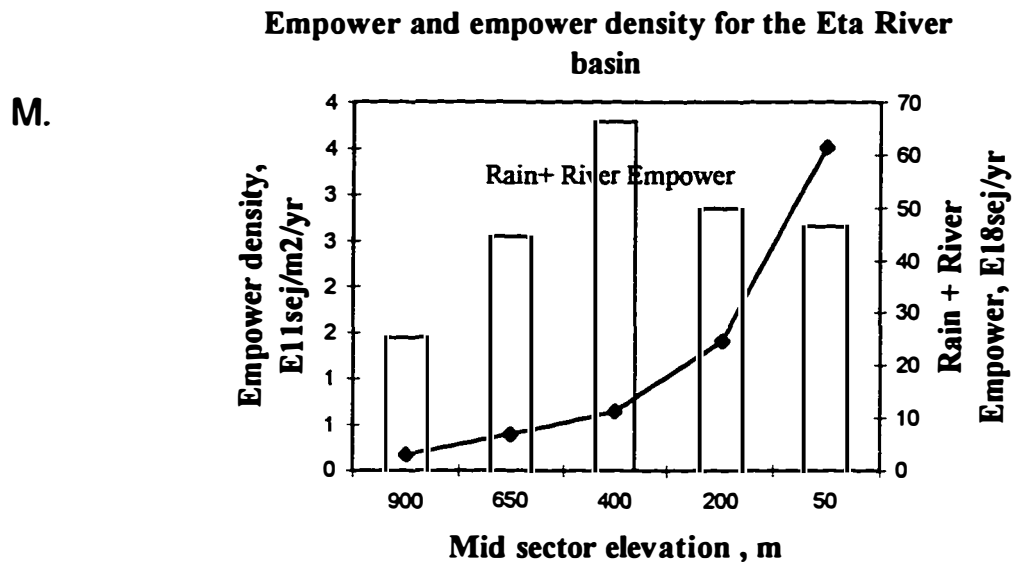


Figure A.1. Continued

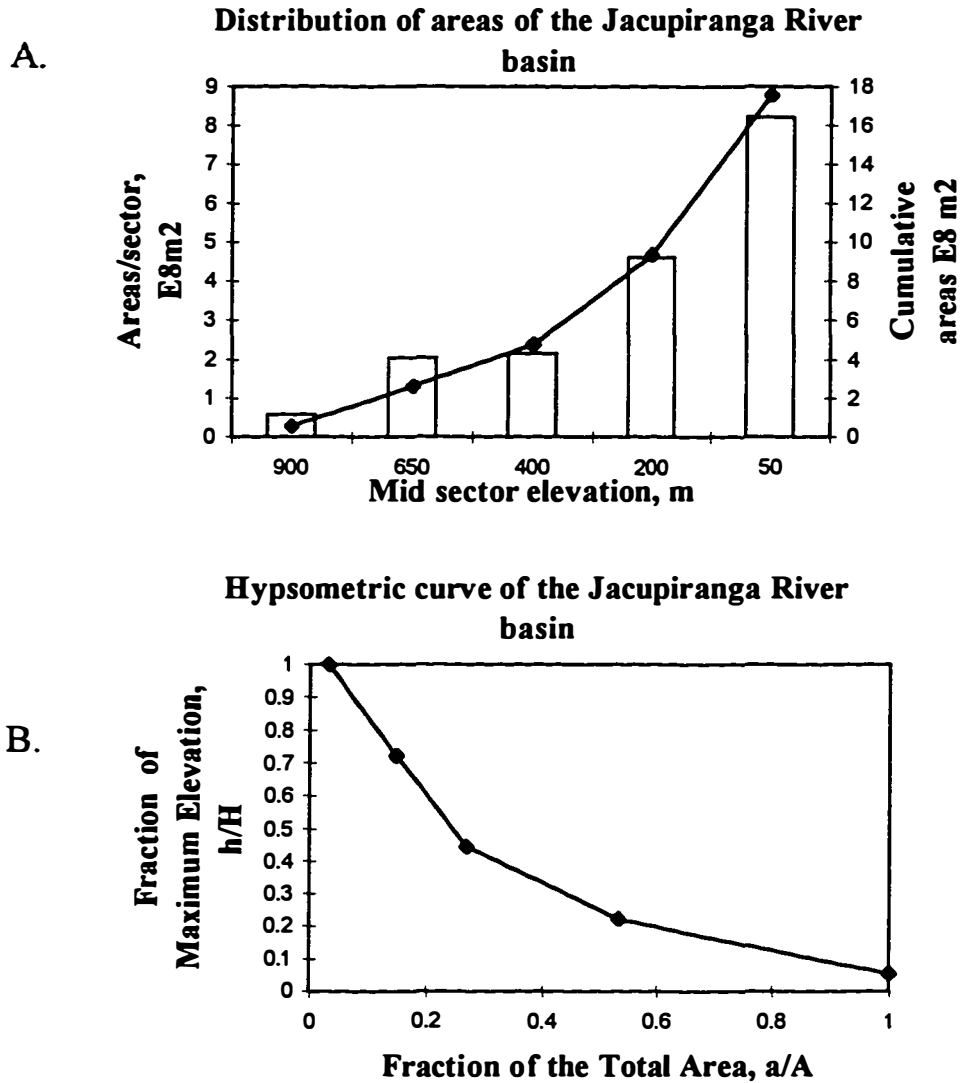
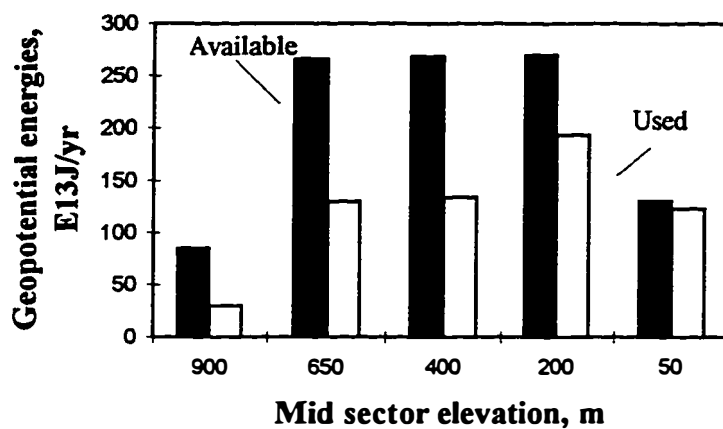


Figure A.2. Areas, energy and energy evaluations for the elevational sectors of Jacupiranga river basin, representing in: **A.** Aerial distribuion; **B.** Hypsometric curve; **C.** Available (G_{ri}) and Used (G_{tu}) geopotential energies; **D.** Proportion of rain (G_{ri}) and river (G_{vo}) in the inflowing geopotential energies; **E.** Available(C_{ri}) and Used (C_{tu}) chemical potential energies; **F.** Proportion of rain (C_{ri}) and river (C_{vo}) in the inflowing chemical potential energies; **G.** Geopotential energies used (G_{ru}, G_{vu}, G_{tu}) and outflow (G_{vo}); **H.** Chemical potential energies used ($C_{ru}, C_{vt}, C_{vu}, C_{tu}$) and outflow(C_{to}) ; **I.** Proportion of rain(G_{ru}) and river(G_{vu}) in the geopotential energy used up; **J.** Proportion of rain (C_{ru}) and river (C_{vu}) in the chemical potential energy used up; **K.** Geopotential used up (G_{tud}) and evapotranspired chemical potential (C_{etd}) power densities; **L.** Emery/ total used energy ($E_t / (G_{tu} + C_{tu})$) ratios; **M.** Total empower(E_t) and empower densities (E_d); **N.** Geopotential (T_{vg}) and chemical potential (T_{vc}) transformities of river outflow.

C. **Water geopotential energies available and used in the Jacupiranga River basin**



D. **Available geopotential energies provided by rain or river for the Jacupiranga River basin**

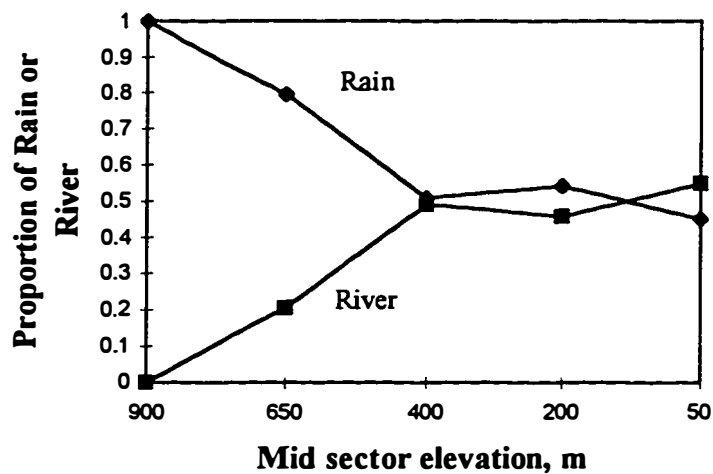
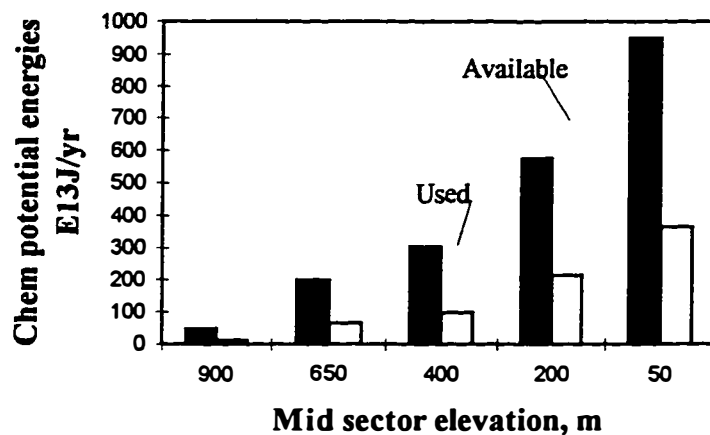


Figure A.2. Continued.

Water chemical potential energies available and used in the Jacupiranga River basin

E.



F.

Available chemical potential energy provided by rain or river for the Jacupiranga River basin

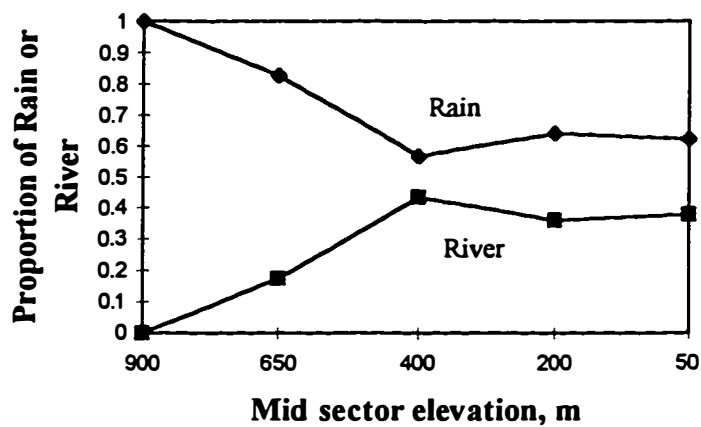


Figure A.2. Continued.

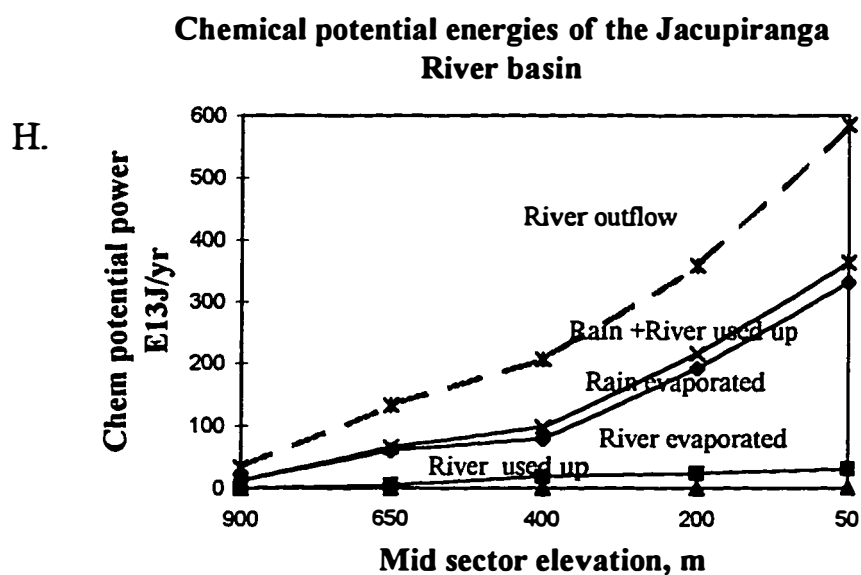
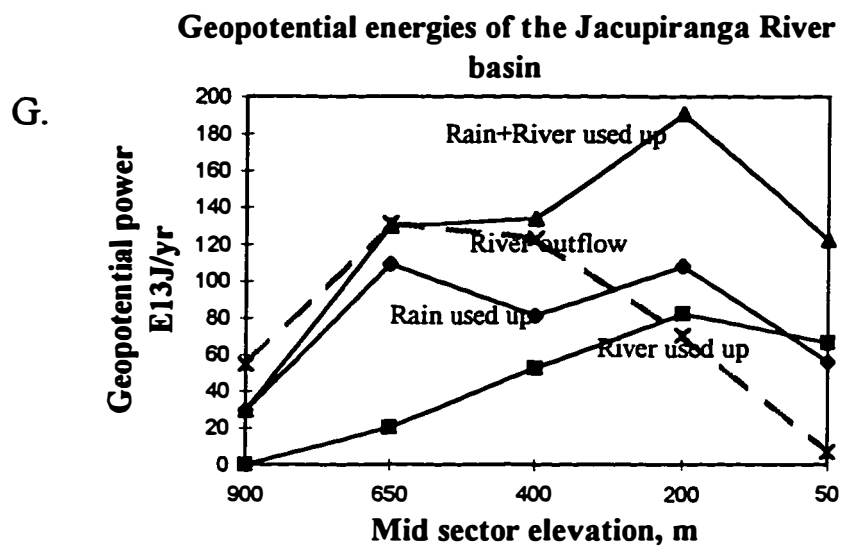
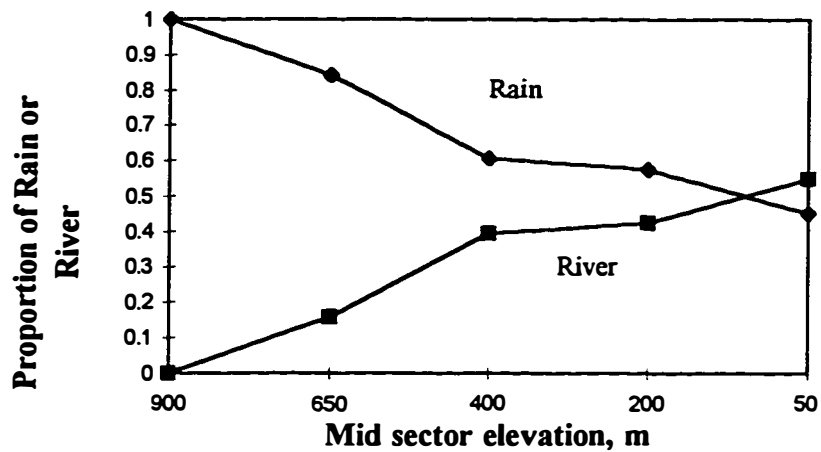


Figure A.2. Continued.

Proportion of Used Geopotential energy from rain or river in the Jacupiranga River basin

I.



Proportion of Used Chemical potential energy from rain or river in the Jacupiranga River basin

J.

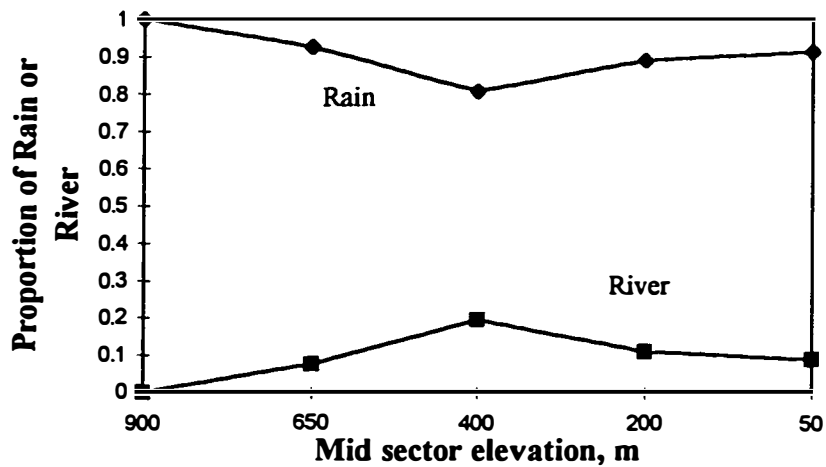
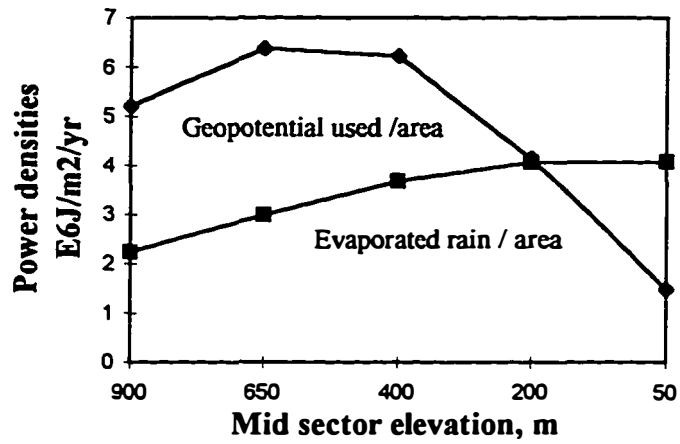


Figure A.2. Continued.

K.

Geopotential and Chemical potential power densities for the Jacupiranga River basin



L.

Ratio of Emergy to energy used up for the Jacupiranga River basin

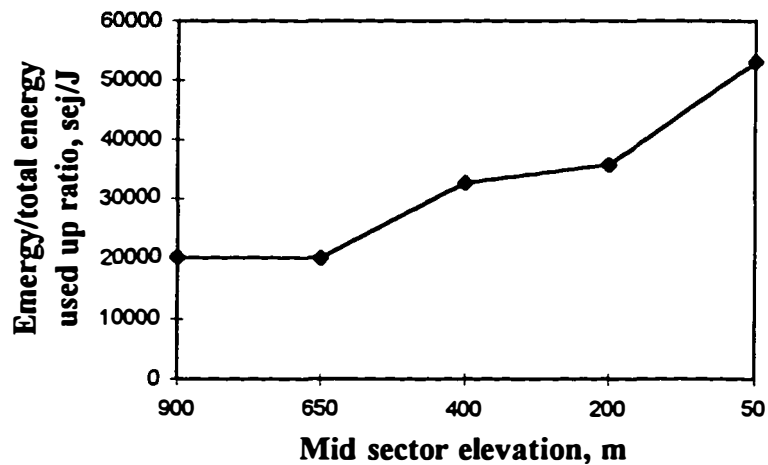


Figure A.2. Continued.

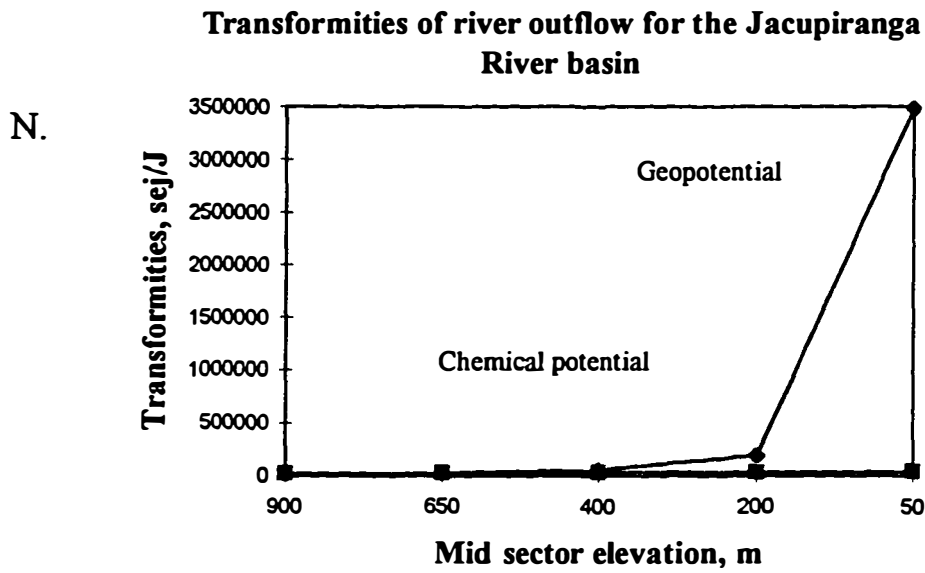
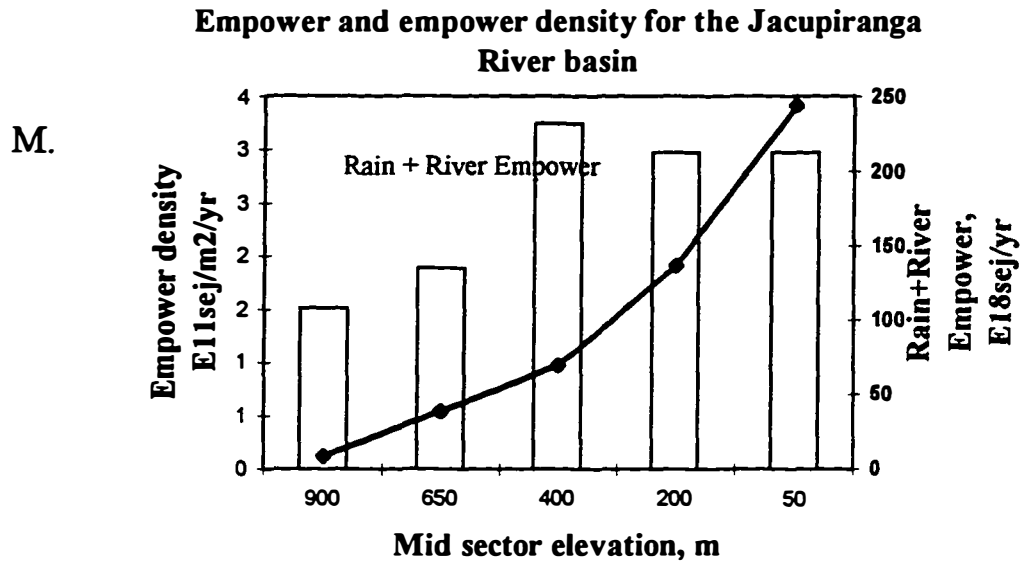


Figure A.2. Continued.

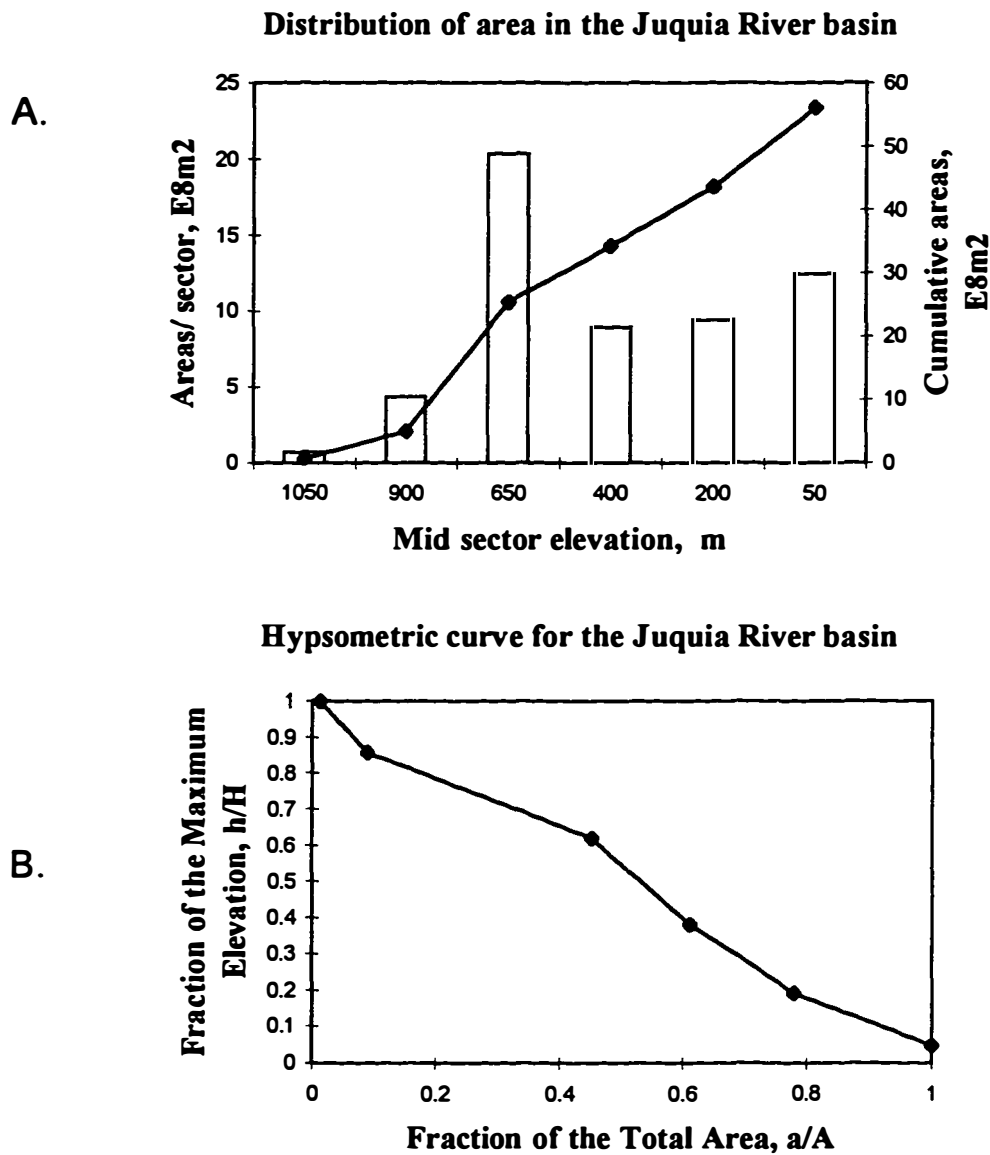


Figure A.3. Areas, energy and energy evaluations for the elevational sectors of Juquia river basin, representing in: **A.** Aerial distribution; **B.** Hypsometric curve; **C.** Available (Gri) and Used (Gtu) geopotential energies; **D.** Proportion of rain (Gri) and river (Gvo) in the inflowing geopotential energies; **E.** Available (Cri) and Used (Ctu) chemical potential energies; **F.** Proportion of rain (Cri) and river (Cvo) in the inflowing chemical potential energies; **G.** Geopotential energies used (Gru, Gvu, Gtu) and outflow (Gvo); **H.** Chemical potential energies used (Cru, Cvt, Cvu, Ctu) and outflow (Cto); **I.** Proportion of rain (Gru) and river (Gvu) in the geopotential energy used up; **J.** Proportion of rain (Cru) and river (Cvu) in the chemical potential energy used up; **K.** Geopotential used up (Gtud) and evapotranspired chemical potential (Cetd) power densities; **L.** Energy/ total used energy ($E_t / (G_{tu} + C_{tu})$) ratios; **M.** Total empower (E_t) and empower densities (E_d); **N.** Geopotential (Tvg) and chemical potential (Tvc) transformities of river outflow.

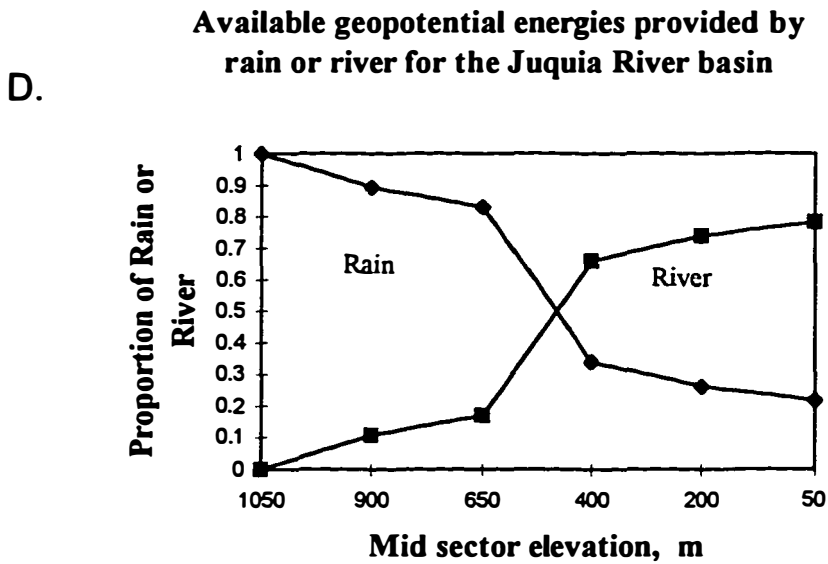
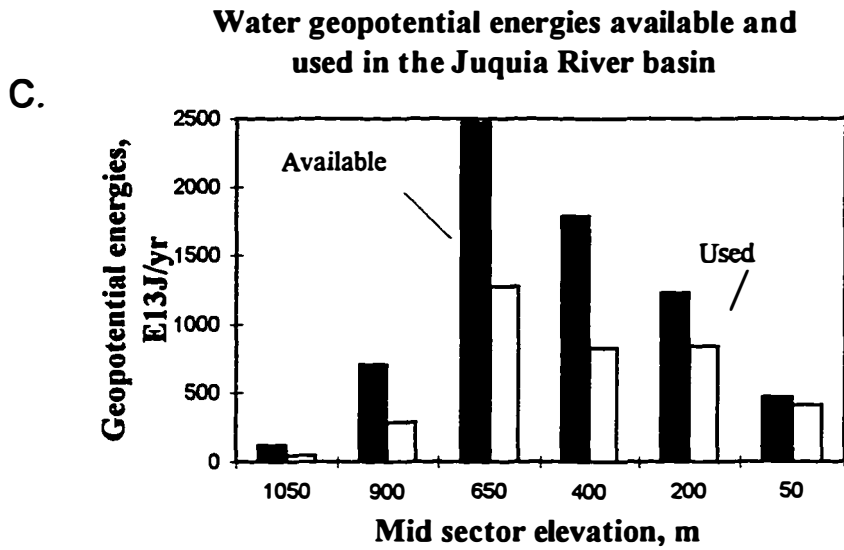
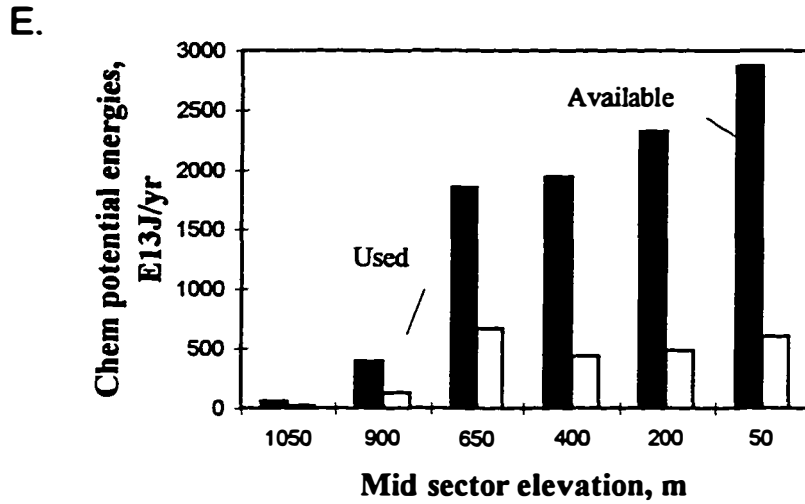


Figure A.3. Continued.

E. Water chemical potential energies available and used in the Juquia River basin



F. Available chemical potential energies provided by rain or river for the Juquia River basin

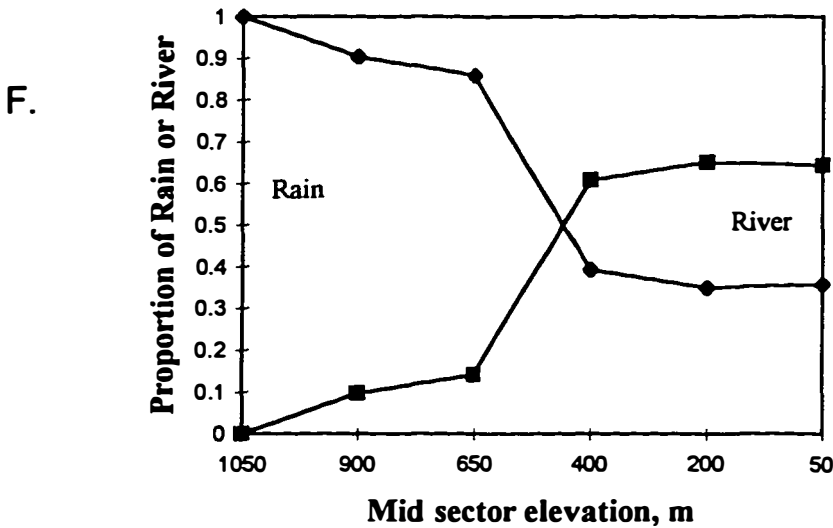


Figure A.3. Continued.

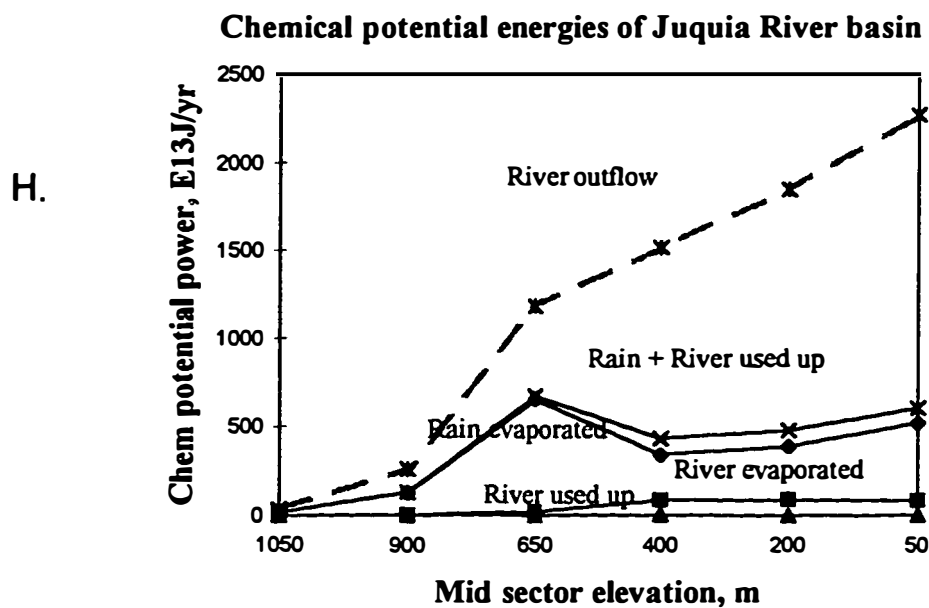
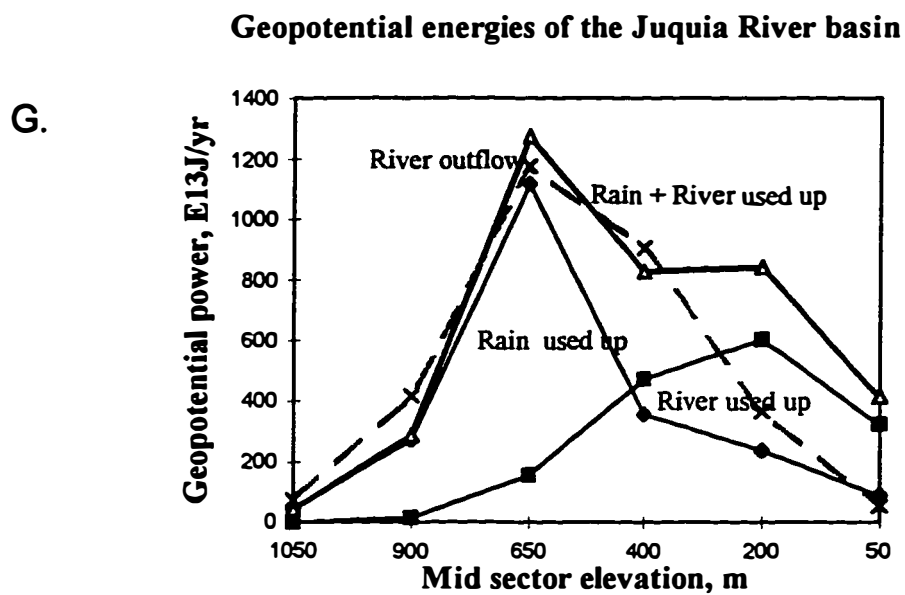


Figure A.3. Continued.

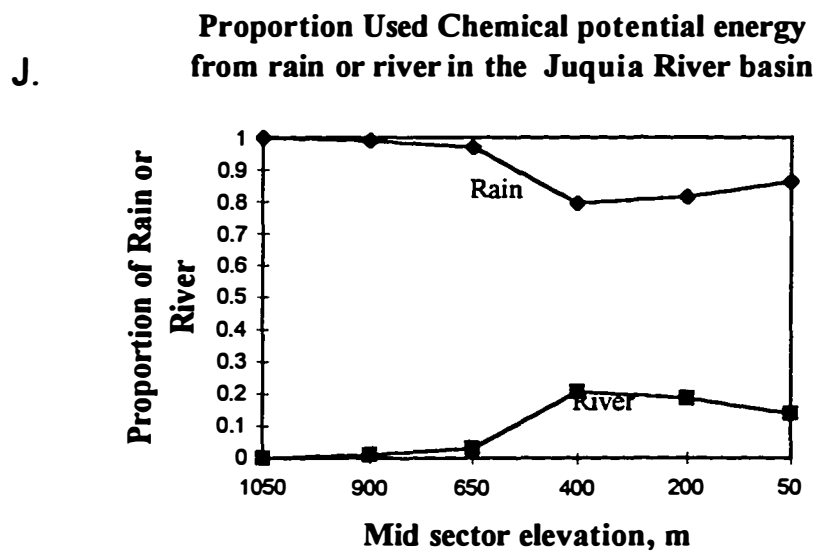
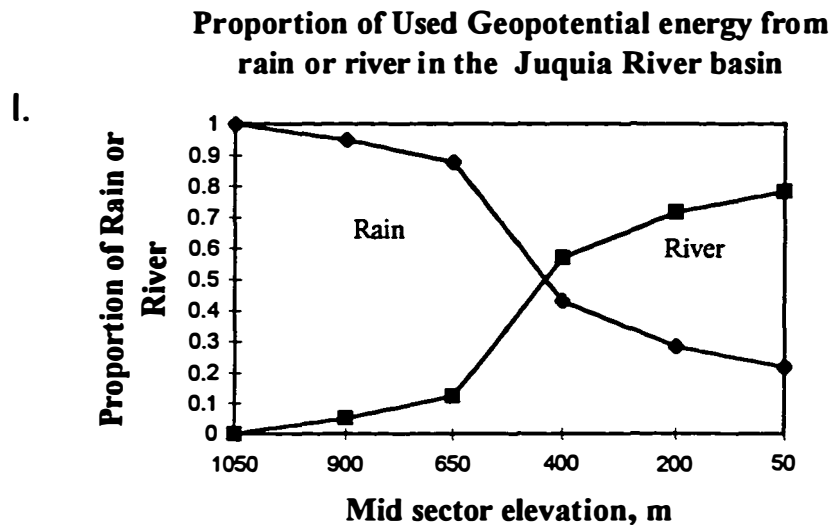
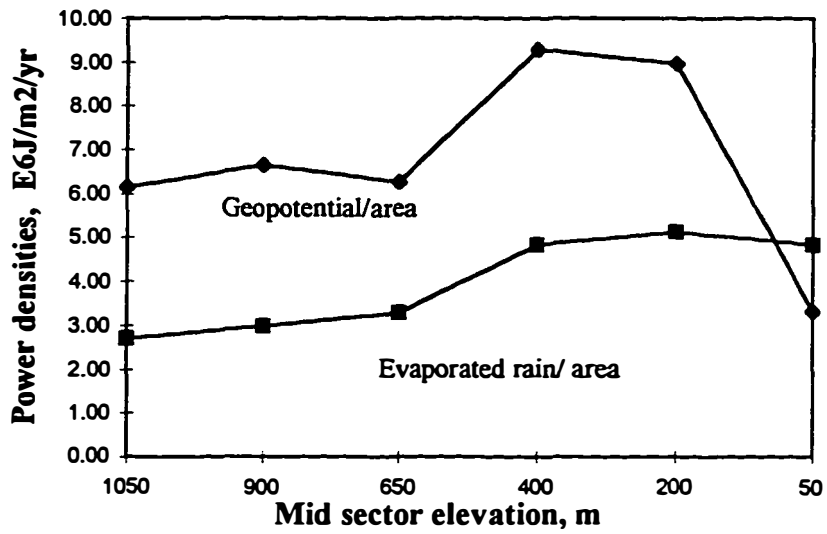


Figure A.3. Continued.

Geopotential and Chemical potential power densities of the Juquia River basin

K.



Ratio of Energy to energy use for the Juquia River basin

L.

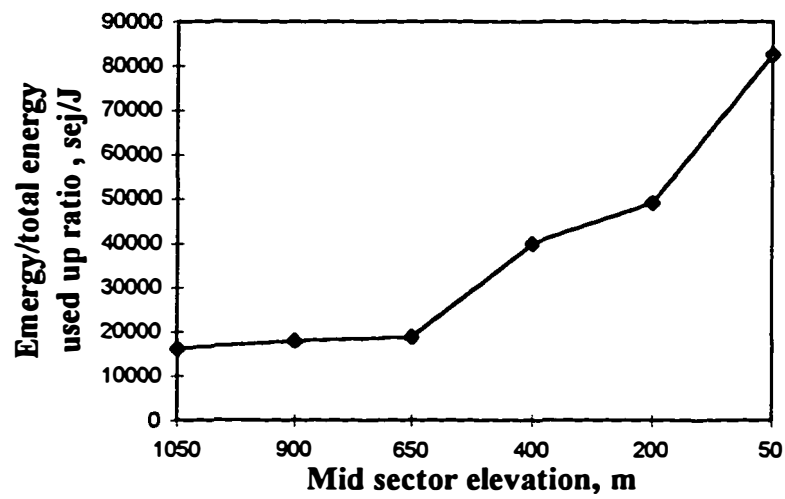
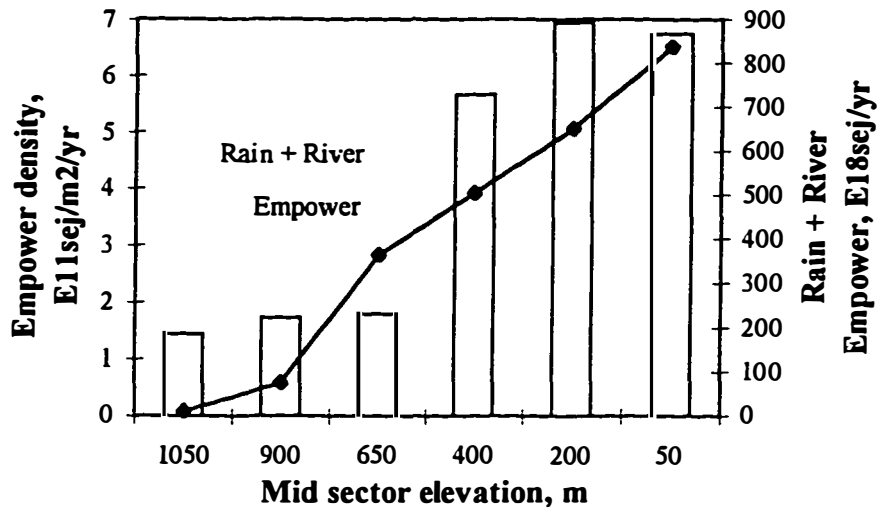


Figure A.3. Continued.

M. Empower and empower density for the Juquia River basin



N. Transformities of river outflow for the Juquia River basin

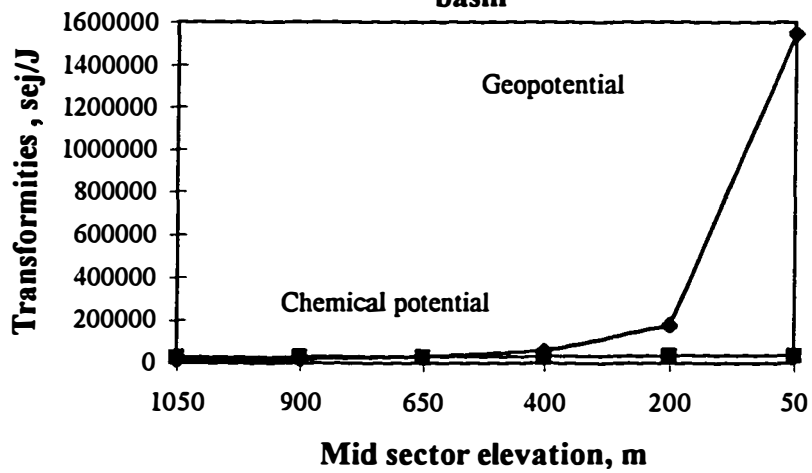


Figure A.3. Continued.

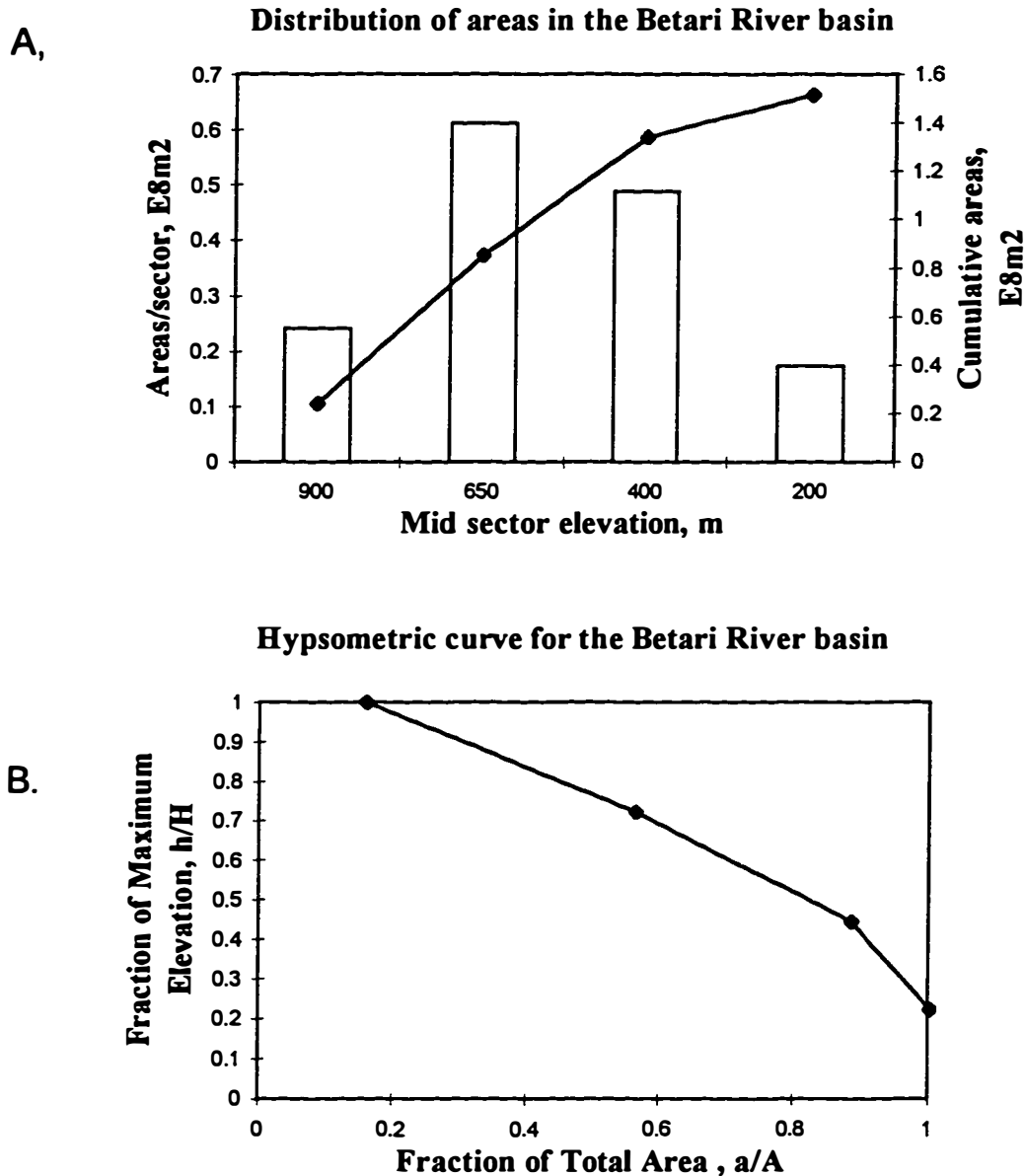
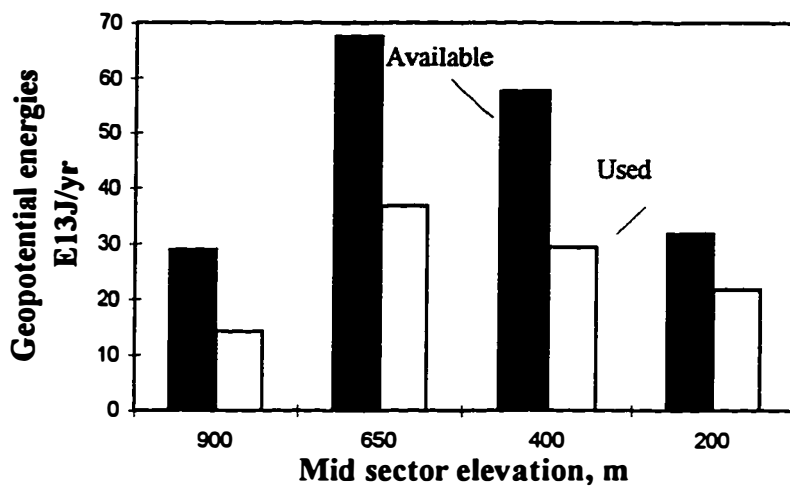


Figure A.4. Areas, energy and energy evaluations for the elevational sectors of Betari river basin, representing in: **A.** Aerial distribution; **B.** Hypsometric curve; **C.** Available (G_{ri}) and Used (G_{tu}) geopotential energies; **D.** Proportion of rain (G_{ri}) and river (G_{vo}) in the inflowing geopotential energies; **E.** Available (C_{ri}) and Used (C_{tu}) chemical potential energies; **F.** Proportion of rain (C_{ri}) and river (C_{vo}) in the inflowing chemical potential energies; **G.** Geopotential energies used (G_{ru}, G_{vu}, G_{tu}) and outflow (G_{vo}); **H.** Chemical potential energies used ($C_{ru}, C_{vt}, C_{vu}, C_{tu}$) and outflow (C_{to}); **I.** Proportion of rain (G_{ru}) and river (G_{vu}) in the geopotential energy used up; **J.** Proportion of rain (C_{ru}) and river (C_{vu}) in the chemical potential energy used up; **K.** Geopotential used up (G_{tud}) and evapotranspired chemical potential (C_{etd}) power densities; **L.** Energy/ total used energy ($E_t / (G_{tu} + C_{tu})$) ratios; **M.** Total empower (E_t) and empower densities (E_d); **N.** Geopotential (T_{vg}) and chemical potential (T_{vc}) transformities of river outflow.

C. **Water geopotential energies available and used in the Betari River basin**



D. **Available geopotential energies provided by rain or river for the Betari River basin**

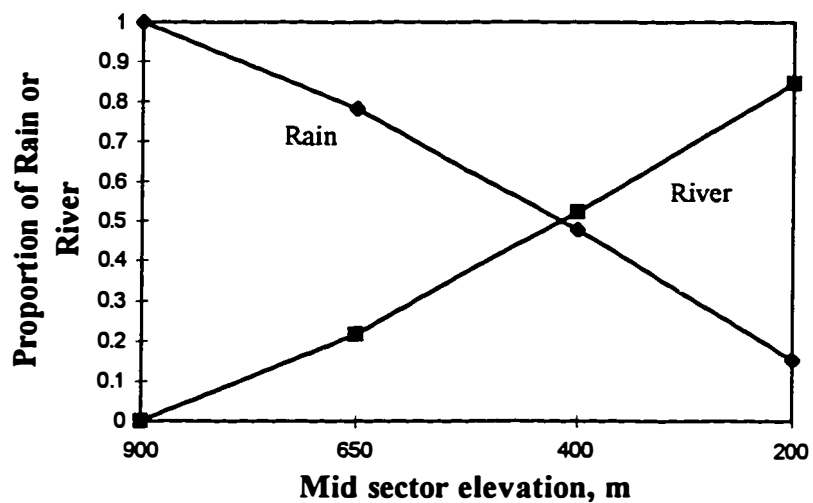
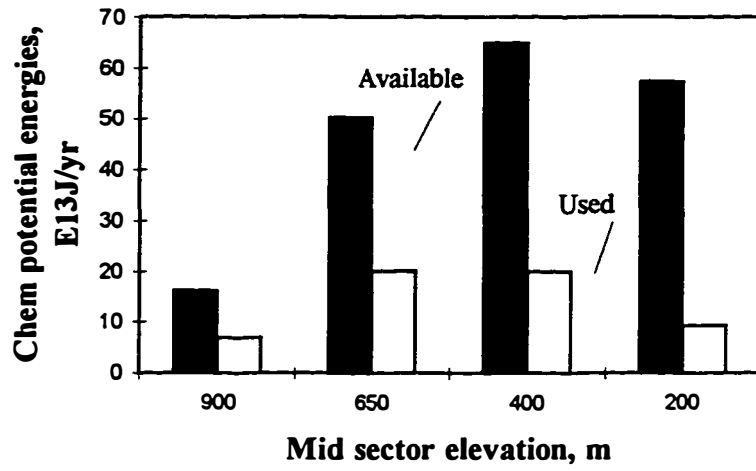


Figure A.4. Continued

F. Water chemical potential energies available and used in the Betari River basin



F. Available chemical potential energies provided by rain or river for Betari River basin

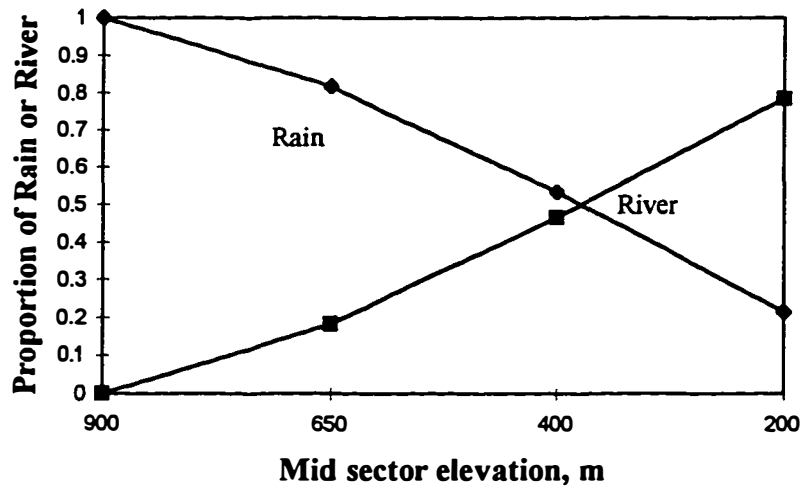
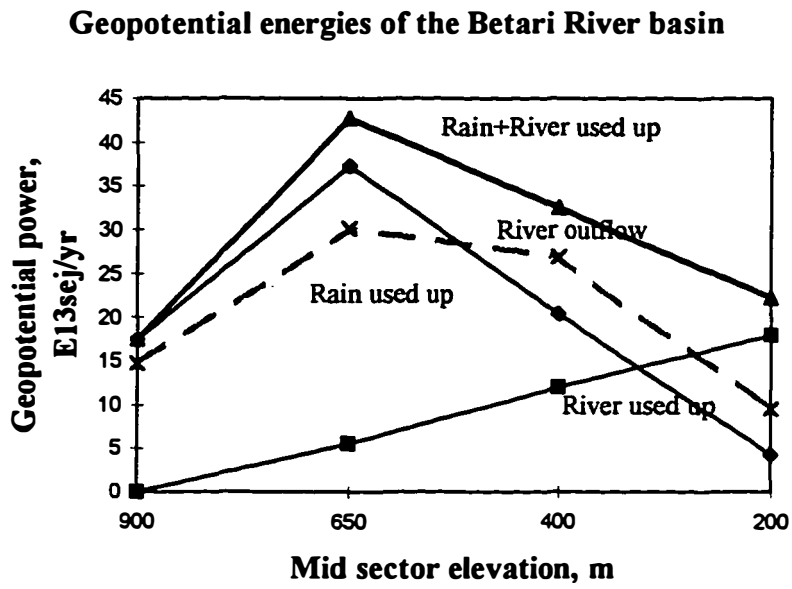


Figure A.4. Continued

G.



H.

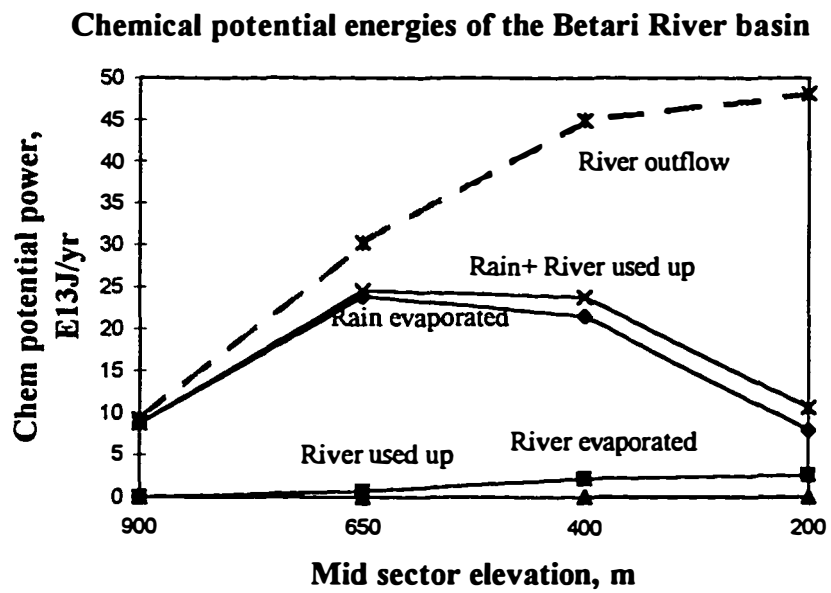


Figure A.4. Continued

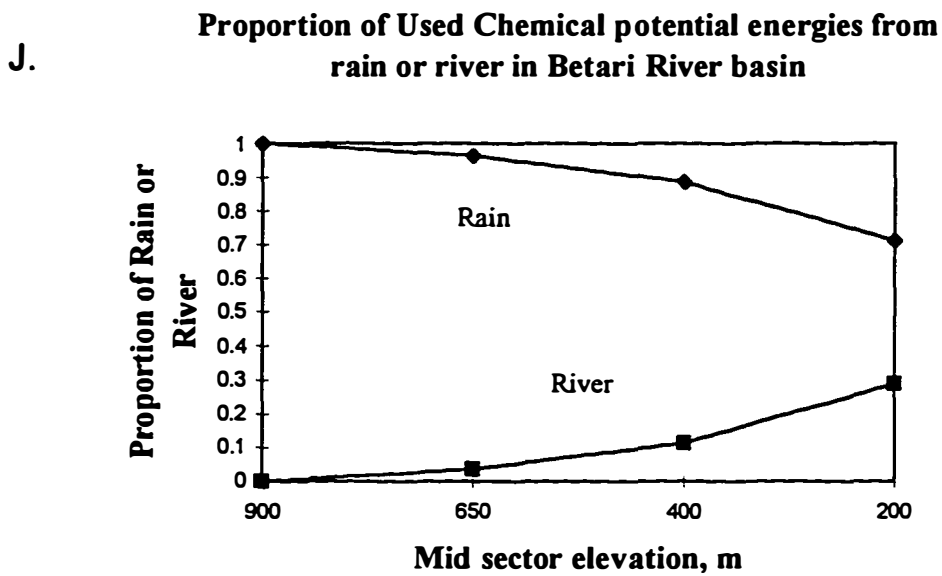
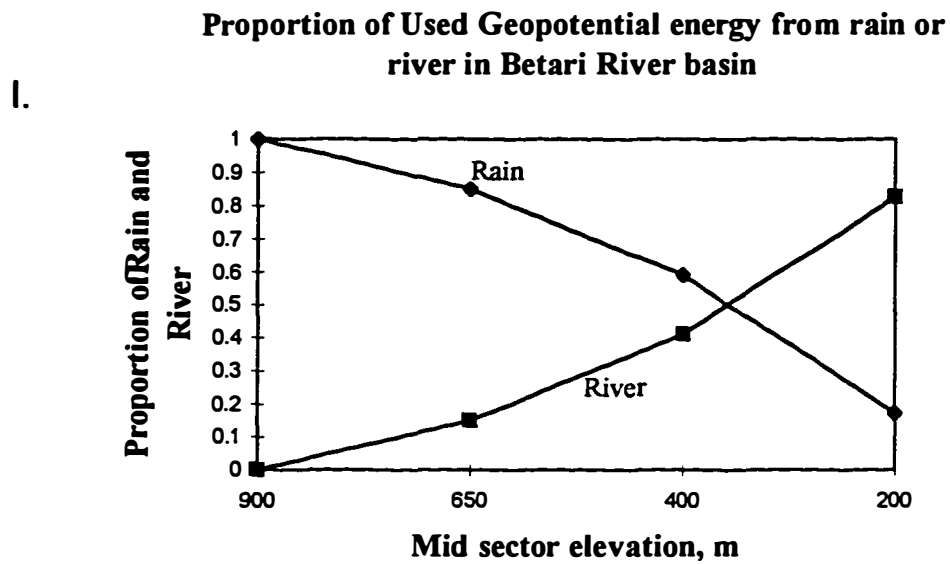
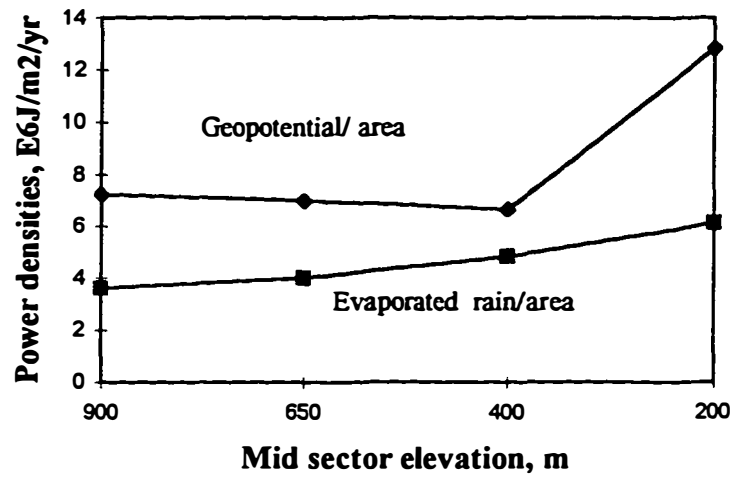


Figure A.4. Continued.

Geopotential and Chemical potential power densities for the Betari River basin

K.



Ratio of Emergy to energy used up for the Betari River basin

L.

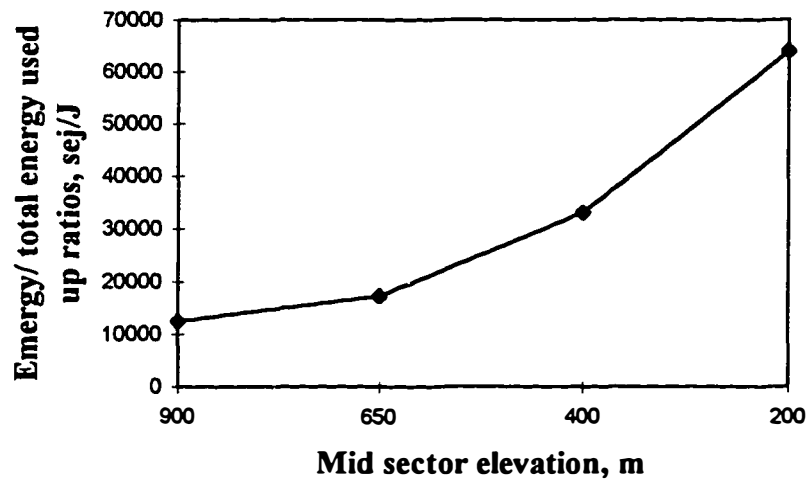


Figure A..4. Continued

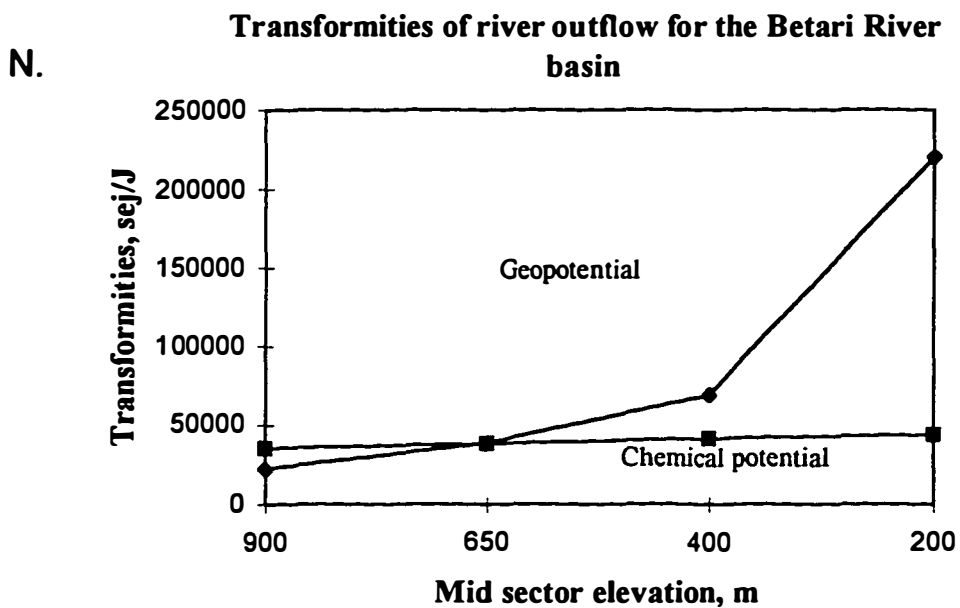
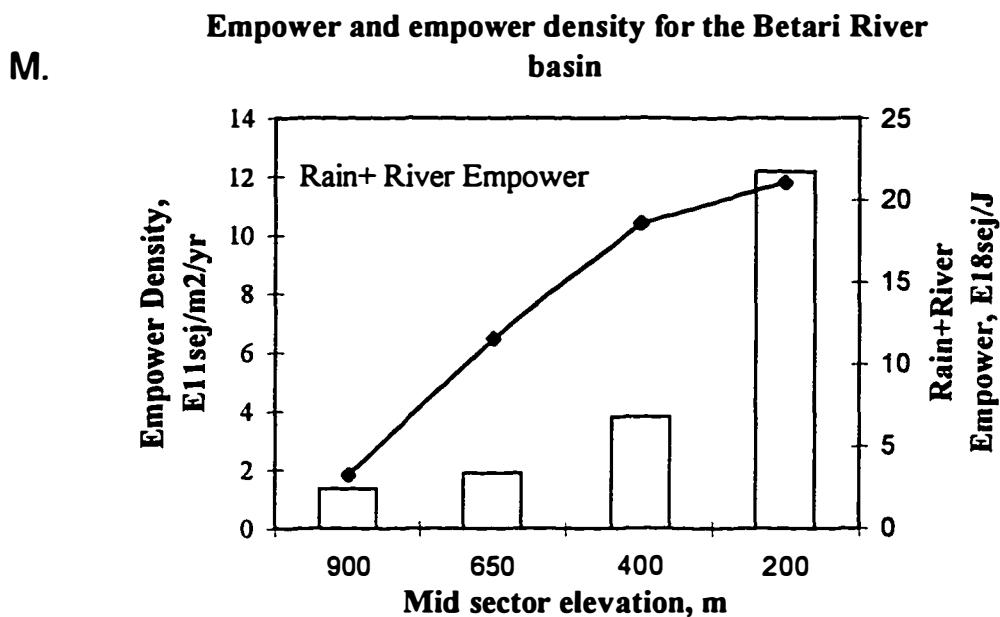


Figure A.4. Continued.

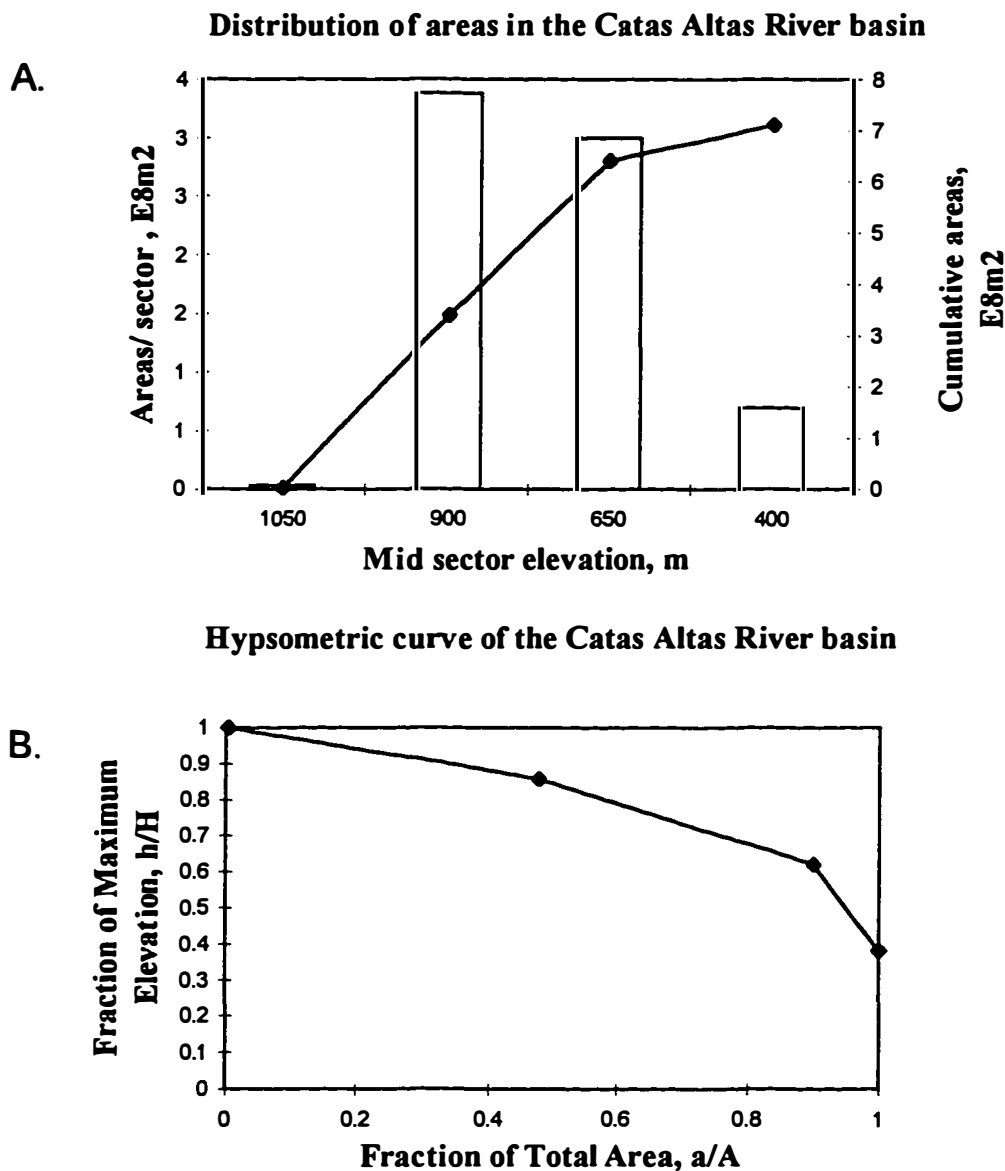
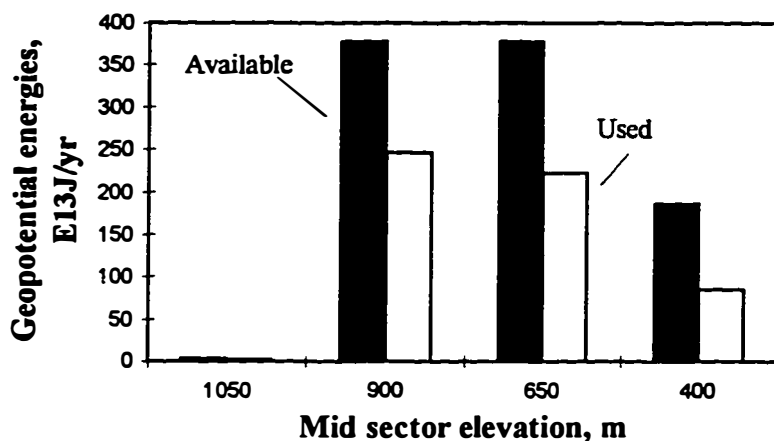


Figure A.5. Areas, energy and energy evaluations for the elevational sectors of Catas Altas river basin, representing in: **A.** Aerial distribution; **B.** Hypsometric curve; **C.** Available (G_{ri}) and Used (G_{tu}) geopotential energies; **D.** Proportion of rain (G_{ri}) and river (G_{vo}) in the inflowing geopotential energies; **E.** Available (C_{ri}) and Used (C_{tu}) chemical potential energies; **F.** Proportion of rain (C_{ri}) and river (C_{vo}) in the inflowing chemical potential energies; **G.** Geopotential energies used (G_{ru}, G_{vu}, G_{tu}) and outflow (G_{vo}); **H.** Chemical potential energies used ($C_{ru}, C_{vt}, C_{vu}, C_{tu}$) and outflow (C_{to}); **I.** Proportion of rain (G_{ru}) and river (G_{vu}) in the geopotential energy used up; **J.** Proportion of rain (C_{ru}) and river (C_{vu}) in the chemical potential energy used up; **K.** Geopotential used up (G_{tud}) and evapotranspired chemical potential (C_{etd}) power densities; **L.** Energy/ total used energy ($E_t / (G_{tu} + C_{tu})$) ratios; **M.** Total empower (E_t) and empower densities (E_d); **N.** Geopotential (T_{vg}) and chemical potential (T_{vc}) transformities of river outflow.

C. **Water geopotential energies available and used in the Catas Altas River basin**



D. **Available geopotential energies provided by rain or river for the Catas Altas River basin**

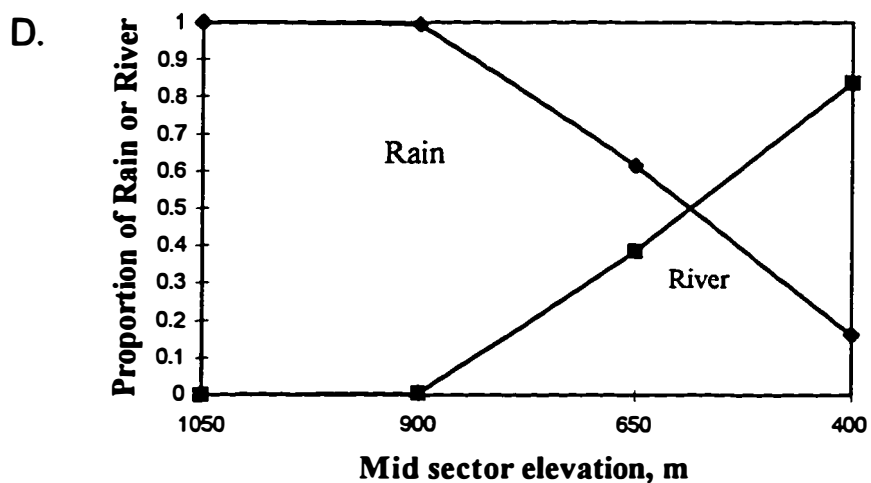
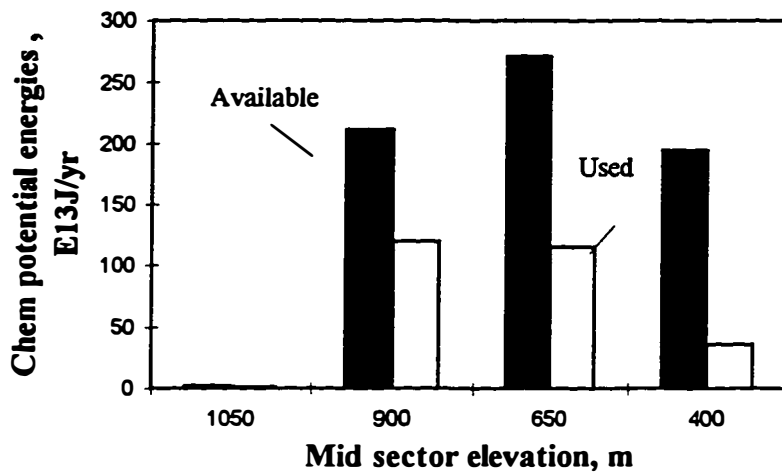


Figure A.5. Continued.

E. **Water chemical potential energies available and used in the Catas Altas River basin**



F. **Available chemical potential energies provided by rain or river for the Catas Altas River basin**

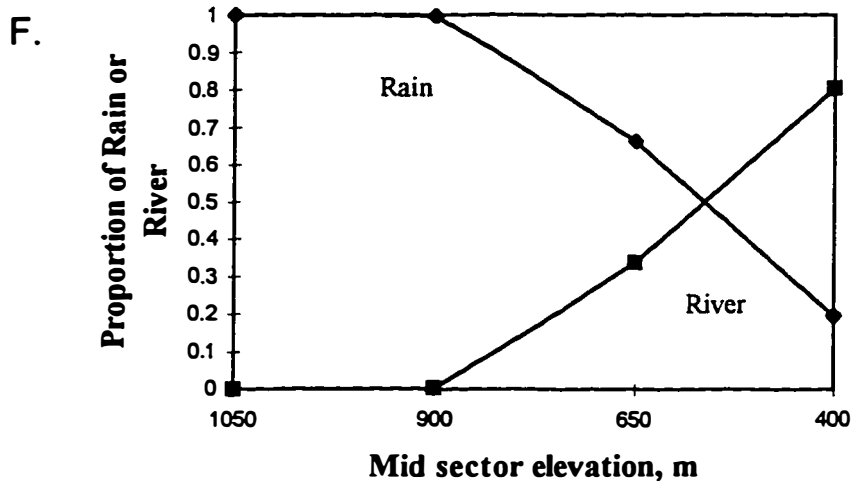


Figure A.5. Continued.

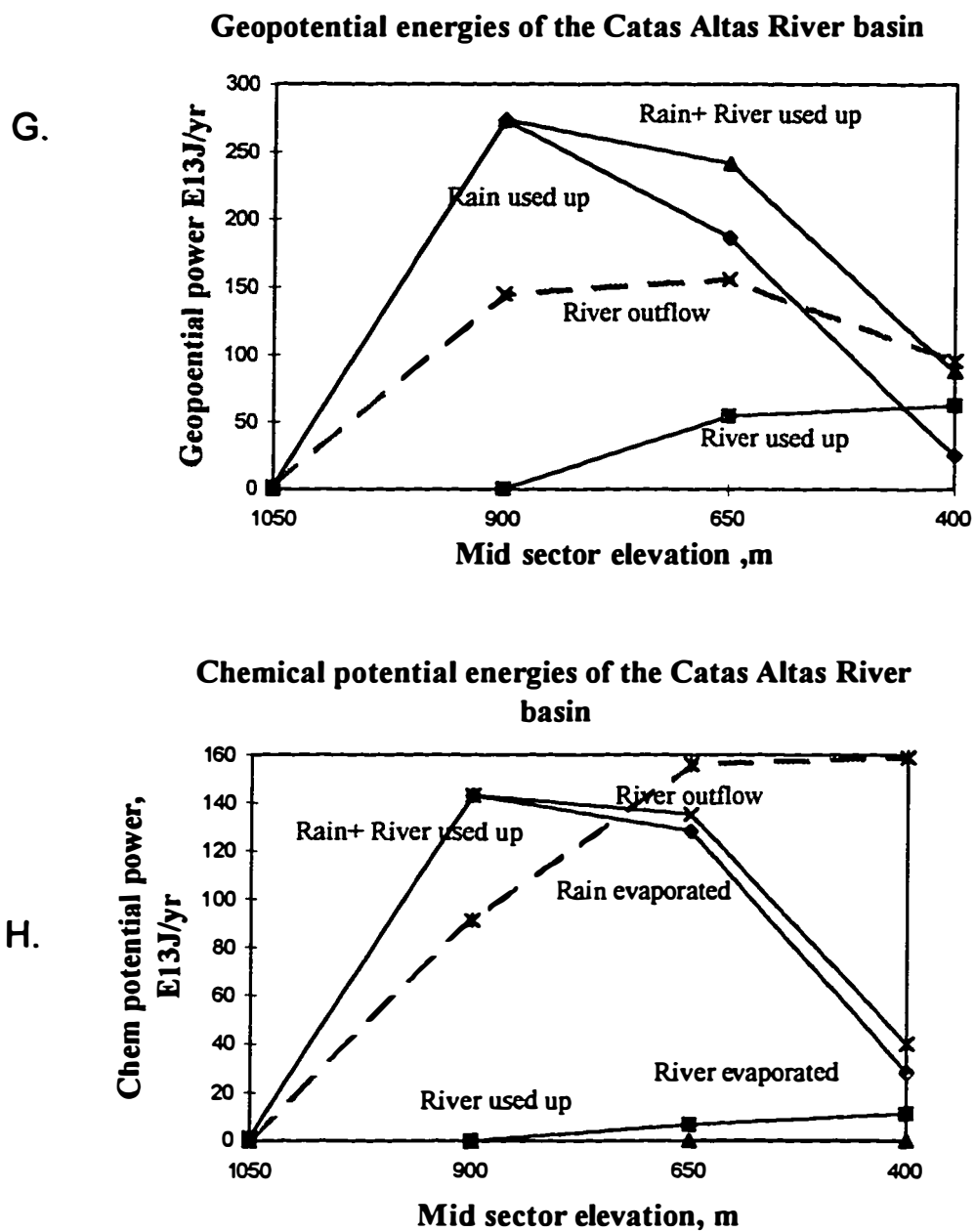


Figure A.5. Continued.

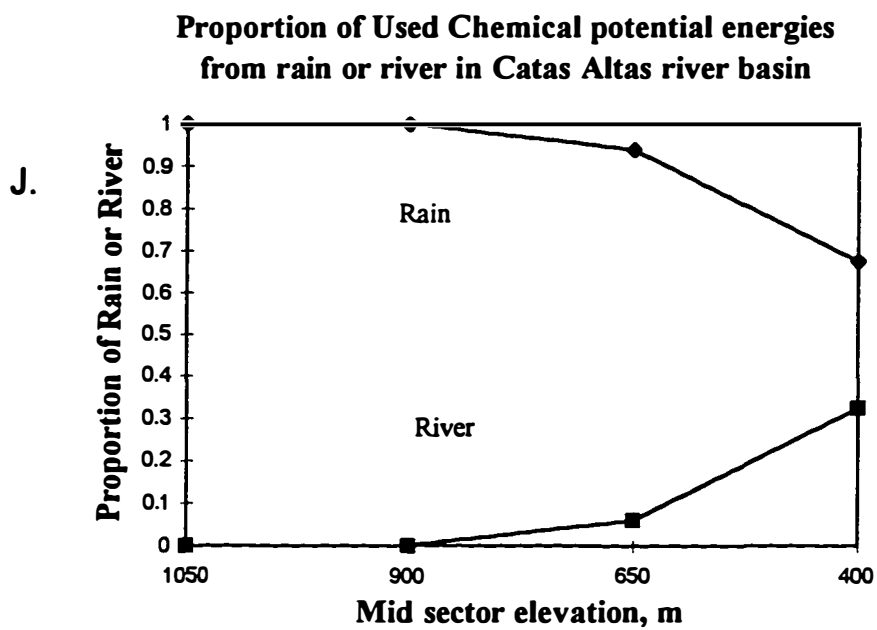
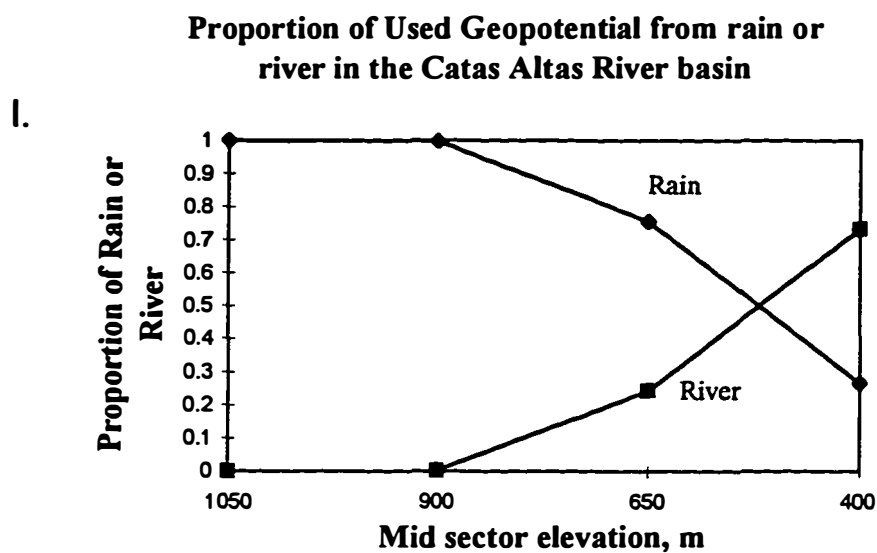
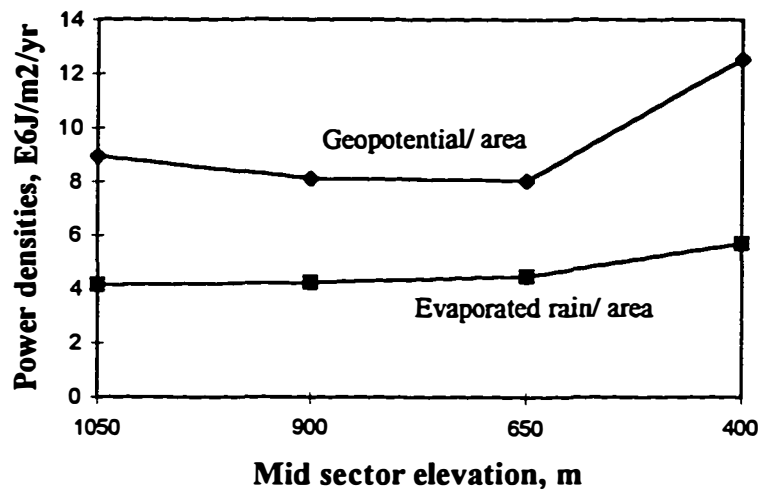


Figure A.5. Continued.

K.

**Geopotential and chemical potential power densities
of the Catas Altas River basin**



L.

**Ratio of Emergy to energy used up for the Catas Altas
River basin**

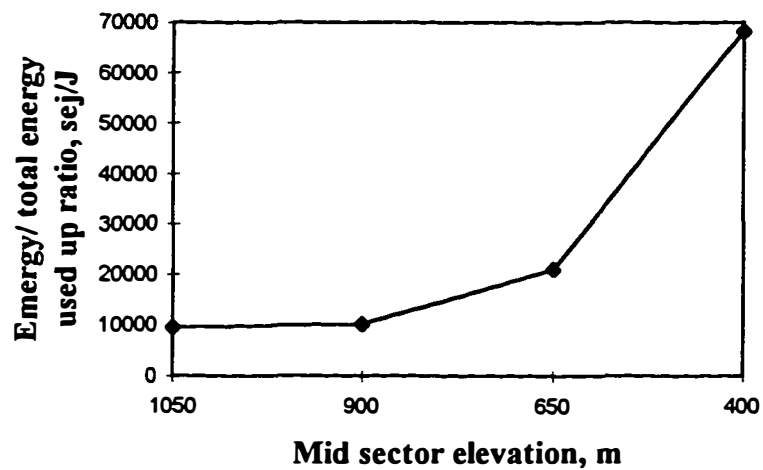


Figure A.5. Continued.

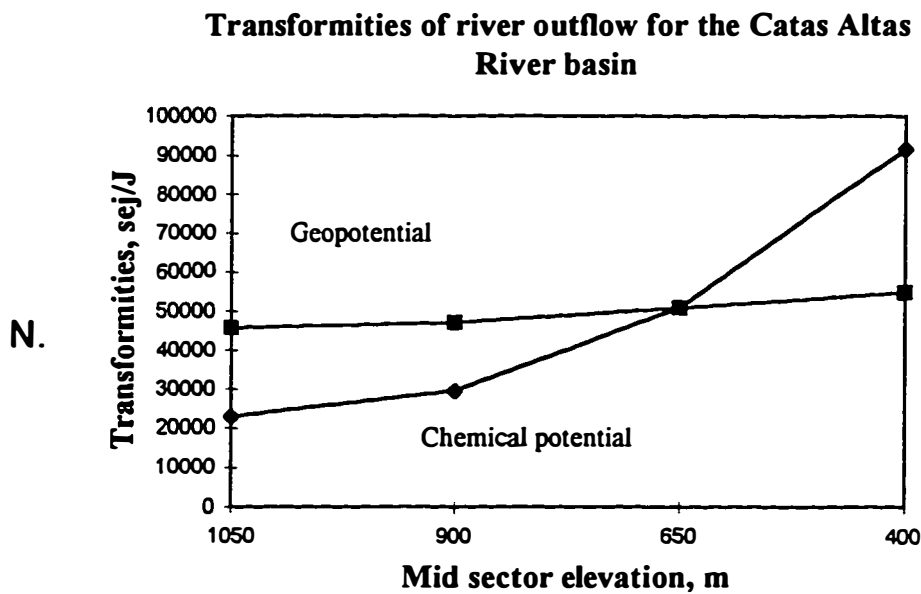
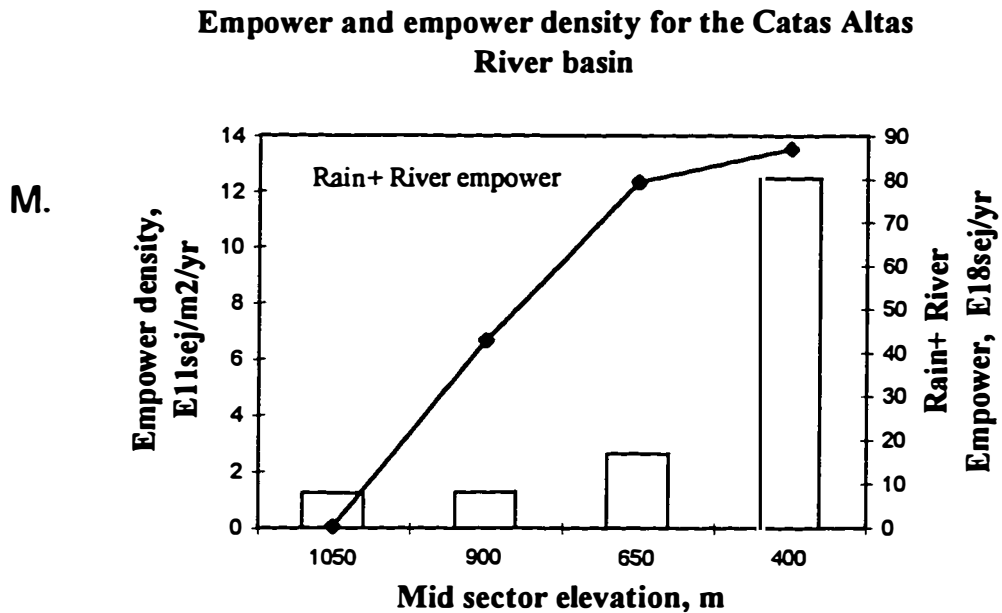


Figure A.5. Continued.

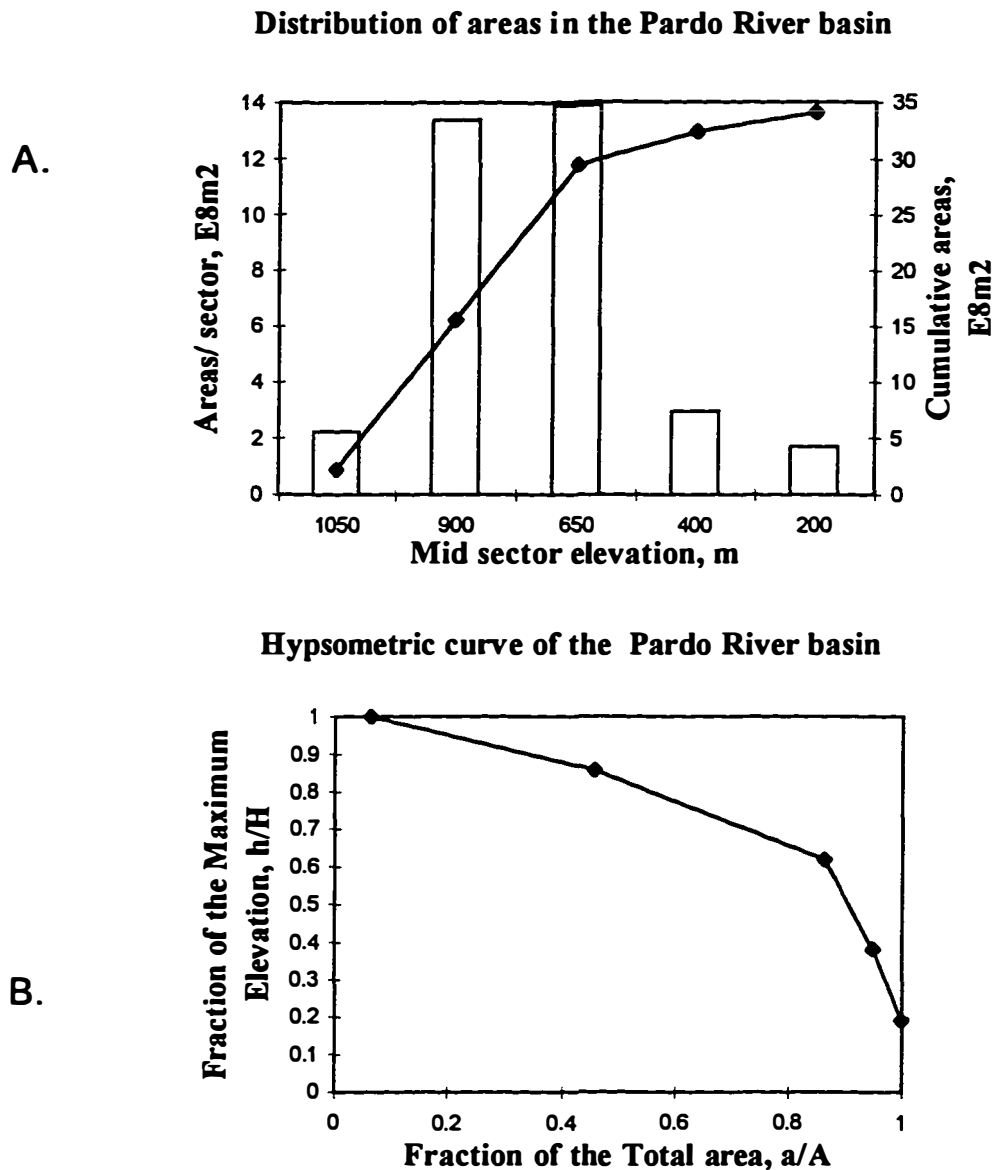


Figure A.6. Areas, energy and energy evaluations for the elevational sectors of Pardo river basin, representing in: **A.** Aerial distribution; **B.** Hypsometric curve; **C.** Available (Gri) and Used (Gtu) geopotential energies; **D.** Proportion of rain (Gri) and river (Gvo) in the inflowing geopotential energies; **E.** Available (Cri) and Used (Ctu) chemical potential energies; **F.** Proportion of rain (Cri) and river (Cvo) in the inflowing chemical potential energies; **G.** Geopotential energies used (Gru, Gvu, Gtu) and outflow (Gvo); **H.** Chemical potential energies used (Cru, Cvt, Cvu, Ctu) and outflow (Cto); **I.** Proportion of rain (Gru) and river (Gvu) in the geopotential energy used up; **J.** Proportion of rain (Cru) and river (Cvu) in the chemical potential energy used up; **K.** Geopotential used up (Gtud) and evapotranspired chemical potential (Cetd) power densities; **L.** Energy/ total used energy ($E_t / (G_{tu} + C_{tu})$) ratios; **M.** Total empower (E_t) and empower densities (E_d); **N.** Geopotential (T_{vg}) and chemical potential (T_{vc}) transformities of river outflow.

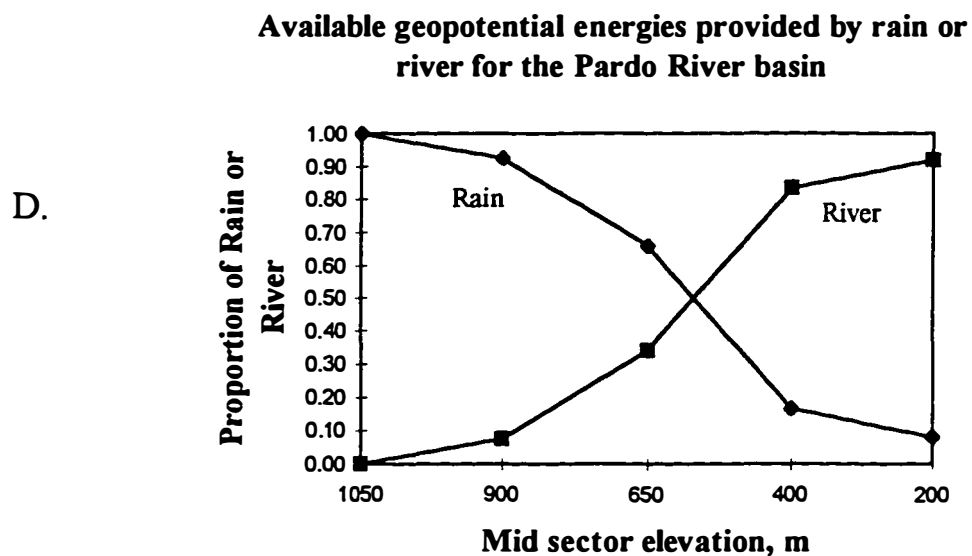
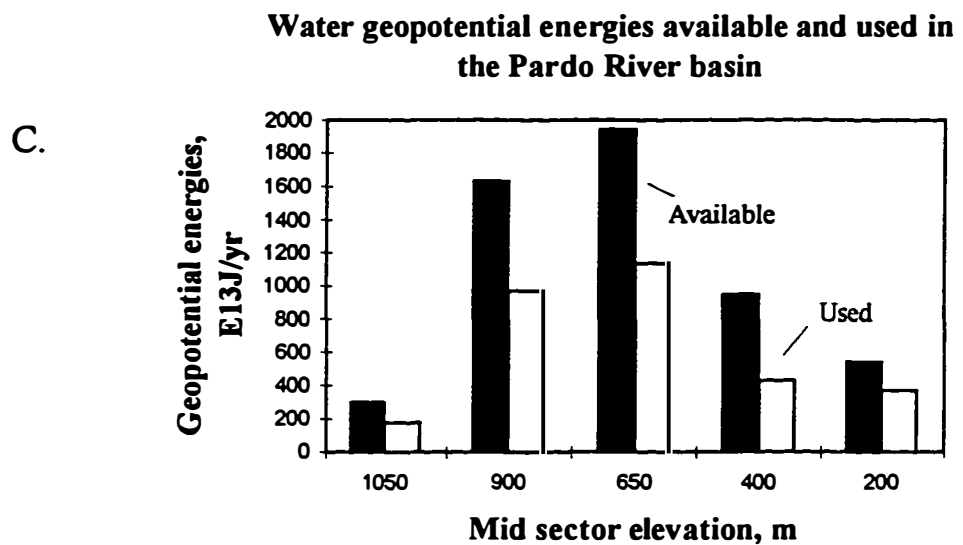
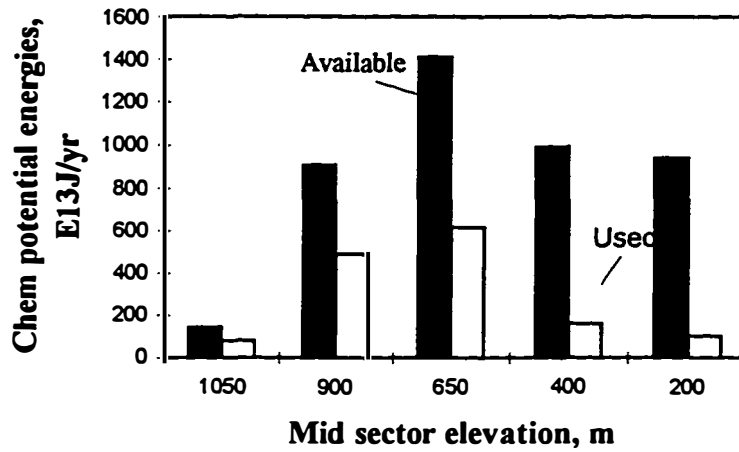


Figure A.6. Continued.

E.

Water chemical potential energies available and used in the Pardo River basin



F.

Available chemical potential energies provided by rain or river for the Pardo River basin

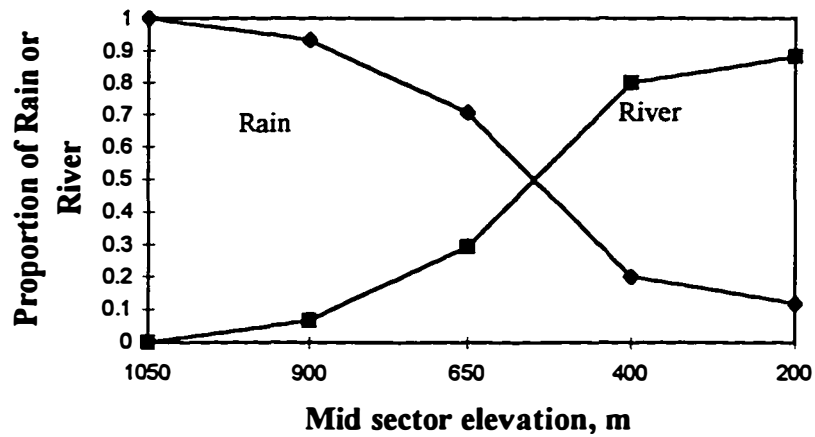


Figure A.6. Continued.

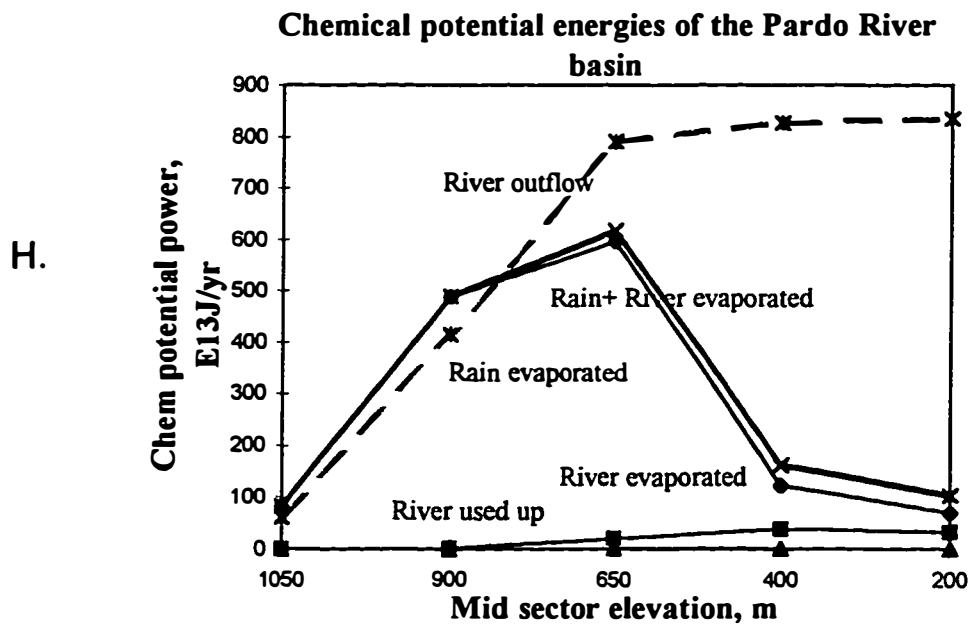
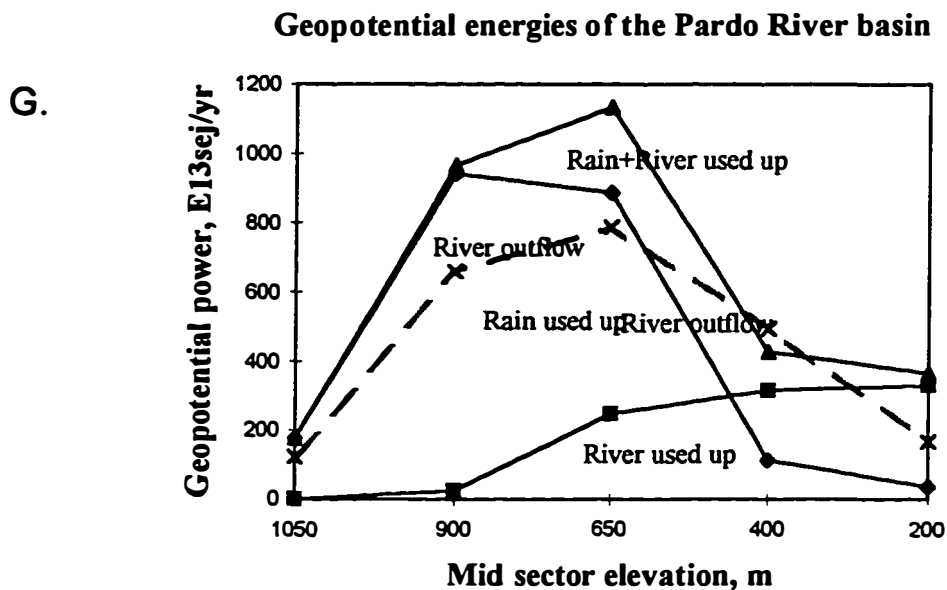
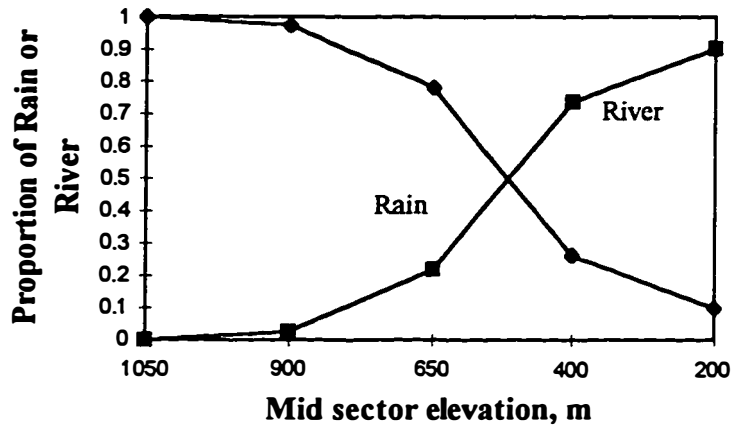


Figure A.6. Continued.

I.

Proportion of Used Geopotential energies from rain or river in the Pardo River basin



J.

Proportion of Used Chemical potential energies from rain or river in the Pardo river basin

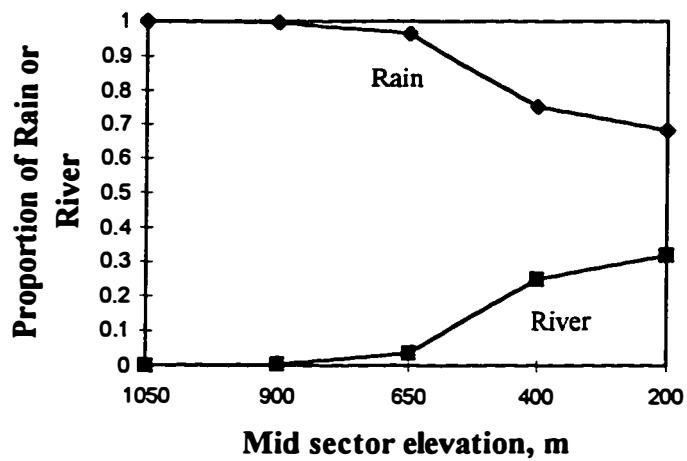
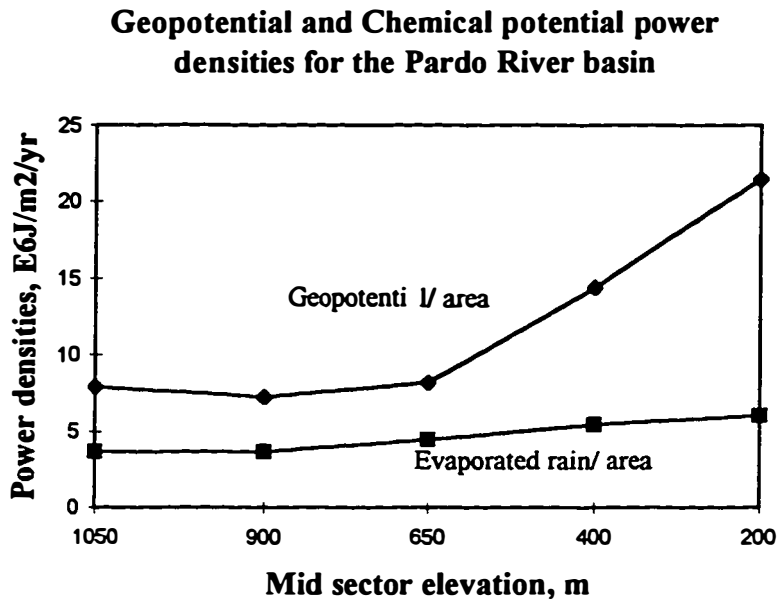


Figure A.6. Continued.

K.



L.

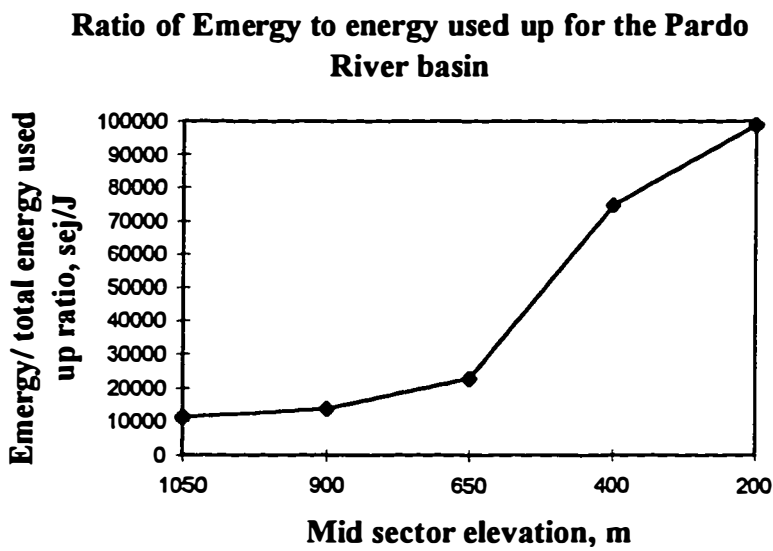
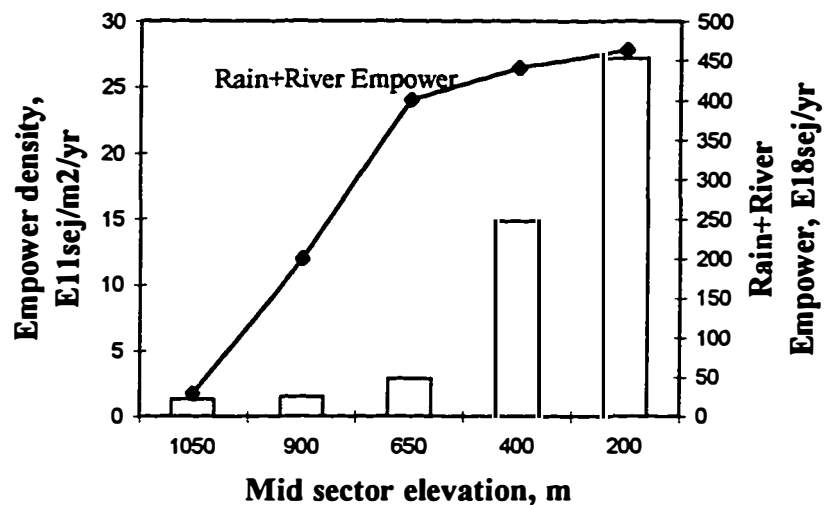


Figure A.6. Continued.

M. **Empower and empower densities for the Pardo River basin**



N. **Transformities of river outflow for the Pardo River basin**

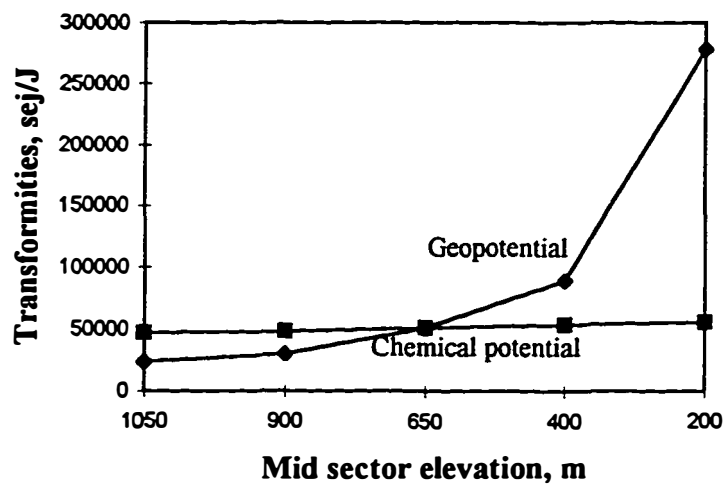
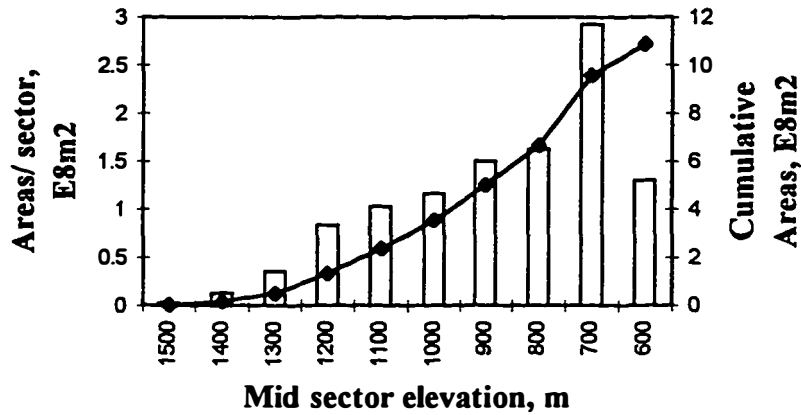


Figure A.6. Continued.

A.

Distribution of areas in the Upper Little Tennessee River basin



B.

Hypsometric curve of the Upper Little Tennessee River basin

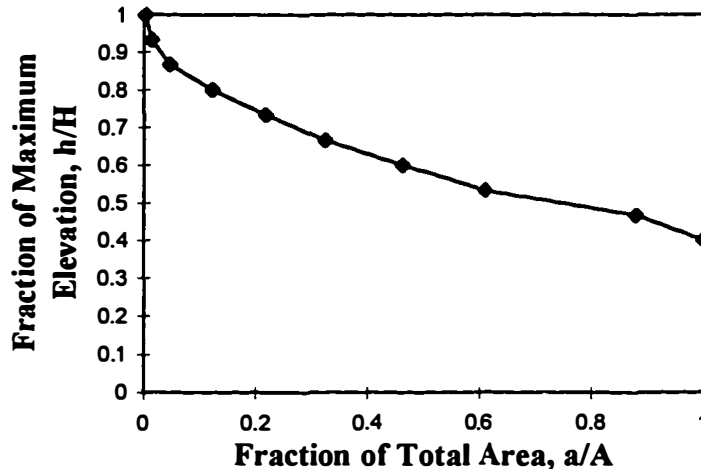
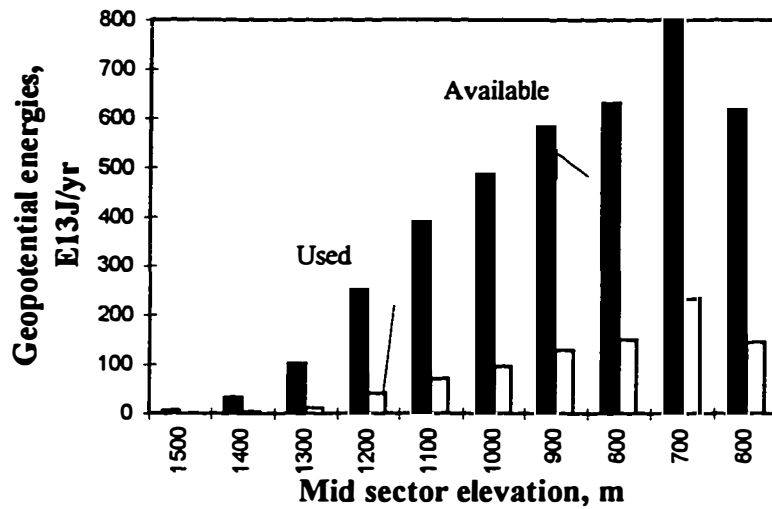


Figure A.7. Areas, energy and energy evaluations for the elevational sectors of Upper Little Tennessee river basin, representing in: **A.** Aerial distribution; **B.** Hypsometric curve; **C.** Available (G_{ri}) and Used (G_{tu}) geopotential energies; **D.** Proportion of rain (G_{ri}) and river (G_{vo}) in the inflowing geopotential energies; **E.** Available (C_{ri}) and Used (C_{tu}) chemical potential energies; **F.** Proportion of rain (C_{ri}) and river (C_{vo}) in the inflowing chemical potential energies; **G.** Geopotential energies used (G_{ru}, G_{vu}, G_{tu}) and outflow (G_{vo}); **H.** Chemical potential energies used ($C_{ru}, C_{vt}, C_{vu}, C_{tu}$) and outflow (C_{to}); **I.** Proportion of rain (G_{ru}) and river (G_{vu}) in the geopotential energy used up; **J.** Proportion of rain (C_{ru}) and river (C_{vu}) in the chemical potential energy used up; **K.** Geopotential used up (G_{tud}) and evapotranspired chemical potential (C_{etd}) power densities; **L.** Energy/ total used energy ($E_t / (G_{tu} + C_{tu})$) ratios; **M.** Total empower (E_t) and empower densities (E_d); **N.** Geopotential (T_{vg}) and chemical potential (T_{vc}) transformities of river outflow.

C. **Water geopotential energies available and used in the Upper Little Tennessee River basin**



D. **Available geopotential energies provided by rain or river for the Upper Little Tennessee River basin**

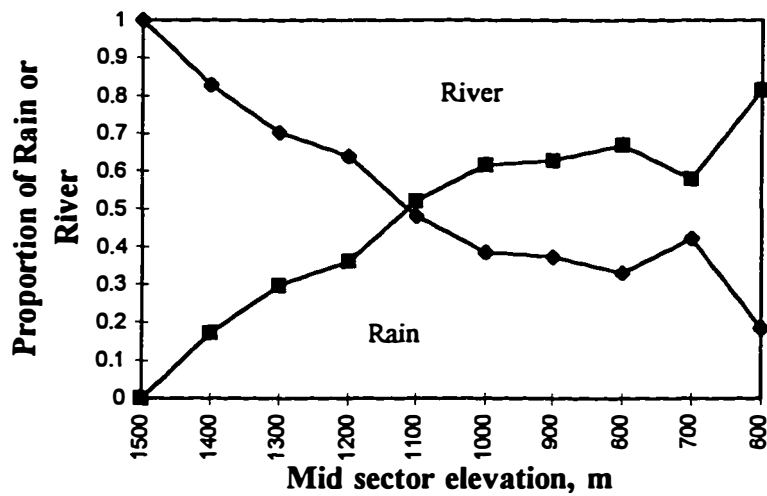


Figure A.7. Continued.

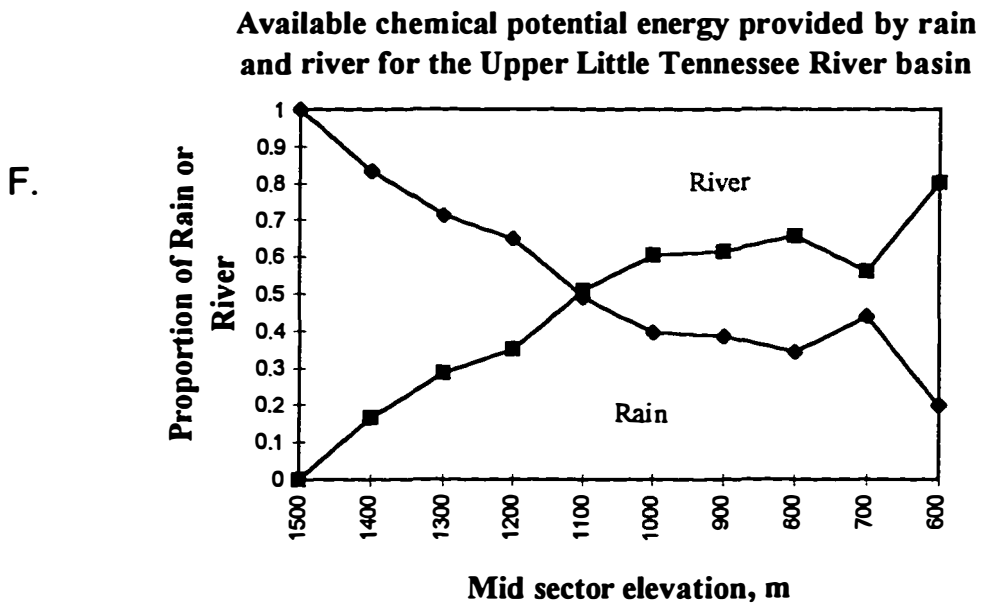
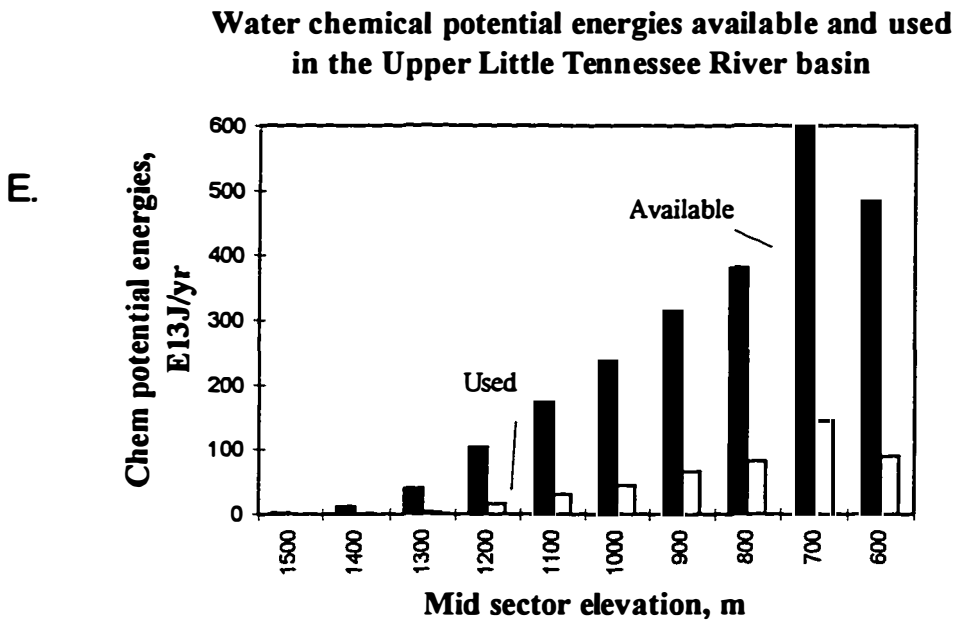


Figure A.7. Continued.

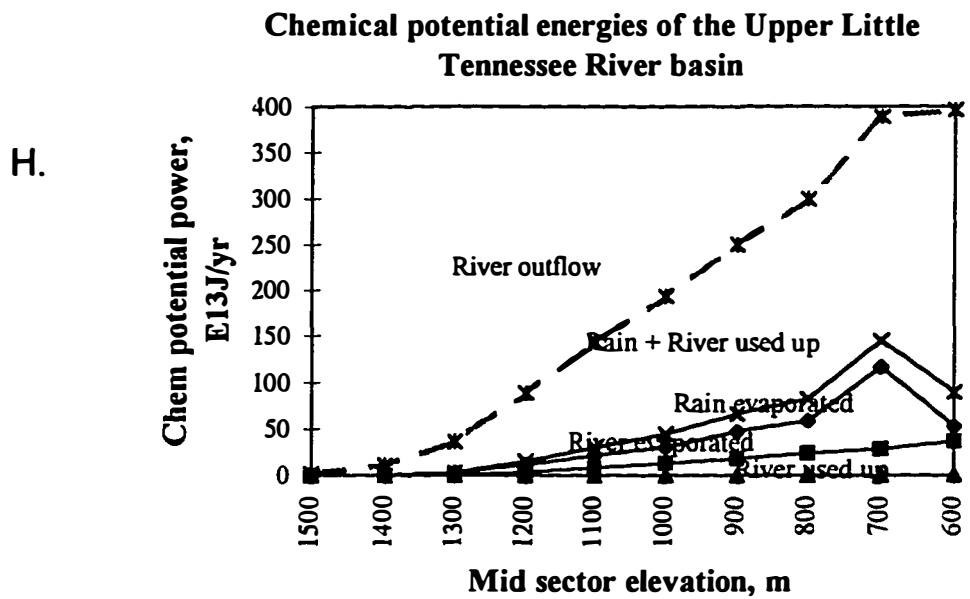
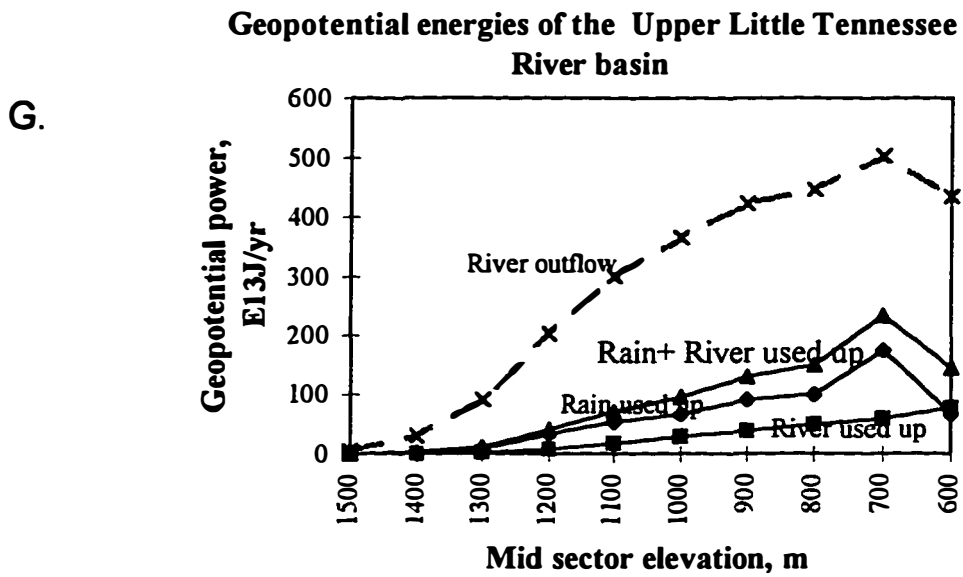
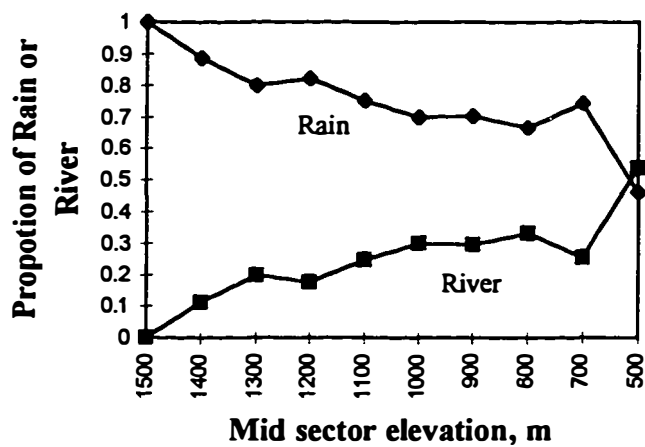


Figure A.7. Continued.

I. **Proportion used Geopotential energies from rain or river from the Upper Little Tennessee River basin**



J. **Proportion of Used Chemical potential energies from rain or river of the Upper Little Tennessee River basin**

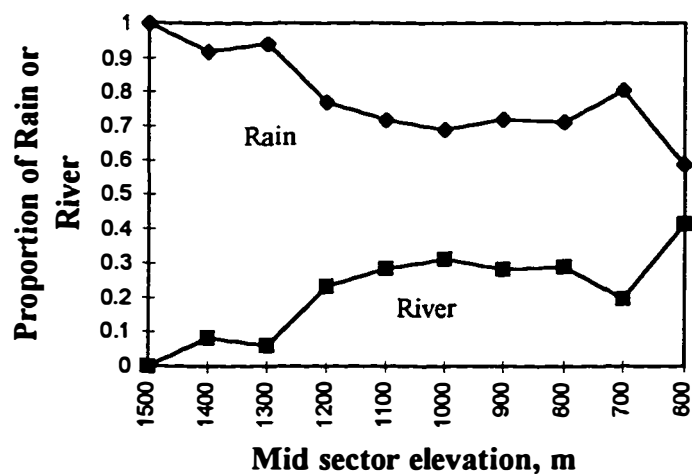
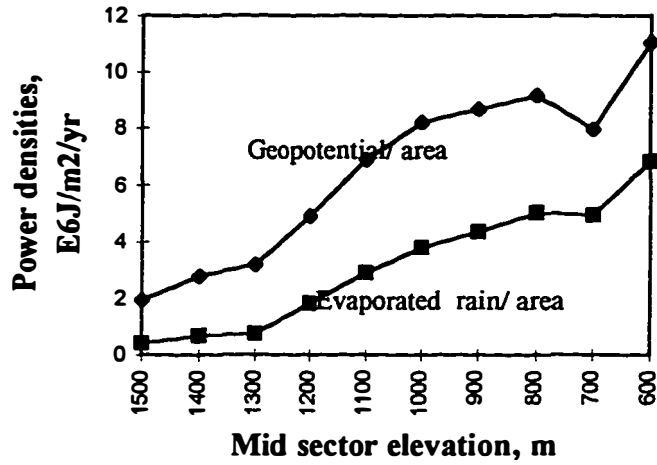


Figure A.7. Continued.

Geopotential and chemical potential power densities for the Upper Little Tennessee River basin

K.



Ratio of Energy to energy used up for the Upper Little Tennessee River basin

L.

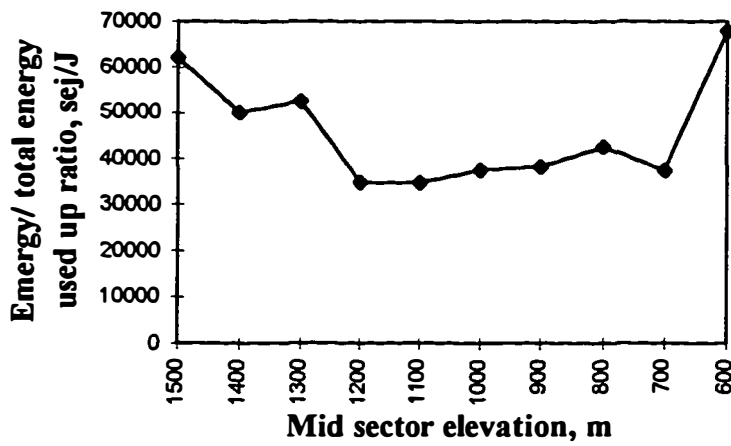
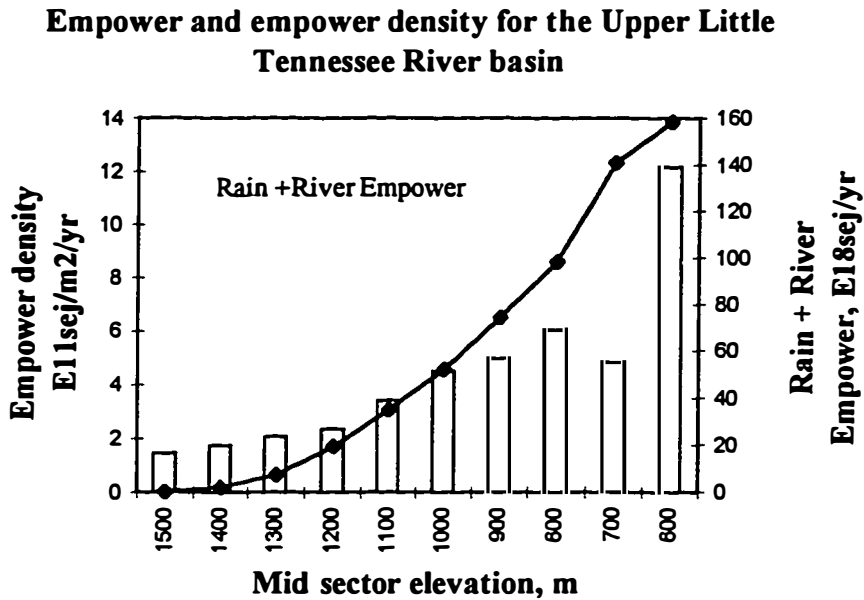


Figure A.7. Continued.

M.



N.

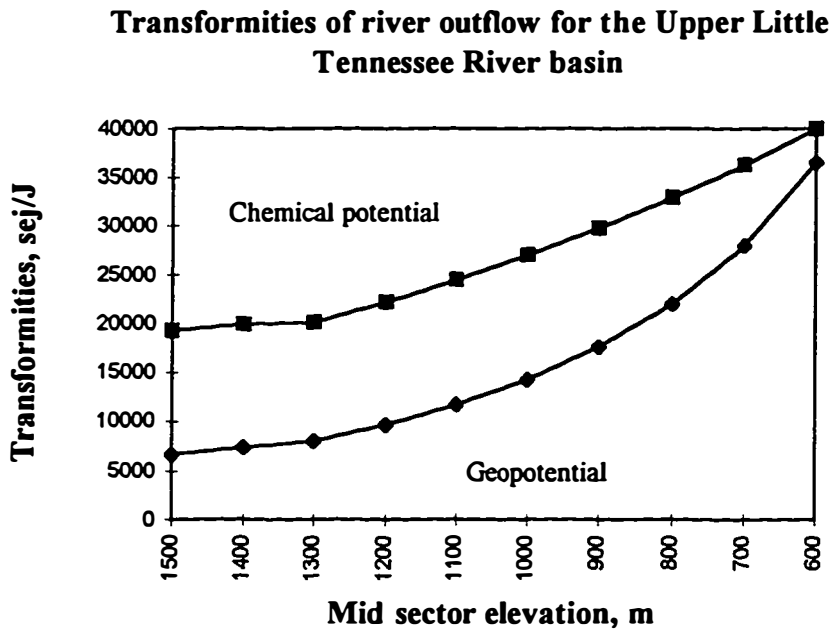


Figure A.7. Continued.

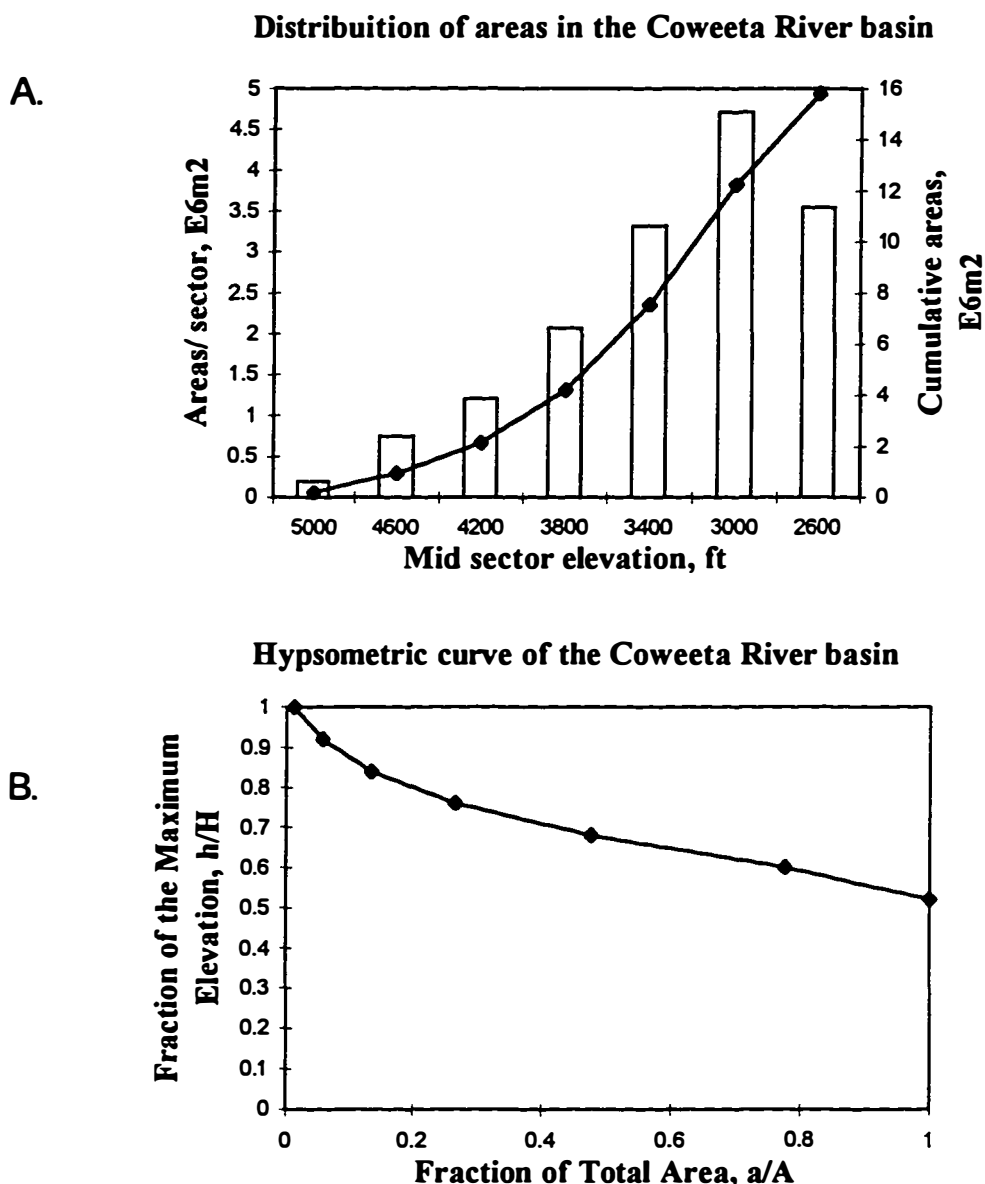
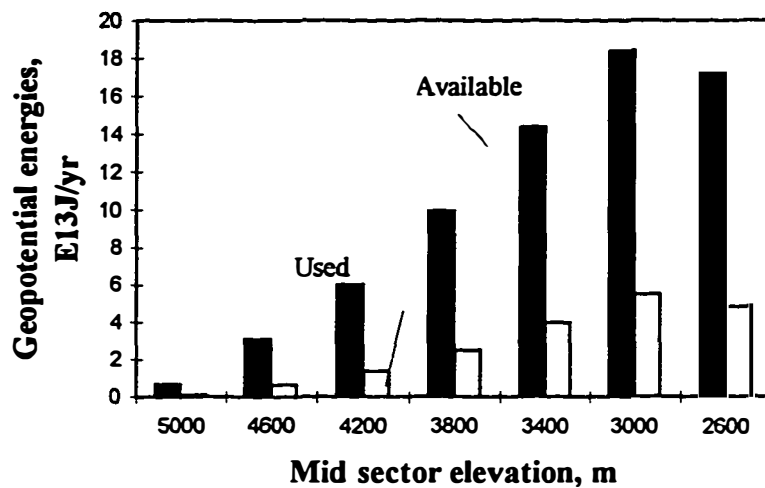


Figure A.8. Areas, energy and energy evaluations for the elevational sectors of Coweeta river basin, representing in: **A.** Aerial distribution; **B.** Hypsometric curve; **C.** Available (G_{ri}) and Used (G_{tu}) geopotential energies; **D.** Proportion of rain (G_{ri}) and river (G_{vo}) in the inflowing geopotential energies; **E.** Available (C_{ri}) and Used (C_{tu}) chemical potential energies; **F.** Proportion of rain (C_{ri}) and river (C_{vo}) in the inflowing chemical potential energies; **G.** Geopotential energies used (G_{ru}, G_{vu}, G_{tu}) and outflow (G_{vo}); **H.** Chemical potential energies used ($C_{ru}, C_{vt}, C_{vu}, C_{tu}$) and outflow (C_{to}); **I.** Proportion of rain (G_{ru}) and river (G_{vu}) in the geopotential energy used up; **J.** Proportion of rain (C_{ru}) and river (C_{vu}) in the chemical potential energy used up; **K.** Geopotential used up (G_{tud}) and evapotranspired chemical potential (C_{etd}) power densities; **L.** Energy/ total used energy ($E_t / (G_{tu} + C_{tu})$) ratios; **M.** Total empower (E_t) and empower densities (E_d); **N.** Geopotential (T_{vg}) and chemical potential (T_{vc}) transformities of river outflow.

C. **Water geopotential energies available and used in the Coweeta River basin**



D. **Available geopotential energies provided by rain or river for Coweeta River basin**

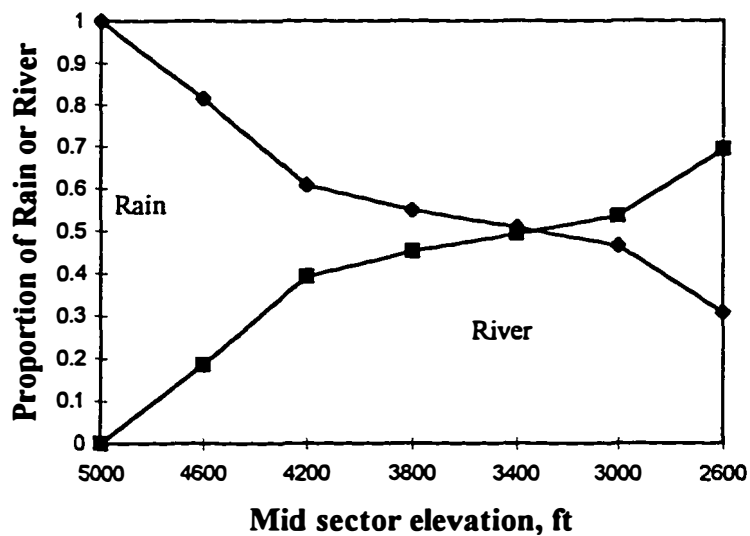
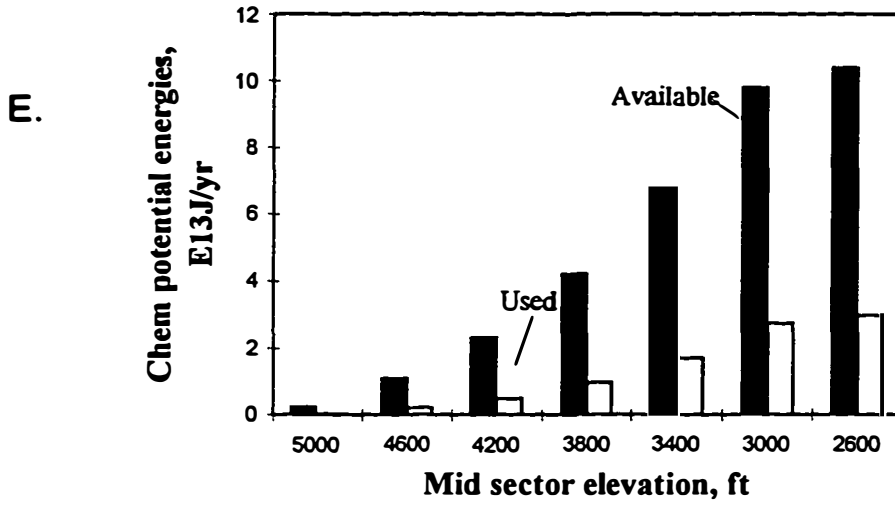


Figure A.8. Continued.

Water chemical potential energies available and used in the Coweeta River basin



Available chemical potential energies provided by rain and river for the Coweeta River basin

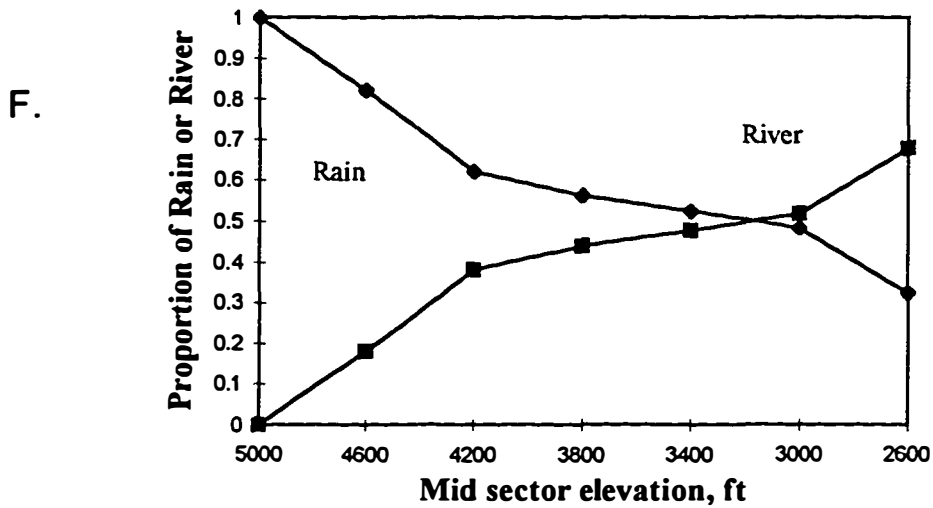


Figure A.8. Continued.

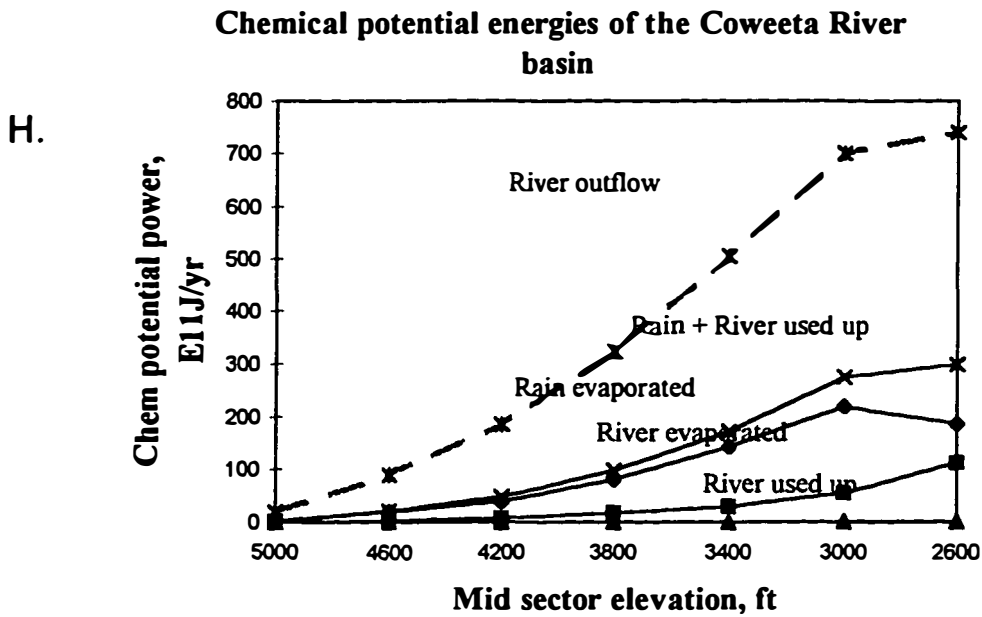
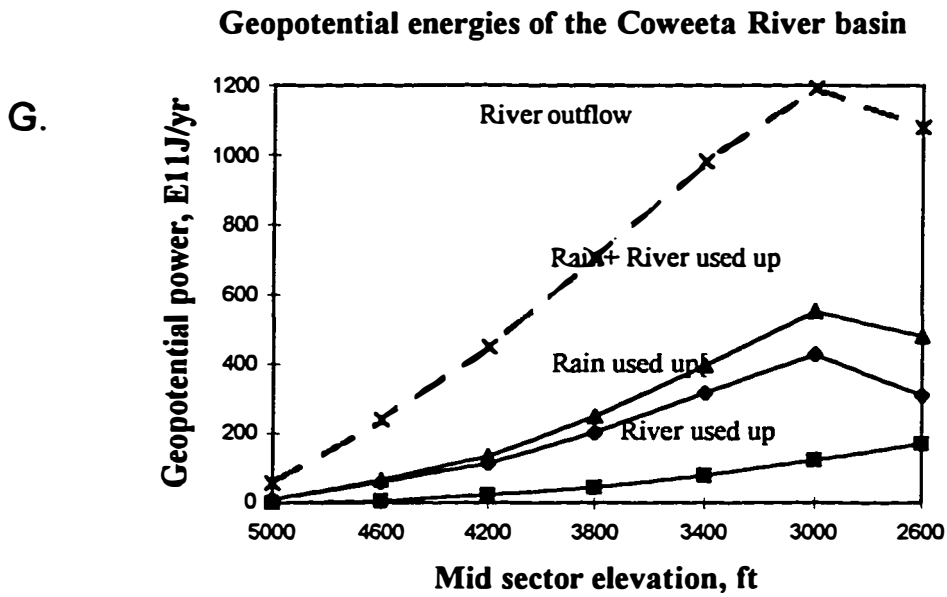


Figure A.8. Continued.

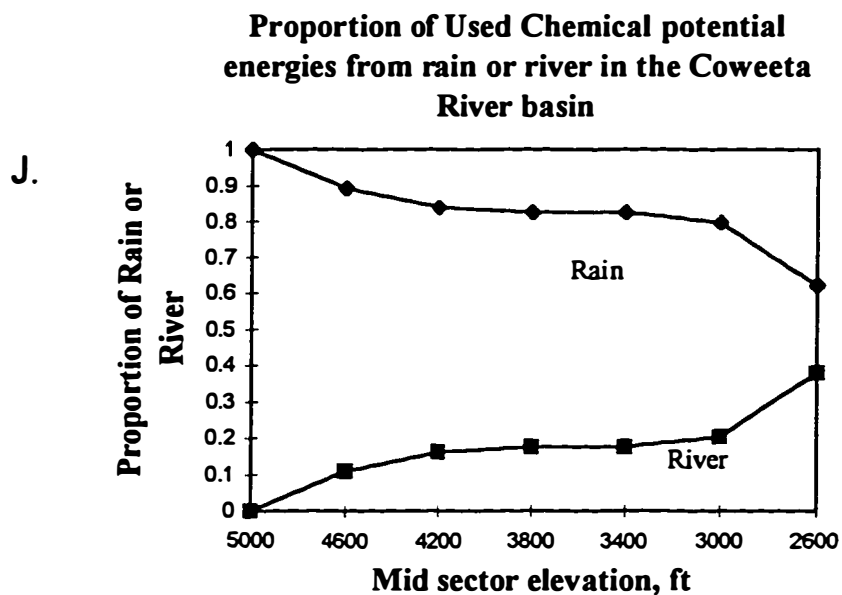
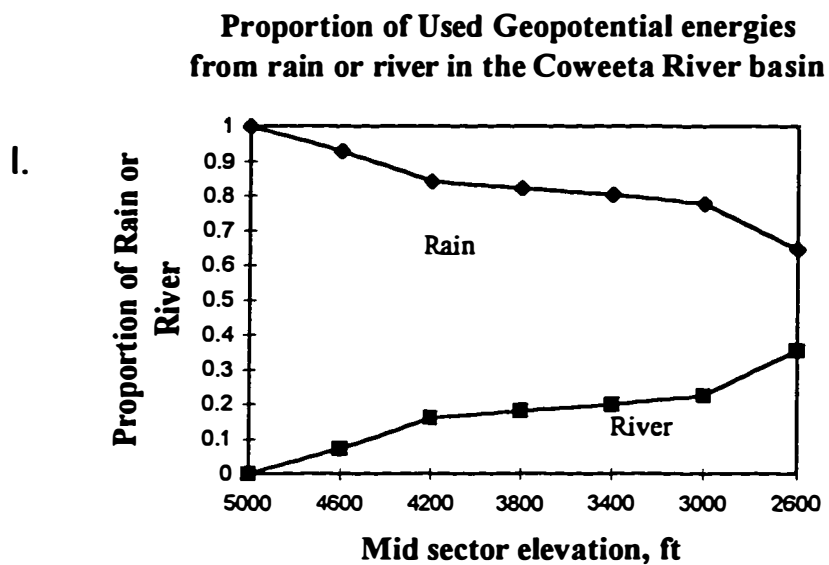


Figure A.8. Continued.

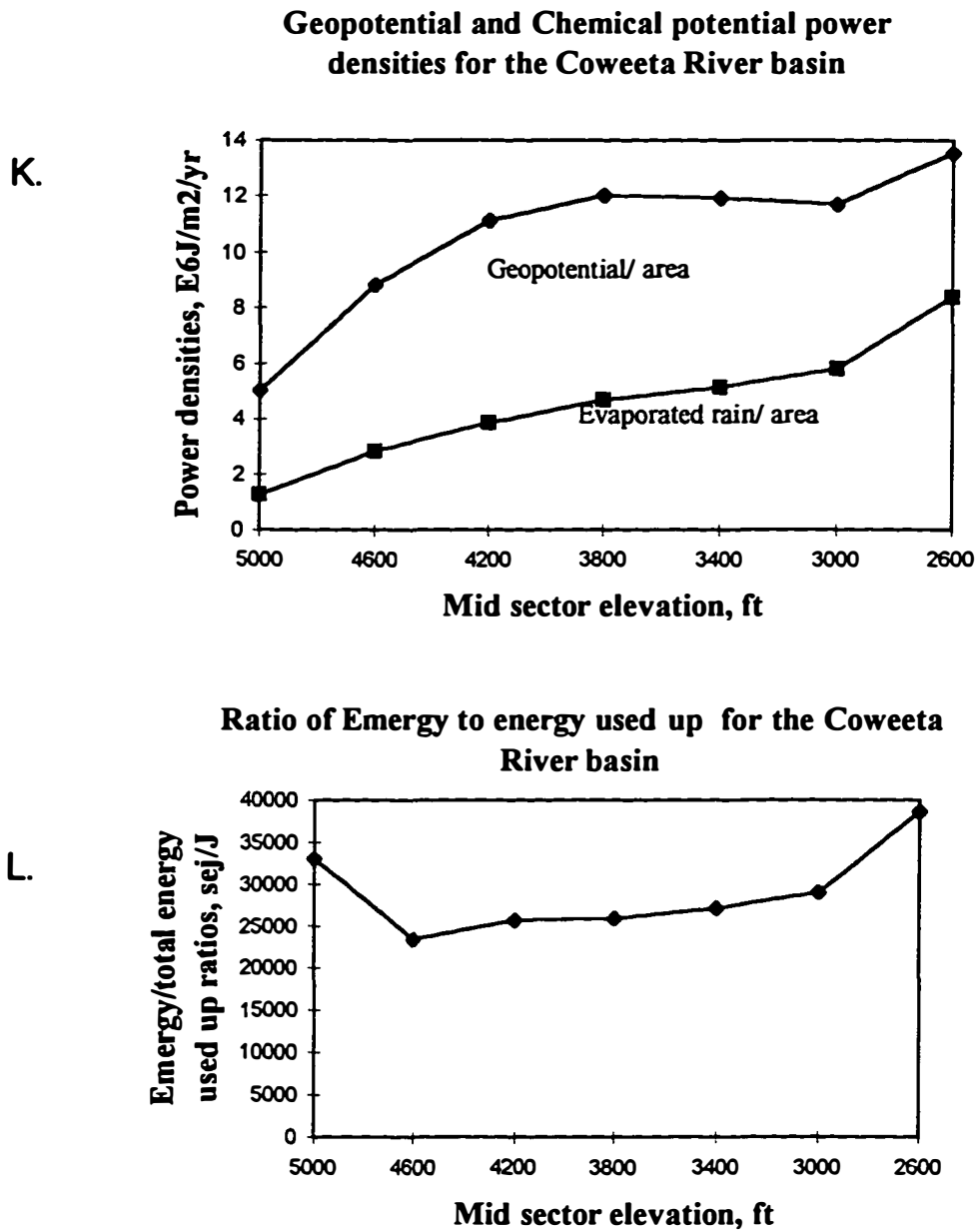


Figure A.8. Continued.

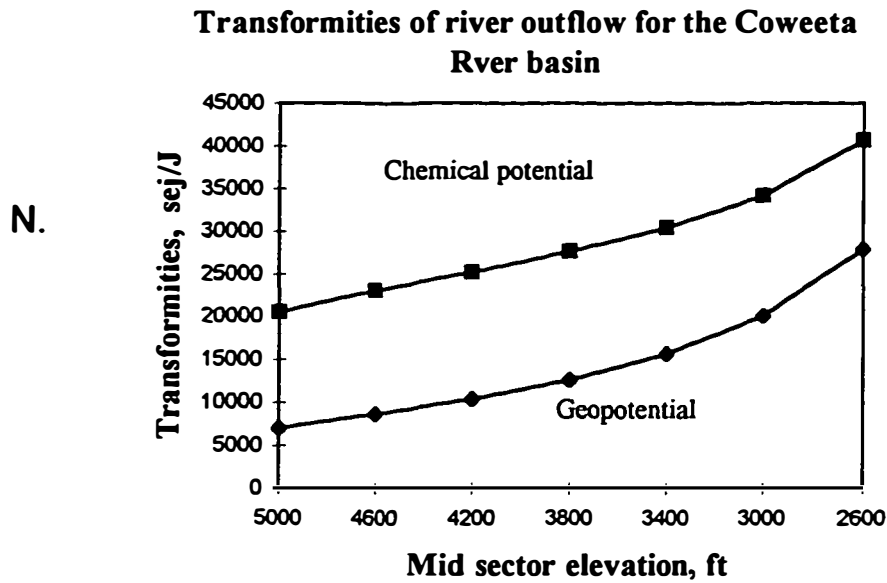
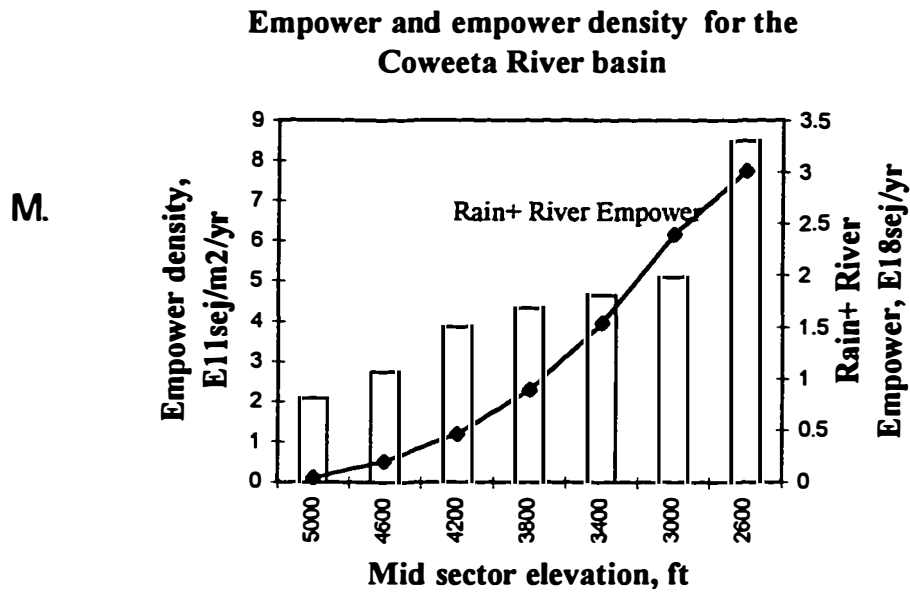
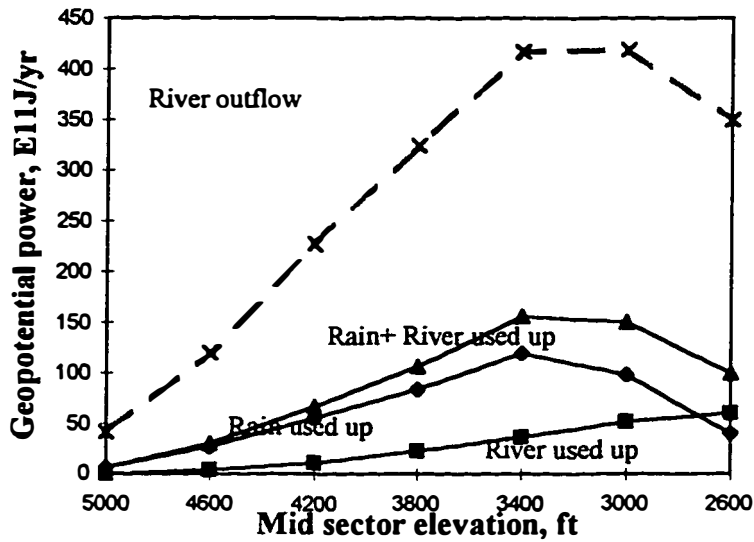


Figure A.8. Continued.

Geopotential energies of the Upper Shope Creek subbasin

A.



Chemical potential energies of the Upper Shope Fork Creek subbasin

B.

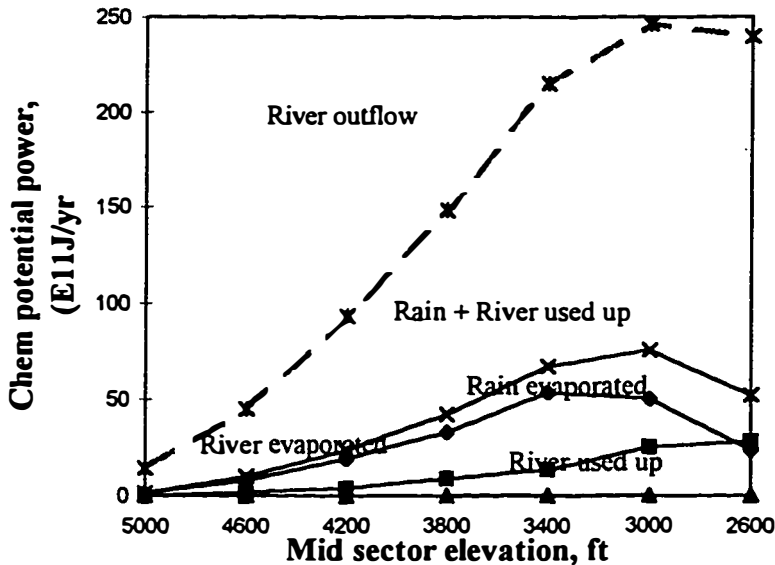
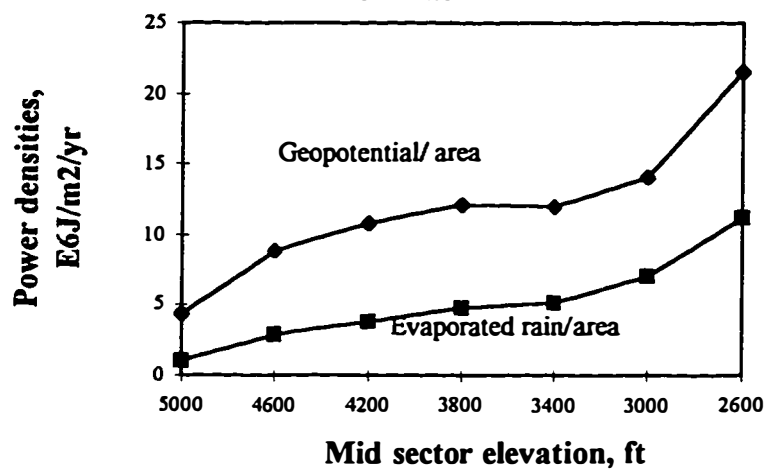


Figure A.9. Areas, energy and energy evaluations for the elevational sectors of Upper Shope Fork creek subbasin, representing in: A. Geopotential energies used (Gru,Gvu,Gtu) and outflow (Gvo); B. Chemical potential energies used (Cru,Cvt,Cvu,Ctu) and outflow(Cto) ; C. Geopotential used up (Gtud) and evapotranspired chemical potential (Cetd) power densities;D. Emery/ total used energy (Et/(Gtu+Ctu) ratios; E. Total empower(Et) and empower densities (Ed); F. Geopotential (Tvg) and chemical potential (Tvc) transformities of river outflow.

C.

Geopotential and chemical potential power densities of the Upper Shope Fork Creek subbasin



D.

Ratio of Energy to energy used up for the Upper Shope Fork Creek subbasin

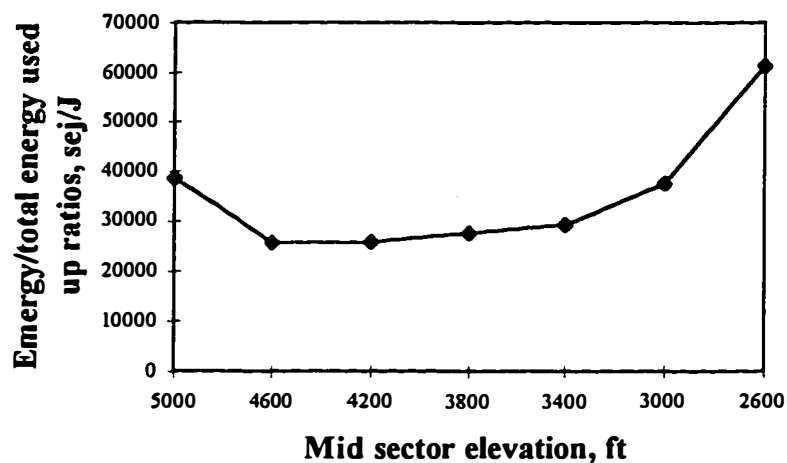
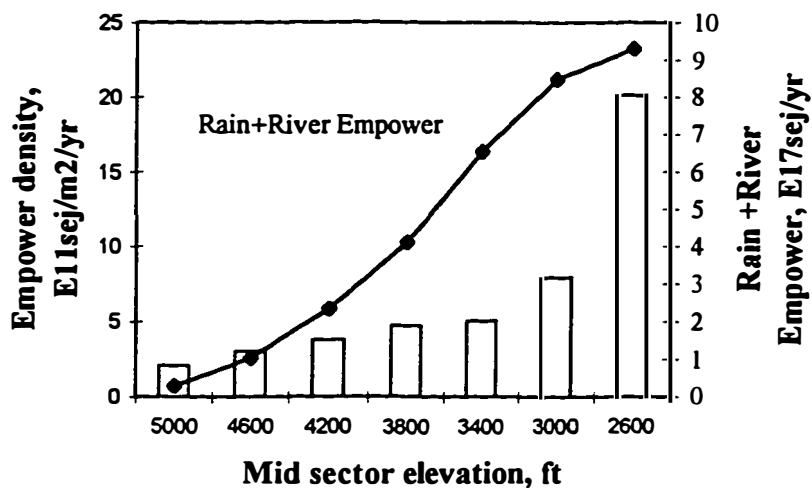


Figure A.9. Continued.

E.

Empower and empower density for the Upper Shope Fork Creek subbasin



F.

Transformities of river outflow for the Upper Shope Fork Creek subbasin

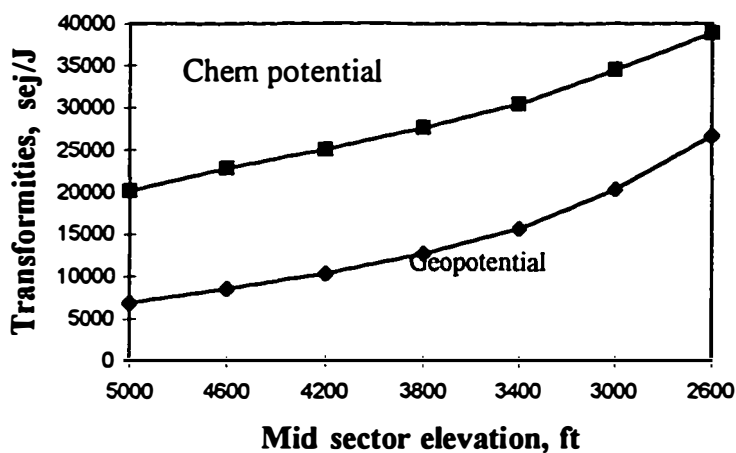
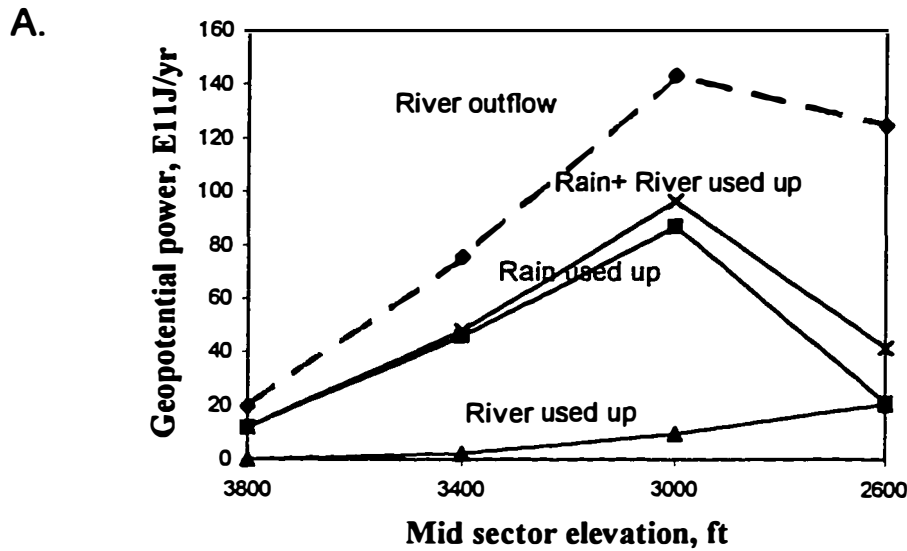


Figure A.9. Continued.

Geopotential energies of the Cunningham Creek subbasin



Chemical potential energies of the Cunningham Creek subbasin

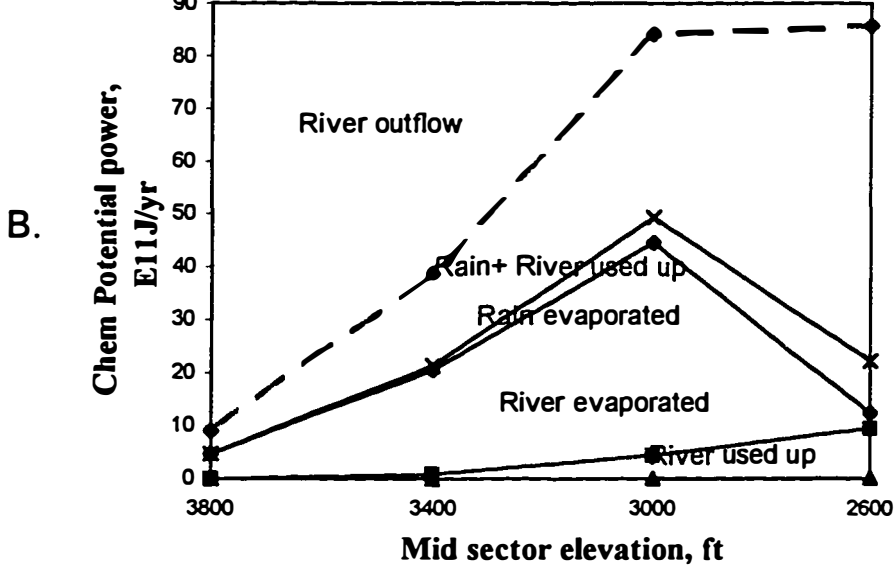
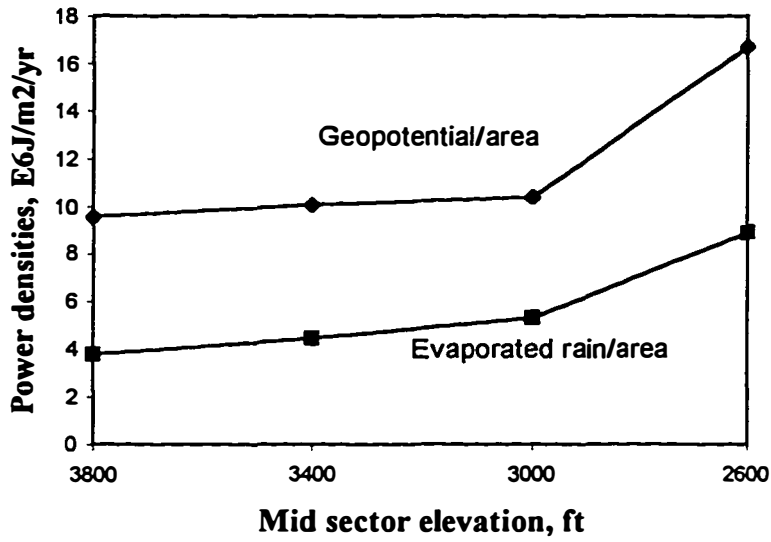


Figure A.10. Areas, energy and energy evaluations for the elevational sectors of Cunningham creek subbasin, representing in: **A.** Geopotential energies used (Gru,Gvu,Gtu) and outflow (Gvo); **B.**Chemical potential energies used (Cru,Cvt,Cvu,Ctu) and outflow(Cto) ; **C.** Geopotential used up (Gtud) and evapotranspired chemical potential (Cetd) power densities;**D.** Emergy/ total used energy (Et/(Gtu+Ctu) ratios; **E.**Total empower(Et) and empower densities (Ed); **F.** Geopotential (Tvg) and chemical potential (Tvc) transformities of river outflow.

C.

Geopotential and Chemical potential power densities of the Cunningham Creek subbasin



D.

Ratio of Emergy to energy used up for the Cunningham Creek subbasin

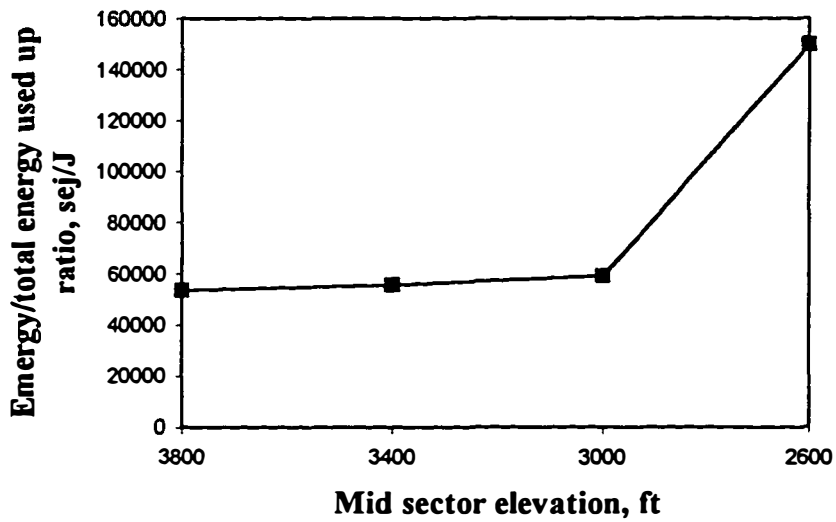
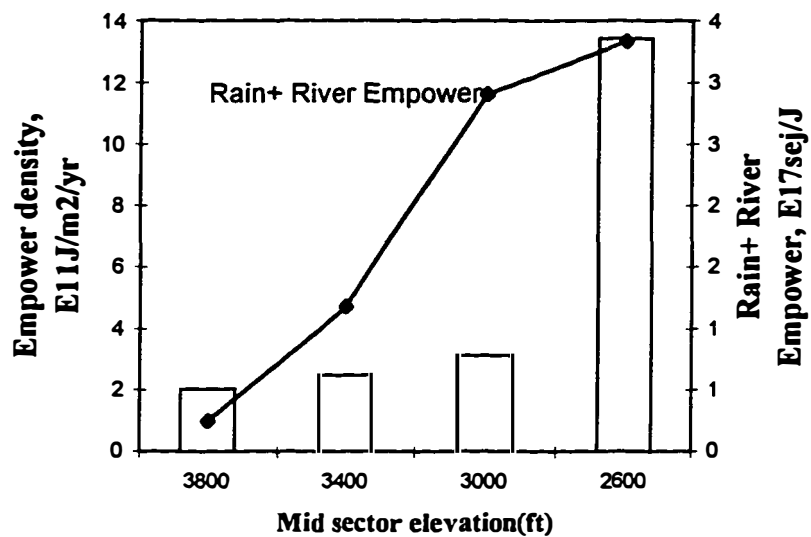


Figure A.10. Continued.

E. Empower and empower density for the Cunningham creek subbasin



F. Transformities of river outflow for the Cunningham Creek subbasin

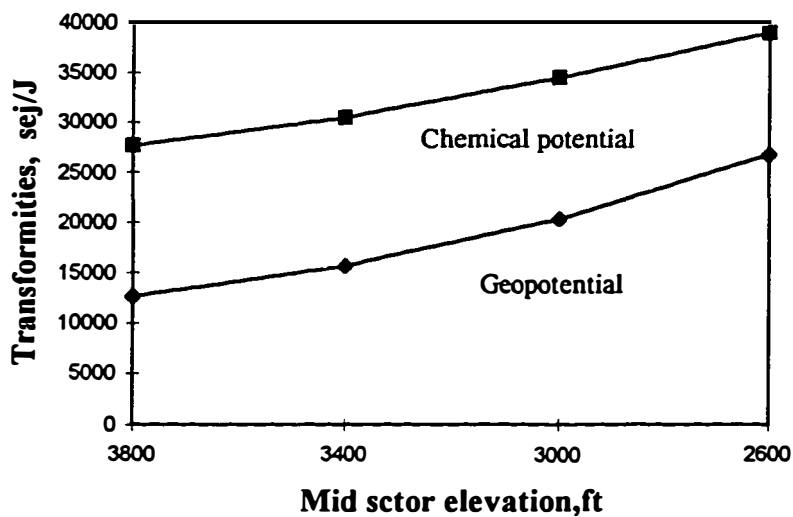


Figure A.10. Continued.

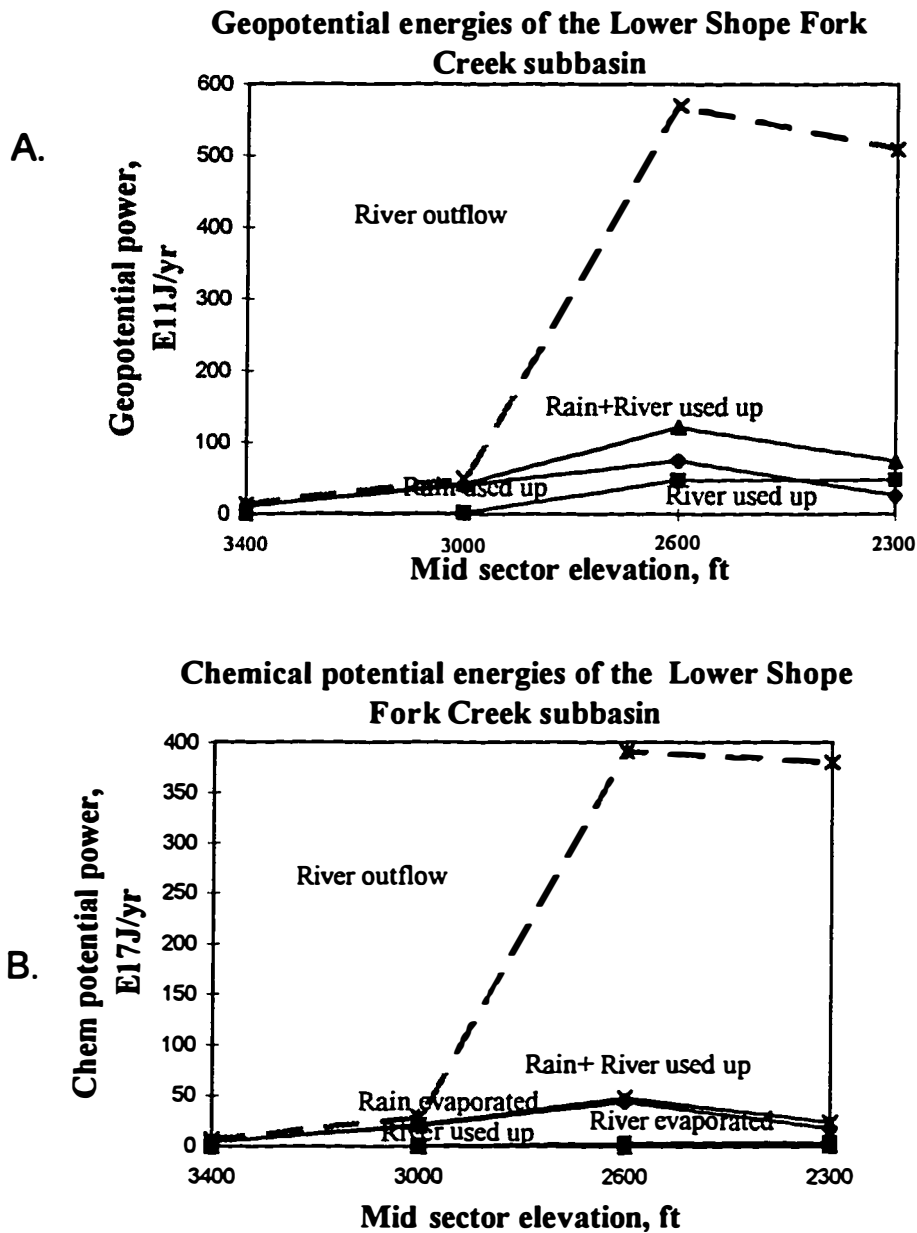


Figure A.11. Areas, energy and emergy evaluations for the elevational sectors of Lower Shope Fork creek subbasin, representing in: **A.** Geopotential energies used (G_{ru}, G_{vu}, G_{tu}) and outflow (G_{vo}); **B.** Chemical potential energies used ($C_{ru}, C_{vt}, C_{vu}, C_{tu}$) and outflow (C_{to}); **C.** Geopotential used up (G_{tud}) and evapotranspired chemical potential (C_{etd}) power densities; **D.** Emergy/ total used energy ($E_t / (G_{tu} + C_{tu})$) ratios; **E.** Total empower (E_t) and empower densities (E_d); **F.** Geopotential (T_{vg}) and chemical potential (T_{vc}) transformities of river outflow.

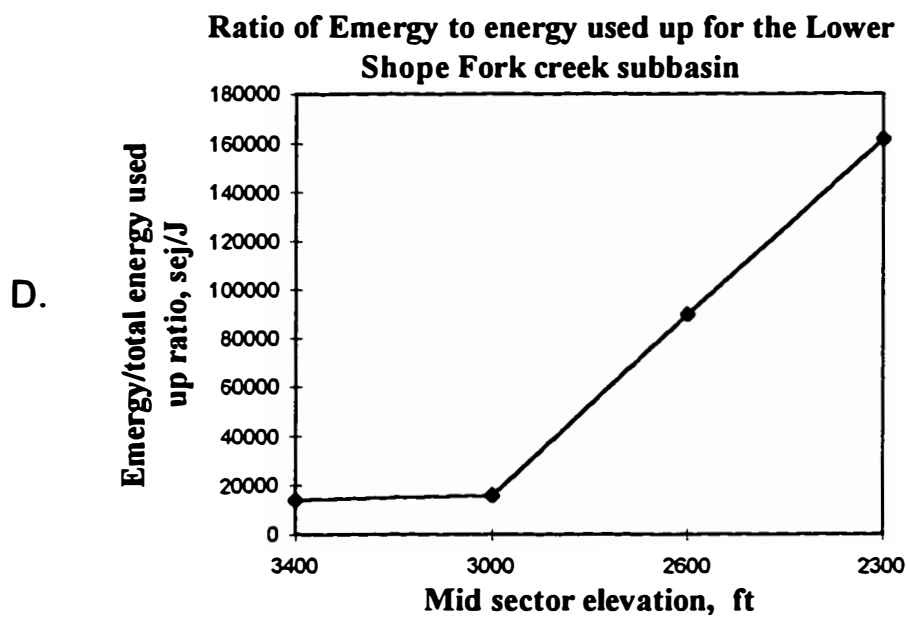
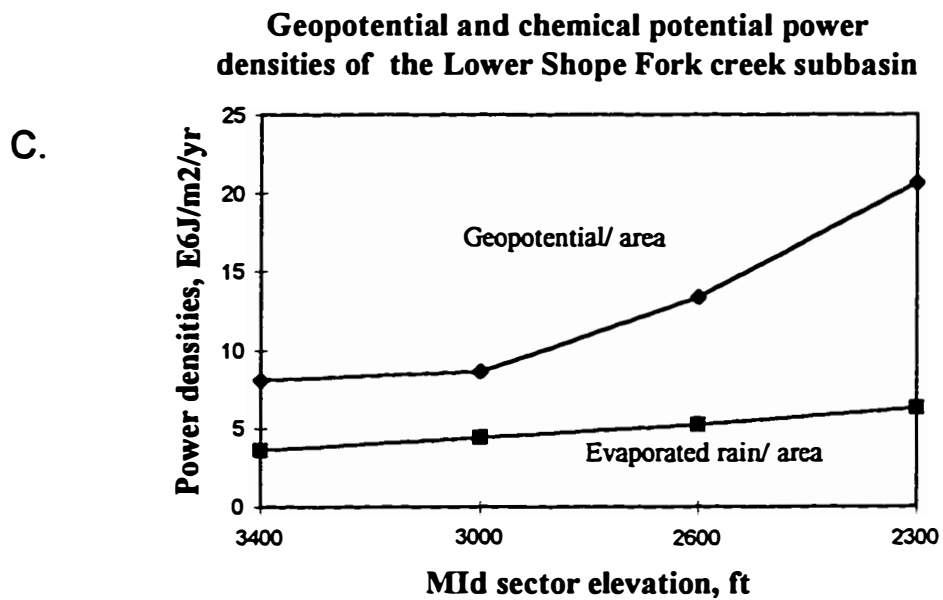
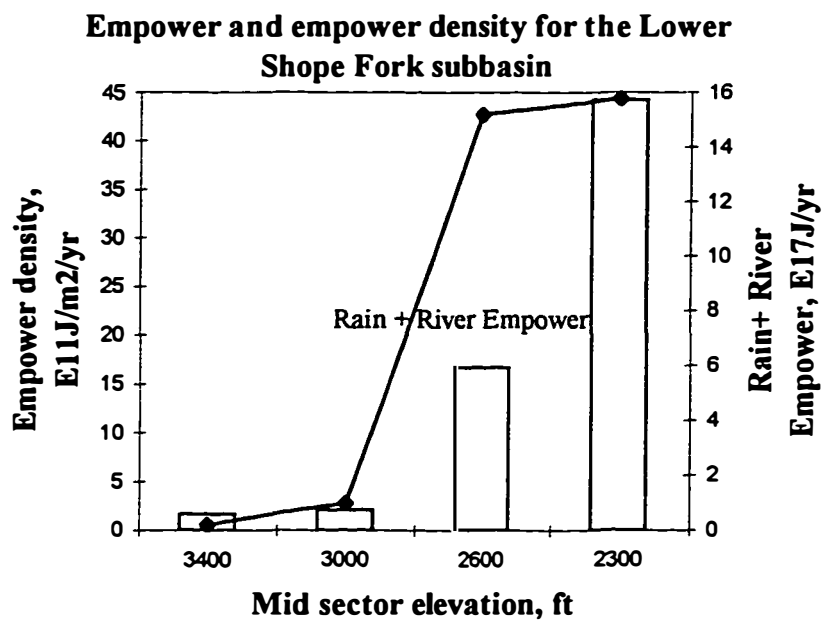


Figure A.11. Continued.

E.



F.

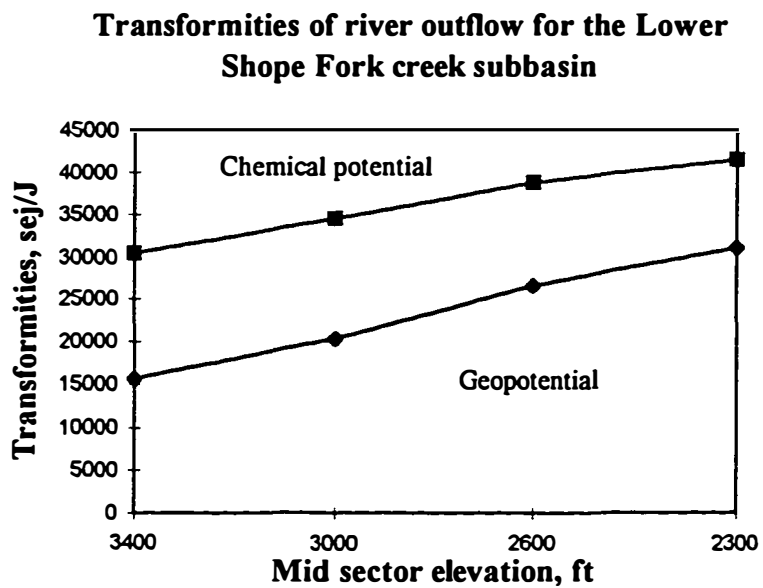


Figure A.11. Continued.

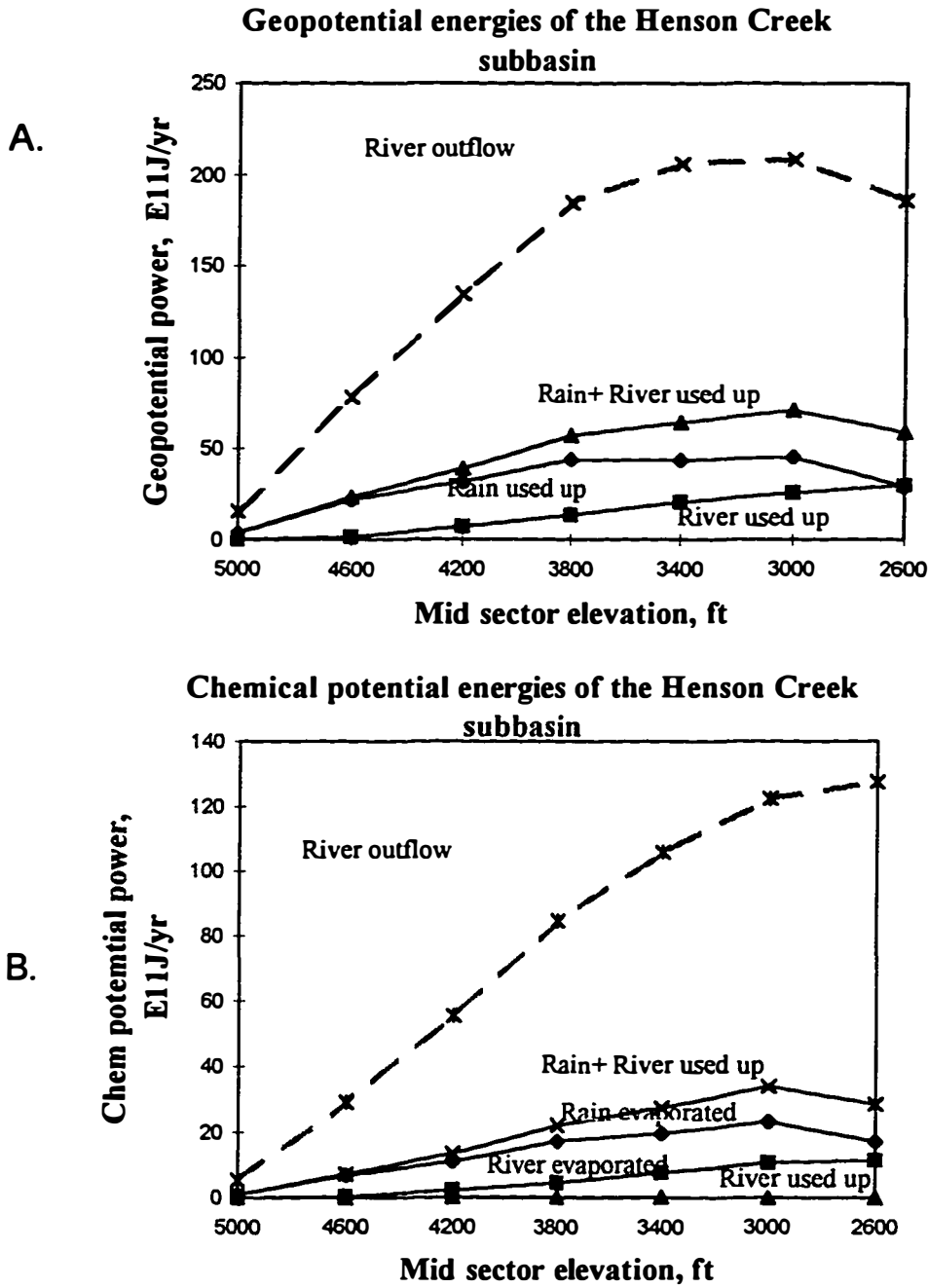


Figure A.12. Areas, energy and energy evaluations for the elevational sectors of Henson creek subbasin, representing in: A. Geopotential energies used (G_{ru}, G_{vu}, G_{tu}) and outflow (G_{vo}); B. Chemical potential energies used ($C_{ru}, C_{vt}, C_{vu}, C_{tu}$) and outflow (C_{to}); C. Geopotential used up (G_{tud}) and evapotranspired chemical potential (C_{etd}) power densities; D. Energy/ total used energy ($E_t / (G_{tu} + C_{tu})$) ratios; E. Total empower (E_t) and empower densities (E_d); F. Geopotential (T_{vg}) and chemical potential (T_{vc}) transformities of river outflow.

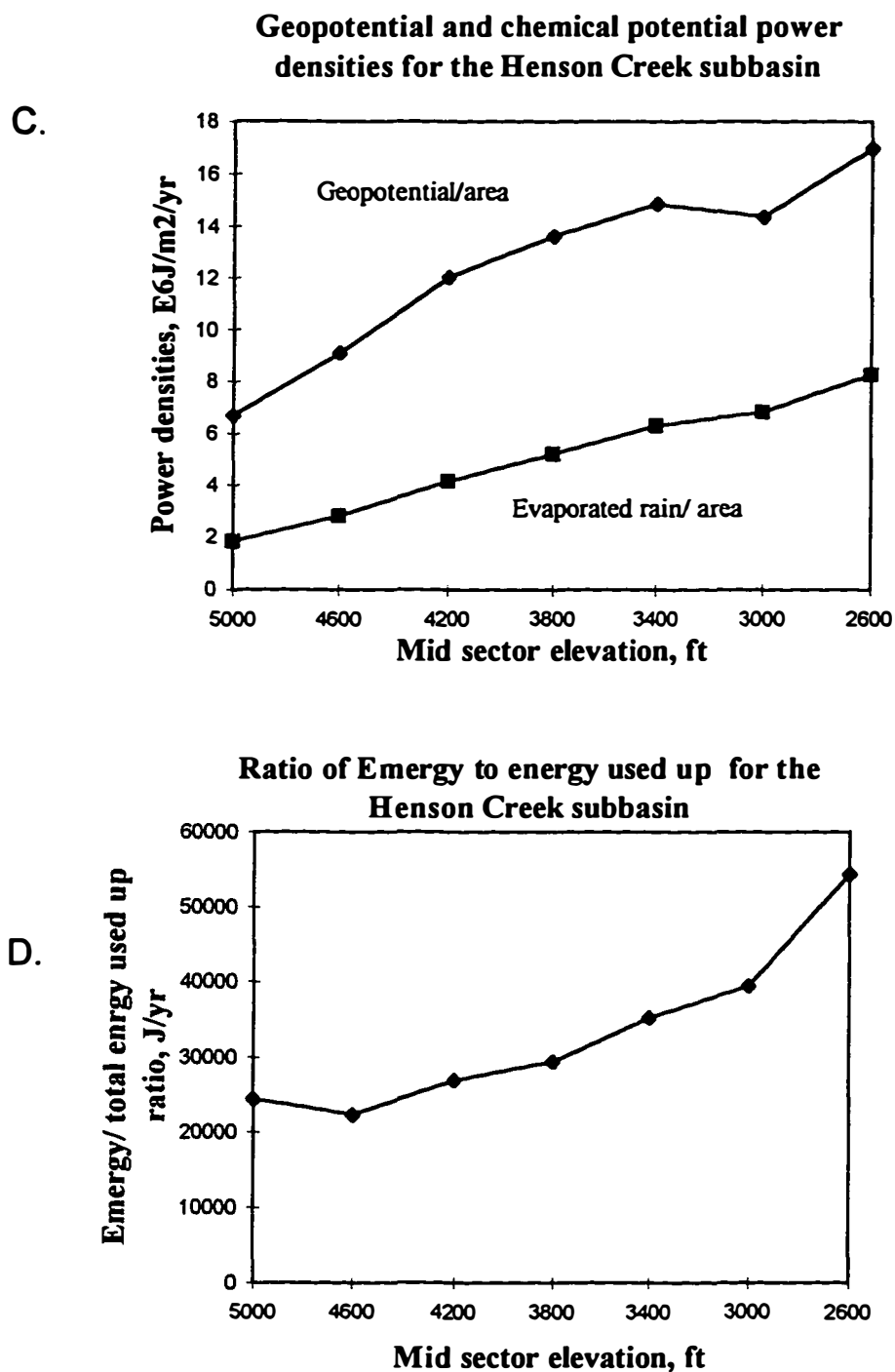
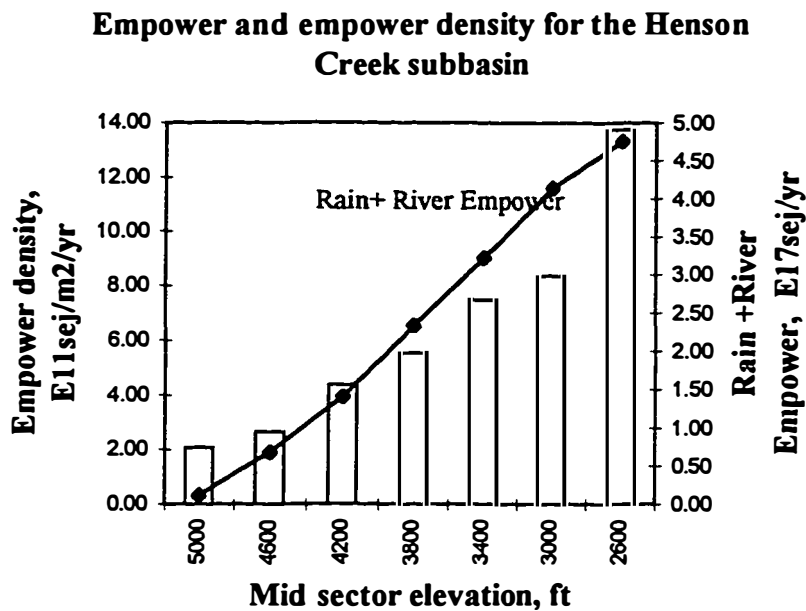


Figure A.12. Continued

E.



F.

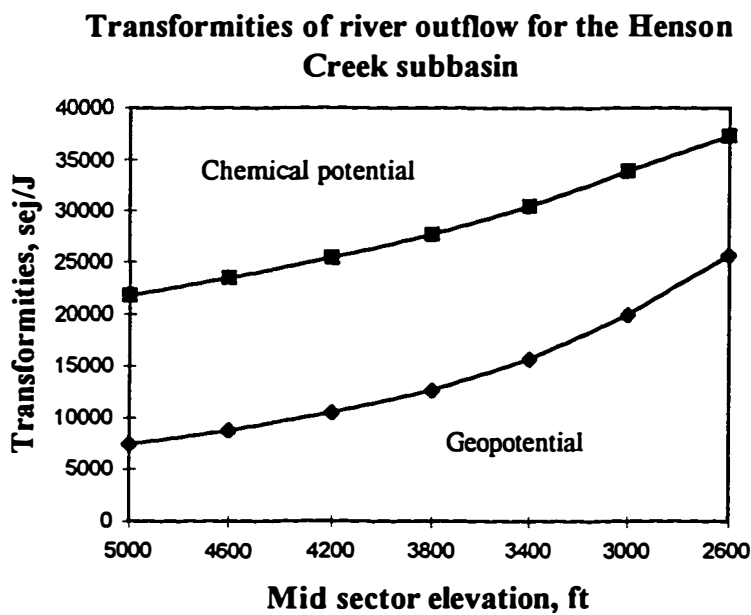


Figure A.12. Continued

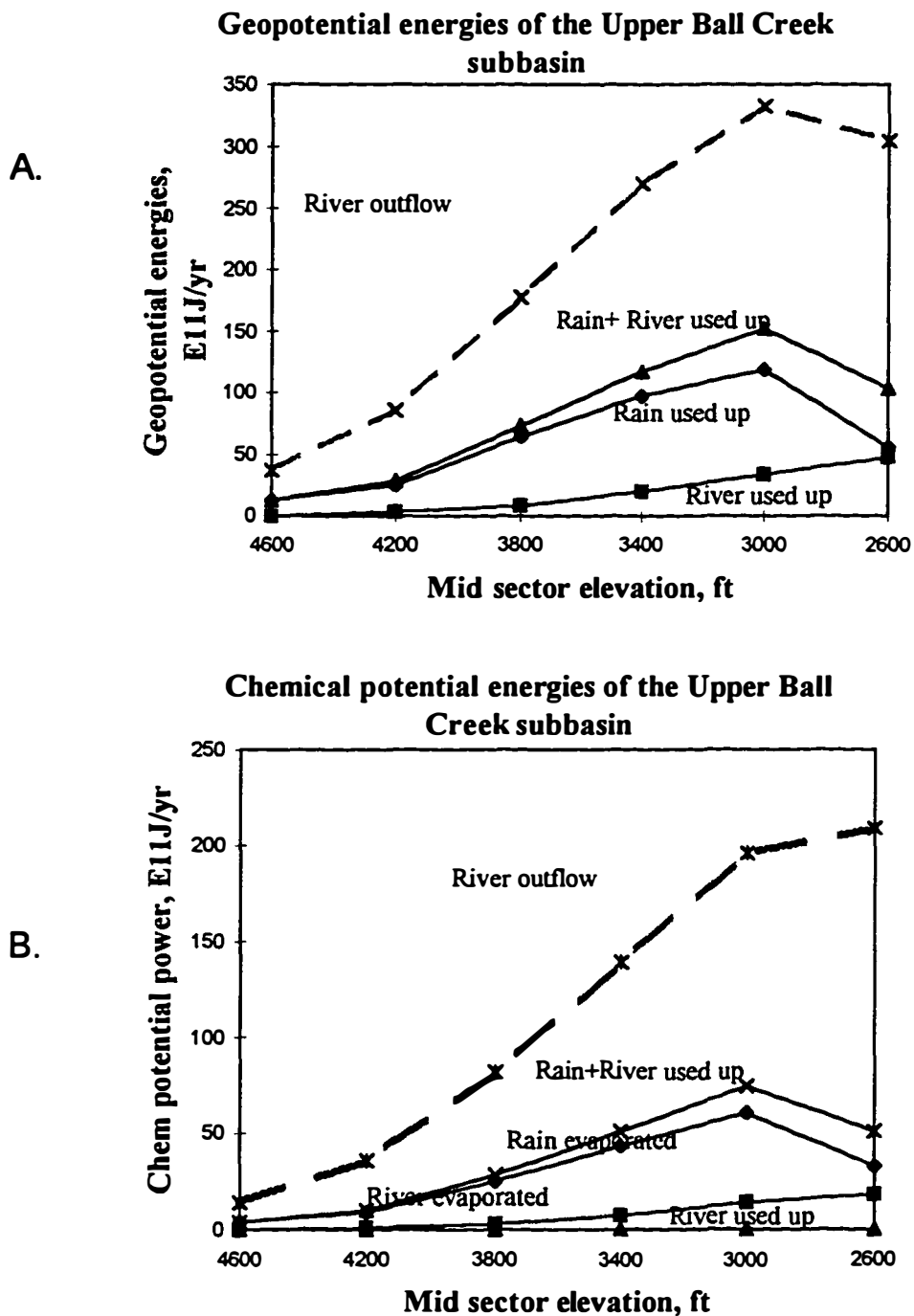


Figure A. 13. Areas, energy and energy evaluations for the elevational sectors of Upper Ball creek subbasin, representing in: **A.** Geopotential energies used (G_{ru}, G_{vu}, G_{tu}) and outflow (G_{vo}); **B.** Chemical potential energies used ($C_{ru}, C_{vt}, C_{vu}, C_{tu}$) and outflow (C_{to}); **C.** Geopotential used up (G_{tud}) and evapotranspired chemical potential (C_{etd}) power densities; **D.** Emergy/ total used energy ($E_t / (G_{tu} + C_{tu})$) ratios; **E.** Total empower (E_t) and empower densities (E_d); **F.** Geopotential (T_{vg}) and chemical potential (T_{vc}) transformities of river outflow.

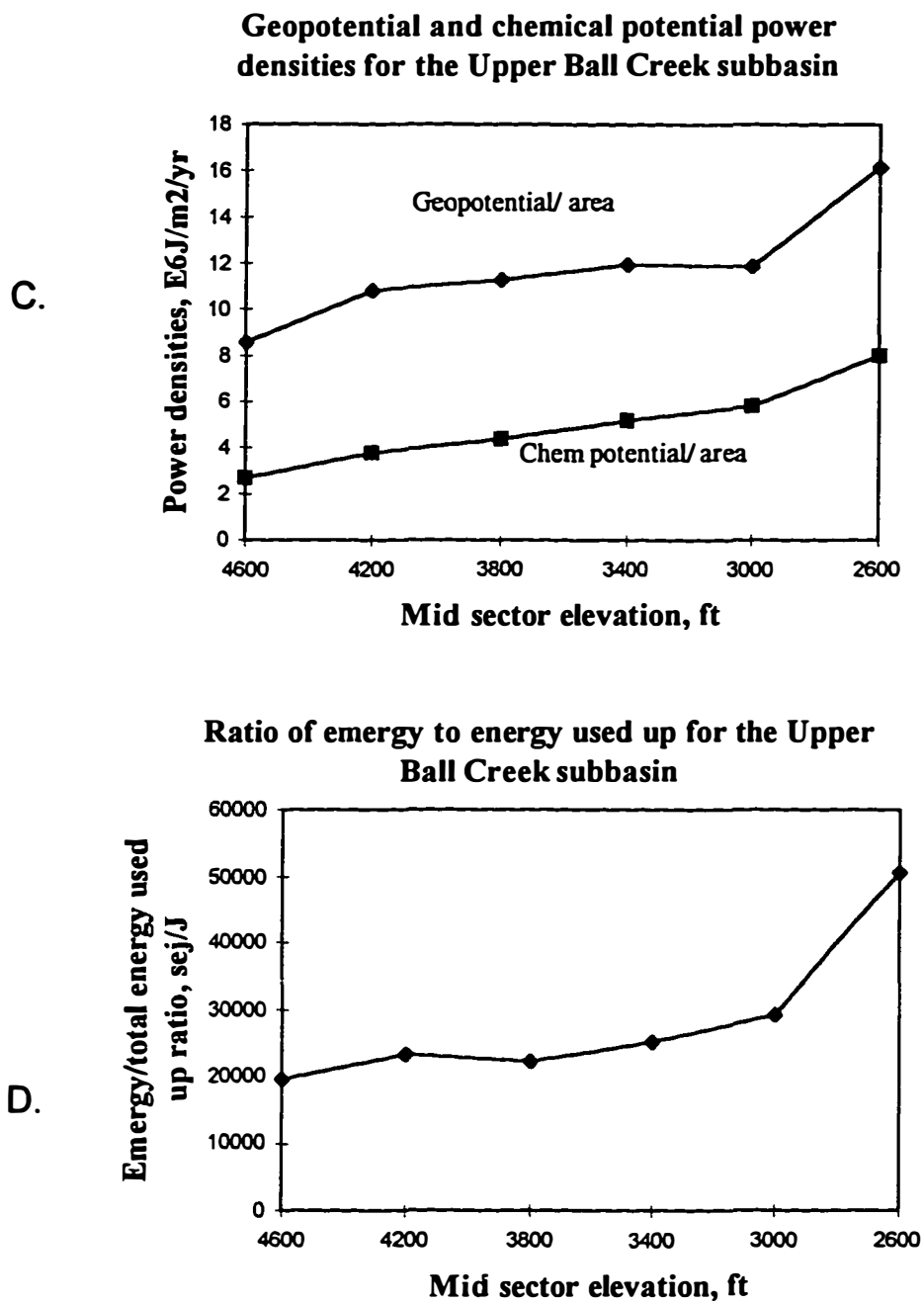


Figure A.13. Continued.

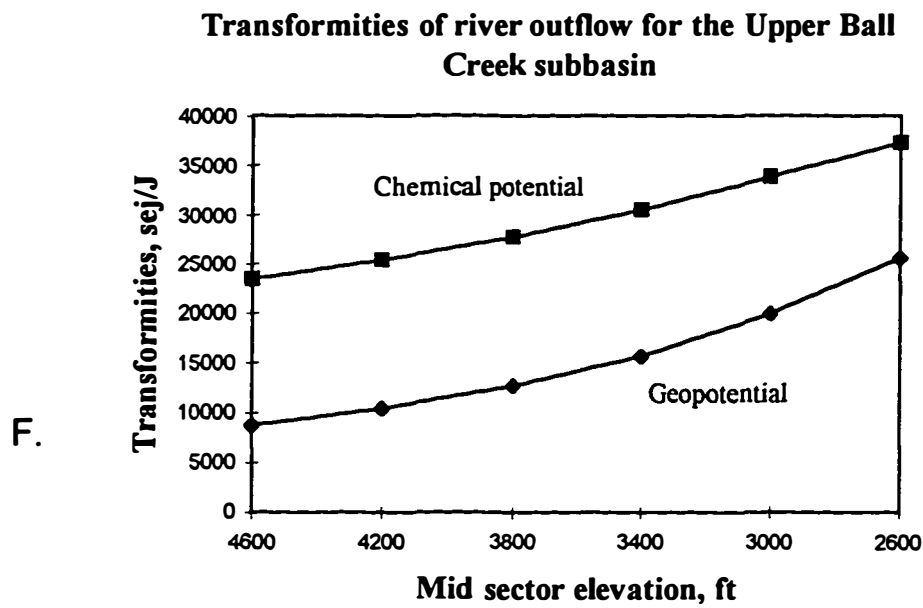
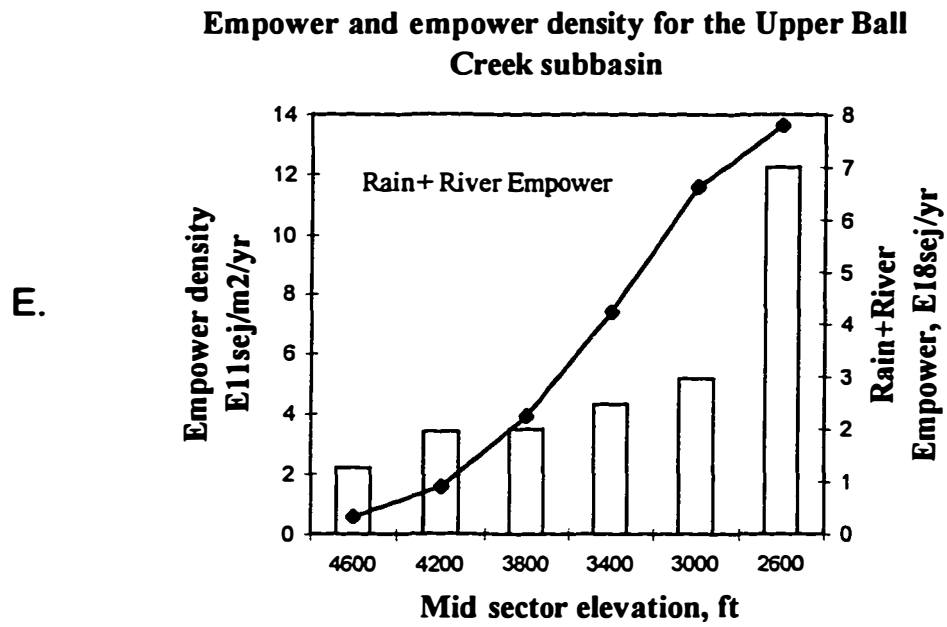


Figure A.13. Continued.

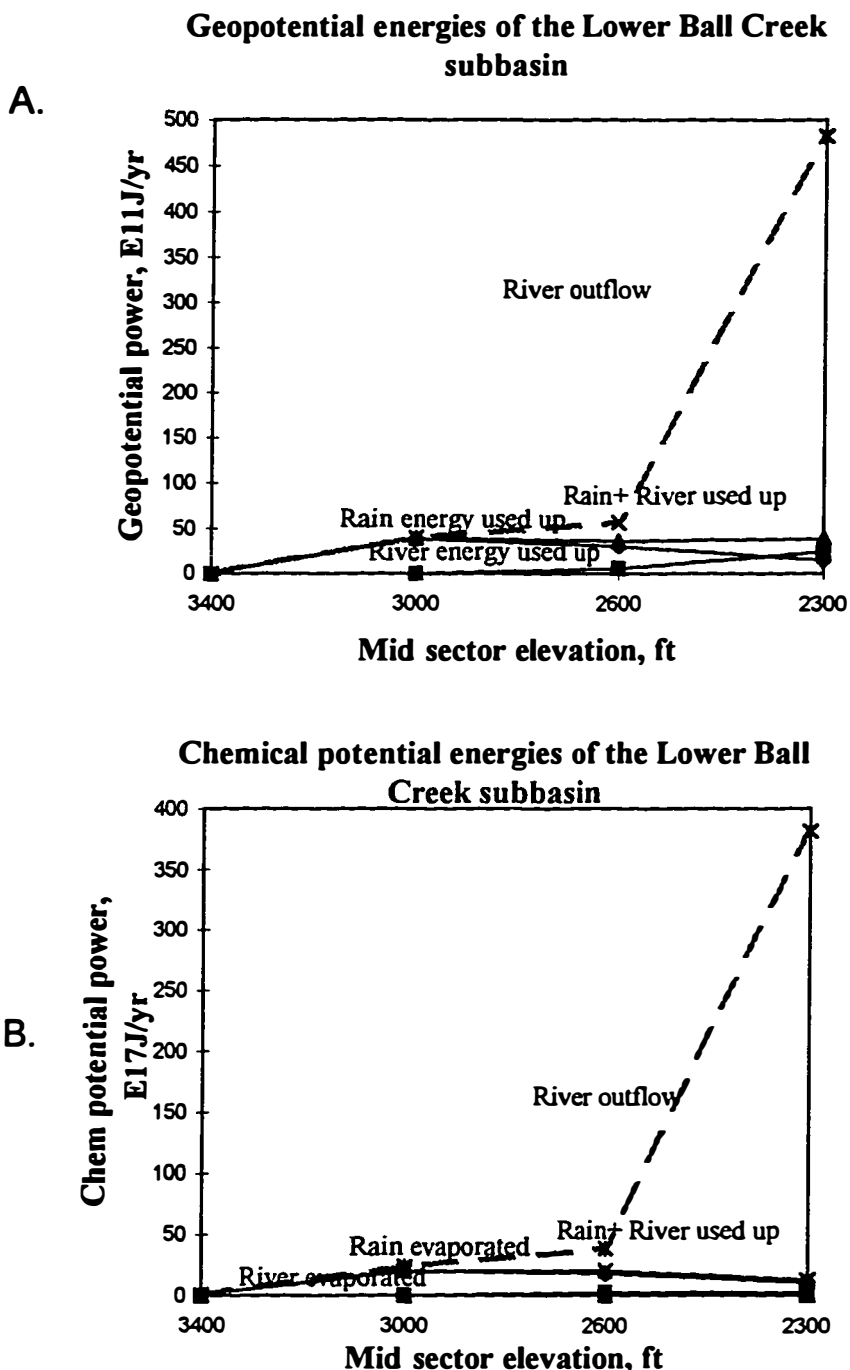


Figure A.14. Areas, energy and energy evaluations for the elevational sectors of Lower creek subbasin, representing in: A. Geopotential energies used (G_{ru}, G_{vu}, G_{tu}) and outflow (G_{vo}); B. Chemical potential energies used ($C_{ru}, C_{vt}, C_{vu}, C_{tu}$) and outflow (C_{to}); C. Geopotential used up (G_{tud}) and evapotranspired chemical potential (C_{etd}) power densities; D. Energy/ total used energy ($E_t / (G_{tu} + C_{tu})$) ratios; E. Total empower (E_t) and empower densities (E_d); F. Geopotential (T_{vg}) and chemical potential (T_{vc}) transformities of river outflow.

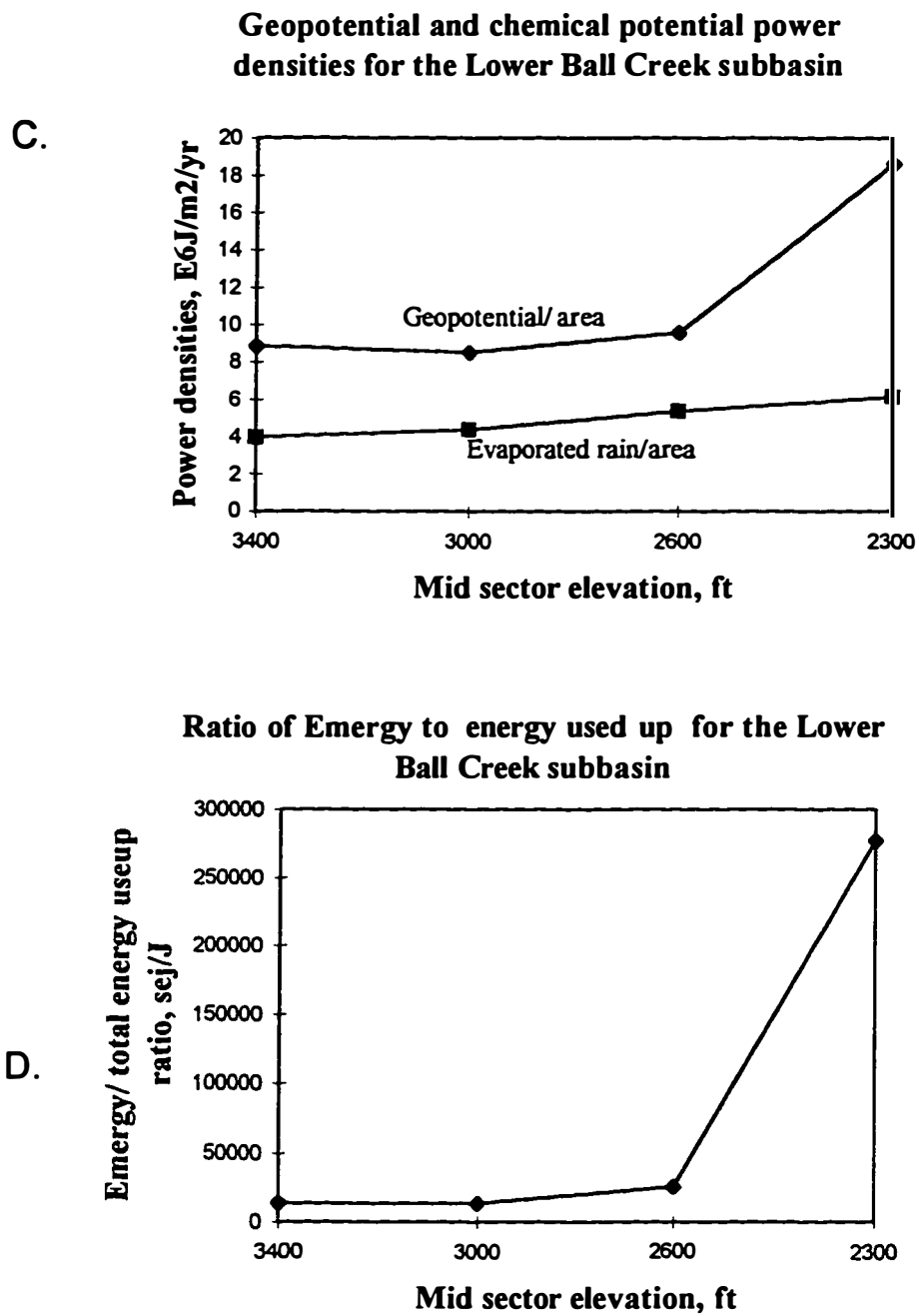


Figure A.14. Continued.

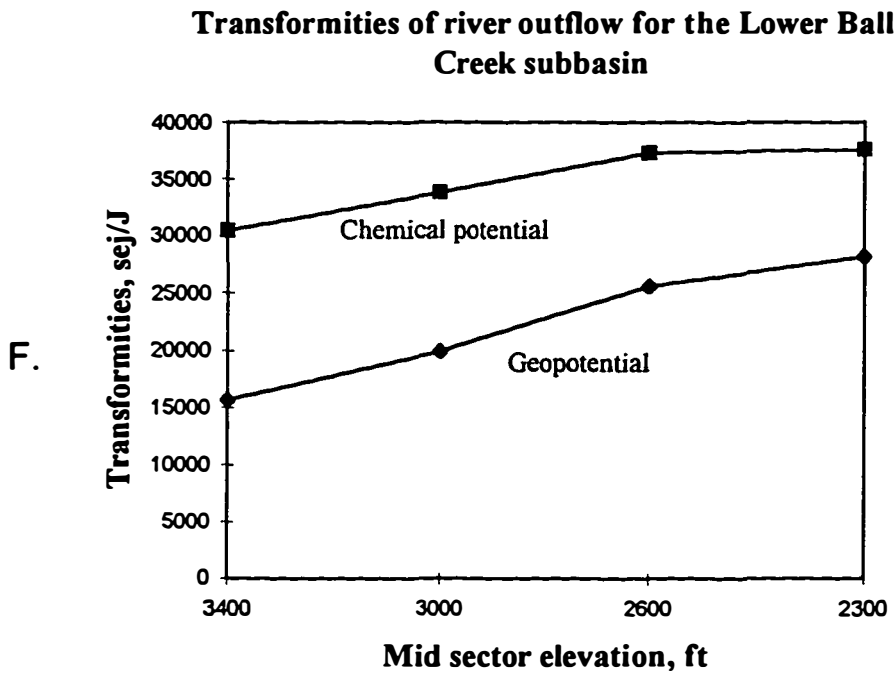
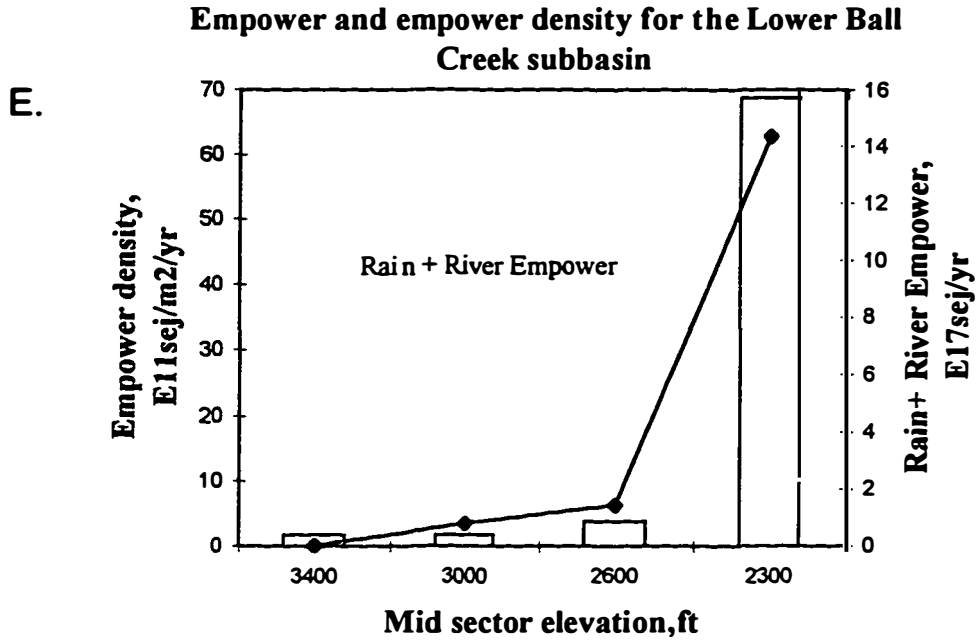


Figure A.14. Continued.

APPENDIX B

TABLES OF ENERGY AND EMERGY INDICES AND RATIOS

Tables B.1 to B.3 show energetic indices and ratios for the large watersheds (Eta, Jacupiranga, Juquia, Betari, Catas Altas, Pardo and Upper Little Tennessee).

Tables B.4 to B.6 show energetic indices and ratios for the Coweeta River basin and sub-basins.

Tables B.7 and B.8 show the EMERGY ratios for the large watersheds and the Coweeta River basin, respectively.

Table B.9 shows ratios of mountain EMERGY and energy to the productivity in the valley for selected watersheds.

Table B.1

Summary of water energies available, used and outflowing the large watersheds

Basins (col 1)	area E6 m2 (col 2)	Flow out E6 m3/yr (col 3)	Geop available E13J/yr (col 4)	Che pot available E13J/yr (col 5)	Total geo used E13J/ yr (col 6)	River geo out E13 J/yr (col 7)	Chem ET E13 J/yr (col 8)	River che out E13J/yr (col 9)
Eta	396.0	318.0	125.3	337.7	114.4	5.0	181.0	156.5
Jacupiranga	1757.0	1190.0	636.9	1341.6	609.0	7.0	753.7	585.5
Juquia	5609.0	4610.0	3835.1	4606.8	3670.0	54.2	2330.0	2268.2
Betari	151.0	97.7	114.3	104.3	102.2	9.6	56.0	48.1
Catas Altas	711.0	323.0	641.9	430.6	556.2	95.0	270.9	159.0
Pardo	3470.0	1697.0	3286.9	2289.2	3069.0	166.4	1450.5	835.3
Little Tennessee	1088.0	805.5	1505.8	871.1	878.8	434.2	474.7	396.3

Footnotes of Table B.1

area -	Area in square kilometers taken from ArcInfo coverage for the basins and subbasins
Flow out-	Average annual flow (in E6 m ³ /yr) leaving the basins and subbasins estimated from predicted runoff ratios for different elevations.
Geop available	Total annual geopotential energy available (in E13J/yr) provided by the rainfall, estimated summing up available rain geopotential energy of the different elevational sectors of the basins or subbasins.
Che pot available	Total annual chemical potential energy available (in E13J/yr) provided by the rainfall, estimated summing up available rain chemical potential energy of the different elevational sectors of the basins or subbasins.
Total geo used-	Total annual (rain + river) geopotential energy used up (in E13 J/yr) in a subbasin or basin, estimated summing up the geopotential energy used up in the elevational sectors of the subbasin or basin.
River geo out	Annual river geopotential energy (in E13 J/yr) outflowing a subbasin or basin , taking as the available geopotential energy of the river waters outflowing the lowest elevational sector of the basin or subbasin.
Che ET	Annual rain and river chemical potential energy (in E13 J/yr) used up in evapotranspiration in a basin , estimated summing up the energy of rain and river evapotranspired in the elevational sectors of the basin.
River che out	Annual river chemical potential energy (in E13 J/yr) outflowing a subbasin or basin , taking as the available chemical potential energy of the river waters outflowing the lowest elevational sector of the basin or subbasin

Table B.2

Ratios of energy per unit area for the large watersheds

Basins (col 1)	Tot used average E6J/m2/yr (col 2)	geo/ area max value E6J/m2/yr (col 3)	chem ET / area average E6J/m2/yr (col 4)	max value E6J/m2/yr (col 5)	avail geo/ area (E6J/m2/yr) (col 6)	avail chem/ area (E6J/m2/yr) (col 7)	Che out/ area (E6j/m2) (col 8)
Eta	2.9	7.7	4.6	5.0	3.2	8.5	4.0
Jacupiranga	3.5	6.4	4.3	4.6	3.6	7.6	3.3
Juquia	6.6	9.3	4.2	5.1	6.8	8.2	4.0
Betari	6.8	12.5	3.7	5.3	7.6	6.9	3.2
Catas Altas	7.8	12.7	3.8	5.1	9.0	6.1	2.2
Pardo	9.0	21.5	4.3	6.0	9.5	6.6	2.4
Little Tennessee	8.1	11.1	4.4	6.8	13.8	8.0	3.6

Footnotes of Table B.2

tot geo/ area	Average and maximum annual values for total (rain + river) geopotential power density for the basins. Average values were estimated dividing " Total geo used"/"area" (col 6/col2 in Table 3.1) Maximum values were taken from tables, referring to the highest total geopotential power densities estimated for the elevational sectors of the basins.
Chem ET/ area	Average and maximum annual values for evapotranspired rain and river per area of the basins. Average values were estimated dividing " Chem ET"/"area" (col 8/col2 in Table 3.1) Maximum values were taken from tables, referring to the highest of the rain+river evapotranspiration per area ratios estimated for the elevational sectors of the basins.
Avail geo/area	Available geopotential energy in the rainfall per area of the basins, estimated dividing "Geop available" to "area" (col4/ col2 in Table 3.1).
Avail chem/area	Available chemical potential energy in the rainfall per area of the basins, estimated dividing the "Che pot available" per "area" (col5/ col2 in Table 3.1).
Che out/ area	Chemical potential energy in the river outflowing the basin divided by the area of the basin, estimated dividing "river che out"per "area"(col 9/col2 in Table 3.1)

Table B.3.
Energetic ratios for the large watersheds

Basins (col 1)	geo out/ flow E6 J/m3 (col 2)	geo out/ geo avail (col 3)	geo out/ geo used (col 4)	che ET/ geo used (col 5)	che ET/ geo avail (col 6)	che ET/ che avail (col 7)	che out/ che avail (col 8)	che out/ geo out (col 9)
Eta	0.16	0.04	0.04	1.58	1.44	0.54	0.46	31
Jacupiranga	0.06	0.01	0.01	1.24	1.18	0.56	0.44	84
Juquia	0.12	0.01	0.01	0.63	0.61	0.51	0.49	42
Betari	0.98	0.08	0.09	0.55	0.49	0.54	0.46	5
Catas Altas	2.94	0.15	0.17	0.49	0.42	0.63	0.37	2
Pardo	0.98	0.05	0.05	0.47	0.44	0.63	0.36	5
Little Tennessee	5.39	0.29	0.49	0.54	0.32	0.54	0.45	1

Footnotes of Table B.3

Geo out/ flow	Average annual rate of geopotential energy per cubic meter of river flow leaving the basins (in E5J/m ³). Estimated dividing "river geo out"/ "Flow out"(col7/ col3 in Table 3.1)
Geo out/geo avail	Average annual rate of geopotential energy outflowing the basins to the geopotential energy provided to the basins by rain, estimated dividing "river geo out"per "geop available" (col 7/col 4 in Table 3.1)
Geo out/ geo used	Average annual rate of geopotential energy outflowing the basins to the total (rain+ river) geopotential energy used in the basins, estimated dividing "river geo out" per "total geo used" (col 7/ col6 in Table 3.1)
Che ET/ geo used	Average annual rate of rain and river chemical potential energy evapotranspired in the basin to the total (rain+ river) geopotential energy used in the basins, estimated dividing "chem ET" per "total geo used"(col 8/col6 in Table 3.1).
Che ET/geo avail	Average annual rate of rain and river chemical potential energy evapotranspired in the basin to the geopotential energy provided to the basins by rain, estimated dividing "chem ET" per "geop available" (col 8/col 4 in Table 3.1).
Che ET/ che avail	Average annual rate of rain and river chemical potential energy evapotranspired in the basin to the chemical potential energy provided to the basins by rain, estimated dividing "chem ET" per "che pot available"(col8/ col5 in Table 3.1)
Che out/ geo out	Average annual rate of chemical potential energy to the geopotential energy of rivers outflowing the basins, estimated dividing "river che out" to "river geo out"(col9/ col7 of Table 3.1)

Table B.4

Summary of water energies available, used and outflowing the Coweeta river system

Basins (col 1)	area E6 m2 (col 2)	Flow out E6 m3/yr (col 3)	Geop available E13J/yr (col 4)	Che pot available E13J/yr (col 5)	Total geo used E13J/ yr (col 6)	River geo out E13 J/yr (col 7)	Chem ET E13 J/yr (col 8)	River che out E13J/yr (col 9)
Sub-basins								
Upper Shope Fork	4.8	4.9	11.1	5.1	6.2	3.5	2.7	2.4
Cunnigham	1.7	1.8	3.5	1.8	2.0	1.3	1.0	0.9
Henson	2.3	2.6	5.7	2.6	3.2	1.9	1.3	1.3
Upper Ball	4.0	4.3	8.6	4.3	4.9	3.0	2.2	2.1
Coweeta river system								
Coweeta	15.8	15.1	33.4	16.5	18.9	10.8	9.1	7.4
Little Tennessee	1088.0	805.5	1505.8	871.1	878.8	434.2	473.2	396.4

Footnotes of Table B.4

area -	Area in square kilometers taken from ArcInfo coverage for the basins and sub-basins
Flow out-	Average annual flow (in $E6 \text{ m}^3/\text{yr}$) leaving the basins and sub-basins estimated from predicted runoff ratios for different elevations.
Geop available	Total annual geopotential energy available (in $E13\text{J}/\text{yr}$) provided by the rainfall, estimated summing up available rain geopotential energy of the different elevational sectors of the basins or sub-basins.
Che pot available	Total annual chemical potential energy available (in $E13\text{J}/\text{yr}$) provided by the rainfall, estimated summing up available rain chemical potential energy of the different elevational sectors of the basins or sub-basins.
Total geo used-	Total annual (rain + river) geopotential energy used up (in $E13 \text{ J}/\text{yr}$) in a subbasin or basin, estimated summing up the geopotential energy used up in the elevational sectors of the sub-basin or basin.
River geo out	Annual river geopotential energy (in $E13 \text{ J}/\text{yr}$) outflowing a subbasin or basin, taking as the available geopotential energy of the river waters outflowing the lowest elevational sector of the basin or sub-basin.
Che ET	Annual rain and river chemical potential energy (in $E13 \text{ J}/\text{yr}$) used up in evapotranspiration in a basin, estimated summing up the energy of rain and river evapotranspired in the elevational sectors of the basin.
River che out	Annual river chemical potential energy (in $E13 \text{ J}/\text{yr}$) outflowing a subbasin or basin, taking as the available chemical potential energy of the river waters outflowing the lowest elevational sector of the basin or sub-basin.

Table B.5

Ratios of energy per unit area for the Coweeta river system

Basins	Tot used average E6J/m2/yr	geo/ area max value E6J/m2/yr	chem ET / area average E6J/m2/yr	max value E6J/m2/yr	avail geo/ area (E6J/m2/yr)	avail chem/ area (E6J/m2/yr)	che out/ area (E6J/m2/yr)
(col 1)	(col 2	(col 3	(col 4)	(col 5	(col 6	(col 7	(col 8)
Sub-basins							
Upper Shope Fork	12.8	21.6	5.7	11.2	23.1	10.7	5.0
Cunnigham	11.1	16.7	5.5	8.9	20.4	10.8	5.1
Henson	13.6	17.0	5.7	8.3	24.5	11.2	5.5
Upper Ball	12.3	16.1	5.5	8.0	21.8	10.8	5.3
Coweeta river system							
Coweeta	11.9	13.6	5.8	8.4	21.1	10.4	4.7
Little Tennessee	8.1	11.1	4.4	6.8	13.8	8.0	3.6

Footnotes of Table B.5

tot geo/ area	Average and maximum annual values for total (rain + river) geopotential power density for the basins. Average values were estimated dividing " Total geo used"/"area" (col 6/col2 in Table 3.4) Maximum values were taken from tables, refering to the highest total geopotential power densities estimated for the elevational sectors of the basins.
Chem ET/ area	Average and maximum annual values for evapotranspired rain and river per area of the basins. Average values were estimated dividing " Chem ET"/"area" (col 8/col2 in Table 3.4) Maximum values were taken from tables, refering to the highest of the rain+river evapotranspiration per area ratios estimated for the elevational sectors of the basins.
Avail geo/area	Available geopotential energy in the rainfall per area of the basins, estimated dividing "Geop available" to "area" (col4/ col2 in Table 3.4).
Avail chem/area	Available chemical potential energy in the rainfall per area of the basins, estimated dividing the "Che pot available" per "area" (col5/ col2 in Table 3.4).
Che out/ area	Chemical potential energy in the river outflowing the basin divided by the area of the basin, estimated dividing "river che out"per "area"(col 9/col2 in Table 3.4)

Table B.6.

Energetic ratios for the Coweeta river system

Basins (col 1)	geo out/ flow E6 J/m3 (col 2)	geo out/ geo avail (col 3)	geo out/ geo used (col 4)	che ET/ geo used (col 5)	che ET/ geo avail (col 6)	che ET/ che avail (col 7)	che out/ che avail (col 8)	che out/ geo out (col 9)
Sub-basins								
Upper Shope Fork	7.2	0.31	0.56	0.44	0.24	0.53	0.47	0.69
Cunnigham	7.1	0.36	0.63	0.49	0.28	0.53	0.47	0.69
Henson	7.2	0.33	0.58	0.42	0.23	0.51	0.49	0.69
Upper Ball	7.2	0.35	0.63	0.45	0.25	0.51	0.49	0.69
Coweeta river system								
Coweeta	7.2	0.32	0.57	0.48	0.27	0.55	0.45	0.69
Little Tennessee	5.4	0.29	0.49	0.54	0.31	0.54	0.45	0.91

Footnotes of Table B.6

Geo out/ flow	Average annual rate of geopotential energy per cubic meter of river flow leaving the basins (in E5J/m ³).Estimated dividing " river geo out"/ " Flow out"(col7/ col3 in Table 3.4)
Geo out/geo avail	Average annual rate of geopotential energy outflowing the basins to the geopotential energy provided to the basins by rain, estimated dividing "river geo out"per "geop available" (col 7/col 4 in Table 3.4)
Geo out/ geo used	Average annual rate of geopotential energy outflowing the basins to the total (rain+ river) geopotential energy used in the basins, estimated dividing "river geo out" per "total geo used" (col 7/ col6 in Table 3.4)
Che ET/ geo used	Average annual rate of rain and river chemical potential energy evapotranspired in the basin to the total (rain+ river) geopotential energy used in the basins, estimated dividing "chem Et" per "total geo used"(col 8/col6 in Table 3.4).
Che ET/geo avail	Average annual rate of rain and river chemical potential energy evapotranspired in the basin to the geopotential energy provided to the basins by rain, estimated dividing "chem ET" per "geop available" (col 8/col 4 in Table 3.4).
Che ET/ che avail	Average annual rate of rain and river chemical potential energy evapotranspired in the basin to the chemical potential energy provided to the basins by rain, estimated dividing "chem ET" per "che pot available"(col8/ col5 in Table 3.4)
Che out/ geo out	Average annual rate of chemical potential energy to the geopotential energy of rivers outflowing the basins, estimated dividing "river che out" to "river geo out"(col9/ col7 of Table3.4)

Table B.7.
Empower, total power and transformities for the large watersheds

Basins (col 1)	Empower E18 sej/yr (col 2)	Empower Density		Total Energy Used (E13J/yr) (col 5)	Power density (E6J/m2/yr) (col 6)	Transformities	
		ave rain E11 sej/m2/yr (col 3)	ave rain+rv E11 sej/m2/y (col 4)			Geopotential sej/J (col 7)	Che Potential sej/J (col 8)
Eta	61.5	1.55	2.65	295.2	7.5	1232462	39278
Jacupiranga	244.1	1.39	2.52	1364.3	7.8	3482240	41617
Juquia	838.4	1.49	4.05	6026.7	10.7	1546354	36962
Betari	21.1	1.39	4.81	158.4	10.5	220164	43854
Catas Altas	87.1	1.22	4.41	827.7	11.6	91623	54750
Pardo	462.9	1.35	9.5	4522.8	13.2	278212	55416
Little Tennessee	158.5	1.46	4.35	1353.5	12.4	36509	39997

Footnotes of Table B.7

Empower	Average annual rain empower contributing to the basin, which was also equivalent to the rain and river empower contribution to the lowest sector of the basin (in E18 sej/yr).
Empower density	Average rain empower density and average rain and river empower density (in E11 sej/m ² /yr). Average rain empower was estimated dividing the rain empower contribution (col 2) by the area of the basin. Average rain and river empower density was calculated as the average values of the rain + river empower density estimated for the elevational sectors of the river basin.
Total energy Used	Average annual geopotential and chemical energy used in the basins (in E13J/yr), estimated summing up all rain and river energy used up in the different elevational sectors of the basins.
Power density	Average rate of total energy use per area of the basin (in E6 J/m ² /yr), estimated dividing the "Total Energy used" (col 5) per "Area"of the basins.
Transformities	Geopotential and chemical potential transformity (in sej/J)of river outflowing the the lowest sector of the river basin, and they were taken from calculation tables.

Table B.8.

Empower, total power and Transformities for the Coweeta river system

Basins (col 1)	Empower E18 sej/yr (col 2)	Empower Density		Total Energy Used (E13J/yr) (col 5)	Power density (E6J/m2/yr) (col 6)	Transformities	
		ave rain E11 sej/m2/yr (col 3)	ave rain+rv E11 sej/m2/yr (col 4)			Geopotential sej/J (col 7)	Che Potential sej/J (col 8)
Sub-basins							
Upper Shope Fork	0.93	1.94	6.67	8.87	18.5	26681	38877
Cunnigham	0.33	1.88	5.27	2.95	16.6	26681	38877
Henson	0.47	2.04	6.31	4.51	19.4	25592	37291
Upper Ball	0.78	1.97	5.14	7.05	17.8	25592	37291
Coweeta system							
Coweeta	3.01	1.91	4.46	28.4	17.7	27897	40648
Little Tennessee	158.5	1.46	4.35	1353.5	12.4	36509	39997

Footnotes of Table B.8

Empower	Average annual rain empower contributing to the basin, which was also equivalent to the rain and river empower contribution to the lowest sector of the basi (in E18sej/yr).
Empower density	Average rain empower density and average rain and river empower density (in E11 sej/m ² /yr). Average rain empower was estimated dividing the rain empower contribution (col 2) by the area of the basin. Average rain and river empower density was calculated as the average values of the rain + river empower density estimated for the elevational sectors of the river basin.
Total energy Used	Average annual geopotential and chemical energy used inthe basins (in E13J/yr), estimated summing up all rain and river energy used up in the different elevational sectors of the basins.
Power density	Average rate of total energy use per area of the basin (in E6 J/m ² /yr), estimated dividing the "Total Energy used" (col 5) per "Area"of the basins.
Transformities	Geopotential and chemical potential transformity (in sej/J)of river outflowing the the lowest sector of the river basin, and they were taken from calculation tables.

Table B.9.
Ratios of mountain Energy and energy to the valley evapotranspiration

Basin	Mountain area E8 m2 col 2	Valley area E8 m2 col 3	Mt geop energy use E15 J/yr col 4	Valley transp E15 J/yr col 5	Mountain Energy E26 sej col 6	Mt Empowe E19 sej/yr col 7	Mt geo En/ transp col 8	Mt Energy/ valley area E18 sej/m2 col 9	Mt Energy/ transp E11 sej/J/yr col 10	Mt Empower/ transp E4 sej/J col 11
Eta	1.64	2.13	0.85	1.15	1.71	2.46	0.74	0.8	1.49	2.14
Jacupiranga	9.44	8.13	4.86	3.63	9.45	13.67	1.34	1.29	2.89	3.76
Itariri	2.37	2.45	1.23	1.05	3.07	3.98	1.17	1.25	2.92	3.79
Little Tennessee	6.65	4.23	5.01	2.34	17.2	9.82	2.14	4.07	7.35	4.2

Footnotes of Table B.9

Mountain area-	(in E8 m ²)-Sum of the areas of the elevational sectors belonging to the " upland or mountain zone"
Valley area	(in E8 m ²)-Sum of the areas of the elevational sectors belonging to the " lowlands or valley zone"
Mt geop energy use	in E15 J/yr)-Sum of Total (rain + river) geopotential energy used in the elevational sectors of the " upland/ mountain zone".
Valley transp	(in E15J/yr)-Sum of Rain chemical potential energy used in the elevational sectors of the " lowlands or valley zone"
Mt Emergy	(in E 26 sej)- Emergy in the rock structure of the " mountain zone". It was estimated multiplying the volume of rock in the mountain zone by rock density (2.6 E 6 g/m ³) and by the rock transformity (1E9 sej/g).
Mt Empower	(in E19 sej/yr) Annual Empower contributing to the lowest elevational sector of the "mountain zone" of the basin. It was estimated accumulating all Empower contribution to the upper elevational sectors.
Mt geo Eng/ transp	Ratio of previously defined " Mt geop energy use " to " valley transpiration".
Mt Emg/valley area	(in E18 sej/m ²) Ratio of previously defined " Mt Emergy " to" valley area".
Mt Emergy/ transp	(in E11 sej/J/yr) Ratio of previously defined " Mt Emergy " to" valley transpiration".
Mt Empower/ transp	(in E4 sej/J) Ratio of previously defined "Mt Empower" to " valley transpiration".

APPENDIX C

SIMULATION TABLES AND PROGRAMS

Tables C.1 to C.4 displaying the coefficients estimated for the simulated No- Dam, One-Dam, Two- Dams and Four-Dams alternatives, respectively.

Figures C.1 and C.2 showing the Qbasic programs used in the simulation of No-Dam and One-Dam alternatives, respectively.

Table C.1. Estimates of coefficients for the No Dam simulation model

R0=	0.1375	Q2=	1.60E+07
L1=	100	M=	1.40E+07
L11=	95	V=	1.50E+07
L2=	100	W1=	6.40E+07
L22=	95	W2=	8.50E+07
A1=	3.20E+08	S1=	32
A2=	2.84E+08	S2=	34
P0=	3.00E-08	Jg=	1.5
		k=	1.00E+07
k1*L11*W1*S1*M=	5	K1=	1.84E-18
k2*L11*W1*S1*M=	2.00E+07	K2=	7.34E-12
k3*L11*W1*S1*M=	0.6	K3=	2.20E-19
k4*L11*W1*S1*M=	1.20E+05	K4=	4.41E-14
K5*M=	1.20E+05	K5=	8.57E-03
K10*L22*W2*S2*V=	5	K10=	1.21E-18
K11*L22*W2*S2*V=	2.90E+07	K11=	7.04E-12
K12*L22*W2*S2*V=	0.8	K12=	1.94E-19
K13*L22*W2*S2*V=	1.60E+05	K13=	3.89E-14
K14*V=	1.60E+05	K14=	1.07E-02
K20*W1=	2.40E+07	K20=	3.75E-01
K21*W1*S1=	2.4	K21=	1.17E-09
k40*(Q2)^2/K=	8.00E+06	K40=	3.13E-01
K41*(Q2^2/K)*S1=	0.8	K41=	9.77E-10
K50*W2=	1.60E+07	K50=	1.88E-01
K51*W2*S2=	0.9	K51=	3.11E-10

Table C.2. Estimates of coefficients for the One-Dam simulation model

Q2=	1.60E+07	A5=	4.40E+07
K=	1.00E+07	A4=	2.40E+08
R0=	0.1375	M=	1.40E+07
L1=	100	V=	1.30E+07
L11=	95	W1=	6.40E+07
L2=	100	W2=	7.20E+07
L22=	95	S1=	32
A1=	3.20E+08	S2=	29
A2=	2.84E+08	Jg=	1.6
P0=	3.00E-08	W3=	2.05E+08
J1=	2.20E+07	S3=	10.25
k1*L11*W1*S1*M=	5	K1=	1.84E-18
k2*L11*W1*S1*M=	2.20E+07	K2=	8.08E-12
k3*L11*W1*S1*M=	0.6	K3=	2.20E-19
k4*L11*W1*S1*M=	1.20E+05	K4=	4.41E-14
K5*M=	1.20E+05	K5=	8.57E-03
K10*L22*W2*S2*V=	5	K10=	1.94E-18
K11*L22*W2*S2*V=	2.50E+07	K11=	9.69E-12
K12*L22*W2*S2*V=	0.68	K12=	2.64E-19
K13*L22*W2*S2*V=	1.35E+05	K13=	5.24E-14
K14*V=	1.35E+05	K14=	1.04E-02
k20*W1=	2.40E+07	K20=	3.75E-01
K21*W1*S1=	2.4	K21=	1.17E-09
k40*(Q2)^2/K=	6.80E+06	K40=	2.66E-01
K41*(Q2^2/K)*S3=	0.34	K41=	1.30E-09
K50*W2=	1.36E+07	K50=	1.89E-01
K51*w2*S2=	0.765	K51=	3.66E-10
k60*W3/A5=	2.40E+07	k60=	5.15E+06
K61*W3*S3/A5=	1.2	k61=	2.51E-02
K62*S3=	1.2	K62=	1.17E-01

Table C.3. Estimates of coefficients for the Two- Dams simulation model

Q2=	1.60E+07	A5=	4.40E+07
K=	1.00E+07	A4=	2.40E+08
R0=	0.1375	M=	1.40E+07
L1=	100	V=	1.30E+07
L11=	95	W1=	6.40E+07
L2=	100	W2=	7.20E+07
L22=	95	S1=	32
A1=	3.20E+08	S2=	29
A2=	2.84E+08	Jg=	1.6
P0=	3.00E-08	W3=	9.80E+07
J1=	2.20E+07	S3=	4.9
k1*L11*W1*S1*M=	5	K1=	1.84E-18
k2*L11*W1*S1*M=	2.20E+07	K2=	8.08E-12
k3*L11*W1*S1*M=	0.6	K3=	2.20E-19
k4*L11*W1*S1*M=	1.20E+05	K4=	4.41E-14
K5*M=	1.20E+05	K5=	8.57E-03
K10*L22*W2*S2*V=	5	K10=	1.94E-18
K11*L22*W2*S2*V=	2.50E+07	K11=	9.69E-12
K12*L22*W2*S2*V=	0.68	K12=	2.64E-19
K13*L22*W2*S2*V=	1.35E+05	K13=	5.24E-14
K14*V=	1.35E+05	K14=	1.04E-02
k20*W1=	2.40E+07	K20=	3.75E-01
K21*W1*S1=	2.4	K21=	1.17E-09
k40*(Q2)^2/K=	6.80E+06	K40=	2.66E-01
K41*(Q2^2/K)*S3=	0.34	K41=	2.71E-09
K50*W2=	1.36E+07	K50=	1.89E-01
K51*w2*S2=	0.765	K51=	3.66E-10
k60*W3=	2.40E+07	k60=	2.45E-01
K61*W3*S3=	1.2	k61=	2.50E-09
K62*S3=	1.2	K62=	2.45E-01

Table C.4. Estimates of coefficients for the Four -Dams simulation model

Q2=	1.60E+07	A5=	4.40E+07
K=	1.00E+07	A4=	2.40E+08
R0=	0.1375	M=	1.40E+07
L1=	100	V=	1.30E+07
L11=	95	W1=	6.40E+07
L2=	100	W2=	7.20E+07
L22=	95	S1=	32
A1=	3.20E+08	S2=	29
A2=	2.84E+08	Jg=	1.6
P0=	3.00E-08	W3=	4.90E+07
J1=	2.20E+07	S3=	2.5
k1*L11*W1*S1*M=	5	K1=	1.84E-18
k2*L11*W1*S1*M=	2.20E+07	K2=	8.08E-12
k3*L11*W1*S1*M=	0.6	K3=	2.20E-19
k4*L11*W1*S1*M=	1.20E+05	K4=	4.41E-14
K5*M=	1.20E+05	K5=	8.57E-03
K10*L22*W2*S2*V	5	K10=	1.94E-18
K11*L22*W2*S2*V	2.50E+07	K11=	9.69E-12
K12*L22*W2*S2*V	0.68	K12=	2.64E-19
K13*L22*W2*S2*V	1.35E+05	K13=	5.24E-14
K14*V=	1.35E+05	K14=	1.04E-02
k20*W1=	2.40E+07	K20=	3.75E-01
K21*W1*S1=	2.4	K21=	1.17E-09
k40*(Q2)^2/K=	6.80E+06	K40=	2.66E-01
K41*(Q2^2/K)*S3=	0.34	K41=	5.31E-09
K50*W2=	1.36E+07	K50=	1.89E-01
K51*W2*S2=	0.765	K51=	3.66E-10
k60*W3=	2.40E+07	k60=	4.90E-01
K61*W3*S3=	1.2	k61=	9.80E-09
K62*S3=	1.2	K62=	4.80E-01

Figure C.1. QBasic Program for No Dam Simulation model.

```

10 REM NDam3
20 CLS
30 SCREEN 1, 0: COLOR 0, 0
40 LINE (0, 0)-(319, 180), 1, B
50 LINE (0, 60)-(319, 60)
60 LINE (0, 120)-(319, 120)
65 REM DEFINING SUNLIGHT(L1),RAINFALL(R0),FLOODING RAIN(F0)
70 DIM L1(36)
75 DATA 154, 143, 107, 83, 66, 57, 64, 77 , 71, 97, 143, 147
76 DATA 154,143, 107, 83,66,57,64,77,71,97,143,137
77 DATA 154,143, 107, 83,66,57,64,77,71,97,143,137
80 FOR I = 1 TO 36
85 READ L1(I)
90 NEXT I
91 DIM R0(36)
95 DATA 0.26, 0.24, 0.21, 0.11, 0.09, 0.08, 0.08, 0.06, 0.10, 0.13, 0.12, 0.18
96 DATA 0.26, 0.24, 0.21, 0.11, 0.09, 0.08, 0.08, 0.06, 0.10, 0.13, 0.12, 0.18
97 DATA 0.29, 0.30, 0.29, 0.12, 0.09, 0.08, 0.08, 0.06, 0.10, 0.13, 0.12, 0.18
100 FOR I = 1 TO 36
105 READ R0(I)
110 NEXT I
136 OPEN "C:\SILVIA\NDWLG.DAT" FOR OUTPUT AS #1
140 R0 = .1375
145 Jg = 1.55
150 P0 = 3E-08
160 A1 = 3.2E+08
170 A2 = 2.84E+08
190 L1 = 100
195 L11 = 95
200 L2 = 100
205 L22 = 95
210 M = 1.4E+07
215 W1 = 6.4E+07
216 S1 = 32
220 V = 1.5E+07
225 W2 = 8.5E+07
226 S2 = 34
230 K = 1E+07
245 dt = 1
250 REM COEFFICIENTS
260 K1 = 1.84E-18
270 K2 = 7.34E-12
280 K3 = 2.2E-19
290 K4 = 4.41E-14
300 K5 = .008571
310 K10 = 1.21E-18
320 K11 = 7.04E-12
325 K12 = 1.94E-19
330 K13 = 3.89E-14
340 K14 = .010667
350 K20 = .375
355 K21 = 1.17E-09

```

Figure C.1. Continued.

```

360 K40 = .313
361 K41 = 9.77E-10
365 K50 = .188235
366 K51 = 3.11E-10
370 REM CONSTANT
371 H20 = .1
372 Q10 = 1000000!
373 PM0 = .00001
375 M0 = 500000!
376 V0 = 500000!
377 Q30 = 600000!
378 W10 = 5000000!
379 S10 = 1
380 W20 = 5000000!
381 S20 = 1
382 RC = .05
385 T0 = 1
390 REM EQUATIONS
395 FOR I = 1 TO 36
405 L11 = L1(I) / (1 + K1 * W1 * S1 * M)
410 L22 = L1(I) / (1 + K10 * W2 * S2 * V)
420 DM = K4 * L11 * W1 * S1 * M - K5 * M
430 DV = K13 * L22 * W2 * S2 * V - K14 * V
440 DW1 = R0(I) * A1 - K2 * L11 * W1 * S1 * M - K20 * W1
450 DS1 = R0(I) * A1 * P0 + Jg - K3 * L11 * S1 * W1 * M - K21 * W1 * S1
451 Q1 = K20 * W1
455 Q2 = (((1 + 4 * (K40 / K) * Q1) ^ .5) - 1) / (2 * (K40 / K))
456 H2 = Q2 / K
457 Q3 = K40 * ((Q2) ^ 2) / K
458 IF H2 <= 1.72 THEN Q3 = 0
460 DW2 = R0(I) * A2 + Q3 - K11 * L22 * W2 * S2 * V - K50 * W2
470 DS2 = K41 * (Q3 / K40) * S1 + R0(I) * A2 * P0 - K12 * L22 * W2 * S2 * V -
K51 * W2 * S2
480 PV = (K13 * L22 * W2 * S2 * V) / A2
490 PM = (K4 * L11 * W1 * S1 * M) / A1
550 REM CHANGING EQUATIONS
570 M = M + DM * dt
580 IF M < 1 THEN F = M
590 V = V + DV * dt
600 IF V < 1 THEN V = 1
610 W1 = W1 + DW1 * dt
620 IF W1 < 1 THEN W1 = 1
630 S1 = S1 + DS1 * dt
635 IF S1 < 1 THEN S1 = 1
640 W2 = W2 + DW2 * dt
645 IF W2 < 1 THEN W2 = 1
650 S2 = S2 + DS2 * dt
655 IF S2 < 1 THEN S2 = 1
656 T = T + dt

```

Figure C.1. Continued.

```
720 REM PRINTING
730 PSET (T / T0, 60 - (M / M0)), 2
740 PSET (T / T0, 60 - V / V0), 1
750 REM PSET (T / T0, 60 - (PM / PM0)), 3
760 REM PSET (T / T0, 120 - Q1 / Q10), 2
765 PSET (T / T0, 120 - W1 / W10), 2
770 PSET (T / T0, 120 - S1 / S10), 3
775 PSET (T / T0, 180 - W2 / W20), 1
780 PSET (T / T0, 180 - S2 / S20), 3
785 PSET (T / T0, 120 - Q3 / Q30), 1
790 REM PSET (T / T0, 180 - Tgv / TGV0), 3
800 PRINT #1, USING "#####.#####"; M; V; W1; W2; S1; S2; Q2; Q3; H2;
PV; R0(I); L1(I)
810 NEXT I
820 IF T / T0 < 319 THEN GOTO 390
830 END
```

Figure C.2. QBasic Program for One Dam Simulation model.

```

10 REM WDEM3
20 CLS
30 SCREEN 1, 0: COLOR 0, 0
40 LINE (0, 0)-(319, 180), 1, B
50 LINE (0, 60)-(319, 60)
60 LINE (0, 120)-(319, 120)
65 REM DEFINING SUNLIGHT(L1),RAINFALL(R0),RIVER FLOWS(JR)
70 DIM L1(36)
75 DATA 154, 143, 107, 83, 66, 57, 64, 77 , 71, 97, 143, 137
76 DATA 154, 143, 107, 83, 66, 57, 64, 77 , 71, 97, 143, 137
77 DATA 154, 143, 107, 83, 66, 57, 64, 77 , 71, 97, 143, 137
80 FOR I = 1 TO 36
85   READ L1(I)
90 NEXT I
91 DIM R0(36)
95 DATA 0.26, 0.24, 0.21, 0.11, 0.09, 0.08, 0.08, 0.06, 0.10, 0.13, 0.12, 0.18
96 DATA 0.26, 0.24, 0.21, 0.11, 0.09, 0.08, 0.08, 0.06, 0.10, 0.13, 0.12, 0.18
97 DATA 0.29, 0.30, 0.29, 0.12, 0.09, 0.08, 0.08, 0.06, 0.10, 0.13, 0.12, 0.18
100 FOR I = 1 TO 36
105   READ R0(I)
110 NEXT I
135 OPEN "C:\silvia\WDLG.DAT" FOR OUTPUT AS #1
140 R0 = .1375
145 Jg = 1.55
150 P0 = 3E-08
160 A1 = 3.2E+08
170 A2 = 2.84E+08
180 A4 = 2.4E+08
185 A5 = 4.4E+07
190 L1 = 100
195 L11 = 95
200 L2 = 100
205 L22 = 95
210 M = 1.4E+07
215 W1 = 6.4E+07
216 S1 = 32
220 V = 1.3E+07
225 W2 = 7.2E+07
226 S2 = 29
230 W3 = 2.05E+08
240 S3 = 10.25
241 K = 1E+07
245 DT = 1
250 REM COEFFICIENTS
260 K1 = 1.84E-18
270 K2 = 8.08E-12
280 K3 = 2.2E-19
290 K4 = 4.41E-14
300 K5 = .008571
310 K10 = 1.94E-18
320 K11 = 9.69E-12
325 K12 = 2.64E-19
330 K13 = 5.24E-14
340 K14 = .010385
350 K20 = .375

```

Figure C.2. Continued.

```

355 K21 = 1.17E-09
360 K40 = .266
361 K41 = 1.3E-09
365 K50 = .188889
366 K51 = 3.66E-10
367 K60 = .117
368 K61 = 5.71E-10
369 K62 = .117
370 REM CONSTANT
375 M0 = 500000!
376 V0 = 500000!
377 RN = .05385
378 W10 = 5000000!
379 S10 = 1
380 W20 = 5000000!
381 S20 = 1
382 Q30 = 5000000!
383 PM0 = .00001
385 T0 = 2
386 EM0 = 1E+18
387 TGM0 = 10000!
388 TGVO = 500000!
390 REM EQUATION
395 FOR I = 1 TO 36
400 L11 = L1(I) / (1 + K1 * W1 * S1 * M)
410 L22 = L1(I) / (1 + K10 * W2 * S2 * V)
420 DM = K4 * L11 * W1 * S1 * M - K5 * M
430 DV = K13 * L22 * W2 * S2 * V - K14 * V
440 DW1 = R0(I) * A1 - K2 * L11 * S1 * W1 * M - K20 * W1
450 DS1 = R0(I) * A1 * PO + Jg - K3 * L11 * S1 * W1 * M - K21 * S1 * W1
454 Q1 = K60 * (W3)
455 Q2 = (((1 + 4 * (K40 / K) * Q1) ^ .5) - 1) / (2 * (K40 / K))
456 H2 = Q2 / K
457 IF H2 <= 1.72 THEN Q2 = 0
458 Q3 = K40 * ((Q2) ^ 2) / K
460 DW2 = R0(I) * A4 + Q3 - K11 * L22 * W2 * S2 * V - K50 * W2
470 DS2 = K41 * (((Q2) ^ 2) / K) * S3 + R0(I) * A4 * PO - K12 * L22 * W2 * S2 * V
- K51 * W2 * S2
480 DW3 = K20 * W1 - K60 * W3
490 DS3 = K21 * W1 * S1 - K61 * W3 * S3 - K62 * S3
491 PM = (K4 * L11 * W1 * S1 * M) / A1
492 PV = (K13 * L22 * W2 * S2 * V) / A4
500 REM CHANGING EQUATIONS
520 M = M + DM * DT
530 IF M < 1 THEN F = M
540 V = V + DV * DT
550 IF V < 1 THEN V = 1
560 W1 = W1 + DW1 * DT
570 IF W1 < 1 THEN W1 = 1
580 S1 = S1 + DS1 * DT
590 IF S1 < 1 THEN S1 = 1

```

Figure C.2. Continued.

```
600 W2 = W2 + DW2 * DT
610 IF W2 < 1 THEN W2 = 1
615 S2 = S2 + DS2 * DT
620 IF S2 < 1 THEN S2 = 1
625 W3 = W3 + DW3 * DT
630 IF W3 < 1 THEN W3 = 1
635 S3 = S3 + DS3 * DT
640 IF S3 < 1 THEN S3 = 1
656 T = T + DT
720 REM PRINTING
730 PSET (T / T0, 60 - (M / M0)), 2
740 PSET (T / T0, 60 - V / V0), 1
750 REM PSET (T / T0, 60 - PM / PM0), 3
760 PSET (T / T0, 120 - W1 / W10), 2
770 PSET (T / T0, 120 - S1 / S10), 3
771 PSET (T / T0, 120 - Q3 / Q30), 1
775 PSET (T / T0, 180 - W2 / W20), 1
780 PSET (T / T0, 180 - S2 / S20), 3
790 REM PSET (T / T0, 180 - Tgv / TGv0), 3
805 PRINT #1, USING "#####.###"; M; V; W1; W2; S1; S2; Q2; Q3; H2;
PV; RO(I); L1(I)
810 NEXT I
820 IF T / T0 < 319 THEN GOTO 390
830 END
```

REFERENCES

- Allan J. D. 1995. *Stream Ecology- Structure and Function of Running Waters*. Chapman & Hall, London, Great Britain.
- Bailey, P. B. 1991. The flood pulse advantage and the restoration of river-floodplain systems. *Regulated rivers: research and management*, vol.6, pp. 75-86.
- Bailey, P.B. 1995. Understanding large river- floodplain ecosystems. *Bioscience*, 45, 3, pp.153-158.
- Blinn D.W., J.P. Shannon, L.E. Stevens and J.P. Carder. 1995. Consequences of fluctuating discharges for lotic community. *J. North American Benthological Society*, 14, 3, pp. 233- 248.
- Bonetto A.A., J.R. Wais and H.P. Costello. 1989. The increasing of the Parana Basing and its effects in the lower reaches. *Regulated rivers- research and management*, 4, pp. 333- 346.
- Boring L.R., W.T. Swank and C.D. Monk. 1988. Dynamics of early successional forest structure and processes in the Coweeta Basin. In: Swank W T & D A Crossley, Jr. *Forest Hydrology and Ecology at Coweeta*. Ecological Studies 66. Springer-Verlag, New York, pp.161-179.
- Burns, L.A. 1978. Productivity, biomass and water relations in a Florida Cypress forest. Ph. D. Dissertation, University of North Carolina, Chapel Hill.
- CETESB. 1991. Aspectos hidrologicos do Rio Ribeira de Iguape- Relatorio preliminar. Companhia de Tecnologia de Saneamento Ambiental. Diretoria de Normas e Padroes Ambientais, Sao Paulo, Brazil.
- Chorley R. J., S.A. Schumm, and D.E. Sugden. 1985. *Geomorphology*. Methuen, London
- Curry R.R. 1972. Rivers- A geomorphic and chemical overview. In: Oglesby R.T., C.A. Carlson, and J.A. McCann., Eds. *River Ecology and Man*. Academic Press, New York.

- Davies B.R. 1979. Stream regulation in Africa- A review . In : Ward J. V. and J.A. Stanford ed. *The Ecology of Regulated Streams*. Plenum Press, New York, pp. 113-142.
- Day, Jr. J.W., C. A.S. Hall, W.M. Kemp, A. Yanez- Arancibia. 1989. *Estuarine Ecology*. John Wiley & Sons, New York.
- De Vries J.J. and T.V. Homadka. 1993. Computer models for surface water. In: Maidment D.R. *Handbook of Hydrology*. Mc Graw Hill, Inc., New York, pp. 21.1-21.39.
- Diamond C. 1984. Energy basis for the regional organization on the Mississippi River Basin. M.S. Thesis, University of Florida, Gainesville.
- Engecops. 1992.a. Macrozoneamento do Vale do Ribeira- Memorial Descritivo, Recursos Hídricos. Governo do Estado de Sao Paulo. Secretaria do Estado do Meio Ambiente, Sao Paulo, Brazil.
- Engecops. 1992.b. Macrozoneamento do Vale do Ribeira- Memorial Descritivo, Climatologia. Governo do Estado de Sao Paulo. Secretaria do Estado do Meio Ambiente, Sao Paulo, Brazil.
- Fawthrop N.P. 1994. Modeling hydrological processes for river management. In: Calow P. and G.E. Petts. eds. *The River Handbook- Hydrological and Ecological Principles- Vol.II*. Blackwell Scientific Publications, Oxford, England, pp. 187- 212.
- Frissell C.A., W.J. Liss, C.E. Warren and M.D. Hurley. 1986. A hierarchical framework for stream habitat classification : viewing streams in a watershed context. *Environmental Management*, 10, 2 , pp. 199- 214.
- Golley F. B. et al. 1975. *Mineral Cycling in a Tropical Moist Forest Ecosystem*. University of Georgia Press, Athens.
- Grubb, P. J. 1977. Control of forest growth and distribution on wet tropical mountains : with special reference to mineral nutrition. *Ann. Rev. Ecol. Syst.* 8, pp. 83-107.
- Hall C.A.S. 1972. Migration and metabolism in a temperate stream ecosystem. *Ecology*, 53, 4, pp. 585-604.
- Holden P.B. 1979. Ecology of riverine fish in regulated stream system with emphasis on the Colorado river. In: Ward J. V. and J.A. Stanford ed. *The Ecology of Regulated Streams*. Plenum Press, New York, pp. 57-74.
- Hynes H.B.N. 1975. Egardo Baldi memorial lecture - The stream and its valley. *Verh. Internat. Verein. Limnol.*, 19, pp. 1-15.

- Jones, H.G. 1992. *Plants and Microclimate : A Quantitative Approach to Environmental Plant Physiology*. Cambridge University Press, Cambridge, England, 2nd edition.
- Krenkel P.A., G.F. Lee and R.A. Jones. 1979. Effects of TVA impoundments on downstream water quality and biota. In: Ward J. V. and J.A. Stanford ed. *The Ecology of Regulated Streams*. Plenum Press, New York, pp. 289-306.
- Leopold L. B., M. G. Wolman and J. P. Miller. 1964. *Fluvial Processes in Geomorphology*. W. H. Freeman and Co., San Francisco.
- Leopold L.B. and W.B. Langbein. 1962. The concept of entropy in landscape evolution. papers in the hydrologic and geomorphic sciences. Geological survey Professional Paper 500-A. U.S. Department of Interior, U.S. Government Printing Office, Washington.
- Lepsch, I.F, I.R. Saraiva, P.L. Donzeli, M. Marinho, E. Sakai, J.R. Guillaumon, R. M. Pfeiffer, I.F. Mattos, W.J. Andrade and C.E.F. Silva. 1990. Macrozoneamento das terras da regio de Rio Ribeira de Iguape, SP. *Boletim Cientifico do Instituto Agronomico*, no. 19, Campinas, Brazil.
- Meentmeyer V., E.O. Box and R. Thompson. 1982. World patterns and amounts of terrestrial plant litter production. *Bioscience*, 32, 2, pp.125-128.
- Ministerio de Minas e Energia- MME. 1984. *Bacia do Ribeira de Iguape- Caracterizacao dos Usos e disponibilidades hidricas* Departamento Nacional de Aguas e Energia Eletrica. Divisao de Controle de Recursos Hidricos, Brasilia, Brazil.
- Ministerio de Minas e Energia- MME. 1970. *Boletim Fluviometrico no. 25- Bacias Litoraneas, Estado do Parana e Santa Catarina*. Departamento de Aguas e Energia Eletrica, Belo Horizonte, Brazil.
- Mitsch W. J., J.R. Taylor and K.B. Benson. 1991. Estimating primary productivity of forested wetland communities in different hydrologic landscapes. *Landscape Ecology*, 5, 2, pp. 75-92.
- Naiman R. J., J.J. Magnuson, D.M. MacKnight, J.A. Stanford, ed.1995. *The Freshwater Imperative- A Research Agenda*. Island Press, Washington.
- Newson M. 1994. *Hydrology and the River Environment*. Claredon Press. Oxford.
- Nilsson C. and R. Jansson. 1995. Floristic differences between riparian corridors of regulated and free-flowing boreal rivers. *Regulated rivers- research and management*, 11, pp. 55-66.

- Odum H. T. 1983. *Systems Ecology: An Introduction*. John Wiley & Sons, New York.
- Odum, H T. 1996. *Environmental Accounting- Energy and Environmental Decision-making*. John Wiley & Sons, New York.
- Odum H. T. and R. P. Pigeon. 1970. *A Tropical Rain Forest*. Division of Technical Information. U. S. Atomic Energy Commission, Oak Ridge, Tennessee.
- Petts G.E. 1984. *Impounded Rivers- Perspectives for Ecological Management*. John Wiley & Sons, London.
- Prigogine, I. 1947. *Study of Thermodynamics of Irreversible Processes*. 3rd ed., John Wiley, New York.
- Reily P.C. and W.C. Johnson. 1982. The effects of altered hydrologic regime on tree growth along Missouri river in North Dakota. *Can. J. Bot.* 60, pp. 2410-2423.
- Ritter D.F. 1978. *Process Geomorphology*. W.C. Brown Company Publishers, Dubuque, Iowa.
- Rosenzweig, M. L. 1968. Net primary productivity of terrestrial communities: prediction from climatological data. *The American Naturalist*, 102, 923, pp. 67- 74.
- Sao Paulo State Secretariat for Environment, 1990. *The rainforest of the Serra do Mar: Degradation and Reconstitution*. Institute of Botany, Forestry Institute, Environmental Technology Company/ CETESB, Document Series, Sao Paulo, Brazil.
- Scheidegger A.E. and W.B. Langbein. 1966. *Probability Concepts in Geomorphology*. Theoretical papers in the hydrologic and geomorphic sciences. Geological survey Professional Paper 500-C. U.S. Department of Interior, U.S. Government Printing Office, Washington.
- Schlesinger W. H. 1991. *Biogeochemistry- An Analysis of Global Change*. Academic Press, San Diego.
- Schumm S.A, M.P. Mosley and W.E. Weaver. 1987. *Experimental Fluvial Geomorphology*. John Wiley & Sons, New York.
- Secretaria do Meio Ambiente. 1990. *Macrozoneamento do complexo estuarino- lagunar de Iguape e Cananeaia : Plano de Gerenciamento Costeiro*. Coordenadoria de Planejamento Ambiental, Serie Documentos, Sao Paulo, Brazil.

- SEP/ DAEE, 1989. Estudo de Impacto Ambiental das Obras complementares da barragem do Valo grande. Relatorio Final V-1, Sao Paulo, Brazil.
- Singh V.P. 1989. Hydrological Systems- vol. II- Watershed Modeling. Prentice-Hall, Englewood Cliffs, New Jersey.
- Stanford J. A., J. V. Ward, W.J. Liss, C.A. Frissell, R.N. Williams, J.A. Lichatowich and C.C. Coutant. 1996. A general protocol for restoration of regulated rivers. *Regulated Rivers: Research & Management*, 12, pp. 391- 413.
- Stanford J.A. and J.V. Ward. 1988. The hyporheic habitat of river ecosystems. *Nature*, 335, pp. 64-66.
- Stikney P. L. , L. W. Swift,Jr. and W. T. Swank, comps. 1994. Annotated bibliography of publications on watershed management and ecological studies at Coweeta Hydrologic Laboratory, 1934-1994. Gen. Tech. rep. SE-86. Asheville, NC. U S Department of Agriculture, Forest Service, Southeastern Forest Experiment Station.
- Swank W.T. and D. A. Crossley, Jr. 1988. Introduction and site description. In: Swank W. T. and D. A. Crossley,Jr. *Forest Hydrology and Ecology at Coweeta. Ecological Studies 66*. Spring- Verlag, New York, p.1-16.
- Swank W.T. and J. B. Waide. 1988. Characterization of baseline precipitation and stream chemistry and nutrients budgets in control watersheds. In: Swank W. T. and D. A. Crossley,Jr. *Forest Hydrology and Ecology at Coweeta. Ecological Studies 66*. Spring- Verlag, New York, p. 57-79.
- Swift L. W., G. B. Cunningham and J. E. Douglass. 1988. Climatology and Hydrology. In: Swank W. T. and D. A. Crossley,Jr. *Forest Hydrology and Ecology at Coweeta. Ecological Studies 66*. Spring- Verlag, New York, p. 35-55.
- Tundisi, J. G.S. 1987. Fitoplancton da regio lagunar de Cananeia: Estudos Ecologicos e interacoes com Fatores Hidrologicos. In : Secretaria de Industria, Comercio, Ciencia e Tecnologia- DCET /SICCT. Simposio sobre ecossistemas da Costa Sul-Sudeste Brasileira, 3, pp. 130-175.
- U.S. EPA. 1995. Watershed protection- A project focus.EPA 841-R-95-003.U.S. Environmental Protection Agency, Washington, DC.
- Vannote R.L., G.W. Minshall, K.W. Cummins, J.R. Sedell and C.E. Cushing. 1980. The river continuum concept. *Can. J. Fish. Aquat. Sci.* 37, p.130-137.
- Viessman Jr W., G.L.Lewis, J.W. Knapp. 1989. *Introduction to Hydrology- 3rd ed.* Harper & Row, Publishers, New York.

Ward J.V. and J.A. Stanford ed. 1979. *The Ecology of Regulated Streams*. Plenum Press, New York.

Ward J.V. and J.A. Stanford. 1985. The ecology of regulated streams: past accomplishments and directions for future research. In: Craig J.F. and J.B. Kemper. Eds. *Regulated Streams- Advances in Ecology*. 3rd Edition. Plenum Press, New York, p. 391-409.

Wittaker R.H. and P. L. Marks. 1975. Methods of assessing terrestrial productivity. In : Lieth H. and R.H. Wittaker. *Primary Productivity of the Biosphere*. Springer-Verlag, New York, pp. 55- 118.

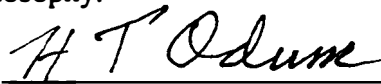
BIOGRAPHICAL SKETCH

Maria Silvia Romitelli was born on April 17, 1953 in Araraquara, Brazil. She received her Bachelor of Science degree in civil engineering from the University of Sao Paulo, Sao Carlos Campus in 1976. She continued working towards her Master of Science in sanitary engineering in the University of Sao Paulo, completing it in 1982. Meanwhile, she spent one year in Madison, Wisconsin where she took classes in sanitary engineering at the University of Wisconsin.

From 1982 to 1987 she worked as a senior engineer in a private environmental consulting company in Brazil, where she developed pilot projects for the treatment of water, wastewater and solid residues. Later, she worked during four years in the Environmental Impact Assessment Division of the Secretariat of Environment of Sao Paulo State where she coordinated a multidisciplinary team reviewing environmental impact statements prepared for large hydraulics and urban developments.

In 1989, she spent three months in Aberdeen, Scotland, in an intensive training course on impact assessment. Since fall of 1991 she has worked towards a Doctor of Philosophy degree in the system ecology program, Environmental Engineering Sciences Department, holding first a Fulbright scholarship and later graduate assistanships.

I certify that I have read this study and that in my opinion it conforms to acceptable standards of scholarly presentation and is fully adequate, in scope and quality, as a dissertation for the degree of Doctor of Philosophy.



H.T. Odum, Chair
Graduate Research Professor of
Environmental Engineering
Sciences, Emeritus

I certify that I have read this study and that in my opinion it conforms to acceptable standards of scholarly presentation and is fully adequate, in scope and quality, as a dissertation for the degree of Doctor of Philosophy.



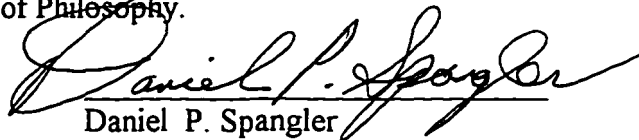
Mark T. Brown
Assistant Professor of Environmental
Engineering Sciences

I certify that I have read this study and that in my opinion it conforms to acceptable standards of scholarly presentation and is fully adequate, in scope and quality, as a dissertation for the degree of Doctor of Philosophy.



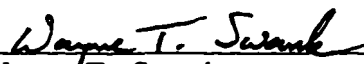
G. R. Best
Scientist of Environmental Engineering
Sciences

I certify that I have read this study and that in my opinion it conforms to acceptable standards of scholarly presentation and is fully adequate, in scope and quality, as a dissertation for the degree of Doctor of Philosophy.



Daniel P. Spangler
Associate Professor of Geology

I certify that I have read this study and that in my opinion it conforms to acceptable standards of scholarly presentation and is fully adequate, in scope and quality, as a dissertation for the degree of Doctor of Philosophy.



Wayne T. Swank
Supervisory Research Forester,
Coweeta Hydrology Laboratory

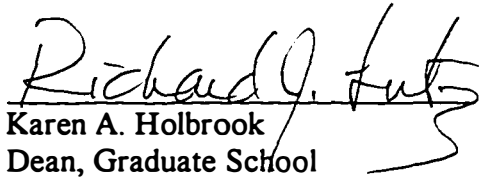
This dissertation was submitted to the Graduate Faculty of the College of Engineering and to the Graduate School and was accepted as partial fulfillment of the requirements for the degree of Doctor of Philosophy.

August, 1997

f



Winfred M. Phillips
Dean, College of Engineering



Karen A. Holbrook
Dean, Graduate School